THE UNIVERSITY *of* EDINBURGH

Holocene Glacier fluctuations and Tephrochronology of the Öræfi district, Iceland

by

Hjalti J. Gudmundsson B.Sc., M.Sc.

Ph.D.

University of Edinburgh

1998

Holocene Glacier Fluctuations and Tephrochronology of the Öræfi District, Iceland.

Abstract

The aims of this thesis are to refine the tephrochronology of the Öræfi district, SE Iceland and assess the Holocene glacier fluctuations of the Öræfajökull ice cap. The pattern and timing of glacier fluctuations are determined using glacial geomorphology and tephrochronology, and the implications for palaeoclimate are assessed. Iceland is important to the study of global and regional climatic change because it is located close to both the marine and atmospheric Polar Fronts widely regarded as the key factors in the climate of the North Atlantic region. Six outlet glaciers were studied: Svínafellsjökull, Virkisjökull, Kotárjökull and Kvíárjökull originating from the Öræfajökull ice cap and Skaftafellsjökull and Morsárjökull originating from the Vatnajökull ice cap. A long history of glacier fluctuations were found with a similar temporal pattern of glacier oscillation between the outlets of Vatnajökull and Öræfajökull. A maximum of eight advances have been identified. The oldest advance is inferred to date from the maximum of the last Glaciation ca. 18000 yrs BP. The first advance in the Holocene occurred ca. 9700 BP during a still-stand of the last Termination. The onset of the Neoglaciation occurred between 6000 BP and 4600 BP with an expansion of all of the studied glaciers. Subsequent smaller advances have been dated to ca. 3200 BP, ca. 1800 BP, ca. 700 BP, ca. 200 BP and ca. 80 BP. The most significant movement of the Polar front during the Holocene is likely to have occurred around 5000 BP, and, as a consequence, an estimated temperature cooling of ca. 2.5°C took place in Iceland, perhaps the greatest cooling since the last Termination. Within the broad pattern of change, glaciers in the study area show variability which represents local precipitation patterns, contrasting topography and change in glacier process. In this thesis a total of 22 silicic tephra layers are identified from over 90 profiles in the study area. The majority of these layers are dated to the latter part of the Holocene. Three silicic tephras were deposited during historical time (post 900 AD) namely, Vö ca. 900 AD, H1104 and Ö1362. The Vö ca. 900 AD and the H1104 tephras are located for the first time. Specific prehistoric (pre 900 AD) tephras identified include Hekla-Ö, Hekla-4 and Hekla-S. The tephrochronology of the Öræfi district is also used to assess the eruption history of the Öræfajökull stratovolcano during the Holocene. Prehistoric eruptions are dated to ca. 9200 BP, ca. 6500 BP(?), ca. 4700 BP, ca. 2800 BP and ca. 1500 BP. Jökulhlaups accompanied the eruptions of 1727 AD, 1362 AD and ca. 1500 BP and are likely to have followed older eruptions of the volcano. A strong relationship occurs between volcanic activity of the Öræfajökull stratovolcano and the pattern of glacier fluctuations. This is explained as a response to isostatic crustal adjustment during ice cap growth and decay, and indicates a general relationship between volcanic activity and climate change.

Sól tér sortna,
sigr fold í mar,
hverfa af himni
heiðar stjörnur;
geisar eimi
við aldrnara,
leikr hár hiti
við himin sjalfan.

"Sun darkens,
earth sinks in sea,
disappear from sky
bright stars;
enduring fire
of ablaze,
encircled by high heat
in heaven itself".

Translation: H.J. Gudmundsson

The 57th stanza of Völuspá written in the late 13th Century in Iceland describing the apocalypse in a form of a volcanic eruption. The author is unknown.

ACKNOWLEDGEMENTS

I gratefully acknowledge my full appreciation to the following people for their help, contribution and inspiration during my 3 years in Edinburgh:

First and foremost to my excellent supervisors Dr Andrew J. Dugmore and Professor David E. Sugden for their valuable support throughout my doctoral study, both in Scotland and Iceland. Their encouragement, patience and constructive criticism were greatly appreciated. Dr Peter Hill, department of Geology and Geophysics, The University of Edinburgh, for his valuable assistance and patience throughout the Electron microprobe work. Dr Gordon T. Cook, Scottish Universities Research and Reactor Centre (SURRC) in East Kilbride, Scotland, for doing the radiocarbon dating. Andrew Macintosh for his help in the field, fruitful discussions on various aspects of science and life, and his continuous friendship. Anthony J. Newton for help on identifying tephras and discussions. Nick Spedding for fruitful discussions and enthusiasm. The computer and secretarial staff in the department for their valuable help at critical moments and for always being ready to help when ever needed. And to all my fellow postgrads and the excellent academic staff in the Geography department who helped making the stay in Edinburgh memorable and pleasant. Finally, to my flatmates in Edinburgh: David, Tom, Martin, Lynton, Joe and Rannveig for their friendship and support.

In Iceland:

The Nature Conservation Agency for the permission to work in the Skaftafell National Park. Gudrun Larsen for her assistance and advise on the tephrochronology. Farmers Ari and Sigrún at Hof in Öræfi for their generosity and support during the field work. I greatly appreciate the financial support from the National Geographic Society, grant no. 5730/96 entitled 'Holocene Glacier and Climate fluctuations in Iceland'. I also want to acknowledge the use of the department's "infamous" Land Rover, a vehicle that will never cease to amaze me. The funding from the Icelandic Student Government Loan Fund is also greatly appreciated. Most importantly, I would like to thank my family in Iceland for their continuous support and encouragement and for generally being there.

TABLE OF CONTENTS

CHAPTER 3
THE GEOMORPHOLOGY OF THE ÖRÆFI DISTRICT

CHAPTER 4
THE TEPHROCHRONOLOGY OF THE ÖRÆFI DISTRICT

CHAPTER 5
THE TIMING AND EXTENT OF GLACIER FLUCTUATIONS

CHAPTER 6
DISCUSSION, IMPLICATIONS AND CONCLUSION

PART I DISCUSSION AND IMPLICATION

PART II SUMMARY AND CONCLUSION

LIST OF FIGURES

CHAPTER 1.

CHAPTER 2.

CHAPTER 3.

CHAPTER 4.

CHAPTER 5

CHAPTER 6

LIST OF TABLES

CHAPTER 2

CHAPTER 3

CHAPTER 4 (Appendix II)

CHAPTER 5

CHAPTER 6

LIST OF SHEETS

(in a pocket attached to the inner site of the back cover):

Chapter 1. Introduction, background and context

1.1 Aim

The overall aim of this research is to use geomorphological and tephrochronological methods to determine the extent and timing of Holocene glacier advances in south east Iceland.

1.2 Scientific rationale

1.2.1 Environmental indicators of climate change

The study of rates and patterns of environmental change is important because it enables us to understand how processes vary both temporally and spatially. During the Northern Hemisphere winter, over half of the world's terrestrial areas and up to 30% of its oceans may be covered by a blanket of snow and ice (Sugden and John, 1988) and this blanket significantly affects the lives of people living in the densely populated areas of the Northern Hemisphere. Understanding the controlling climatic factors is important. One effective way to tackle this is through the terrestrial record because it provides a window of past environmental records which in turn can be used to test against models of climatic change. There are many proxy climate indicators available such as flora and fauna micro- and macro-fossils, landscape and landform evolution and glaciers. In general, terrestrial records tend to reveal higher resolution data of environmental change due to higher sedimentation rates than in the oceans. Although the terrestrial record is frequently fragmentary, several proxies can be observed and compared with each other in order to identify different elements of climatic change. A good dating control is important to effectively integrate the climatic proxies from terrestrial and oceanic records.

Glaciers can be key indicators of climatic change. They have been used for many decades as climatic proxies because they have great spatial coverage and a variety of characteristics which can be linked to climatic change. Moreover, glaciers respond relatively quickly to changes in temperature and precipitation, making it possible to create a high resolution record of climate change. Therefore, the use of glaciers as climatic proxies can act as a complementary method to other commonly used

ecological techniques. However, a caveat has to be introduced. Although glaciers show good 'fixes' at particular times the temporal record is often incomplete.

One of the major advantages of studying glacier fluctuations is the possibility of assembling a climatic model from the history of glacier oscillations (e.g. Payne and Sugden, 1990; Hulton, *et al.*, 1995; Hubbard, 1996). This can be conducted using numerical modelling. Furthermore, the likelihood for synchroneity in climatic trends can be tested between regions where it is important to identify broad trends of glacier fluctuations. Additionally, connections between processes and landforms can be studied in detail, thus opening the opportunity of linking a certain landforms with a particular climate. These tests are of importance in environmentally sensitive areas like the North Atlantic, where the records can be very diverse and complex, because of its importance in being able to interpret them as changes in the North Atlantic environmental system (Björck, *et al.*, 1996).

Glaciers are of particular proxy climatic interest in the North Atlantic because they cover vast areas in Greenland, Scandinavia and Iceland. High resolution records have been deduced from characteristics of glaciers in these areas by studying glacier behaviour, for example Greenland ice cores, glacier moraine records and processes and glacio-lacustrine data (e.g. Dugmore, 1989a; Karlén and Matthews, 1992; Kroç, *et al.*, 1993; Meese, *et al.*, 1994; Mayewski, *et al.*, 1994). These have complemented palaeoecological records of former environments which in turn has led to better understanding of the environmental history of the North Atlantic (e.g. Rousseau *et al.*, 1994; Björck, *et al.*, 1996; Klitgaard-Kristensen *et al.*, 1998).

1.2.2 Iceland and its sensitivity to climate change

About 10.8% of Iceland (11.200 km^2) is covered by glaciers (Björnsson, 1979). The ice caps conceal unexplored landforms and geological structures, active volcanoes and geothermal areas. Icelandic glaciers are warm-based or temperate glaciers and respond actively to climate by advancing or retreating (Björnsson, 1979; Jóhannesson, 1997; Mackintosh *et al.*, in press). Because of their profound effects upon the environment and the features associated with them, the Icelandic glaciers have long been of interest (Pálsson, 1774; Thoroddsen, 1911). A need to map glacier fluctuations in space and time is necessary in Iceland to understand how glaciers behave, especially because meltwater from glaciers has been harnessed for power plants. On the other hand, the dynamic nature of Icelandic glaciers have frequently

threatened inhabited areas by surging, flooding, damaging vegetation, disrupting the Icelandic road system and even temporarily inhibiting fish from entering coastal waters (Björnsson, 1988).

In a wider context, the position of Iceland close to the boundaries of two oceanic currents, namely the cold Polar Front and the warm North Atlantic Drift offers a unique opportunity to study glacier fluctuations in response to the oscillations of these oceanic boundaries. Furthermore, Iceland is very important in establishing a detailed Holocene environmental record for the sub-Arctic region. Because of the late human settlement of the island occurring around 900 AD, the Holocene changes in the environment are almost entirely lacking anthropogenic influences.

The difficulty of linking climatic data with observed environmental changes has inhibited the study of the wider significance of the environmental record in Iceland. Evidence has recently emerged from Greenland ice core studies indicating that abrupt changes in climate were relatively common over the last glacial epochs (Dansgaard *et al.*, 1993). The ice core data show an excellent continuous record of temperature change over the last approximately 200 ka years which can be compared with environmental data sets from all over the world. For example, the GISP2 project has revealed that the Holocene experienced dramatic temperature fluctuations (Meese *et al.*, 1994). Chronological correlation between Iceland and Greenland is made possible by identifying tephras originating in Iceland buried in the Greenland ice cores (Hammer, 1984; Grönvold *et al.*, 1995). This permits the identification of leads and lags between the two regions. One other way of correlating different (tephra-) records is by using acidity spikes; however, this method can be ambiguous because the chemistry of the spikes in the ice is not known in detail. Correlation is a challenge because conventional dating methods lack the precision obtained by tephras of known age in ice cores. For example, when using the radiocarbon method, the accuracy is considered high when the error bar is ±50 BP years at 1σ; excluding the calibration errors.

Correlation between climatic and environmental data is not always straightforward since all responses are not primarily forced by climate variations. Climatically-induced environmental changes can be magnified or completely swamped by other changes in the environment unrelated to climate. This is very likely to happen in Iceland because of the very dynamic environment associated with volcanic and geothermal activity. Therefore, it is crucial to identify local anomalies when identifying climatic signals

which was done by Dugmore and Sugden (1991) in their study of Sólheimajökull, south Iceland.

Relatively recent theories of glacier fluctuations describing the last Termination and glacier behaviour over the Holocene in Iceland indicate a different pattern than previously described for Iceland (i.e. Ingólfsson and Norddahl, 1994; Stötter, 1994; Gudmundsson, 1997). These studies indicate a complex environmental history and one that is not necessarily the same as in Europe. Focusing on the Holocene epoch, which spans the last ten millennia (Mangerud *et al.*, 1974, Wohlfarth, 1996), the traditional school of thought was that glacier activity was limited during much of the Boreal to Subatlantic time (i.e. Björnsson, 1979). This view was based on the first effort to investigate Holocene environmental change in Iceland, published in the early 1960s (Einarsson, 1961; 1963). A shift of emphasis came as a result of studies conducted in the mid 1980s by scientists from the UK and Germany (Dugmore, 1987, 1989a; Stötter, 1994). They proposed that the glaciers were active in all parts of the country throughout the Holocene. Details of the newly emerging Holocene record are reviewed in a recently published paper (Gudmundsson, 1997: Appendix I).

1.3 Approach

It has become clear that the environmental record in Iceland is much more complicated than previously thought which underlines the fact that more sites need to be investigated. One of the best sites in Iceland to study the Holocene glacier fluctuations is Öræfi, south east Iceland, where glaciers form on the highest mountain in Iceland and flow into one of the warmest regions (Fig. 1.1). Glaciers in the area form relatively small valley outlets with southerly aspect which means they receive high precipitation and thus respond rapidly to climatic change. During the Holocene epoch outlets from the Öræfajökull ice cap left sequences of moraines around the south and south eastern side of the ice cap. The outlets have advanced onto a sandur plain or andisols with little organic material which means that radiocarbon dating of moraine sequences is nearly impossible. But due to the high volcanic activity of Iceland an alternative means of dating can establish the accurate chronology required. Tephra layers, produced by volcanic eruptions and deposited in soils formed between moraines after the glacier retreated, make it possible to date moraines with precision. Abundant tephra layers can be found in soils in the Öræfi district, spanning the whole Holocene. Öræfajökull ice cap is therefore a promising site in Iceland for refocusing recent ideas about environmental change during the Holocene.

1.4 Specific objectives

The overall aims of this research are to establish a detailed chronological record of glacier fluctuations in south east Iceland to identify climatic signals and hence improve the present knowledge of Holocene glacier fluctuations in Iceland. More specifically this research will:

1. Use geomorphological techniques to determine the extent of glacier advances of four different outlets of the Öræfajökull ice cap (Svínafellsjökull, Virkisjökull, Kotárjökull and Ķviárjökull) and two outlets from Vatnajökull ice cap (Skaftafellsjökull and Morsárjökull) in south east Iceland. The two latter outlets are selected to obtain comparison between small ice cap (Öræfajökull) outlets and larger ice sheet (Vatnajökull) outlets. This helps in identifying the role of factors such as varying response time, climate and catchment size. Furthermore, Öræfajökull ice cap is an active ice-capped central volcano whereas the catchment areas of the two outlets of Vatnajökull are not. Volcanic activity could alter the subglacial environment and thus the pattern of glacier oscillation.
2. Refine the Holocene tephrochronology in the Öræfi district.
3. Date the glacier advances using tephrochronology.
4. Assess the relative importance of local and regional climate, local topography, volcanic activity and glacial processes in explaining glacier fluctuations.

These objectives raise a series of specific questions:

- Are fluctuations of outlet glaciers from Öræfajökull ice cap in phase or out of phase with other similar outlets in Iceland?

- Is there a synchroneity with other regions in the North Atlantic?

- If not, what inhibits or amplifies advance or retreat of a glacier in Iceland?

Answering these questions will improve the knowledge of the climatic history of Iceland and consequently the North Atlantic.

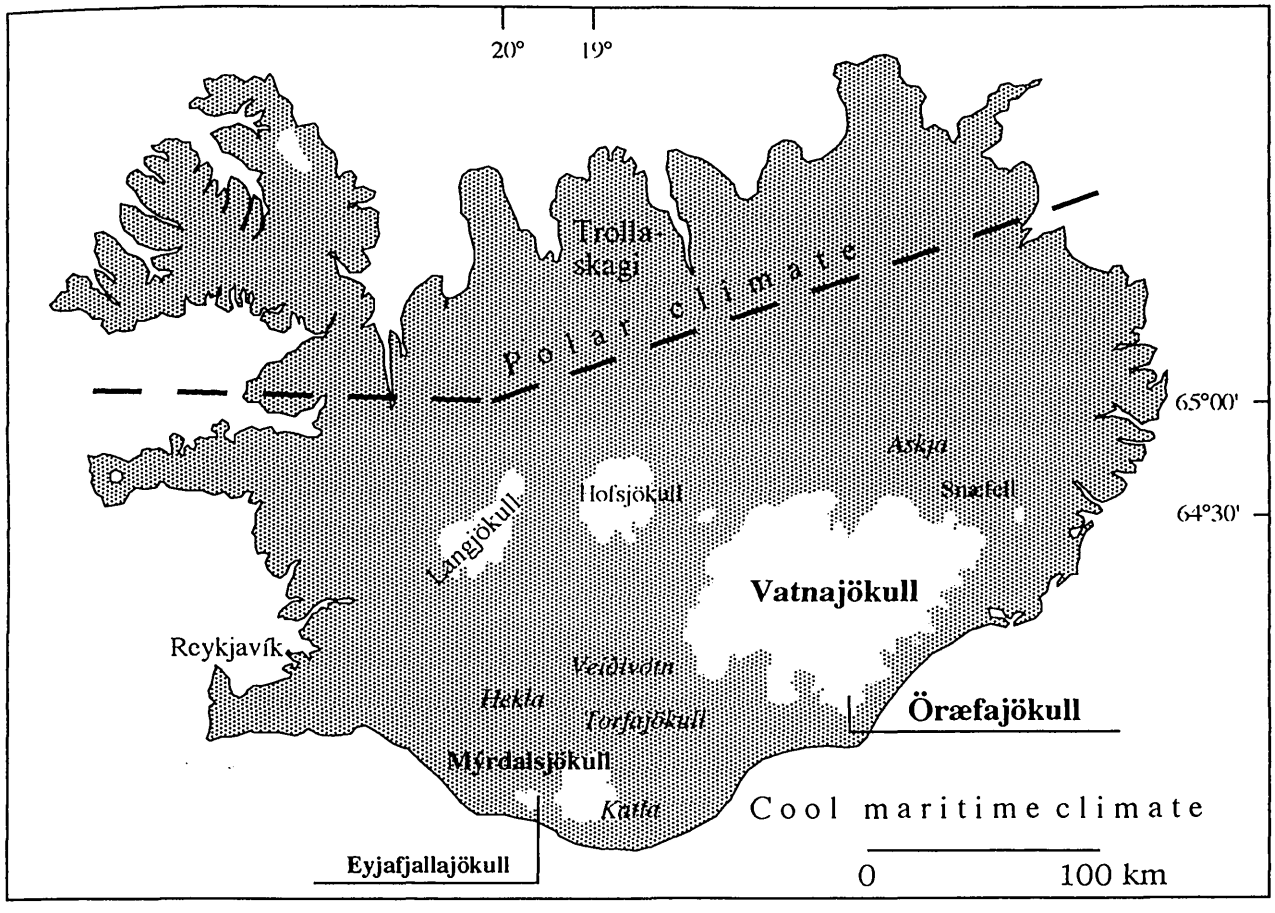

Fig. 1.1. Iceland. An island of about 103.000 km^2 in the North Atlantic. Glaciers mentioned in the text are shown in bold, volcanoes in italics and other place names in lower case text.

Chapter 2. The Study Area and Methods

Part A. The Study Area.

2.1 The Icelandic environment

Iceland is an island of approximately 103.000 km^2 in area lying in the North Atlantic Ocean between 63.4°N and 66.5°N latitudes (Fig. 1.1). Topographically about 25% of the island lies below 200 m and about 50% rises above 400 m. Most of the uplands form a highland plateau between 500 - 700 m extending approximately 300 km from east to west and 100 km from north to south. Several peaks rise above the plateau, the highest being Hvannadalshnúkur in Öræfajökull, at 2119 m.

The topography is primarily a result of the geology of Iceland. Geologically, Iceland is a very young country and has been mainly built up during the latter part of Cainozoic era. It is almost entirely made of lava flows and eruptive móberg (hyaloclistites) (90%) while in between are widespread thin consolidated sedimentary beds (10%) (Jakobsson, 1979). Igneous intrusions are also common in older geological formations. The bedrock of Iceland has been divided into three major chronological formations that are topographically distinct and have important implications for the location and nature of glaciation (Fig. 2.1). These are the Tertiary Basaltic Formation, of Tertiary and early Pleistocene age, Grey Basalt Formation from the late Pliocene and early Pleistocene and Móberg Formation of late Pleistocene age (Sæmundsson, 1979). The Tertiary Basalt Formation consist largely of subaerial plateau basalt cut by glacially formed valleys. During the Pleistocene Glaciation, which ended about 10 ka BP years ago, Iceland was almost entirely glaciated on several occasions. During the Pliocene and Pleistocene a 100.000 yrs periodicity of glaciations has been identified in Iceland (cf. Einarson and Albertsson, 1988) where an islandwide glaciation has been identified at 2.2 - 2.1 myr (Geirsdóttir and Eiríksson, 1994). This led to subglacial volcanic eruptions resulting in the formation of the hyaloclistites which is easily eroded. The Pleistocene materials are

largely made of pyroclastic tuffs and breccias, subglacial pillow lavas and altered glass (palagonite) formed by subglacial volcanism (Jakobsson, 1979). These materials are interbedded with glacial and alluvial deposits together with interglacial lava flows. The implications are that glaciers are easily formed and the bedrock is relatively soft and ideal for dynamic glacier erosion.

Volcanism is important to this study because it creates topographic heights where glaciers can form and it is the source of tephras. The present volcanism in Iceland is restricted to volcanic belts that cut through the island from south west to north east as a part of the mid-Atlantic constructive plate boundary. Here, the North American plate is moving apart from the Eurasian plate and as a result Iceland is widening about 1 cm per year (Kristjánsson, 1979). The volcanically active zones in Iceland may be divided into four areas; the axial zone and three flank zones (Jakobsson, 1979; Fig. 2.2). Tholeiitic basalts are produced in the axial zone but alkali rocks are limited to the flanks, resulting in a thick pile of alkali olivine basalts and transitional alkali basalts superimposed on the tholeiitic rocks. The volcanic zones can be further subdivided into twenty-nine volcanic systems which can be delimited petrologically, i.e. according to the chemical composition of the volcanic products (Jakobsson, 1979). Volcanic activity in Iceland has been more varied than in any other area of equal size in the world. The activity has been very high since the time of Settlement in Iceland around 900 AD. Large quantities of tephra are ejected in some eruptions, for example Hekla and Katla (Fig. 1.1; 2.2), greatly affecting the formation and character of superficial deposits. The implication is that tephras can be used as a dating tool for various human and environmental changes in Iceland.

The present day geomorphic environment of Iceland is highly dynamic and subject to significant changes over short periods of time. Being a relatively heavily glaciated volcanic island the landscape changes actively through erosion and deposition. Consequently, the presently contrasting plateau topography is a combination of glacier erosion and volcanism. Most of the glaciers in Iceland are located on top of volcanically active areas. Björnsson (1988) has shown that a subglacial topography

with high relief exists in these areas. The implication of a glacier being on top of a volcanically active centre, such as the Öræfajökull ice cap, means that the subglacial topography must change as a result of changes in the rates of eruption and glacial erosion. If the eruption rate is high, the subglacial topography changes rapidly making it necessary for the glacier to find a new equilibrium with the changed subglacial conditions. Geothermal heatflux, connected with volcanically active areas, must also contribute to change in the subglacial conditions in terms of subglacial melting, and may even change the flow mechanism of the ice.

The height and extent of the highland plateau results in a dry climate in the north because the dominant precipitation source is from the south. Due to orographic effects, the winds dry up as they go over the highlands and the ice caps located on the south and south eastern part of the plateau. This means that mountains on the southern side of the island receive high amounts of precipitation encouraging the formation of glaciers.

The movement and intensity of cyclonic activity is of great importance for the climate and consequently the growth and decay of glaciers in Iceland. As part of the westerlies, a major feature of the Northern Hemisphere atmospheric circulation, depressions are usually formed or regenerated around Newfoundland. They follow a route guided by the boundaries of cold Polar and warm Atlantic air masses and often reach a maximum intensity around Iceland (Fig. 2.3). This means that if this boundary fluctuates the temperature and precipitation can vary significantly in Iceland. For example, if depressions slow and intensify to the south west of the island it can result in more persistent cold and rainy weather in the summer months or a thaw in the winter. Consequently, the climate of Iceland is very changeable, but relatively mild for its latitudinal location.

According to Einarsson (1976) the climate of Iceland is typical maritime, cold temperate in the lowlands but can be categorised as sub-Arctic at higher altitudes in North Iceland. The mean lowland July temperature ranged between 7.7°C and

11.1°C between 1901 and 1990 while the mean lowland January temperature, usually the coldest month in Iceland, ranged between -2.0°C and 0.0°C during the same period. The temperature difference between the lowlands and the highlands for the period between 1936 - 1985 is rather small. The mean winter (January - March) temperature in the highlands is commonly between -3°C and -6°C and the mean summer (June - August) highland temperature is commonly 6°C to 9°C (Einarsson, 1991; Fig. 2.4).

The mean annual precipitation varies with altitude and latitude (Fig. 2.5). In all areas, precipitation is greater in the winter months (October - April) compared to the summertime (May - September) (Eythórsson and Sigtryggsson, 1971). Commonly, the mean annual precipitation in the southern lowlands is about 700 - 1600 mm but ranges between 400 and 700 mm in the northern lowlands (Einarsson, 1984). Mean annual precipitation on the accumulation areas of the ice caps in the southern and south eastern parts of the country (ca. >1100 m a.s.l.) can be more than 4000 mm (Sigfúsdóttir, 1975). Recent mass balance studies conducted on top of the Öræfajökull caldera, at ca. 1850 m a.s.l., indicate that the precipitation was as much as 6400 mm for the 1995 - 1996 accumulation season (Gudmundsson, pers. com). On the other hand, the precipitation in the lowlands at the southern foot of the mountain is about 1800 mm/a (Fagurhólsmýri) but on the south eastern side (Kvísker) it is about 3300 mm/a. The result is a very steep precipitation gradient to the north and north west, sometimes more than 2 mm/m in glaciated areas. Consequently, precipitation variations of the order of metres/100 m (vertical) can occur over a couple of kilometres distance (horizontal) in a single year. The reason is that the prevailing precipitation source is from the south and south east as the cyclone path travels along the south and south eastern coast of the island. The overall pattern and distribution of precipitation has great implications for glaciers in Iceland. Where high precipitation totals occur, as in south and south eastern Iceland, glaciers are likely to respond quickly to any precipitation change.

As can be seen above, glaciers in Iceland form because of low summer temperatures, high winter precipitation and elevated topography. Inferring climate change from glaciers involves measurements of the Equilibrium Line Altitude (ELA). According to Paterson (1994) the ELA is defined as the boundary between the accumulation area, where the net balance of the glacier is positive and ablation area where the net balance is negative on a yearly basis. Consequently, identification of the ELA is very important in mass balance studies of glaciers. Moreover, any oscillations of this line imply changes in the mass balance and variability in the local climate. In the mountain climate of Iceland the snow line (lowest limit to snow cover) at the end of the summer is a good approximation of the ELA (Paterson, 1994). The match between the snowline and ELA, however, can be imprecise because the summer snow melt can refreeze as superimposed ice, resulting in an ELA lower than the snowline.

Snowline is a useful feature since, despite imprecise relation to ELA, it can be inferred from maps, photographs and by observation, whereas ELA measurements have rarely been undertaken. The snowline in Iceland is very much dependent on the precipitation and is therefore very variable in different parts of the country (Fig. 2.6). Along the southern coast the snowline lies presently at about 1100 - 1300 m (Björnsson, 1979; Einarsson, 1994) but due to a heavy precipitation shadow, resulting from the Vatnajökull ice cap, the snowline just north of the ice cap is about 1700 m (Björnsson, 1979). This results in a relatively small ice cap on Mt. Snæfell (1833 m; Fig. 1.1) just north of Vatnajökull ice cap which, in a more maritime situation, would carry a larger ice field because of its high elevation. On Tröllaskagi in the extreme north of Iceland (Fig. 2.6) small corrie glaciers have formed. There the snowline lies at about 900 - 1000 m reflecting cold temperatures and heavy winter precipitation. In the north west of Iceland the snowlinefalls to about 550 - 600 m (Einarsson, 1994, Björnsson, 1979; Fig. 2.6). This variability of the snowline in Iceland implies great environmental sensitivity of the island to any changes in the climate, not only from north to south but also with altitude. It also implies a geographically diverse response to climate change.

Although glaciers in Iceland reflect and respond to the prevailing climate (cf. Björnsson, 1979; Jóhannesson *et al.*, 1989), the bigger ice caps exist above the snowline partly as a result of their own thickness. About 70% of Vatnajökull is above the regional snowline whereas a much a smaller part of the bedrock is above this height (Björnsson, 1988). In other words, a large ice cap like Vatnajökull might not form under contemporary climate forcing because of the low altitude of the bedrock in south Iceland. Such feedback mechanisms are important to recognise when climate is inferred from glacier fluctuations in Iceland.

2.2 The Öræfajökull Massif

The Öræfi district comprises the area between Skeiðarárjökull in the west and Breiðamerkurjökull in the east (Fig. 2.7). The dominating feature of the region is Öræfajökull (2119m), an active stratovolcano located outside the presently active volcanic zones of Iceland (Jakobsson, 1979; Fig. 2.2). Topographically, the volcano forms an extension of the Vatnajökull ice cap connected by a ridge 1352 m high. Commonly, the ice-capped volcano rises about 1700 m in about 10 km distance from the south to the caldera rim on top of the massif. From the foot of the mountain, at about 100 m a.s.l., an extensive sandur plain covers the area from the north west around the mountain towards the east (Fig. 2.7). This high topographic relief and southerly aspect creates an ideal situation for a growth of a climatically sensitive ice cap. The massif is presently capped by an ice field which nourishes eight well-constrained valley glaciers (Fig. 2.7).

The geology of Öræfi is a key factor in affecting the landscape and glaciation. The structural relations of the area around Öræfajökull are not well understood. Thórarinsson *et al.* (1973) discussed the tectonic relationship of the Vatnajökull area and came to the conclusion that a north west - south east trending structural feature immediately south west of Öræfajökull represents a left lateral transcurrent fault. Walker (1975) came to the conclusion that Öræfajökull reflects the southernmost active part of a largely dormant rift zone which can be traced through Mt. Snæfell (Fig. 2.1; 2.2). The Öræfajökull massif might therefore be situated at the intersection

of a fracture zone and a spreading axis, a structural position in which volcanic activity is often closely connected. This tectonic setting has important implications for the isostatic response of the landscape to glacier growth and decay.

The age of the volcano is important to determining the long-term volcanic and glacier history. The earliest studies of the geology of the mountain comes from Nielsen and Noe-Nygaard (1936) and Noe-Nygaard (1953) who suggested that the base of the massif is mostly of Pleistocene age. Later, Hospers (1953), Henson (1955) and Einarsson (1957) suggested that the lower part of Skaftafellsfjöll, just north west of the Öræfajökull massif, was of Tertiary age. They concluded that the normally magnetised rocks of the Öræfajökull massif should all be of Pleistocene age and probably younger than the Gunz-Mindel interglacial. The central part of the Öræfi district is dominated by various rocks discharged from the still active Öræfajökull central volcano (Prestvik, 1979). The peripheral areas, Skaftafellsfjöll in the west and Breiðamerkurfjall in the east, are made up of basic and silicic rocks below an unconformity, indicating that both these areas belong to older central volcanoes. The abundance of hyaloclistites and tillites within the piles of these older volcanic rocks and their relationship to the presently active volcano indicates that those volcanoes were active during the Quaternary. Thórarinsson (1963) came to the conclusion that the fossiliferous lacustrine Svínafell layers at the base of Öræfajökull massif were deposited during the Mindel-Riss interglacial period. Albertsson (1976) concluded that the lacustrine Svínafell layers were deposited at any time between post-Jaramillo (ca. 0.89 Ma) and the beginning of the Elster glaciation (ca. 0.60 Ma). The hyaloclastites deposited between the Svínafell sediments and the overlying dated lavas probably formed during the Elster glacial period, indicating that the Öræfajökull massif has been active for more than 0.5 Ma (and the base for the presently active centre should be found in the late Matuyama or early Bruhnes). Assuming that a central volcano in Iceland normally has an active record of about 0.5 - 1.0 Ma (Piper, 1971), then Öræfajökull might be nearing its end.

A recent study by Helgason and Duncan (1996) indicates a slightly different age for the lacustrine Svínafell layers and therefore the Öræfajökull massif. The Svínafell strata have been divided into 19 units containing lavas, sedimentary deposits and pillow lavas. Furthermore, the units have been separated into 6 glacials and 7 interglacials based on stratigraphical mapping, rock magnetism and absolute dating. Measurements of rock magnetism of lavas under and above the lacustrine Svínafell layers revealed an age between 1.65 Ma and 0.78 Ma. On the basis of stratigraphical correlation and K-Ar dating in Mt. Hafrafell, the youngest lava formation in Mt. Svínafell is 215 ka years old.

The implications of this considerable age is that the present valleys, through which the outlets flow, may be pre-Weichselian in age. This also means that the age of the caldera is at least of equal age. Consequently, the development of the contemporary subglacial landscape has probably gone through several changes over the same time period. These changes might occur very abruptly when volcanic eruptions take place. For example, the caldera rim might be breached in a new location or even an old gap filled in. This might affect the glacier behaviour in such a way that an advance could be inhibited or temporarily exaggerated while a new equilibrium is reached.

The Öræfajökull massif has erupted twice since the Settlement of Iceland, i.e. 1362 AD and 1727 AD (Thórarinsson, 1958). These eruptions were hydromagmatic (phreatic) eruptions with high production of tephra causing devastating Jökulhlaups (glacier meltwater bursts) onto the sandur plain in the south. Thórarinsson (1958) identified two pre-Settlement eruptions from Öræfajökull ($Ö_2$ and $Ö_3$) but the precise age of these eruptions is not known. The 1362 AD eruption has successfully been used as tephra isochrone in south eastern Iceland and has recently been identified in Greenland ice cores (Palais, *et al.*, 1991), underlining the continental-scale dispersion of the tephra grains. Thus, the potential for using tephra from Öræfajökull and other major volcanic centres in Iceland as isochrones for the study of glacier fluctuations in the region is high.

2.3 Previous glacial geomorphological studies of the Öræfi district and limits to knowledge

Ives and King (1954, 1955), King and Ives (1955) and Ives (1956) have studied the historical glacier fluctuations and recent mass balance of Morsárjökull (Fig. 2.7). Ives and King (1954) came to the conclusion that the conspicuous alternating light and dark ogive banding, found on the glacier surface, reflected the annual movement of the glacier. Ives and King (1955) and King and Ives (1955) described the budget and flow of the glacier for three consecutive seasons 1951-52, 1952-53 and 1953-54. Their results indicated that a close correlation occurred between ice flow and weather conditions over the given period. Additionally, there was evidence for rapid retreat of about 1 km and thinning of the glacier from 1904 to the mid-1950s. Further, they noted that remains of a moraine near Bæjarstaðarskógur indicated a possible late glacial extension of Morsárjökull and suggests the line along which this glacier may have been in contact with Skeiðarárjökull.

Ives (1956, 1991, 1996), Ives and King (1955), Thompson and Jones (1986) and Thompson (1988) described the historical glacial geomorphology and landform development of the proglacial zone of Skaftafellsjökull (Fig. 2.7). These studies concluded that Skaftafellsjökull retreated about 2 km from the outermost moraine on the outwash plain dated to the late 19th Century. Thompson (1988) argued for a rapid retreat from an extensive area of subglacial ground moraine between the outermost extension and the early 1980s position of the glacier. The ground moraine is moulded by minor oscillations of the retreating ice front into a series of low concentric ridges. Eyles (1978, 1979, 1983) described the processes responsible for the moraine formation during the historical retreat of the glacier. Pushing and squeezing mechanisms were responsible for producing series of well defined ridges of low relief, diversified by numerous small proglacial lakes. This was explained by the nature of Skaftafellsjökull landsystem, reflecting the transitional form of the glacier as a piedmont outlet, with a relatively limited supply of englacial and supraglacial debris. Douglas and Harrison (1996) investigated turf-banked terraces in Gimludalur north of Skaftafellsheiði and on Illuklettur in Hafrafell. They concluded that these features

were formed above the Neoglacial trimlines of the Öræfi region under a variety of different environmental controls including aspect, slope angle and altitude. At Gimludalur corrie, to the north of Skaftafellsheiði, over 1000 individual terraces can be found in the area extending from about 450 - 650 m a.s.l. Similar to Gimludalur over 100 individual turf-banked terraces could be located on platforms cut into the Illuklettur spur extending from 300 - 370 m a.s.l.

Thórarinsson (1956) determined the age of Stóralda moraine in front of Svínafellsjökull outlet glacier using tephrochronology (Fig. 2.7). His results indicated that the moraine predates the 1362 AD tephra found on top of it. He went on to suggest a Subatlantic age as knowledge of the Holocene climate change in the late 1950s suggested that this was the coldest period since the last Glaciation. Thompson and Jones (1986) studied the timing of proglacial river terrace formation in front of Svínafellsjökull, using lichenometry, and concluded that the timing and rates of down cutting have been closely related to frontal movements of the Svínafellsjökull glacier over the last century. Thompson (1988) concluded that, in contrast to Skaftafellsjökull, alternate episodes of slow retreat and readvance of Svínafellsjökull produced a more complex and higher series of push moraines. He inferred the mode of moraine formation to be repeated 'bulldozing' of sediment released by ablation at the glacier snout as oppose to the combination of pushing and squeezing mechanism operating in front of Skaftafellsjökull. It is inferred here that this might be the same process. Pushing and squeezing could be understood as 'bulldozing' because there is no apparent difference in the mode of formation. Douglas and Harrison (1996) investigated small-scale turf-banked terraces of Svínafellsheiði to the east of Svínafellsjökull and on Illuklettur spur of Mt. Hafrafell (Fig. 2.7). These solifluction type terraces were prominent above 500 m a.s.l on Svínafellsheiði implying that glacier did not occupy surfaces above this height in the Holocene.

The fluctuations of the Virkisjökull outlet glacier have not been studied in detail (Fig. 2.7). Eyles (1978), however, conducted studies on the origin of the moraines deposited during the last decade of the 19th Century. According to his study, these

moraines were mainly superimposed push ridges, or composite push ridges and consisted of supraglacial morainic till. They were defined by inner enclosed basins in which ice-cored supraglacial morainic till survived. Eyles (1978) further defined the type of the supraglacial morainic till as being of 'facies 1' which occurred where supraglacial morainic till slowed the rate of ice melt such that till was slowly superimposed on the subglacial surface in the form of stagnation or disintegration topography. Thórarinsson (1958) has described in detail the eruption of Öræfajökull in 1362 AD and to a lesser extent, the eruption of 1727 AD. He mapped the routes of the consequent jökulhlaups (glacier bursts) and concluded that Virkisjökull was one of the main pathways for both of the jökulhlaups. The chemical composition of the 1362 AD tephra is more silicic compared with the 1727 AD tephra. This results in a colour difference of the two deposits; the matrix of the 1362 AD jökulhlaup is light coloured or white as a result of its silicic composition, but the matrix of the 1727 AD jökulhlaup is black because of the more basic nature of the tephra. Thórarinsson also stated that the 1362 AD deposit contains more fine tephra compared with the coarse grained pumice of the 1727 material. Thórarinsson (1958) has given an account of the 1727 jökulhlaup deposits in front of Kotárjökull. He mainly described the flood as it rushed forward according to eye witness accounts from the description of Rev. Jón Thorláksson written half a century after the eruption. Thórarinsson (1958, p 31-33) used the English translation from Henderson (1818) of Thorláksson's report. To summarise, Rev. Thorláksson wrote how the glacier rushed forward and left the proglacial zone covered with ice blocks, rocks, pumice and ash which could not be travelled over many years after the eruption. The eastern part of the area is still called Svartijökull (Black glacier) due to the black jökulhlaup deposits. Thompson and Jones (1986) studied the rates and causes of the terraces in front of Kotárjökull. They concluded, on the basis of overall geomorphic evidence, that these terraces were formed by the recent downcutting of the major meltwater streams. The Kotá terraces, in contrast to Svínafellsá terraces in front of Svínafellsjökull, have been formed independently of glacier fluctuations and are thought to represent stages in the gradual recovery of the stream from the aggregation effects of the 1727 jökulhlaup. During 257 years of river incision, eight terraces have been formed. More recent, but

unpublished, work on the 1996 jökulhlaup from Skeiðarárjökull suggests that flood terraces, resulting from a jökulhlaup, are formed during the waning stage of the original flood.

Thórarinsson (1956) studied the recent fluctuations of Kviárjökull outlet. His results indicated that the big moraine amphitheatre, called Kambsmýrarkambur (right lateral) and Kviármýrarkambur (left lateral) (Fig. 2.7), was of Subatlantic age as determined by tephrochronology and the knowledge of the climate history in the late 1950s. He also concluded from documentary sources that the maximum advance during the LIA was in the 1870s. Thórarinsson (1956) made an attempt to explain why the outlets of the Vatnajökull ice cap did not advance in the early Subatlantic time as far as the outlets of Öræfajökull. One explanation was that at the end of the Postglacial Warm period (presumably before the Subatlantic period) Vatnajökull ice cap was reduced by a much more substantive area than the higher and more alpine Öræfajökull. The rise of the ELA during the Early Holocene Warm Period had a bigger impact on the big Vatnajökull outlets with their relatively flat accumulation areas than on the steep alpine Öræfajökull outlets. Black (1990) studied the late Holocene glacial chronology of Kviárjökull. He identified three main periods of Holocene advance using tephrochronology and lichenometry. A Subatlantic moraine complex was identified and with the aid of a single radiocarbon date it was constrained to 2040±80 BP years (GX-15181). A period of pre-settlement advance deposited Kviármýrarkambur and Kambsmýrarkambur which, according to soil accumulation depicted from tephras of known age, was dated to 728±395 AD years. The third advance was the LIA maximum dated to the early 1870s by lichenometry, but other dates were deduced by using tephrochronology and radiocarbon dating. Björnsson (1993) concluded that the present valley in which Kviárjökull is flowing was initially a volcanic fissure which the glacier used as a pathway when it later grew in response to climatic change sometime during the Holocene. He stated the origin of the lava flows was a volcanic cone, located where the present Kviárjökull bed is today, which was subsequently blasted away by the last eruption of the cone during the end of the last Termination. The

explosive activity was due to water flowing over the vent as a consequence of the sea level being higher than at present.

Figures 2.8, 2.9, 2.10, 2.11, 2.12 and 2.13 are photographs of the study area showing various outlet glaciers and their proglacial areas.

Part B Methods

In this research, geomorphological mapping was used to pinpoint various glacial depositional and erosional features associated with glacier fluctuations. Tephrochronology, lichenometry and radiocarbon dating were applied to date landforms. In addition, where appropriate, annals and written sources were employed to offer complementary dating of historical glacier positions.

2.4 Geomorphological mapping, aerial photos and field work

Mapping of glacial features as observed on aerial photos was carried out with the aid of a handheld non-zooming stereoscope. The original mapping scale was 1:36000, but, to enhance details, the original photos were enlarged to approximately 1:25000, thus allowing features of about 10 m in diameter to be observed. The final stage in the mapping process was to test and check the mapping with fieldwork. Fieldwork involved logging profiles, sampling sediments for further analysis in the laboratory, such as sieving and measurements of roundness and finally, measurements of the spatial extent and relationship of glacial features. The final step was to construct a series of 1:25.000 geomorphological maps, in digital form, and link them to environmental processes. Macdraw Pro, a drawing program for Macintosh personal computer, was used to draw the maps.

The six outlet glaciers were selected on the basis of the abundant glacial geomorphological features located in their proglacial areas. Therefore, the best record of any changes in the position of the ice would be found in front of the selected outlets.

The identification criteria of each landform and processes for the geomorphologic mapping are shown in Table 2.1. The criteria are adopted from Goudie (1981), Small and Witherick (1986), Sugden and John (1988), Greene (1995) and Bentley (1996). The table shows the landforms distinguished in the Öræfi district and defines the key to identification, process and depositional environment. The symbols for the superficial deposits on the geomorphologic maps were adopted from a standard used by the National Energy Authority in Iceland (Kaldal and Víkingsson, 1995).

2.5 Tephrochronology

Thórarinsson (1981) has written an historical review of the studies of ash fall deposits in Iceland. He points out that the knowledge goes far back in Icelandic history. Fourteenth Century chroniclers already recognised the difference between three types of airborne volcanic deposits, namely pumice, sand and ash. Detailed accounts of the ash fall were written for all major Icelandic eruptions. Thórarinsson (1944) acknowledged the fact that a collective scientific term was needed to define ash fall deposits. In the mid 1940s the modern term *tephra* was suggested by Thórarinsson (op. cit.) as a collective term for all pyroclasts, and consequently the term *tephrochronology* describes the dating method based on the tephra layers. After defining the terms he used the tephras, tephrochronology and soil erosion to date the abandonment of settlements in Thjórsárdalur valley in south Iceland.

Tephrochronology is well established but not widely used. This is mainly because the availability of tephra layers is scarce. The complex and active volcanism of Iceland, however, makes it possible to use tephras to aid the study of environmental change. Furthermore, the geochemical fingerprinting of each tephra layer makes it possible to trace the origin of each ash layer by relating it to a distinct volcanic system. The chronology of tephra deposits in Iceland is relatively well known, with a few exceptions such as in the Öræfi region. This means that dating environmental change becomes possible by using layers of volcanic ash, which form widespread chronostratigraphic marker horizons, or tephra *isochrones*. The implication is that a detailed environmental history dated with tephras is possible over an extended time

scale. Since tephra grains can travel great distances the tephrochronology can be applied not only in Iceland but also in Europe (e.g. Dugmore *et al.*, 1995a).

The first direct mention of tephra fall in Icelandic annals refers to the Hekla eruption in 1104. Both Annales regii and Lögmannsannáll, written in the 13th and 14th Century respectively, have entries of a volcanic eruption in the winter of 1104/1105. Over the succeeding centuries volcanic eruptions are often mentioned in the annals and sometimes in great detail. Several contemporary annals, such as Skálholtsannáll, Gottskálksanáll, Flateyjarbók and Lögmannsannáll, mention the 1362 AD and 1727 AD eruptions of Öræfajökull and describe the vast devastation following the ash fall and jökulhlaups. They are therefore an important source in identifying the age of historical tephra layers and have been used for that purpose by various authors (e.g. Thórarinsson, 1944; 1958; 1967; Larsen, 1978).

Tephrochronological studies conducted over the period between 1940 and 1975 were mostly based on field studies, combined with investigations of written sources in order to trace a tephra's origin and the year of eruption. Little chemical work was done, although not completely ignored (e.g. Thórarinsson, 1958), mainly because of the lack of suitable techniques to carry out the analysis. According to Larsen (1981), the stratigraphic location, thickness and grain size variations of individual tephra layers was, up to the late 1970s, considered sufficient to relate the source of tephra and establish a dispersal pattern in proximal areas. In distal areas, however, this was sometimes problematic due to the thinness of the tephra layers which also inhibited bulk chemical analysis.

This perspective changed with new techniques developed to analyse very small minerals in rocks. This led to the identification of the 29 individual volcanic systems each having a distinct chemical fingerprinting (Jakobsson, 1979). Subsequently, various authors began to point out the need for rigorous chemical work in order to determine the correct origin (Imsland, 1978; Jakobsson, 1979). In the early 1980s, Larsen (1981) developed a new method to analyse the distal tephra by using electron

probe micro analysis (EPMA). The advantage of the EPMA technique is the small sample size, rapidity of the method and the favourable cost/efficiency ratio (Larsen, 1981). The EPMA can be used to analyse volcanic glass and minerals separately and the grains need only to be >30 microns in diameter for effective work. This means that very thin tephra layers can be analysed, and problems of contamination/heterogeneous samples that limit bulk analysis, can be avoided.

There are some limitations to the use of chemical 'fingerprinting' of tephras. Some overlap occurs between both systems and some individual eruptions, analytical techniques can vary and the tephra can undergo post-depositional modifications of the geochemical composition due to weathering. There is a substantial literature available on the weathering of tephra in a different range of environments which indicates that such processes occur (Lowe, 1986). Further complications could be introduced by the techniques used to isolate tephra grain samples from the enclosing material, for example peat, using acid digestion. However, Dugmore *et al.* (1992) have shown that fine-grained silicic tephras from Iceland can retain their overall chemical integrity on at least a four millennial time-scale and that the exposure to acid conditions does not significantly bias the results of major element analysis by EPMA. In other words, biases due to weathering and sample preparation of Holocene tephra grains in Iceland can be eluded. This means that using EPMA technique is a valid method of analysing and correlating tephra horizons in Iceland. However, the problem of equifinality can occur because the Holocene is a limited time period. Volcanoes are of different ages/stage of development but all systems tend towards the same end-point. Where exactly each volcanic system is located in the development in space and time is not known which underlines that caution is needed when tephras are correlated, especially the older layers.

In this study, soil sections were measured at a sub-centimetre scale in the field. Each tephra layer in the section was described in terms of depth, grain size and colour. All silicic and basaltic tephras of possible chronostratigraphical importance were sampled and prepared for the EPMA in the tephra laboratory in the department of Geography

using the technique suggested by Dugmore *et al.* (1992; 1995a). Tephra grains were then analysed in the Cambridge Instrument Microscan V at the Grant Institute of Geology and Geophysics, the University of Edinburgh. A standard WDS (wavelength dispersive) technique was used with an accelerating voltage of 20 kV and a beam current of 15 nA, as measured across a Faraday cup. Nine major elements were analysed using two spectrometers and involved a counting time of 10 seconds for each element. The Cambridge Instrument Microscan V was calibrated using standards of known composition, involving a mixture of pure metals and simple silica compounds. Counter dead time, fluorescence and atomic number effects were corrected using a ZAF correction programme (Sweatman and Long, 1969). At regular periods throughout the analytical session an andradite standard of known composition was analysed to guard against unexpected variation in machine operating condition.

The terminology of igneous petrology used in this thesis is based on recommendations of Le Maitre (1989). The description of the general composition of the glass is termed basic (45 - 52% SiO_2) and intermediate (52 - 63% SiO_2) and silicic (>63% SiO_2). Dugmore *et al.* (1992) have suggested the use of the term 'silicic' for 'acid' to avoid confusion with volcanic aerosols ('acid' layers) in ice cores (Hammer, 1984). The same usage will be adopted in this thesis.

The selection of sites for tephrochronology was not systematic. It was based on finding the best sedimentary traps between moraines. A more detailed criteria can be found in section 5.2. In all 120 profiles were dug but 88 profiles were used to compile the final tephrostratigraphy. The failure rate was therefore 27% meaning that one of every three profiles was not used.

2.6 Lichenometry

Lichenometry was used to date the Little Ice Age (LIA) advances in the research area. The largest inscribed circle of the lichen *Rhizocarpon geographicum* aggr. was measured on each substrate as suggested by Innes (1985). The mean of the 5 largest

lichens on each substrate was calculated. A mean growth curve for the research area (Gudmundsson, 1992) was used to infer the relative age of individual moraines. Limitations of the method in general have been described by Innes (1985) and in Iceland by Gudmundsson (1992).

One key limitation to the accuracy of lichenometry in Iceland depends on the number and age ranges of lichens used in the growth curve. The importance of using error bars on the inferred dates has been reported by Gudmundsson (1992). The method seems to be valid in Iceland to date surfaces as old as the mid 19th Century (Gudmundsson, 1992, 1997). However, unknown environmental factors seem to inhibit the lichen growth in Iceland for earlier dates (Caseldine and Baker, 1998). It has to be emphasised that lichenometry is a relative dating method and gives a close (±10 years) estimation of the true age of the exposure/formation of the landform. Errors increase when dating older features close to the maximum limit (150-160 years).

2.7 Soil or aeolian sediment accumulation rates

Aeolian sediment or soil accumulation rates during the Holocene are the principal dating method in this study. The method is based on estimating rates of soil accumulation between two stratigraphically distinct marker horizons of known age. This is done by measuring the distance in millimetres between the two marker horizons. Numbers of similar profiles are used to generate typical rates for certain soil types. However, local rates are recognised and applied if the profile shows unusual variability from other profiles. This estimated rate is then used to extrapolate or interpolate dates of unknown stratigraphical horizons. This method has been widely used in Iceland to date environmental change (Thórarinsson, 1961; Dugmore, 1987 and Dugmore and Erskine, 1994) and is considered reliable if the reference marker horizons are well dated with widely recognised methods (Dugmore, 1987).

2.8 Radiocarbon dating

Radiocarbon dating is limited to areas with organic material and was used to date tephras and other important stratigraphic markers. Four ^{14}C dates were obtained in front of Kviárjökull and analysed by the Scottish Universities Research and Reactor Centre (SURRC) in East Kilbride, Scotland, supervised by Dr Gordon T. Cook. The dates are quoted in conventional years BP (before 1950 AD) and the errors are expressed at the one sigma level of confidence.

Radiocarbon dating was used to date the maximum age of the tephras. Only one tephra was dated with the aid of ^{14}C because of the lack of organic material in the study area. Other important tephras detected had already been dated elsewhere in Iceland with ^{14}C, for example the Hekla-4 tephra. Here, the same method was used, i.e. the maximum date was obtained for Hekla-4 (Dugmore *et al.*, 1992). The method adopted in this study is further explained in section 4.2.

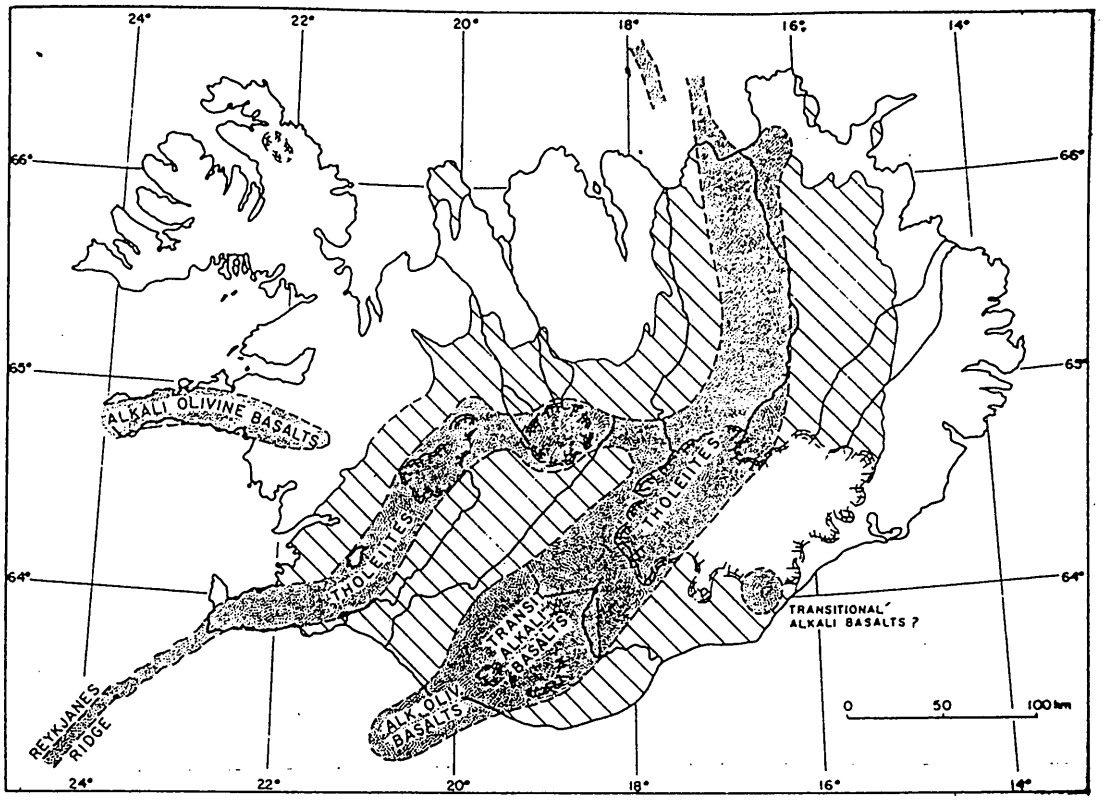

Fig. 2.1. The bedrock of Iceland. Postglacial petrological zones (shaded), Plio-Pleistocene formations (oblique lines) and Tertiary formations (white). From Jakobsson (1979).

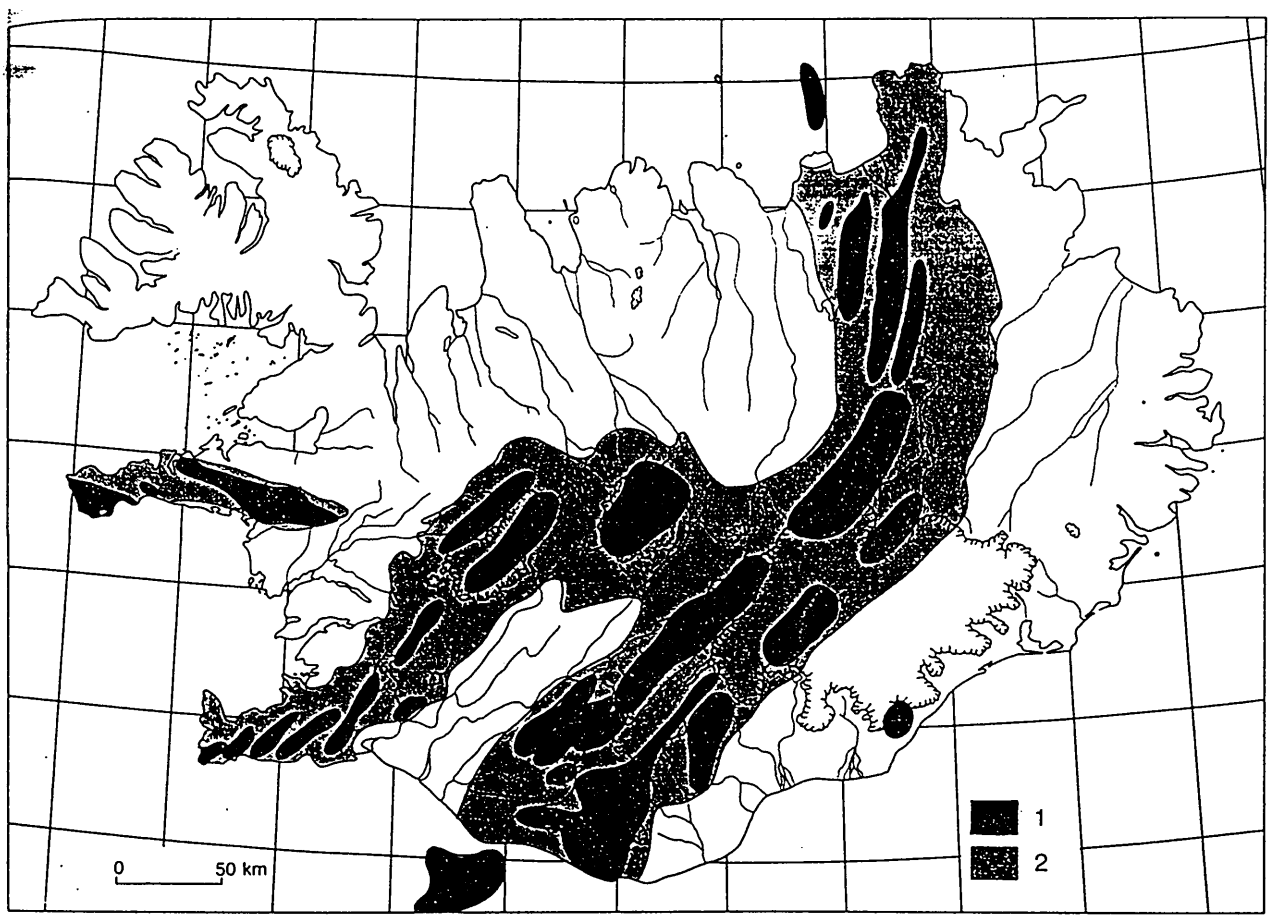

Fig. 2.2. Active volcanic systems in Iceland. Symbols: 1) individual volcanic systems and 2) active volcanic zones. From Jakobsson (1979).

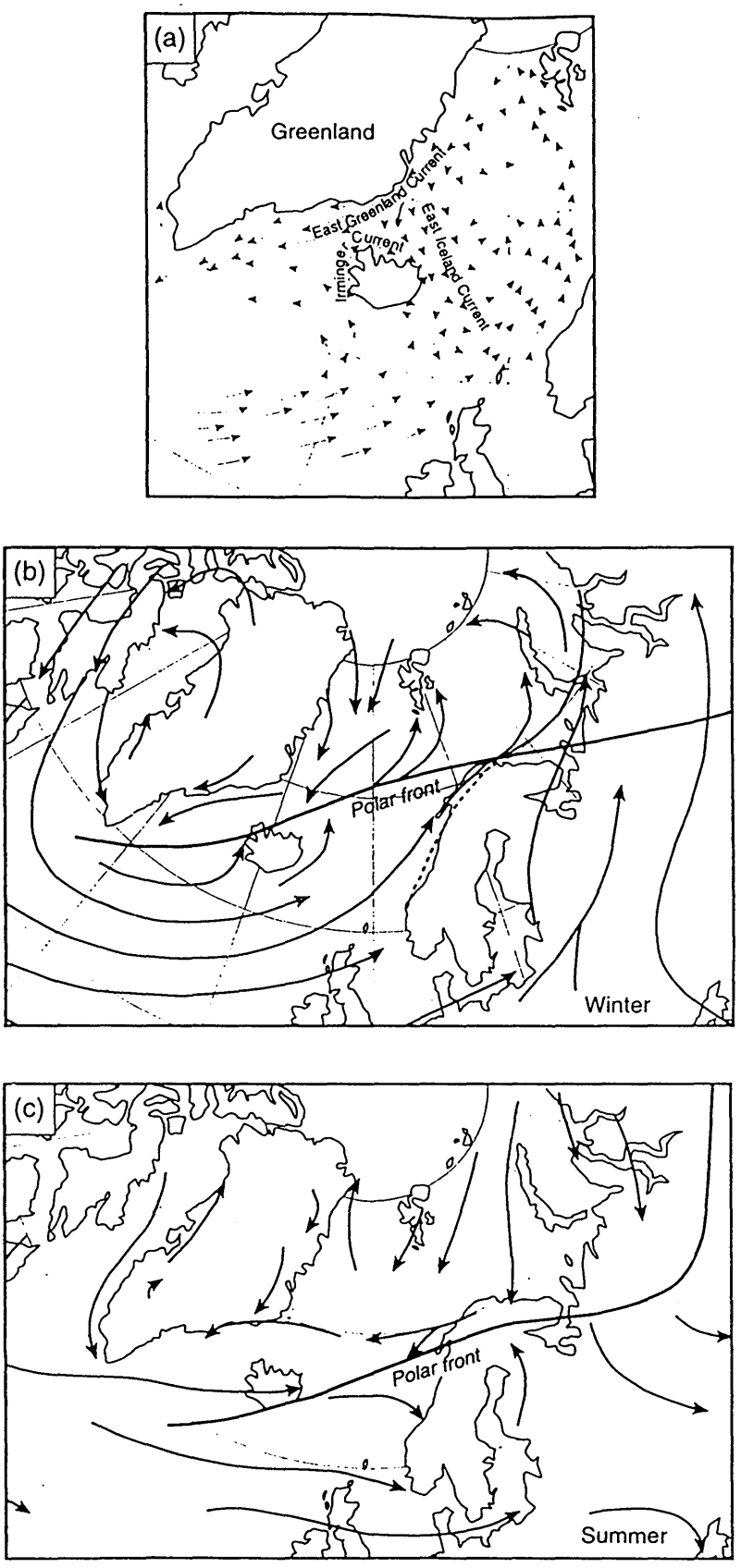

Fig. 2.3. Sea currents showing convergence of the warm Gulf Stream and cold Polar water around Iceland (a). Principal frontal zones (b) in winter and (c) in summer and the mean wind flow. From Meteorological Office (1963).

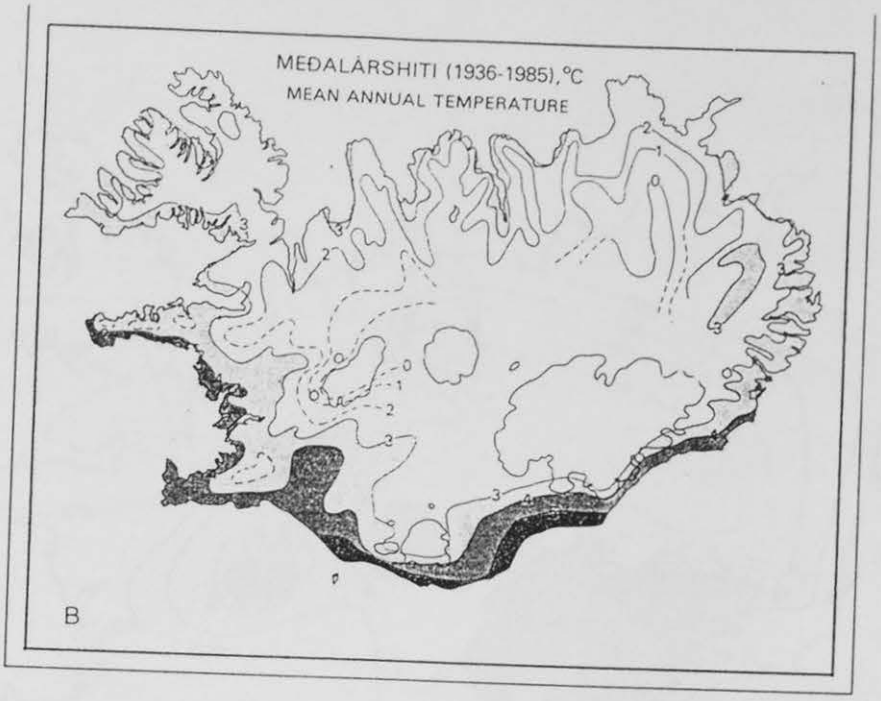

Fig. 2.4. Mean annual temperature in Iceland. From the Icelandic Meteorological Office in Einarsson (1994).

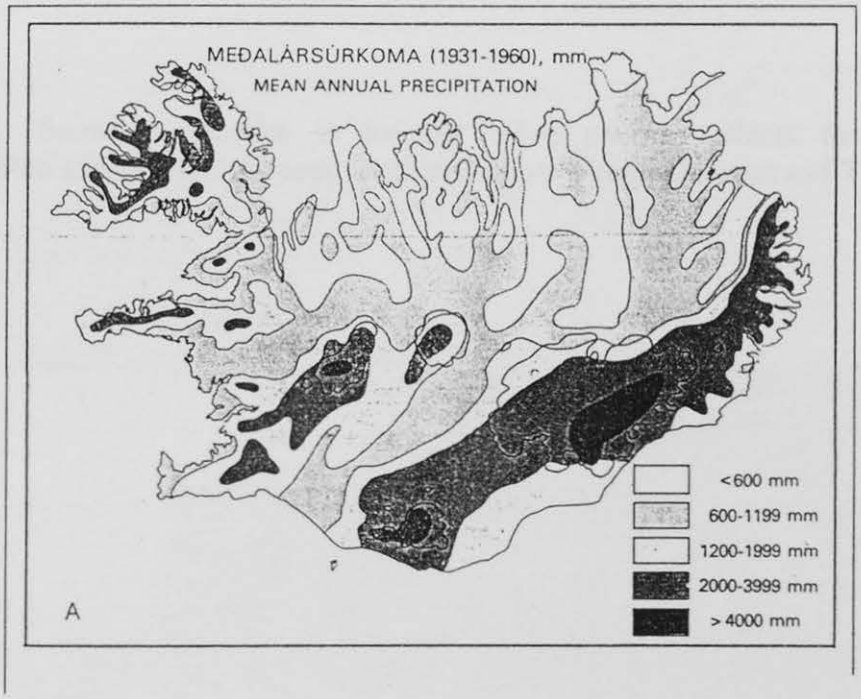

Fig. 2.5. Mean annual precipitation in Iceland. From the Icelandic Meteorological Office in Einarsson (1994).

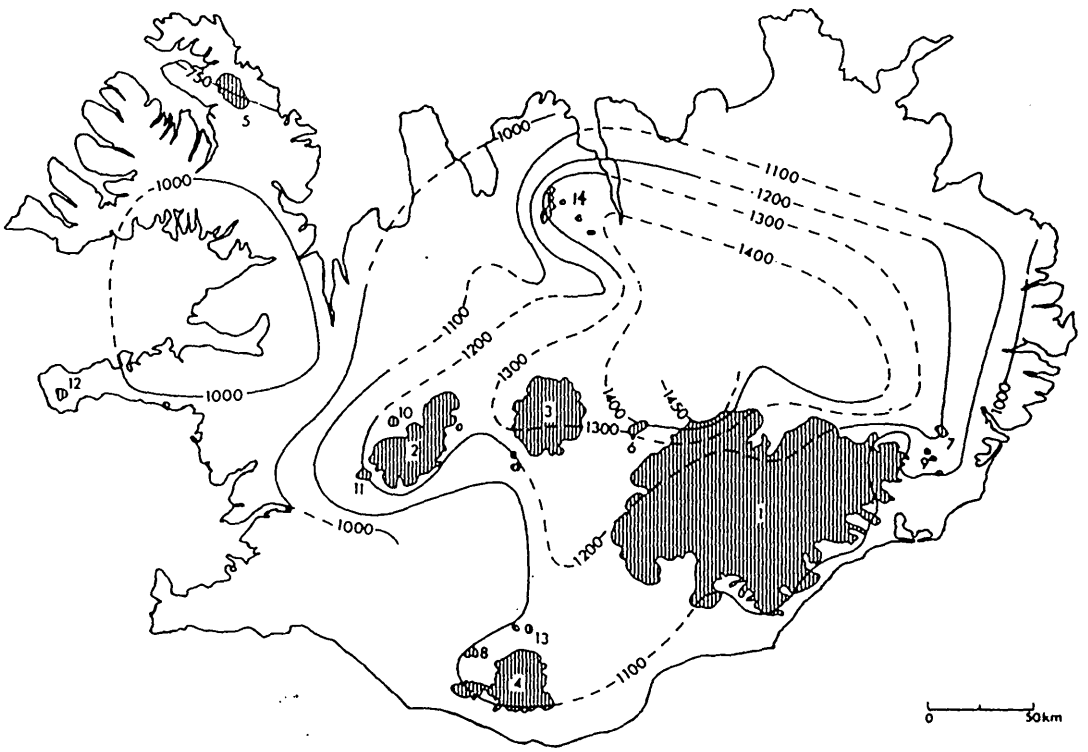

Fig. 2.6. Snowline altitudes in Iceland. The pattern reflects the prevailing precipitation source from the south east in Iceland. From Ahlmann and Thórarinsson (1937).

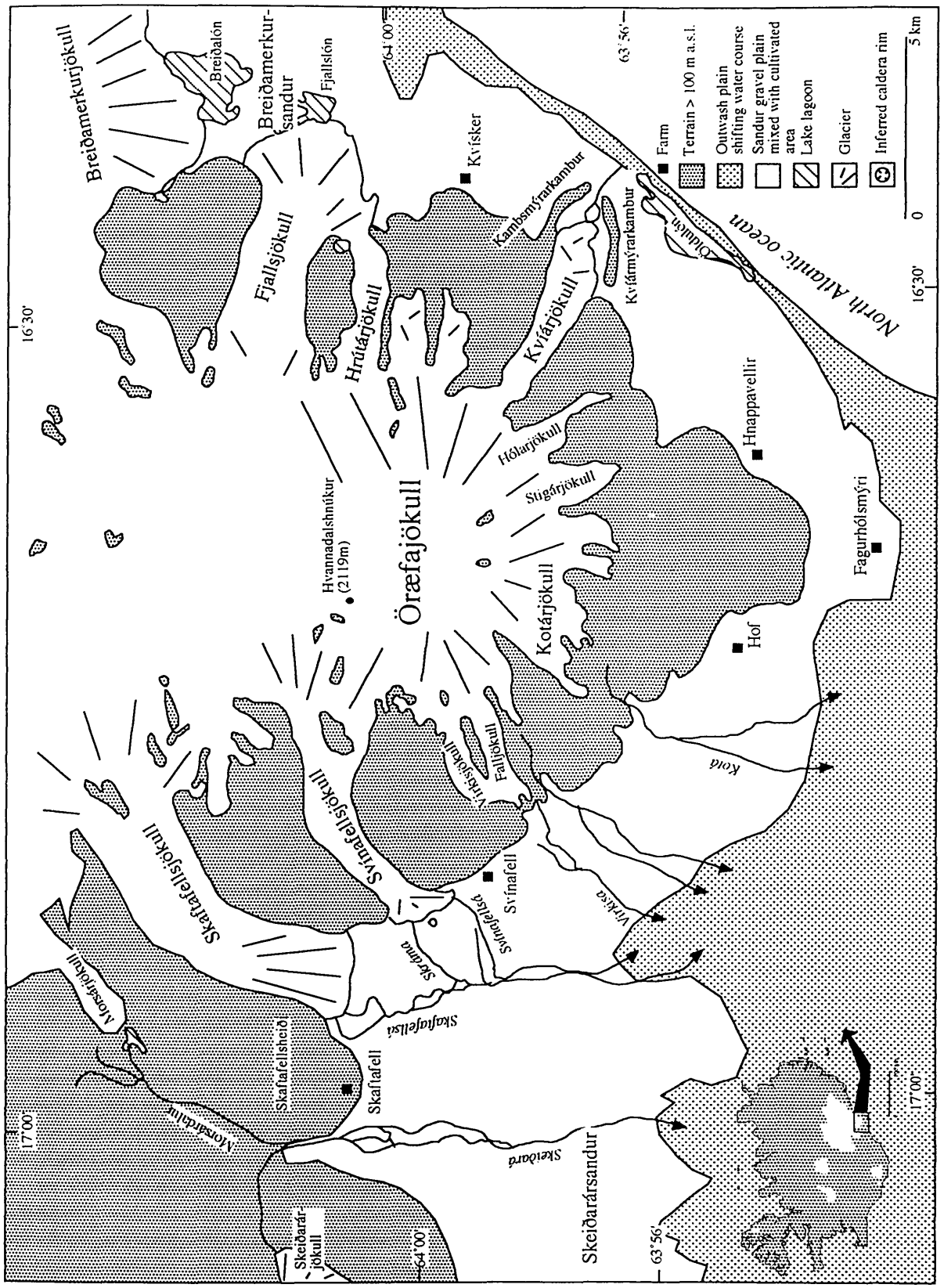

Fig. 2.7. The Öræfi district, SE Iceland. The map shows the macro-geomorphology of the region and important names mentioned in the thesis.

Fig. 2.8. Morsárdalur and Morsárjökull in the background. Note the medial moraine on top if the ice. The view is towards north. The snow-covered mountains on the left are Skaftafellsfjöll.

Fig. 2.9. Skaftafellsheiði in the background viewed from east to west. Skaftafelljökull is on the right. Kristínartindar peaks are in the far background on the right.

Fig. 2.10. A view from Skaftafellsheiði towards the east. The proglacier areas of Skaftafellsjökull (left foreground) and Svínafellsjökull (left background) are clearly shown. The southern part of Svínafellsheiði and Svínafellsfjöll mountains can be seen in the far left corner.

Fig. 2.11. The proglacier area of Virkisjökull viewed towards north east. Rauðikambur nunatak divides the two ice streams. Note the bulk sediment accumulation in the snout area.

Fig. 2.12. The proglacier area of Kotárjökull viewed towards north east. Note the jökulhlaup deposit in area and the white tephra from the Ö1362 eruption of Öræfajökull in the highlands.

Fig. 2.13. Kviármýrarkambur viewed towards east. The big moraine is in the background. Note the lava margin in the centre of the photo and the moraines on top of it. The Stórugrjót jökulhlaup is in the foreground.

Landform	Characteristics	Orientation in terms of ice flow		Link with the glacier			Environmental condition surrounding the formation				
		Parallel	Transverse	Ice-contact	Marginal	Proglacial	Subglacial	Marginal	Supraglacial	Glacio-fluv.	Glacio-lac.
Medial moraines	Usually angular matrix supported material, found commonly in throughput situation often on moving ice surface. Source is usually upland spurs	●							●		
Lateral moraines	Usually angular matrix supported material. Source is valley sides where it falls onto the glacier flanks.	●		●	●			●			
Terminal moraines	Usually angular matrix supported material. Variable origin, usually push or recessional in terms of ice movements		●	●	●			●			
Sandur plain	Outwash deposit usually sand and gravel of various grain size.					●				●	
Striation	Abrasion of becrock by debris in the basal layer of a glacier.	●					●				
Trimlines	Erosional or depositional former limit of a glacier on valley sides.	●			●			●			
Jökulhlaup	Volcanically induced glacier meltwater burst.					●	●				
Meltwater channels	Ravines cut by glacial meltwater.	●			●	●	●	●	●	●	
Dead ice landscape	Hummocky landscape formed by melting unactive glacier. Similar material as in moraines.					●		●	●		
Boulders	A rock fragment which has been transported by a glacier over a substantial distance.					●			●		
Glacio-lacustrine sediments	Silt/clay deposited by suspension in a glacially fed lagoon.				●	●		●			●

Table 2.1. Classification and criteria used in the geomorphological mapping. Landforms identified in the Öræfi district are exclusively categorised. For references see text.

Chapter 3. The Geomorphology of the Öræfi district

3.1 Introduction

The aim of this chapter is to describe and interpret the geomorphology of the study area with special emphasis on glacial landforms and features associated with volcanic eruptions. The goal is to define ice limits from the geomorphic evidence in order to determine Holocene fluctuations from the extent of different outlet glaciers.

The Öræfi region has experienced extensive Holocene environmental change. The rapidly changing geomorphology is directly linked with the presence of glaciers, an active stratovolcano and cool temperate maritime climate. The geomorphology of Öræfi has been investigated by Ives (1956, 1991, 1996), Ives and King (1954, 1955), King and Ives (1955), Thórarinsson (1956, 1957, 1958), Eyles (1978, 1979, 1983) Thompson and Jones (1986), Thompson (1988), Black (1990) and Douglas and Harrison (1996). These studies involve the description and interpretation of late-Holocene and historical glacier fluctuations, permafrost, jökulhlaups, volcanoes and climatic change. Each investigation is limited to either a single outlet glacier or limited time span and there is no overall view of the geomorphology in the region. They do, however, provide a thorough set of case studies for a regional synthesis.

This chapter describes the geomorphology of four outlet glaciers of the Öræfajökull ice cap, namely Svínafellsjökull, Virkisjökull, Kotárjökull and Kviárjökull. Additionally, Morsárjökull and Skaftafellsjökull which are two adjacent outlets of the Vatnajökull ice cap, were studied for comparison (Fig. 3.1). Each geomorphic entity, or map, will be discussed separately with specific relevant geomorphic features, such as moraines and meltwater channels. Landforms will be put in a local and regional context, where appropriate, in an interpretation of the geomorphic results at the end of section. At the end of the chapter the general results will be discussed.

The geomorphological criteria used in the study have been reported in Table 2.1 (Chapter 2). They are based on morphology, glacier-landform relationships and materials.

Each geomorphic map has the same legends based on Kaldal and Víkingsson (1995). Many of the symbols have been modified and changed in order to maintain consistency of the maps and to improve the visual cartographic presentation. The legends for all geomorphologic maps are shown in Fig. 3.2.

3.2 Morsárjökull

3.2.1 General Description

Morsárjökull is a 4 km long valley glacier flowing SSW from the southern part of Vatnajökull ice cap (Fig. 3.1). It drains about 27 km^2 of the ice cap according to maps of supraglacial ice topography (Fig. 3.3) and terminates on a sandur outwash plain nearly 200 m a.s.l. The glacier is divided into two parts by a conspicuous medial moraine originated from a rock wall exposed at its head. The two sections are called the Northwest and Southeast streams (Ives and King, 1954). The north west stream is fed by an ice fall descending about 400 m in a horizontal distance of 500 m while the south east stream is supplied by an ice fall descending about 400 m over a horizontal distance of 700 m. The latter has not been connected to the main ice stream since 1937-38 according to Ives and King (1955) and instead it has been fed by avalanches from the main ice cap. Further down, the two ice streams converge to form a single valley glacier. This can be inferred from the pattern of crevasses and the comparable numbers of ogives on both sides of the medial moraine.

3.2.2 The Moraines

There are two sets of arcuate terminal moraines about 1 km from the glacier where Morsárdalur valley meets its tributary Kjós (Fig. 3.4). In the south they can be divided into three moraine clusters I, II and III (Fig. 3.5). Kjósarlækur flows between moraine clusters I and II. The outermost moraine of unit I extends ca. 1.2 km from the 1990 position of the glacier (Fig. 3.4). The moraine ridges are usually ca. 1-3 m

high from base to crest and typically about 7-10 m apart. A total of 11 crests can be found reflecting the history of glacier retreat (Fig. 3.5). The moraines mainly consist of basaltic material with odd hyaloclastic boulders on top of finer matrix. The moraine material has a typical bimodal grain size distribution with a matrix of medium sand and boulders up to a few meters in diameter. The cobbles and boulders are usually subangular.

At the foot of Mt. Háls, three prominent arcuate terminal moraine stages with three small intermediate crests can be located (Fig. 3.4; Fig. 3.6). The bigger moraines are usually 4 - 6 m high and ca. 40 - 60 m apart. The intermittent crests are usually about 1 m high (Fig. 3.6). The outermost moraine is ca. 1.5 km from the 1990 position of the snout (Fig. 3.4). The moraine material is slightly different from the moraine series in south. The grain size and roundness are similar but there are no big hyaloclastic boulders.

A possible former ice-contact occurs on a slope opposite the glacier about 1.5 km south west from the 1990 position (Fig. 3.4). This deposit is about 900 m where it is widest but the thickness is not known. On the surface, the deposit is made of coarse predominantly angular material, mainly pebbles and cobbles, but lacking the finer matrix at the foot of the slope where it has been cut by fluvial erosion. It merges with an alluvial fan deposit approximately half way up the slope. Despite an extensive search, no subangular, striated cobbles or boulders were found. But the location, size, structure and overall appearance of this deposit indicate a glacier origin. An ice contact here would mean that the Kjós tributary was temporarily dammed up by ice probably forming a lake in the valley.

About 5 km south of the present glacier, at the eastern end of Bæjarstaðarskógur, are ice limits first described by Ives and King (1955). The limits (Fig. 3.4) form two sets of hummocky moraines indicating two glacier still-stands or advances, about 300 m apart. The moraines are about 2 m high on average and consist of medium-grained

sand-supported gravel. Odd subangular to subrounded cobbles can be found on top of the moraines but overall the deposit is lacking material coarser than cobbles.

3.2.3 Trimlines

On the north-western side of Mt. Háls are trimlines continuous with the northern terminal moraines. They dip about 4° down valley as they reach the moraine limits, but are slightly steeper, or about 6°, closer to the glacier (Fig.3.4). The trimlines are composed of subangular to sub-rounded, greyish boulders resting on the valley slope.

3.2.4 Summary and interpretations of Geomorphological findings

The moraine record and trimlines (Table 3.1) shows that at least 4 stages of advance can be identified in front of Morsárjökull (Fig. 3.4a, 3.5; 3.6). The maximum advance reached about 1.5 km from its 1990 position. Thickness estimations, as seen from the trimlines, indicate that during this stage the ice was probably about 100 m thicker than in 1990.

A moraine limit close to Bæjarstaðarskógur was formed by the Skeiðarárjökull outlet glacier (Fig. 3.4B; Table 3.1). Although Ives and King (1955) interpreted this limit as a line along which Morsárjökull and Skeiðarárjökull formerly met, it is more easily explained as a terminal moraine from the Skeiðarárjökull outlet. Reasons for this interpretation are the loop of the moraines indicating that the glacier flowed from the south to south west, the dip of the sandur plain inside the limit and the grain size distribution of the surface material which varies from coarse to fine away from the limit. This reflects the development of the sandur environment as the glacier retreated south west.

3.3 Skaftafellsjökull

3.3.1 General description

Skaftafellsjökull is 10 km long and about 2 km wide and flows due south from the southern part of the Vatnajökull ice cap (Fig. 3.1). The catchment of the glacier is 89 km² (Fig. 3.3). Skaftafellsjökull terminates on a coastal sandur outwash plain ca. 100 m a.s.l. It is fed at present by two ice falls from the Vatnajökull ice cap and a single ice fall originating from the western side of the Öræfajökull ice cap. The ice falls are steep; the northernmost falls about 200 m over 1 km while the southernmost one falls about 400 m over 1 km. The two ice falls are separated by a nunatak called Súlukambur, forming a conspicuous medial moraine stretching south west. The two ice streams converge to form a valley glacier.

3.3.2 The Moraines

The Skaftafellsheiði area exhibits a variety of lateral moraines (Fig. 3.7, Table 3.2) classified on the basis of spatial orientation, location and extent. Three different sets of moraines have been identified called Vesturheiði, Miðheiði and Austurheiði. The outermost moraine, here called the Sjónarsker moraine, is located on Vesturheiði approximately 2 km west from the 1990 lateral position of the glacier (no. 3 on Fig. 3.7, Table 3.2). This moraine stage enclosed by the Sjónarsker moraine is called the Vesturheiði stage. A second set of moraines can be found on Miðheiði located approximately 1 km west from the 1990s position of the ice (Fig. 3.7; Table 3.2). This moraine stage is called the Miðheiði stage. The third innermost set of moraines on Skaftafellsheiði can be seen on Austurheiði (Fig. 3.7; Table 3.2) about 0.5 km west from the 1990 position of the glacier. This moraine stage is called the Austurheiði stage.

3.3.3 Channels

Channels, collectively named Bæjargil, can be located along the proximal site of the Sjónarsker moraine (Fig. 3.7). The northern ravine begins with a 20 m high waterfall

called Svartifoss and ends in a similar fashion in a second waterfall, about 10 m high, called Magnúsarfoss. The southern ravine starts at Magnúsarfoss and ends at the edge of the sandur plain about 500 m due south (Fig. 3.7). The northern and the southern ravines are about 20 m and 10 m deep, respectively, and ca. 30 - 50 m wide.

Another channel, running south by south west, converges with the Bæjargil channel near the edge of the sandur plain. It is called Eystragil but about 1 km further north it is named Austurgil (Fig. 3.12). Like Bæjargil, it forms a stair-like feature. The uppermost waterfall is called Efri-Austurheiðarfoss, the second Neðri-Austurheiðarfoss and the third Heygötufoss (Fig. 3.12). They are all approximately 10 m high. Associated with these waterfalls are ravines with the same maximal depth as the height of each relevant waterfall. These ravines are usually about 50 - 60 m wide and collectively named Austurgil.

3.3.4 The Trimlines and Striations

Trimlines can be found on western and eastern side of the Gimludalur corrie north of Skaftafellsheiði (Fig. 3.7). These trimlines are about 560 m a.s.l. and marked by a matrix supported gravel and cobbles, usually heavily frost shattered. The trimline on the western side of the corrie dips about 3° towards the south west.

Striated bedrock covered with boulders is located in Botn just north of Skerhóll. The orientation of the striae is 266°, indicating glacier flow towards the west in this area (Fig. 3.7). The height of the striated surface is about 490 m a.s.l or approximately 70 m lower than the trimline on the western slope of Gimludalur corrie.

3.3.7 Summary and interpretations of the Geomorphological findings

The moraine record on Skaftafellsheiði, west of the present glacier margin, indicates three distinct advances of Skaftafellsjökull (Fig. 3.7; 3.8; Table 3.2). These stages are called the Vesturheiði, Miðheiði and Austurheiði stages and represent advances of 2.0 km, 1.0 km and 0.5 km, respectively, from the 1990 position of the western margin of the ice. During these events, the ice was probably at least about 200 m, 170 m and

150 m thicker, respectively, compared with the 1990 glacier. This is depicted from the moraine record on Skaftafellsheiði. Extrapolating ice thickness profiles, the Vesturheiði stage advanced about 3.0 km onto the outwash plain from its 1990 glacier position. The same ice gradient is assumed. Other advances extended about 2 km from the 1990 glacier position (Fig. 3.9a,b). The Vesturheiði stage was drained by the Bæjargil channel and the Miðheiði and Austurheiði stages by the Eystragil (Austurgil) channel. During the Vesturheiði stage the channel along the proximal margin of the ice suggests that the drainage was subglacial until it reached the mouth of Bæjargil at the edge of the sandur plain (Fig. 3.7; 3.9c).

In Gimludalur corrie, just north of Skaftafellsheiði, remnants of a cirque glacier can be inferred from trimlines on the corrie slopes (Fig. 3.7). South west of the corrie mouth is a hanging valley called Botn. The bedrock of Botn is striated by the former occupying glacier indicating westerly ice flow. From the evidence it is inferred that the ice flowed from the corrie in two main directions separated by Skerhóll. The southern ice stream flowed onto Skaftafellsheidi. The western ice stream evidently flowed over Botn and probably merged with former Morsárjökull when it was in a more advanced position than at present. The former ice stream in Morsárdalur was at least 400 m thick at this location, given that the altitude of the base of Morsárdalur and Botn at present is about 100 m and 490 m, respectively. The Gimludalur cirque glacier was drained by a single channel running south from the snout, ending on the sandur plain (Fig. 3.7). The subglacial drainage was probably collected in a single conduit running at the lowest point underneath the ice as occurs in the case of the present stream, Gimludalsá, verifies.

The size of the meltwater channels associated with the different position of the glacier termini indicates that these conduits must have been important in the overall drainage system of the glacier. The flow must have been considerable over extended time in order to form the waterfalls and associated ravines.

3.3 Svínafellsjökull

3.4.1 General description

Svínafellsjökull is about 8 km long, 1 km wide and flows south west from the Öræfajökull ice cap (Fig. 3.1). Like Skaftafellsjökull it terminates on a coastal sandur outwash plain about 100 m a.s.l. According to maps of supraglacial topography, the catchment size is ca. 31 km^2 (Fig. 3.3). The glacier is fed by two ice falls, with a 700 m drop over ca. 1.5 km, separated by a steep rock face (Fig. 3.1). The northern ice fall is the main supply of ice. The southern ice fall drops about 1000 m over 4 km beginning along the foot of Hvannadalshnúkur (2119 m), the highest summit in Iceland.

3.4.2 The Moraines

Two areas contain series of moraines, namely in the proglacial area and on Svínafellsheiði east of the glacier margin. The most conspicuous record is on the outwash plain at about 100 m a.s.l. and is called the Stóralda moraine complex (Thórarinsson, 1956; (Fig. 3.10)). It is defined to represent the moraines in front of the big LIA moraine mapped by Thompson (1988; Fig. 3.10; Table 3.3). Five moraine limits were distinguished. Moraines similar in size and shape were found about 200 m north east of the Stóralda moraine complex. They are called the Freysnes moraines (Fig. 3.10; Table 3.3). On the eastern flanks of the LIA limit (Thompson, 1988), to the west and east of Svínafellsá, small subdued end moraine segments are visible (Fig. 3.10; 3.11 (Breiðatorfa A,B); Table 3.3).

The second area where moraines are found is located on Svínafellsheiði in front of the Svínafellsheiði corrie (Fig. 3.10). These moraines were not measured but are located at ca. 550 m a.s.l.

3.4.3 The valley slope

The topography of the area between the eastern border of Svínafellsjökull and the summit of Skerhóll (503 m) is characterised by a frost-shattered till slope dipping about 27° towards the glacier (Fig. 3.10; 3.12). The slope is confined on its upper and lower margins. The foot of the upper cliff face is at about 400 m a.s.l. and the edge of the lower cliff face is at about 200 m a.s.l. On this slope, a set of striations is located at about 330 m a.s.l., showing an orientation of 185°S, which is parallel to the present ice flow. Another set of striations is located on top of Skerhóll at about 500 m a.s.l. These striations show a glacier flowing WSW with an orientation of 244°.

A scatter of boulders occurs at about 340 m a.s.l. ca. 500 m SSW of the mouth of Hrútagil ravine (Fig. 3.10). The boulders are usually over 2 m in diameter and rest on highly frost-shattered till cover. They are quite dispersed and do not form any particular line or horizontal feature.

3.4.4 Channels

There are several prominent ravines to the east of Svínafellsjökull. The biggest ravine is Svarthamragil on the eastern side of Svarthamrar (Fig. 3.10). This channel is about 40 m deep, 2 km long and 100 m wide, narrowing towards the glacier. Two other ravines are located south of Svartagil on the western side of Skerhóll. The ravine closer to Skerhóll has no name and is about 5m deep, roughly 1 km long and is ca. 30 m wide. The ravine further east of Skerhóll is called Hrútagil and about 1 km long, 10 m deep and 20 m wide (Fig. 3.10). The Svartagil channel drains Svarthamragil corrie. The third set of channels drains Svínafellsheiði corrie and are orientated east-west. The channels are of similar size as Hrútagil (Fig. 3.10).

3.4.5 Summary and interpretation of Geomorphological findings

Two areas of different geomorphology are defined in the area around Svínafellsjökull. Glacial erosion features characterise the highlands east of Svínafellsjökull, called

Svínafellsheiði and Svarthamragil. However, in front of Svínafellsjökull depositional landforms are more common, namely moraines (Fig. 3.10; Table 3.3).

The striations on top of Skerhóll indicates ice flow towards the west hinting at a glacier at least 500 m a.s.l. which flowed from the summit area of Öræfajökull (ca. 2000 m a.s.l.). It is likely that this glacier covered Svínafellsheiði and Svarthamragil (Fig. 3.10). This stage is called the Svínafellsheiði stage. The valley slope below Skerhóll (200 - 400 m a.s.l.), the second set of striations on this slope and the boulders on Svínafellsheiði (ca. 350 m a.s.l.) reflect a distinct ice limit. The eastern margin of this glacier was at 330 m a.s.l. This glacier flowed parallel to the present glacier towards the south. This stage is called the Skerhóll stage. Moraines in front of Svínafellsfjall corrie represent the limit of a corrie glacier (Fig. 3.10). Turf-banked terraces, which are small-scale solifluction-type terraces, have been located above 500 m a.s.l. and are inferred to be located above the Neoglaciation limits of the area (Douglas and Harrison, 1996). This concurs with the present study and complements the interpretation of an ice limit on Skerhóll and on the valley slope. The solifluction terraces are located above the inferred Skerhóll stage but below the inferred Svínafellsheiði stage.

The area in front of the LIA limit (Thompson, 1988) is characterised by a series of moraines called the Stóralda moraine complex (Fig. 3.10). Thórarinsson (1956) concluded that at least six spatially discrete moraine limits can be identified. However, it is inferred in this study that five different stages exist (Fig. 3.10). Two other limits were found but these crests have very limited spatial distribution. It is suggested from the geomorphic evidence that the Stóralda moraine complex was deposited after the Skerhóll stage. This can be seen from the spatial relationship of the lateral limit (at least 330 m a.s.l.) on Svínafellsheiði representing the Skerhóll stage. By using the current long profile gradient of Svínafellsjökull and then extrapolating the limit onto the sandur plain, the termini of the Skerhóll stage are likely to have been beyond the Stóralda moraine complex (Fig. 3.13). The Stóralda moraine complex can be seen on Fig. 3.14

3.5 Virkisjökull

3.5.1 General description

Virkisjökull comprises two south west facing ice lobes originating from the ice-filled caldera of Öræfajökull (Fig. 3.1). The two ice streams drain about 18 km^2 according to maps of supraglacial topography (Fig. 3.3) and span altitudes ranging from 180 m a.s.l. at the glacier snout to 1800 m a.s.l. at the edge of the caldera rim. This altitude difference occurs over ca. 7 km. The two ice lobes are separated by a ridge called Rauðikambur where the southern ice stream is called Falljökull but the northern lobe is named Virkisjökull (Fig. 3.3). Both of the outlets are about 5 km long and about 900 m wide. Both glaciers have ice falls. The Virkisjökull ice fall drops about 400 m over 1 km but the Falljökull ice fall drops about 400 m over about 800 m. From the top of the ice falls at about 1000 m a.s.l., the ice slope continues to the caldera rim at about 1800 m a.s.l. with a surface slope of about 13°.

3.5.2 The Moraines

The moraine record of Virkisjökull is complicated. A combination of terminal and lateral moraines, usually only fragments, are scattered over the proglacial area indicating different advances or still-stands. In order to clarify the moraine record, its description and interpretation, a number was given to each moraine. Moraines were then measured and geomorphic correlation suggested on the basis of spatial distribution. Moraine characterisation and correlation can be seen in Table 3.4. According to the table, 53 moraines, or fragments and series of moraines, were mapped and measured. The best preserved moraine record is located on Sandfellsheiði, east of the glacier, suggesting 3 stages of advance called Virkisjökull I, II and III (Fig. 3.15). A single stage is identified in front of the glacier called Virkisjökull IV (Fig. 3.15). Cross sections of the moraines on Sandfellsheiði and in front of the glacier can be seen on Fig. 3.16a and b.

3.5.3 The supraglacial deposit

The landscape inside moraine 1 and 2 is characterised by chaotic mounds and push ridges cut by small channels and pits sometimes randomly orientated (Fig. 3.15). The ridges and mounds usually show rather high relief, about 2 - 8 m. Outside the moraines, just west of Virkisá, the relief is different. The ridges show a more regular north west - south east crest orientation.

3.5.4 Channels

The channels associated with the outermost and the intermittent stages on Sandfellsheiði are about 20 m deep, 70 m wide and about 500 - 700 m long following the moraine limit to the end. The channel running along the innermost limit is about 26 m deep and ca. 200 m wide (Fig. 3.15, 3.16).

Several meltwater channels can be detected on the outwash plain. These channels vary from 50 m to 100 m in width and are very shallow ca. 1 m to 3 m deep (Fig. 3.15).

3.5.5 The Jökulhlaups

Pronounced evidence of the 1362 and 1727 AD jökulhlaups are detectable on the outwash plain in front of Virkisjökull outlet glacier. The 1362 AD jökulhlaup is most obvious in the western part of the area, especially on both sides of Virkisá. Large boulders are scattered over the outwash plain and the matrix is fine grained white ash with occasional pumice grains. The boulders are usually a few metres in diameter. The extent of this 1362 AD jökulhlaup deposit was traced as far as Veilulækur to the west about 500 m from the western margin of Fig. 3.15. Towards Sandfellsheiði and Falljökulkvísl the material of the 1727 AD jökulhlaup becomes more apparent. Big chunks of black/bluish pumice are mixed in the fluvial deposits on the outwash plain beginning just south of moraine no. 12 and increase eastwards (Fig. 3.15). The largest 1727 AD jökulhlaup material is deposited just south and south-east of moraine no. 16 where it forms three distinct terraces at the same altitude (Fig. 3.15). The

terraces are on average 6 m high and cut by meltwater erosion implying that the jökulhlaup deposit was much bigger at the time of formation, probably filling up most of the channel between moraine no. 18 and 50 (Fig. 3.15).

3.5.7 Summary and interpretations of Geomorphological findings

The geomorphology of the proglacial zone of Virkisjökull comprises complex moraines, fluvial meltwater channels and jökulhlaups. Four major advances of the glacier are identified and named Virkisjökull I, II, III, IV in order of formation (Fig. 3.15). These advances can be detected by lateral moraines on Sandfellsheiði on the basis of orientation and location (Fig. 3.17). Fragments of lateral and terminal moraines exist on the outwash plain but were shaped by glacial meltwater and jökulhlaups following the eruption of Öræfajökull in 1362 AD and 1727 AD. The inferred moraine correlation (Table 3.4) is based on the present shape of the Virkisjökull IV stage by using the lateral moraines on Sandfellsheiði as a reference. The fragments of moraines between Virkisjökull I and II (Fig. 3.15) clearly reveal repeated small advances or still-stands. This is best shown by moraine series 48 and 49 (Fig. 3.18). However, it can not be ascertained how many stages they represent.
It is difficult to establish the ice thickness during the different advances. Estimates would suggest that the glacier was perhaps about 50 - 100 m thick on the outwash plain during the outermost advance. Rough estimates can be applied to assess how far onto the outwash plain the glacier extended during different stages. By combining the ice thickness estimations and the geomorphic record the indications are that the glacier extended about 3 km, 1.2 km and 0.9 km onto the outwash plain during the different stages, respectively (Fig. 3.19a and b).

Two geomorphologically distinct environments occur outside and inside moraines 1 and 2 (Fig. 3.15). This geomorphic difference can be explained by the different availability of supraglacial material before and after the deposition of moraine no. 1 and 2. If the inferred ice thickness profiles (Fig. 3.19a and b) are used to estimate the thickness of the glacier at the time when the landscape outside the big moraines was formed, it can be concluded that the ice covered Rauðikambur nunatak which is the

main source of the supraglacial material at present. This would imply that the medial moraine did not exist, or at least it was considerably smaller. When the glacier had thinned sufficiently to expose Rauðikambur, it could sustain a formation of a medial moraine. The geomorphological evidence suggests that this happened when the glacier retreated from moraines 1 and 2.

The pattern of jökulhlaup deposits implies that the 1727 jökulhlaup rushed onto the outwash plain mainly from the eastern side of the glacier, thus coming from underneath Falljökull. The eastern boundary of the 1362 AD jökulhlaup is not clear because of the gradual increase of 1727 AD deposit towards moraine no. 12. It is therefore impossible to draw a line marking the boundary between these two jökulhlaup deposits. Despite this, it is highly likely that the 1362 AD jökulhlaup had a much larger spatial extent than the 1727 AD jökulhlaup simply because of the size of the event. In fact, Thórarinsson (1958) cites one of the annals, i.e. Gottskálksannáll, as plainly saying that Knappafellsjökull (Öræfajökull) "rushed over Lómagnúpssandur (i.e. Skeiðarársandur) cutting off all roads" (Isl. Ann., 1888, p. 279). A huge dispersal pattern like this would indicate that the whole of the glacier terminus simply burst and flowed onto the sandur plain as far as Skeiðará about 5 km to the west of Rasshólar (Fig. 3.15).

A huge flood like this can be reconstructed from other evidence. The morphology of moraines no. 32 to 45 indicate that these features have been flooded by a water mass flowing to the south west. The mean orientation of these moraines is 208° (SSW) (Fig. 3.20) or the same as an expected flow direction of the jökulhlaup. The shape of the moraines also sustain this. The mean length/width ratio is 1:3, the mean proximal slope 10° and the distal 16°. This would give a ratio of 1:1.6 implying that the distal slope is 60% steeper than the proximal side on average. Further, the mean length/width ratio states that the feature is three times longer than it is wide. These morphological characteristics emphasise the direction the flood. The Ö1362 tephra is found immediately on top of the moraines. It is reworked by fluvial activity which

would suggest that the moraines were shaped into the present form by the Ö1362 jökulhlaup.

The ephemeral maximum discharge of the 1362 AD jökulhlaup has been estimated by Thórarinsson (1958) to be approximately 100.000 m^3/s or about that of the river Amazon. This estimate can be improved by simple calculation. The flooded moraines are usually about 5 m to 7 m high on the outwash plain. This would give a minimum depth of the flood water at its peak discharge. The distance between Svínafellssfjall and Sandfellsheiði, which is about 1 km, would give the approximate width of the constraining slopes. This would give an area of ca. 6000 m^2. Maizels (1986) and Tómasson (1996) have estimated that the flow of the 1918 AD jökulhlaup from Katla volcano in South Iceland, which would be of similar type as Öræfajökull jökulhlaups, was about 10 - 14 m/s depending on whether the estimation is conducted on an open outwash plain or in a well constrained ravine. Using an average of 12 m/s to estimate the velocity and then multiplying that with the approximate area of the flood gives a rough ephemeral minimum of the 1362 AD jökulhlaup of about 72.000 m^3/s.

3.6 Kotárjökull

3.6.2 General description

Rótarfjallsjökull and Kotárjökull, south westerly facing ice lobes, form what is here collectively called Kotárjökull (Fig. 3.1). The real Kotárjökull, i.e. the western outlet, is a steep valley glacier rising from ca. 300 m a.s.l. to about 700 m a.s.l. over a distance of 1700 m. From there an ice-fall about 100 m high extending over ca. 120 m exists as a step to the southern slope of the Öræfajökull ice cap from where the glacier is fed. Rótarfjallsjökull, on the other hand, has two outlets, both initiated by the same ice-fall. These outlets are shorter and not as steep. They rise about 240 m over 1 km to the common accumulation area at about 920 m a.s.l. From this altitude to the caldera rim, at about ca. 1820 m a.s.l., the mean average gradient is about 14°.

3.6.3 The Moraines

The moraine record of Kotárjökull is scarce compared with other proglacial regions in the study area. To clarify the record, numbers were given to each moraine (Fig. 3.21). The characteristics of the moraines are listed in Table 3.5. Three distinct advances can be identified called Kotárjökull I, II and III. The outermost advance is marked by two lateral moraines at the foot of Goðafjall and in the gorge between Slaga and Goðafjall numbered 5 and 7 (Fig. 3.21). The intermediate limit is delineated by moraines no. 4 and 6 (Fig. 3.21). Moraine no. 1, 2 and 3 marks the innermost limit of Kotárjökull as mapped on Fig. 3.21.

3.6.4 Channels

Pronounced meltwater channels are associated with each set of moraines. The most conspicuous routes are on the east side of moraines no. 4 and 5 cut into an escarpment starting at the southern tip of the moraines. These channels are about 10 m deep and ca. 50 m wide and extend along the slope surface for approximately 160 m. The innermost limit is associated with a meltwater route as well. The channel is on the western side of moraine no. 1 between the ridge and a small ridge just off the western slope of Goðafjall. Meltwater channels also occur on the western side of Mt. Slaga (Fig. 3.21).

3.6.5 The Jökulhlaups

Extensive areas of black pumice are located in front of Kotárjökull indicating the 1727 AD jökulhlaup (Fig. 3.21). The pumice flow is dissected by meltwater activity forming terraces (Thompson and Jones, 1986; marked I, II and III on Fig. 3.21). The boulders west of moraine no. 1 are probably remnants of a jökulhlaup (Fig. 3.21). This can be seen from the dispersal pattern of the boulders covering a large range of altitudes. Huge kettle holes occur on the terraces in front of Kotárjökull. The biggest kettle hole is located on terrace I. It is 35 m in diameter and about 8 m deep. It is located about 2.5 km south east from the glacier terminus (Fig. 3.21). Remnants of the 1362 AD jökulhlaup deposits can be detected in dead ice areas of the 1727 AD

event. This is based on the preservation of widespread patches of fine grained light brown sediments in such areas.

3.6.6 Summary and interpretations of Geomorphological findings

The moraine record in front of Kotárjökull reveals three distinct advances of the glacier called Kotárjökull I, II and III where Kotárjökull I is the outermost advance (Table 3.5; Fig. 3.21). These advances are associated with meltwater channels. It is difficult to infer the ice thickness from the moraine record. The local relief west of moraines 4 and 5, indicates variable subglacial topography and, since the ice retreated, the landscape has been incised by glacial meltwater and jökulhlaups as seen from the deep ravines. This is in sharp contrast to the more typical U-shape of the valley closer to the glacier. The lithology of the till cover on top of Mt. Slaga would suggest that, during Kotárjökull I and II advance, the ice covered the mountain. This would mean that the ice advanced a maximum 150 m in the gully west of Mt. Slaga. However, near the moraine limits, the ice was considerably thinner, about 50 m (Fig. 3.22; 3.23). It is difficult to estimate how far onto the outwash plain the glacier extended during the different advances because of the lack of terminal moraines. However, if a conceptual long profile of a hypothetical glacier is drawn, assuming an ice thickness of 150 m around Mt. Slaga and an extrapolation of the looped moraines 6 and 7 (Fig. 3.21), it would suggest that the ice extended about 3 km onto the outwash plain during the Kotárjökull I advance.

Kotárjökull was the main route of the 1727 AD jökulhlaup as reported by documentary evidence (Henderson, 1818; Isl. Ann, 1888, p. 279). One of the most compelling pieces of evidence of the 1727 AD jökulhlaup is the abundant black pumice deposition forming a fan in the glacier foreland. The jökulhlaup deposit is cut by post glacio-fluvial drainage activity resulting in a formation of terraces in a range of altitudes. Deep kettle holes can be found on the surface of the jökulhlaup. These were formed by stagnant disintegrating ice bergs brought onto the sandur plain by the jökulhlaup. In the bottom of some of the kettles brown patches of light brown pumice can be observed. This is interpreted as remnants of the 1362 AD jökulhlaup which in

turn is buried beneath the younger black pumice. From this evidence it can be inferred that Kotárjökull was also a pathway of the 1362 AD jökulhlaup. It is likely that Kotárjökull played a more vital role as a pathway for the 1727 AD event in comparison with the 1362 AD episode. This can be deduced because the spatial distribution of the former event is bigger since the 1362 AD pumice can only be found in kettles within the boundary of the 1727 AD event.

The discharge of the 1727 AD jökulhlaup can be estimated by using the same method applied in front of Virkisjökull to calculate the ephemeral discharge of the 1362 AD event. By using the narrow ravine north west of moraine no. 4 as a throughput area and then use the height of the jökulhlaup terrace in that gully the minimal ephemeral discharge would be in the order of 45.000 m^3/s. It has to be noted that this is a very rough estimate but implies that the 1727 AD eruption and the subsequent jökulhlaup was smaller than the 1362 AD event. This is in concordance with the spatial mapping of the two jökulhlaup deposits.

3.7 Kvíárjökull

3.7.1 General description

Kvíárjökull is a steep south east facing valley glacier originating in the Öræfajökull ice cap. The glacier directly faces the main precipitation source in Iceland which is at a maximum in the coastal areas along the south east part of the country. The glacier is about 6.5 km long and ca. 1.5 km wide at the bottom of the ice-fall. The main ice-fall drops about 800 m over a distance of ca 800 m and the accumulation area rises about 1000 m over 2.4 km to the rim of the caldera. The terminus of the glacier is at about 70 m a.s.l. and the highest point of the accumulation area is about 1820 m a.s.l., 10 km to north west. This results in a relatively steep mean altitude gradient between the snout and the highest point (1:0.175 implying that for every 1 km distance the elevation interval is 175 m). The elevation gradient above the ice-fall to the rim of the caldera is 1:0.21 which is similar to other gradients above the ice-falls to the caldera rim in the area. The catchment of the glacier is ca. 26 km^2 which includes a part of the caldera (Fig. 3.3).

3.7.2 The Moraines

Three distinct sets of moraines were identified in front of Kvíárjökull and named Kvíárjökull I, II and III. The main feature around Kvíárjökull is a big moraine amphitheatre composed of two lateral moraines called Kambsmýrarkambur and Kvíármýrarkambur. Outside this limit are three moraine sequences (Fig. 3.24). Each ridge was given a number for descriptive clarification. The characteristics of each moraine ridge are described in Table 3.6. The moraines vary greatly in size from 3 - 100 m high. Morphologically, they comprise arcuate hillocks (11), single hillocks (8 and 9) and discontinuous subdued crescent-like ridges (5 and 6). A cross section of the moraines underlines the size difference (Fig. 3.25). One of the most distinguishing characteristics of the ridges outside the big moraine amphitheatre (7, 10 and 14) is their frost-shattered surfaces.

3.7.3 Channels

The big moraine amphitheatre is breached in five places. These breaches are typically 10 - 50 m deep and 100 m to 500 m in width (Fig. 3.24). These gaps have been related to meltwater shifting as a consequence of a fluctuating glacier within the big moraine amphitheatre (Thórarinsson, 1956). The present drainage was established in the mid 1930s (Thórarinsson, 1956). The Dýlækur stream sits in a channel about 40 m deep running parallel to Kambsmýrarkambur moraine (Fig. 3.24). This channel has incised terraces into a loosely consolidated volcanic substrate. No channels can be related to other moraines in the area.

3.7.4 The Lava flow

A part of a lava flow can be found just south of the western end of Kvíármýrarkambur (Fig. 3.24) and first detected by Thórarinsson (1956). It is rhyolitic, not basaltic as concluded by Thórarinsson (1956), according to a chemical analysis conducted on a sample of the lava (SiO_2>70%). Sections found in the eastern part of Kambsskarð breach show that the lava flow is at least 10 m thick and it can be followed to where it disappears under Kvíármýrarkambur. According to Thórarinsson (1956) the origin is

to the east of Kviárjökull and the lava probably flowed to the south west at a time when the glacier was much smaller and did not reach the lowlands. This would echo the results of Björnsson (1993) indicating the source was Vatnafjöll, north of Kviárjökull. No evidence of the lava flow has been found on the northern side of the glacier.

3.7.5 The Jökulhlaup

To the south of Kviármýrarkambur is an area called Stórugrjót (Big rocks) covered with boulders and occasional large pieces of black pumice about 30 cm in diameter. The matrix is composed of coarse-grained black sand and pumice. Similar material exists at the foot slopes of Staðarfjall mountain to the south of the Kviármýrarkambur breach. Two well delineated terraces, cut later by meltwater activity, are located at the foot of the mountain (Fig. 3.24). These terraces dip due west and north west. The material in these terraces is black basaltic unconsolidated pumice and coarse-grained basaltic sand similar to the material from the 1727 AD jökulhlaup. The upper terrace ends abruptly just south of a small ravine cutting into Staðarfjall mountain. On the other side of the ravine some patchy remnants of these deposits occur. Similar type of black pumice deposits can be traced on the northern side of Kviárjökull where they have been incised by recent meltwater activity. These deposits dip north and east in general (Fig. 3.24).

3.7.6 Summary and interpretations of Geomorphological findings

The geomorphological record in front of Kviárjökull is a complex mixture of glacial and volcanic sediments. At least three distinct glacier advances can be deduced from the moraines in the area and will be called Kviárjökull I, II and III where the first stage is the oldest (Fig. 3.24: Table 3.6). However, the number of advances is likely to be underestimated because the big moraine amphitheatre is most likely a composite moraine formed by several advances of the glacier. This can be substantiated by the existence of a moraine loop on the western side of Kambsmýrarkambur which rests on top of the big moraine; the implication is that the ice advanced partly over the southern end of Kambsmýrarkambur and that these smaller moraines are younger than

the big moraine. This can be sustained by a clear morphological change in the crest of the big moraine where the ice overrode it. Here, the moraine crest becomes progressively less sharp and the moraine height sharply declines.

The Kvíárhólar moraines (Fig. 3.24) are interpreted as being a continuation of Kvíármýrarkambur but breached by meltwater activity during the retreat of the ice. It is not clear from the geomorphic evidence whether this limit represents an individual advance or several advances.

Evidence of a big jökulhlaup event is pronounced. It is inferred to be younger than the lava flow, which is the oldest landform in the area, and the moraines (Kvíárjökull I and II) which lie on it. This can be deduced from the flow pattern of the jökulhlaup which partly stripped the glacial deposits on the surface of the lava (Fig. 3.24). No evidence showing the jökulhlaup deposit stratigraphically under the big moraine amphitheatre could be found despite an extensive search. Therefore, it is concluded that the jökulhlaup occurred after the initial formation of the big moraine amphitheatre and was probably responsible for partly breaching Kvíármýrarkambur at the foot of Staðarfell (Fig. 3.24). It is likely that the bulk of the jökulhlaup material rushed down the canyon south of Staðarfell, as inferred from the geomorphic record. On the northern side, the jökulhlaup rushed down Stóralækjagljúfur and probably breached Kambsmýrarkambur at the eastern foot of Vatnafjöll, flowing along the big lateral moraine but then turning to the north east (Fig. 3.24). The dip of the northern jökulhlaup surface is interesting, i.e. generally towards north east. This flow direction would not occur under the present topographic conditions. A drastically different shoreline is likely. At the time of the jökulhlaup the coastline was probably closer to the foot of Vatnafjöll thus encouraging the jökulhlaup to flow north of the big moraine. On the southern side, however, the flood probably went straight into the ocean.

3.8 Conclusion of the Geomorphological findings in the Öræfi district

The geomorphology of the Öræfi district of south east Iceland reveals a complex combination of glacial erosion and volcanic activity. Distinct glacial advances have been identified in front of four outlets of Öræfajökull ice cap and two outlets of the Vatnajökull ice cap. These glacier fluctuations are indicated by glacial sediments and landforms, mainly moraines. From the evidence it is clear that various outlet glaciers expanded about 2.5 - 3 km beyond their present limits and were up to 200 m thicker at their present snouts. The principal implication is that the area has experienced periods of glacier activity since the decay of the last inland ice sheet in Iceland.

Jökulhlaup deposits are common in the study area due to the volcanic activity of the Öræfajökull stratovolcano since the last Termination. Three distinct jökulhlaup deposits were identified dating from 1362 AD, 1727 AD (Thórarinsson, 1956, 1958) and a third jökulhlaup which is later argued to date from ca. 1500 BP. The origin of the historical jökuhlaups is in the western part of the Öræfajökull caldera. However, the older jökulhlaup was found only in front of the Kviárjökull outlet flowing from the eastern side of the ice cap. This could indicate that the source of any prior eruptions were in the eastern part of the caldera. If so, the eruption side shifted from east to west within the caldera sometime before the 1362 AD eruption. However, the possibility that jökulhlaup deposits from the early eruptions have been buried by younger deposits can not be ruled out.

The implications of a volcanic eruption occurring within the accumulation area of relatively small valley glaciers is profound and raises specific problems when using such glaciers as indicators of climate change. New mass balance equilibrium can be temporarily disrupted and different relationships between the ice and the underlying bedrock are possible. For example, an eruption in the caldera can breach it in new places or even enlarge old ice flow routes and alter the flow pattern of the ice. Alternatively, an eruption could inhibit ice flow by blocking-up existing breaches.

Whether this is the case for Öræfajökull can only be tested when the timing of the fluctuations is discussed later in the thesis.

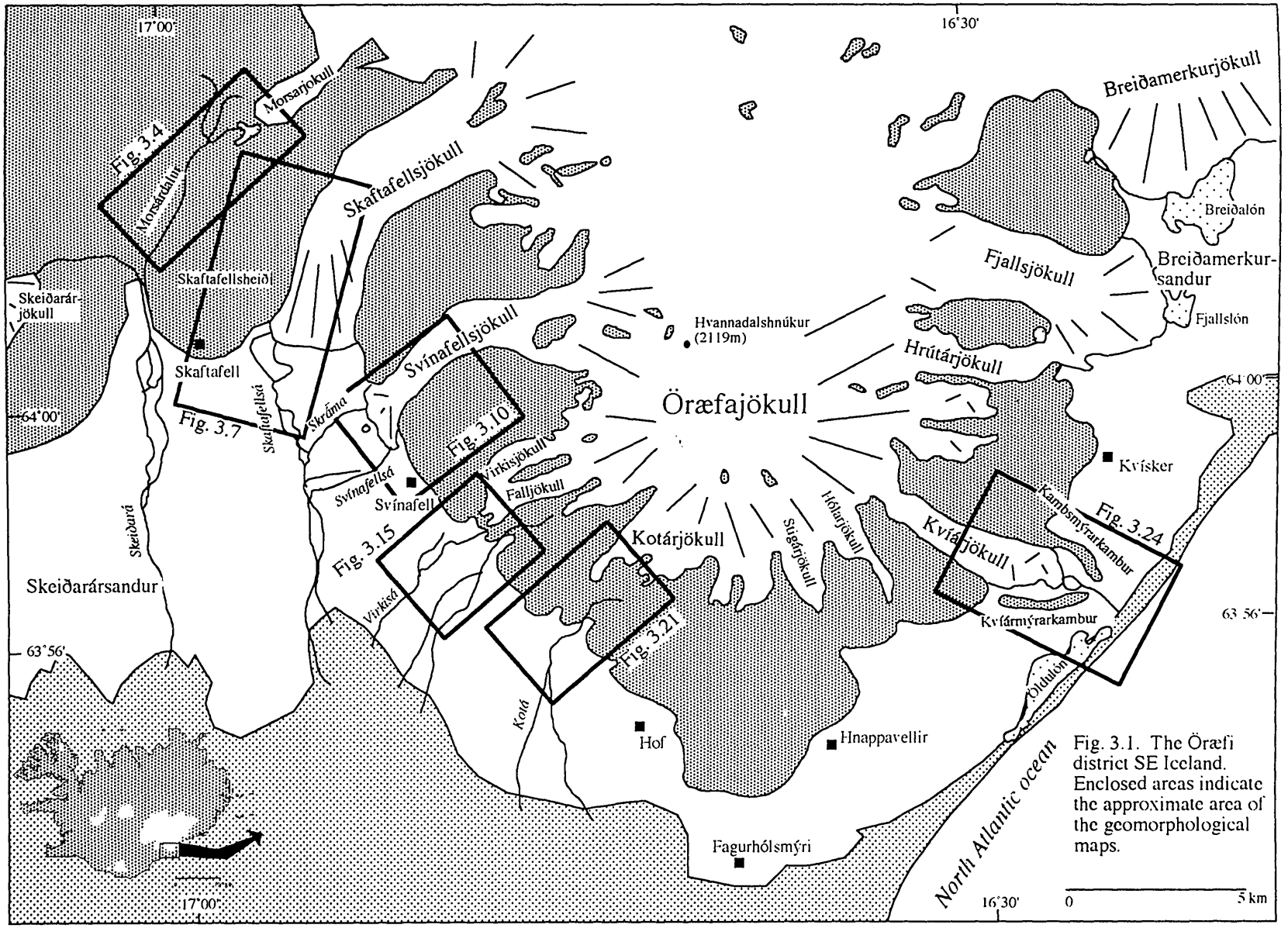

Fig. 3.1. The Öræfi district SE Iceland. Enclosed areas indicate the approximate area of the geomorphological maps.

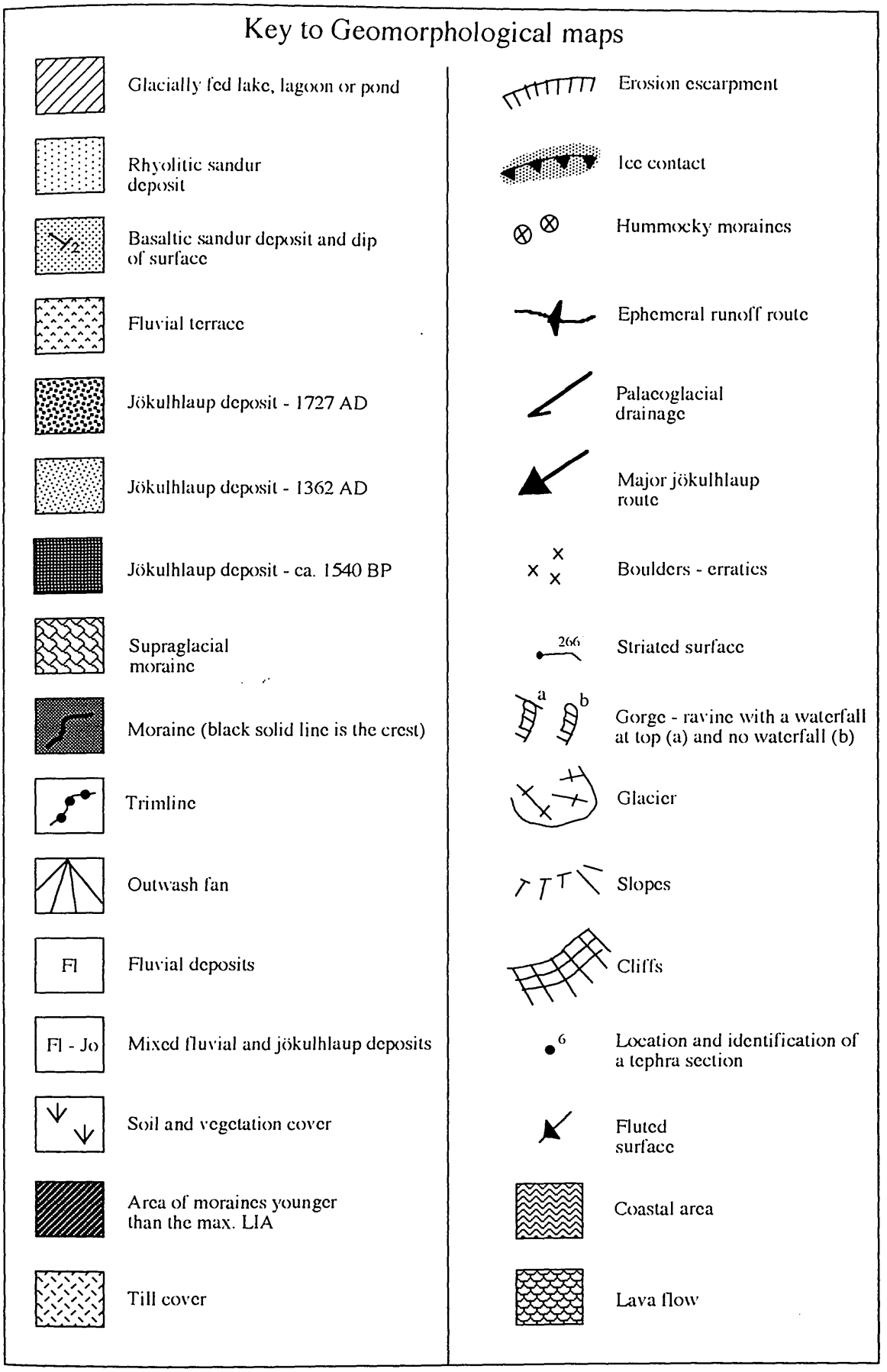

Fig. 3.2. Legends of geomorphological features.

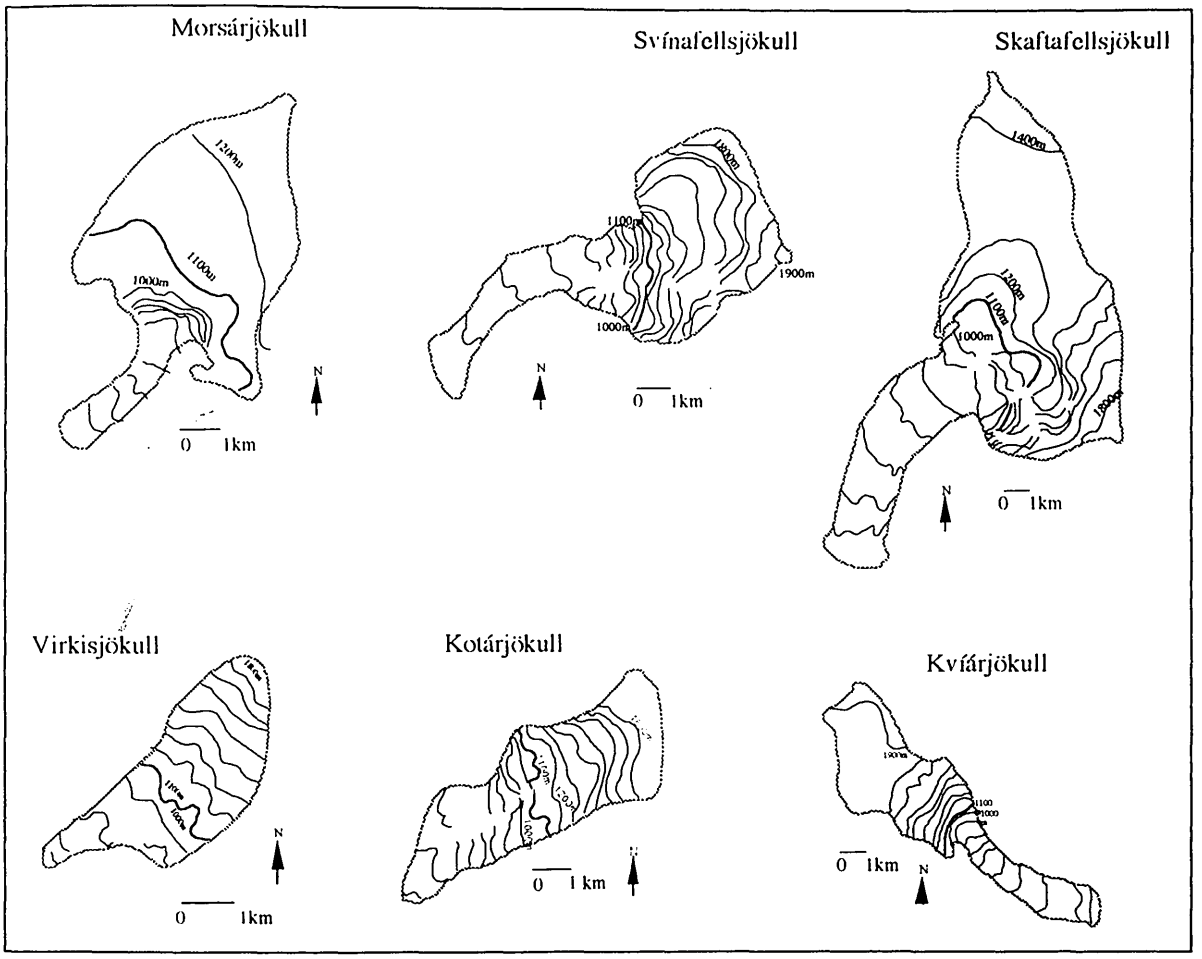

Fig. 3.3. The catchments of the outlets studied. Catchments were defined according to contour lines on the ice (of a map of the glaciers (1:100 000)) and then the area measured. The ELA is at 1100 m a.s.l. as indicated by a bold black line on each map.

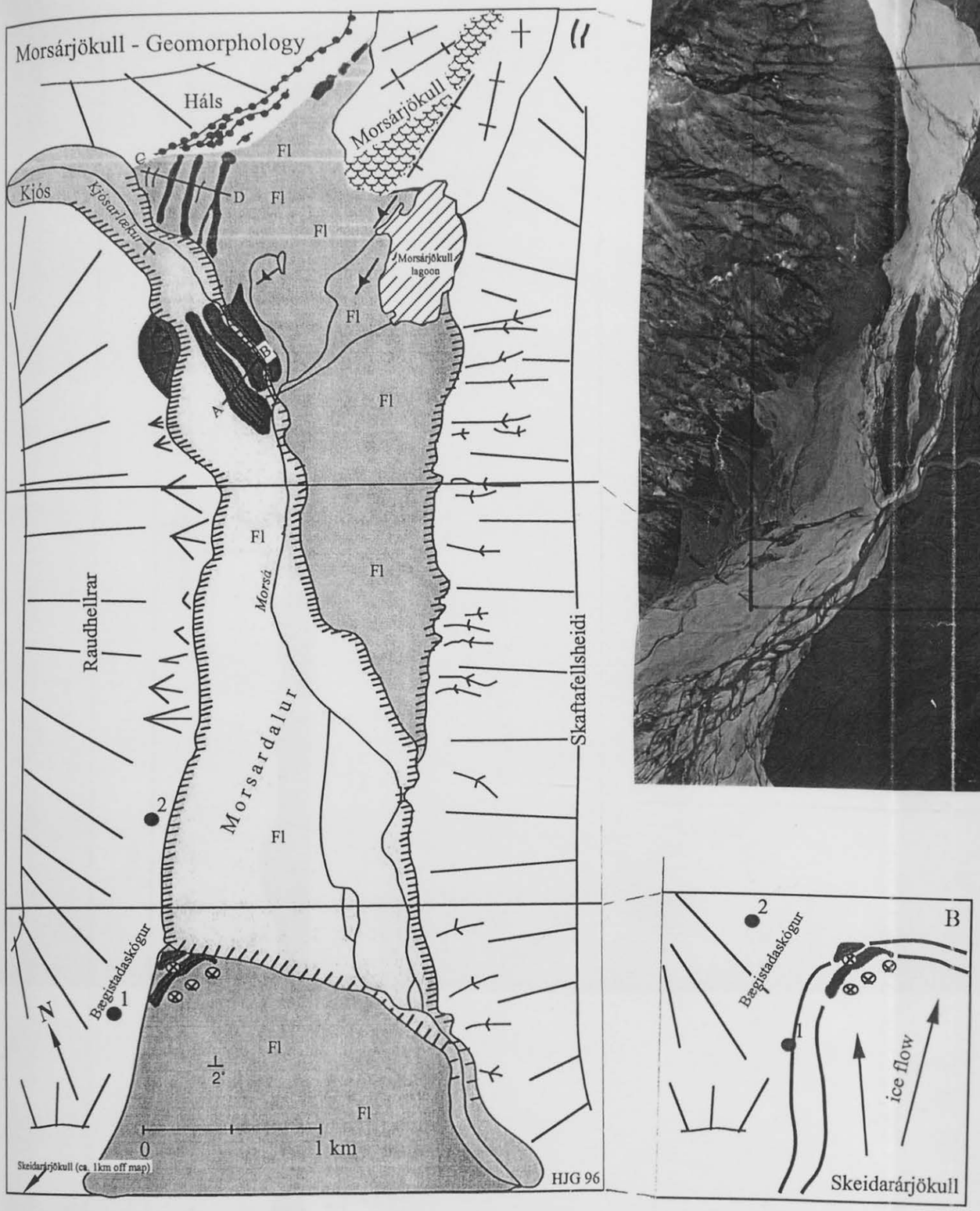

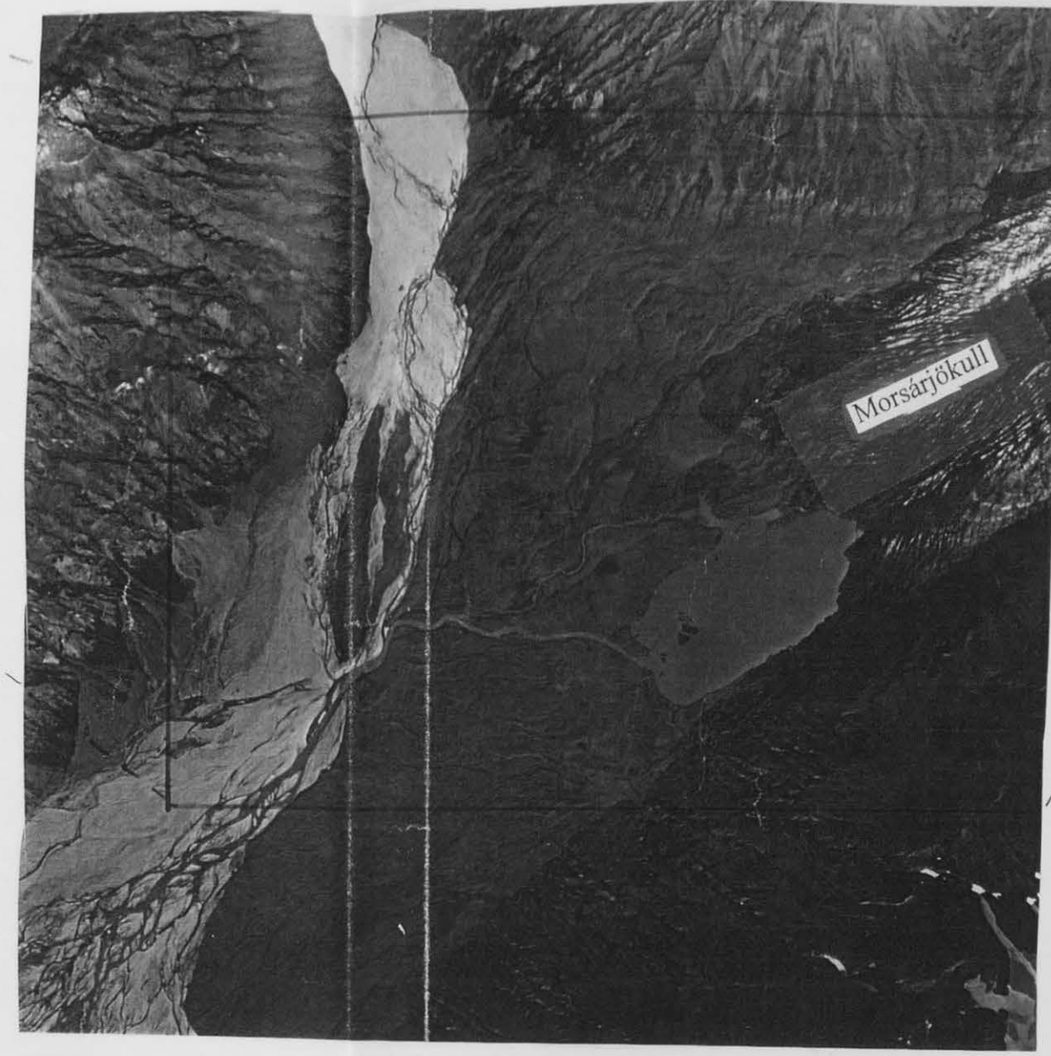

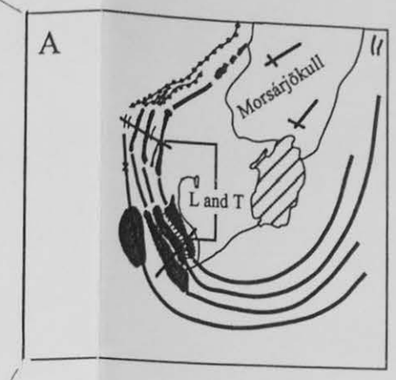

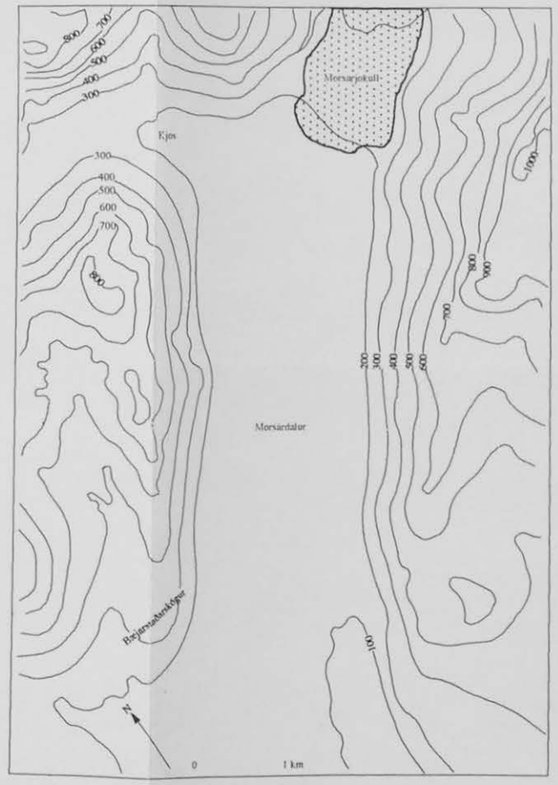

Fig. 3.4. The Geomorphology of Morsárdalur. The small inset maps A and B show the reconstruction of the ice limits (bold curved black lines) in relation to the observed glacial geomorphology (L=lichens, T=tephra). Inset map A shows the Morsárjökull limits but inset map B shows the Skeiðarárjökull limits. Skeiðarárjökull outlet glacier (from the Vatnajökull ice cap) is not visible on the maps. Topography of the whole area is shown on the map in the lower right corner. Contour interval is 100 m. Moraine limits indicate former glacier positions. The base of the Morsárdalur valley is coverd by glacio-fluvial deposit, mainly sandur. The colour difference of the sandur plain is due to its origin, white is rhyolitic and black is basaltic.

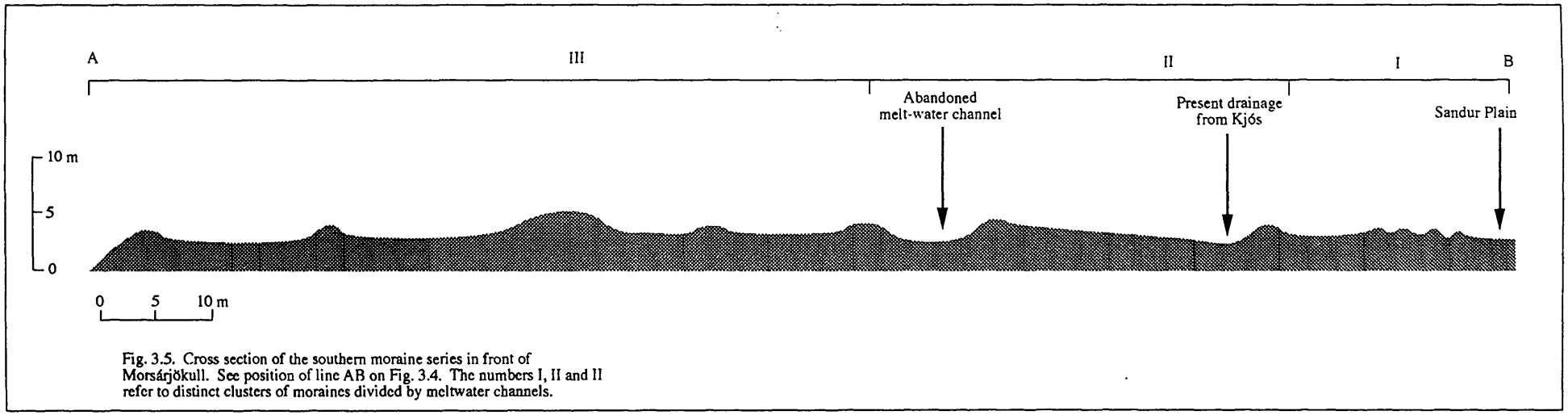

Fig. 3.5. Cross section of the southern moraine series in front of Morsárjökull. See position of line AB on Fig. 3.4. The numbers I, II and II refer to distinct clusters of moraines divided by meltwater channels.

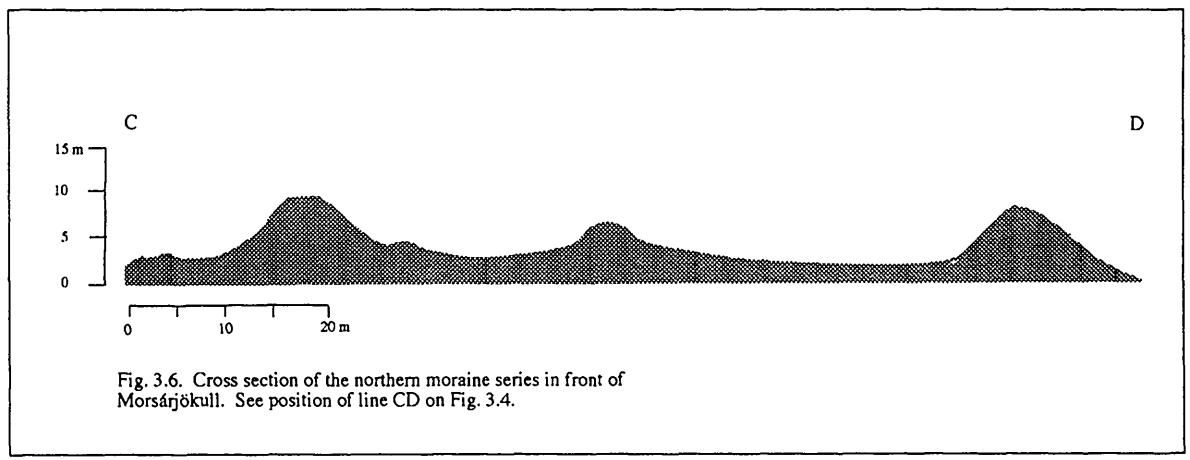

Fig. 3.6. Cross section of the northern moraine series in front of Morsárjökull. See position of line CD on Fig. 3.4.

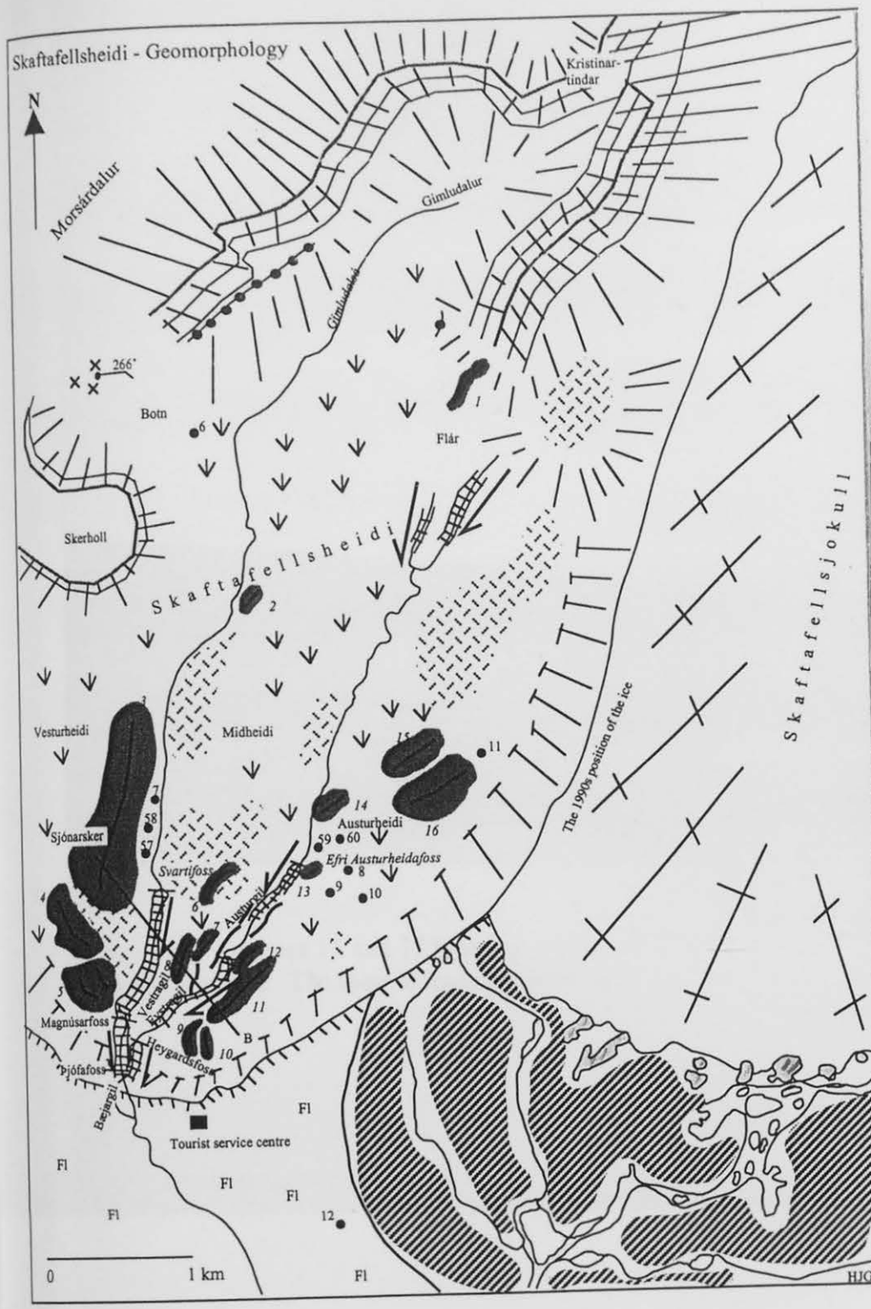

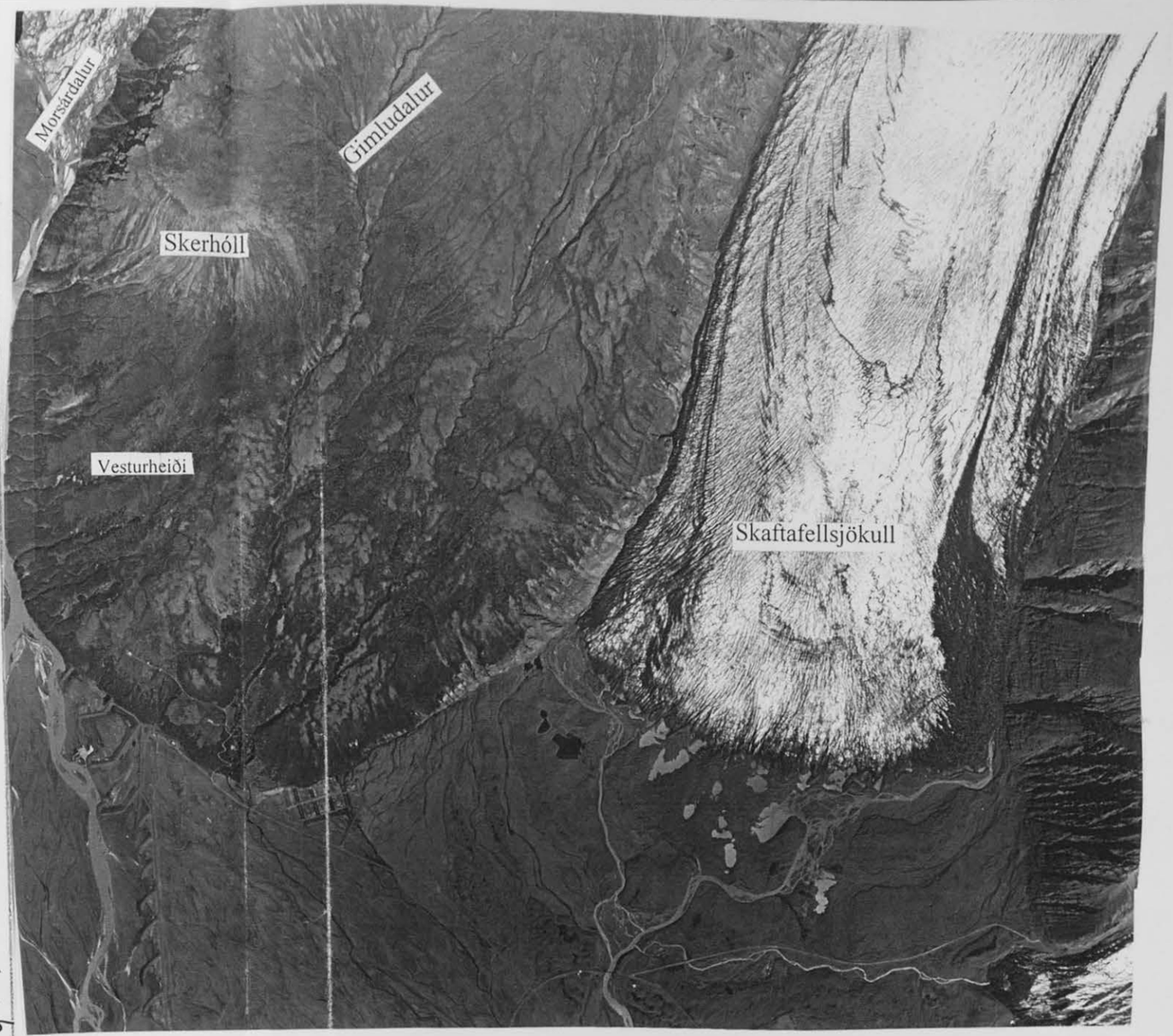

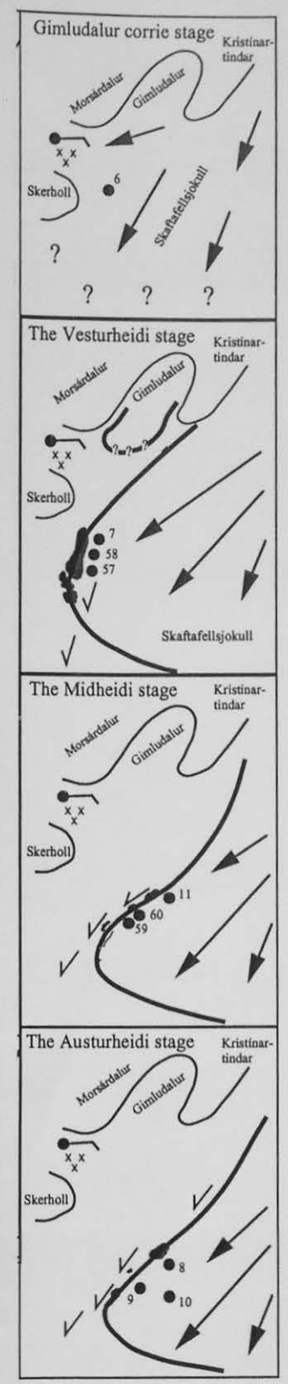

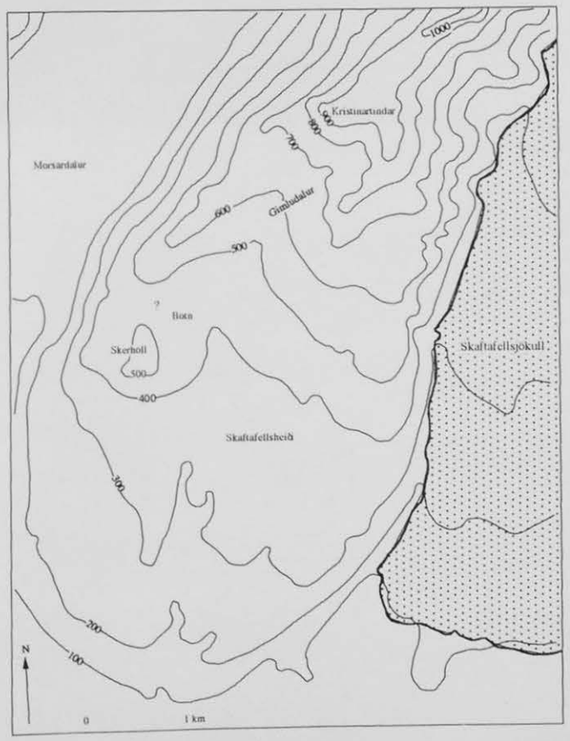

Fig. 3.7. The Geomorphology of the proglacier area of Skaftafellsjökull. The small inset maps on the right show the reconstruction of the ice limits (bold curved black lines) in relation to the observed glacial geomorphology. The small inset maps on the right show single advances of the Skaftafellsjökull outlet. The insets cover approximately the same area as the geomorphic map on the left. The letters in *italics* represent a specific number given to each moraine and black circles show the location of tephra profiles. Topography of the area is shown on the map in the lower right corner. Contour interval is 100 m. The geomorphology of Skaftafellsheiði is characterised by moraines, till-covered surfaces and glacio-fluvial drainage routes indicating former glacier activity. These landforms and deposits are preserved because of minimum recent glacier activity on the Skaftafellsheiði highlands. The geomorphology of the area in front of the outlet is characterised by arcuate terminal moraines resting on black basaltic sandur plain.

Fig. 3.8. Moraines 11 and 12 (see Fig. 3.7) representing the Miðheiði advance on Skaftafellsheiði. The view is towards south east.

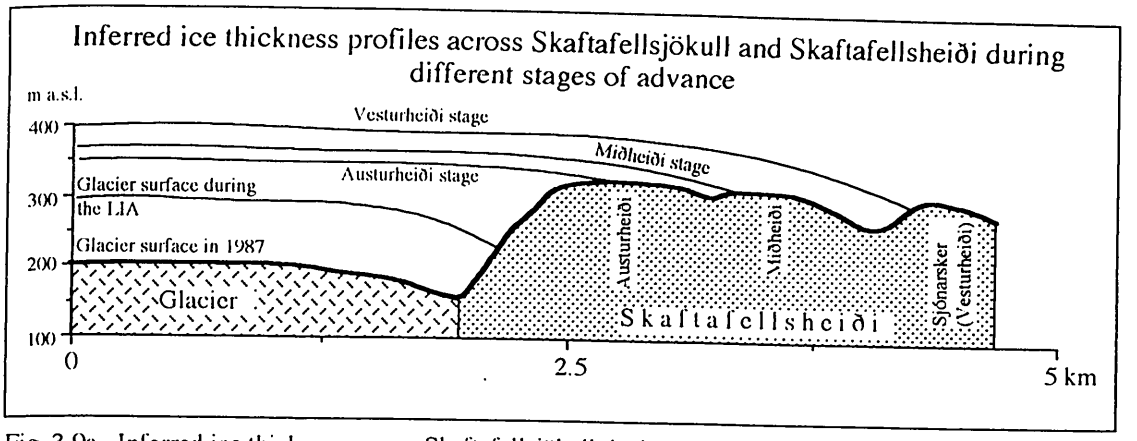

Fig. 3.9a. Inferred ice thickness across Skaftafellsjökull depicted from geomorphic evidence. Note that the profiles are drawn with the same ice surface dip as the present glacier. It is highly probable that the profile was steeper during the advances. For location of transect see a line marked A to B on Fig. 3.7.

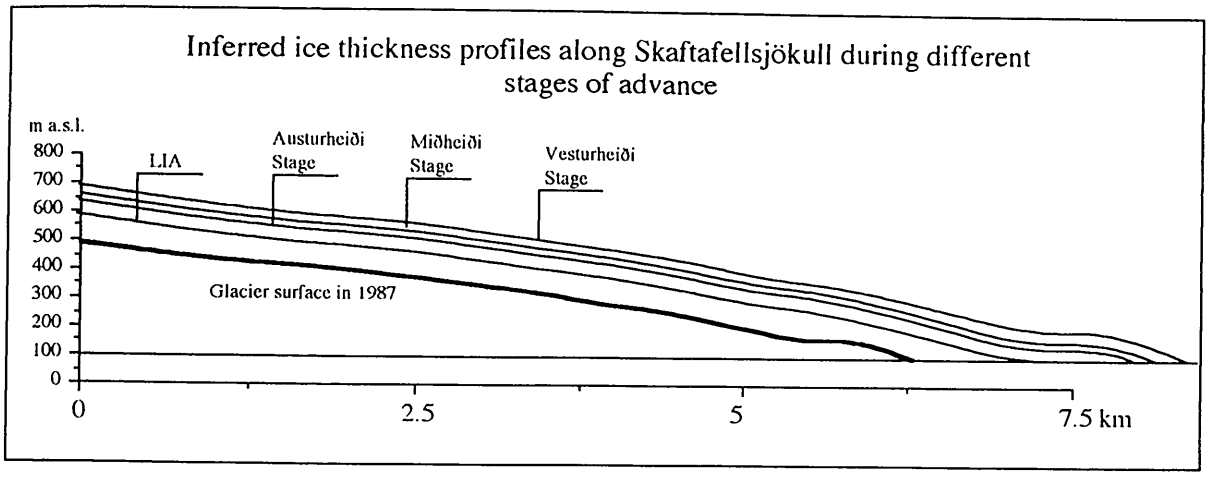

Fig. 3.9b. Inferred ice thickness along Skaftafellsjökull depicted from geomorphic evidence on Skaftafellsheidi. The ice thicknesses from cross profiles as seen on Fig. 3.9a are used to estimate the terminal extent of the glacier during its various stages of advance. Note that the profiles are drawn with the same ice surface dip as the present glacier. It is highly probable that the profile was steeper during the advances. The profile begins about 7.2 km up glacier from the 1990 position of the snout as seen on Fig. 3.7.

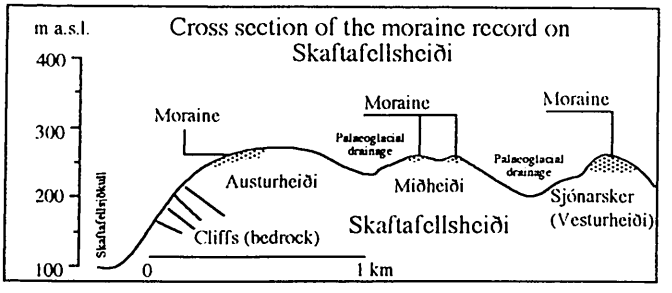

Fig. 3.9c. A cross section of the topography on Skaftafellsheiði. The dark gray areas indicate location and spatial extent of the moraines in the area. The white area is mostly bedrock covered with till. The vertical scale is slightly exaggerated to better reveal the site of the moraines. For location of section see line marked AB on Fig. 3.7.

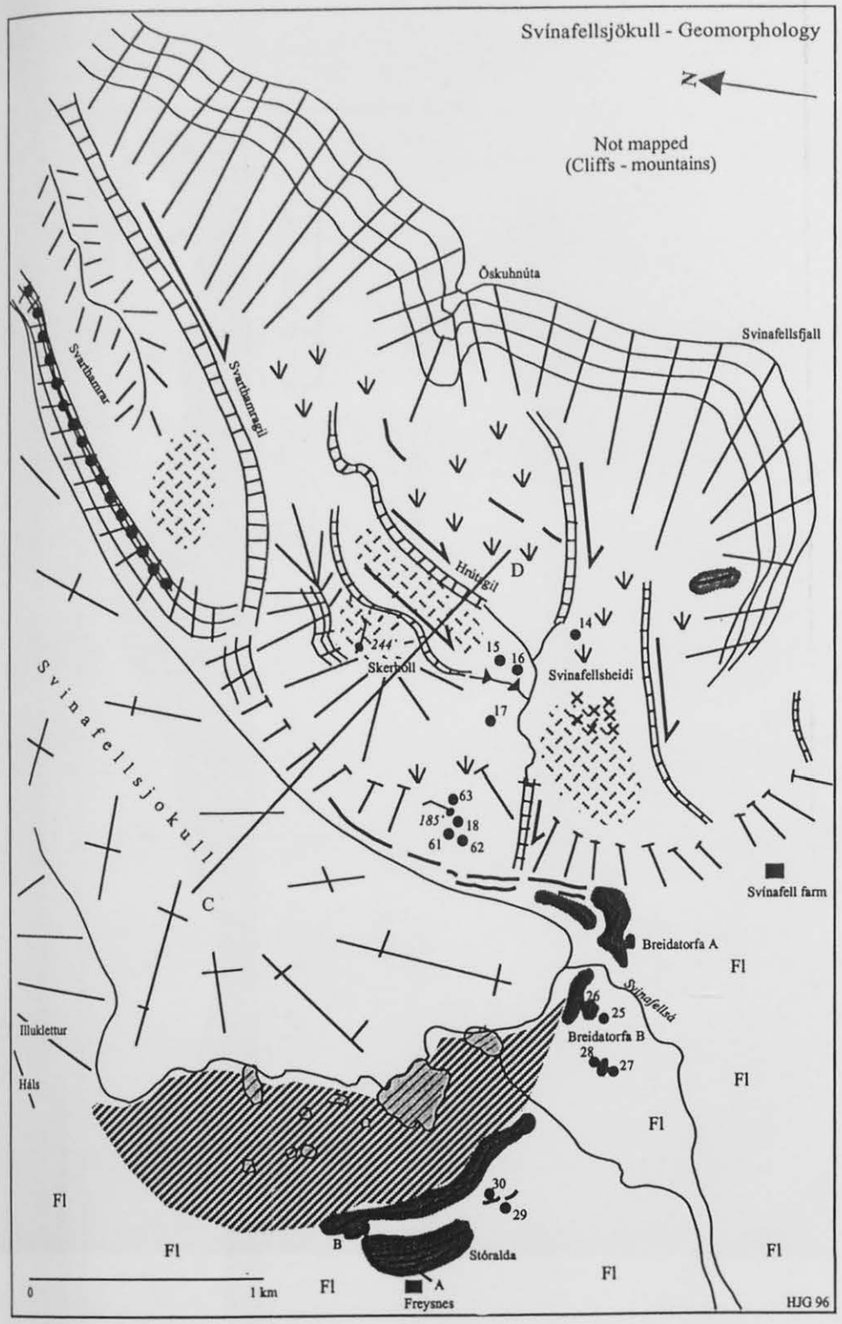

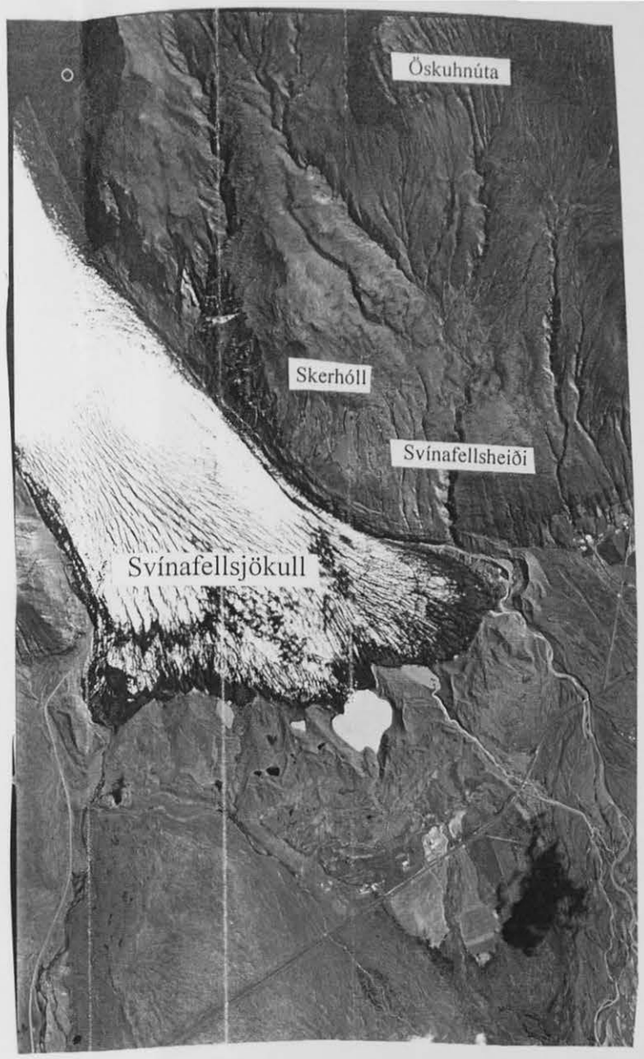

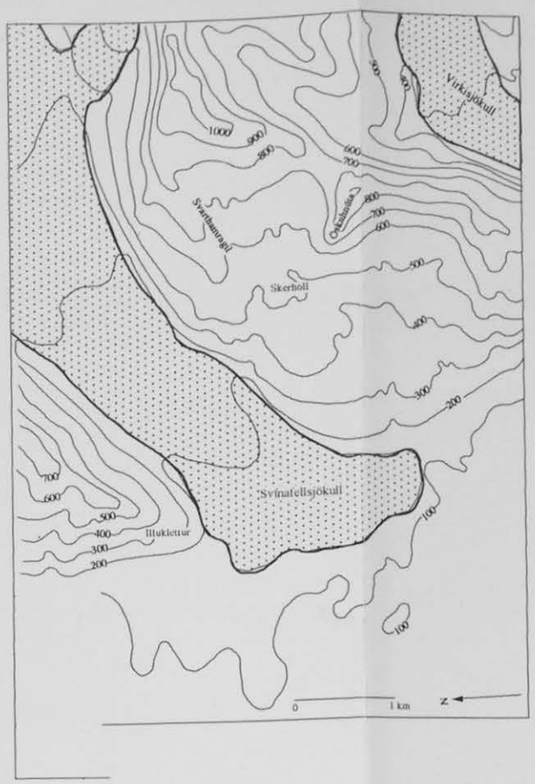

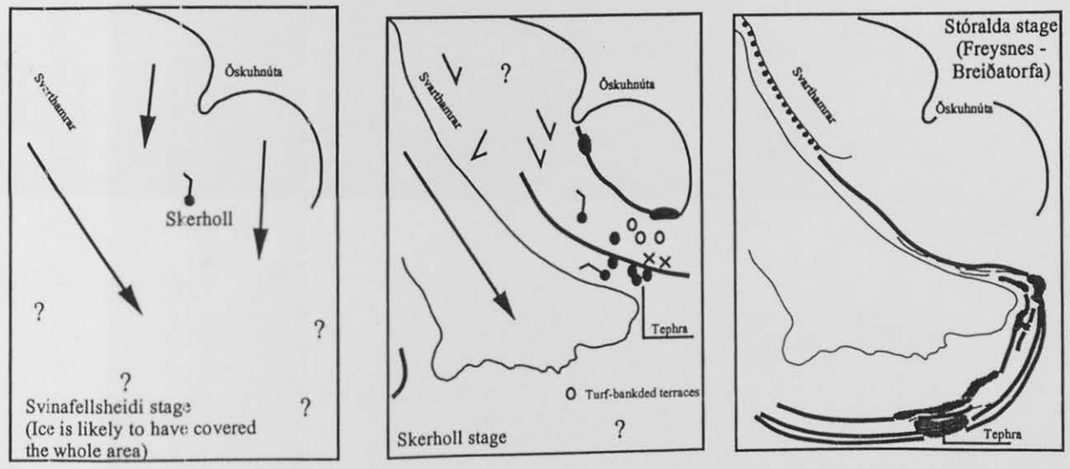

Fig. 3.10. The Geomorphology of the area around Svínafellsjökull. The small ins maps below the aerial photo show the reconstruction of the ice limits (bold curve black lines) in relation to the observed glacial geomorphology. Each inset shows single advance of the Svínafellsjökull outlet and covers approximately the same are as the geomorphic map on the left. The highland area to the east of Svínafellsjöku (Svínafellsheiði highland) is characteristed by glacier erosion and till-covered surfac exhibiting glacier activity. The proglacier area in front of the outlet is characterise by terminal moraines varying in size. The moraines rest on black basaltic outwash sandur plain.

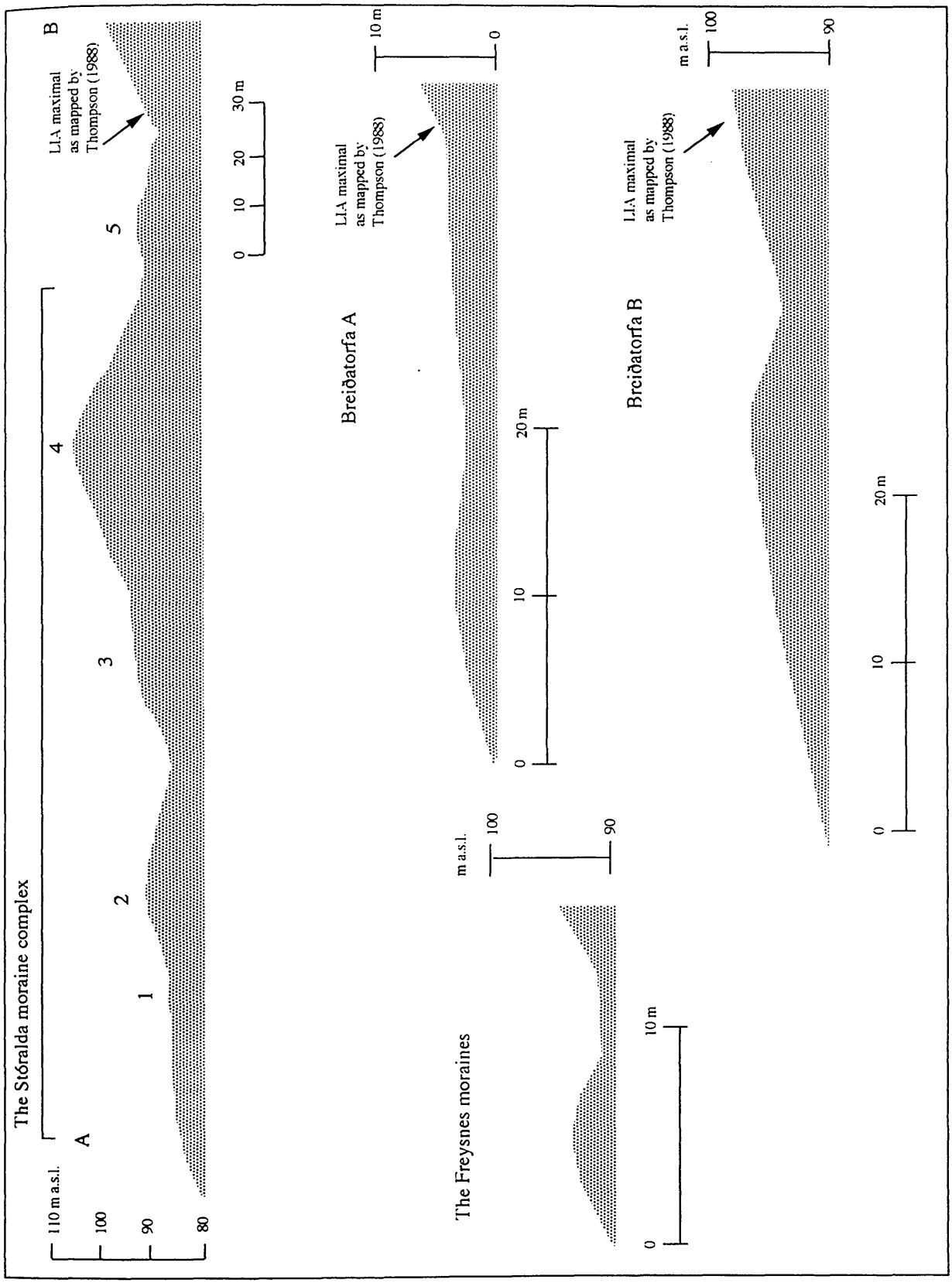

Fig. 3.11. Cross section of the Stóralda moraine complex, Breidatorfa A and B moraines and the Freysnes moraine. For location see Fig. 3.10. The moraine series demonstrate pre-LIA glacial advances of Svínafellsjökull. Note the size difference of the moraines.

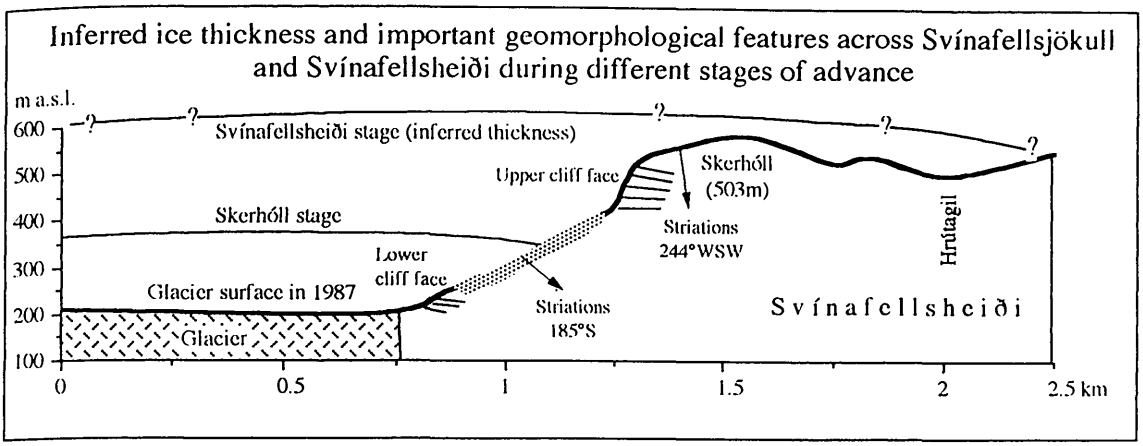

Fig. 3.12. Inferred ice thickness across Svínafellsjökull depicted from geomorphic evidence. The dark grey area indicates an ice contact slope covered with till. For location of transect see a line marked C to D on Fig. 3.10.

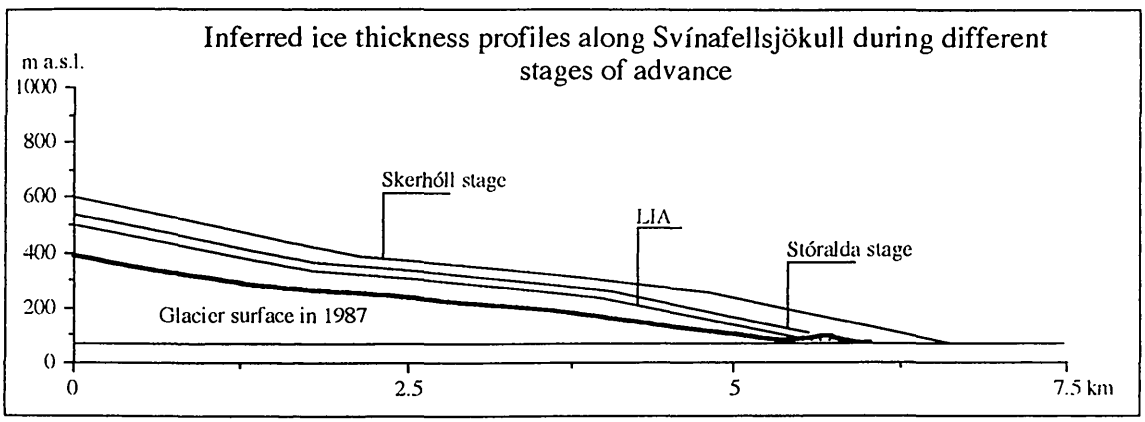

Fig. 3.13. Inferred ice thickness along Svínafellsjökull depicted from geomorphic evidence. Note that the porfiles are drawn with the same ice surface dip as the present glacier. It is highly probable that the profile was steeper during the advances. The Stóralda moraine complex is thought to represent multiple stages of advance. However, the thickness of the ice is inferred to be similar, perhaps >50m difference. This is depicted from the short interval between individual limits of the moraine complex. The inferred thickness line is drawn with the highest moraine of the complex as a reference (no. 4 in Fig. 3.11). The profile begins about 5km up glacier using the 1990 snout position as seen on Fig. 3.10.

Fig. 3.14. The Stóralda moraine complex, in foreground, as viewed from south east towards north west. The photo is taken near the Svínafell farm. The highest crest is marked no. 4 on Fig. 3.11. Skaftafellsheiði is in the centre background and Skaftafellsfjöll, to the north west of Morsárdalur, in the far background.

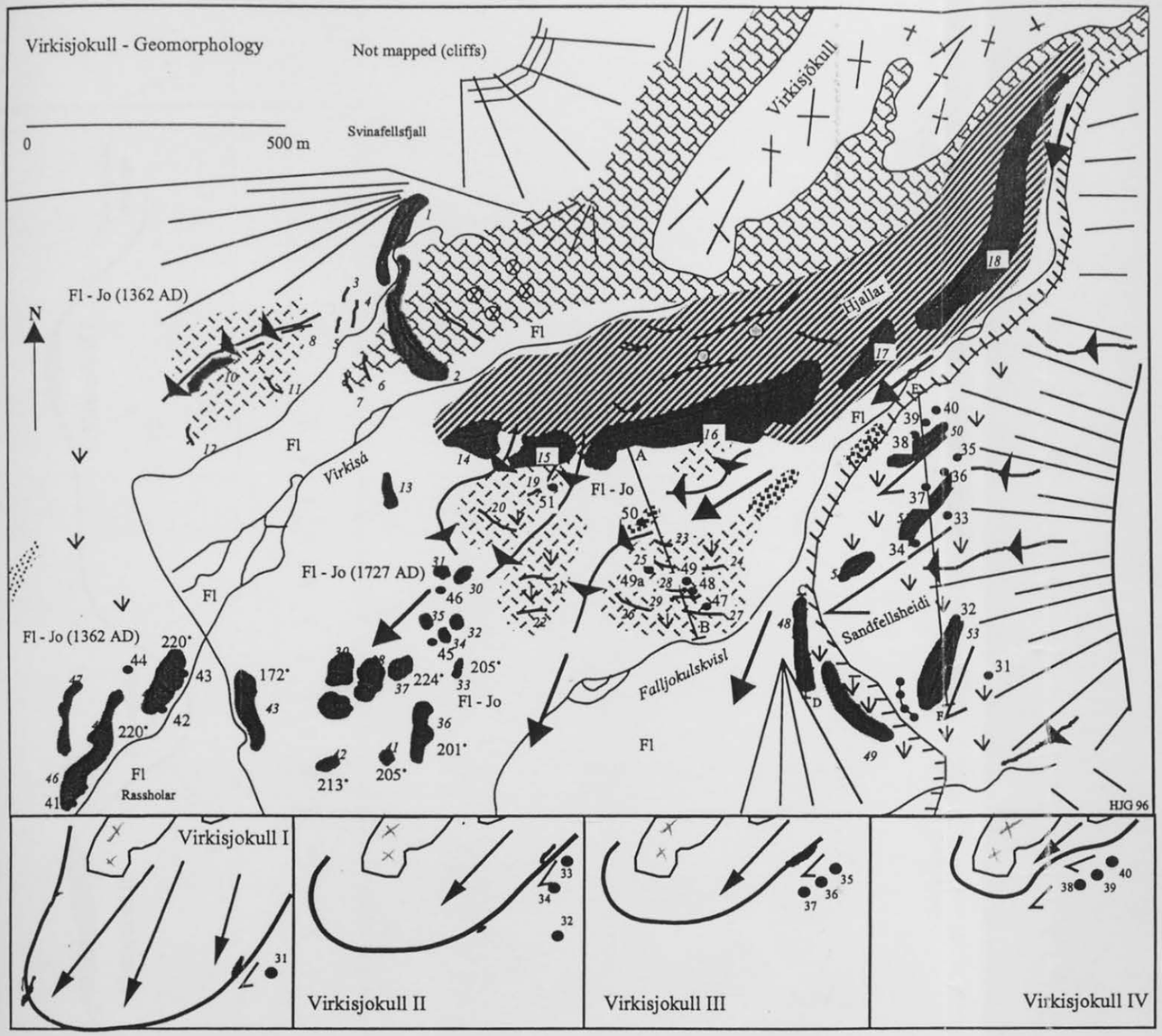

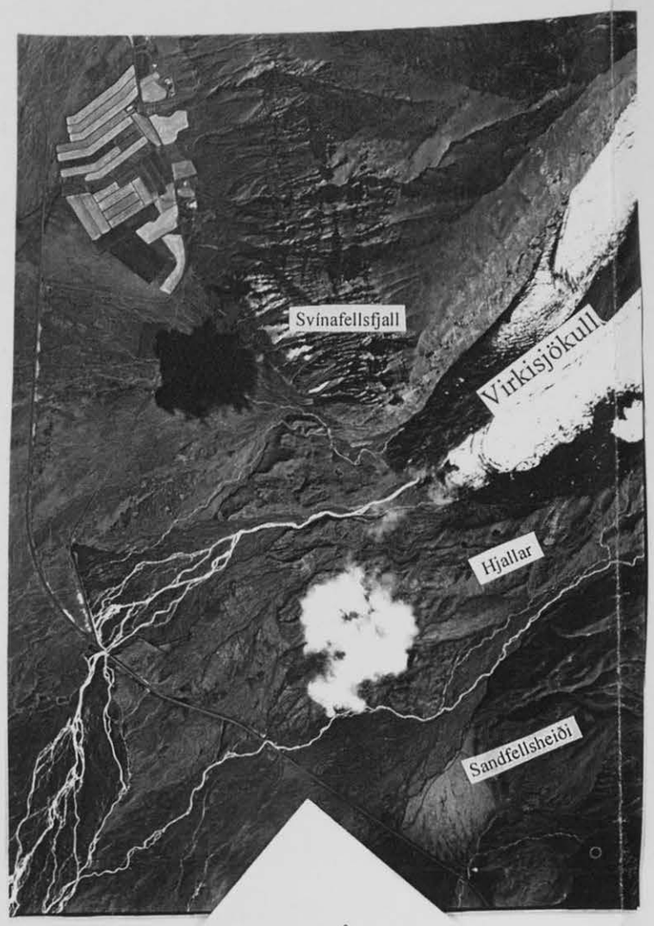

Fig. 3.15. The Geomorphology of the area around Virkisjökull. The small inset maps below the geomorphology map show the reconstruction of the ice limits (bold curved black lines) in relation to the observed glacial geomorphology. Each inset shows a single advance of the Virkisjökull outlet and covers approximately the same area as the geomorphic map. The letters in *italics* represent a specific number given to each moraine and black circles show the location of tephra profiles. The proglacier area of Virkisjökull is chararcterised by terminal and lateral moraines. The area in front of the glacier is covered by jökulhlaup deposits where moraines have been cut and washed by the flood.

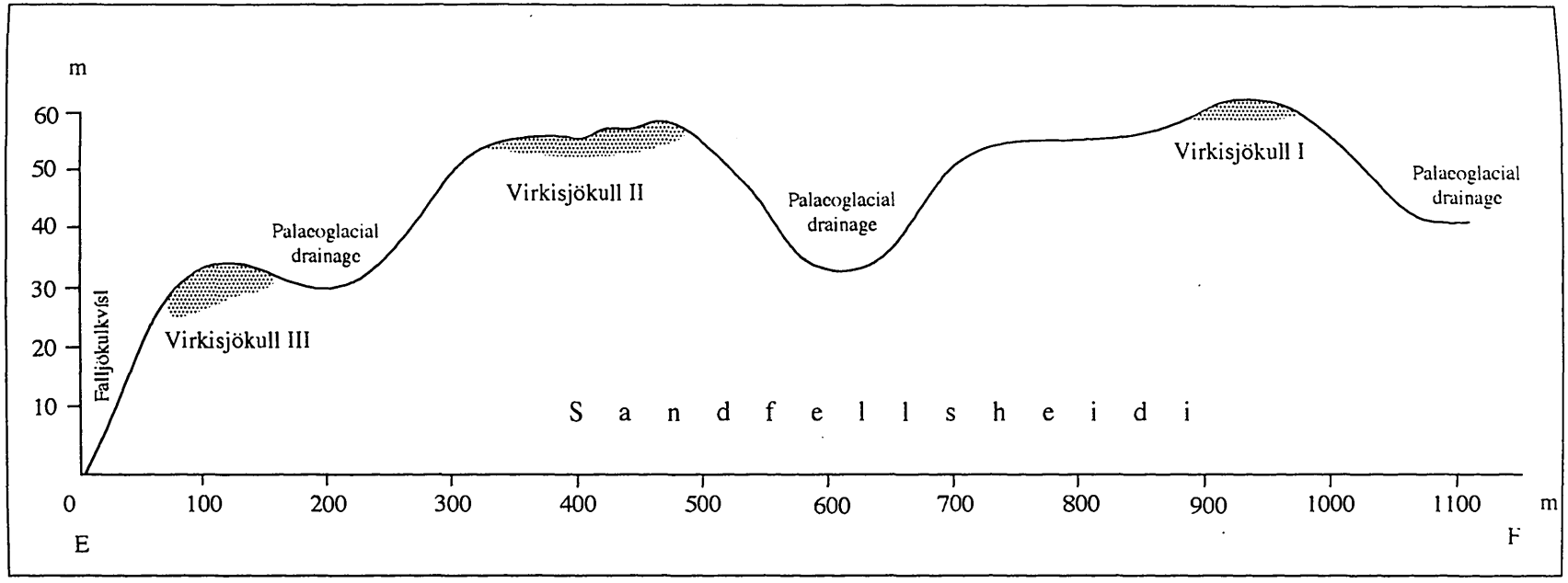

Fig. 3.16a. A cross section of moraines on Sandfellsheidi indicating three different advances. Dark grey areas mark the approximate spatial position of the moraines. For location of profile see line marked E to F on Fig. 3.15.

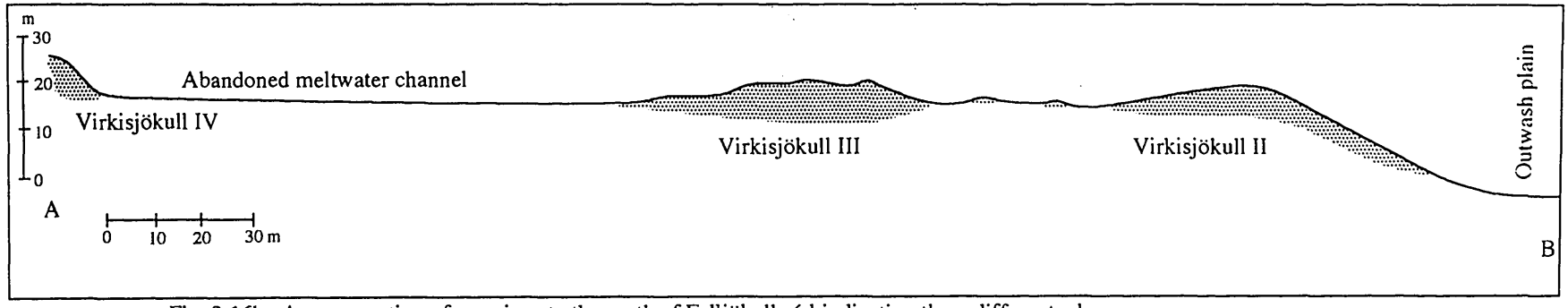

Fig. 3.16b. A cross section of moraines to the north of Falljökulkvísl indicating three different advances interpreted as representing Virkisjökull II, III and IV. Dark grey areas mark the approximate location of the moraines. For location of profile see line marked A to B on Fig. 3.15.

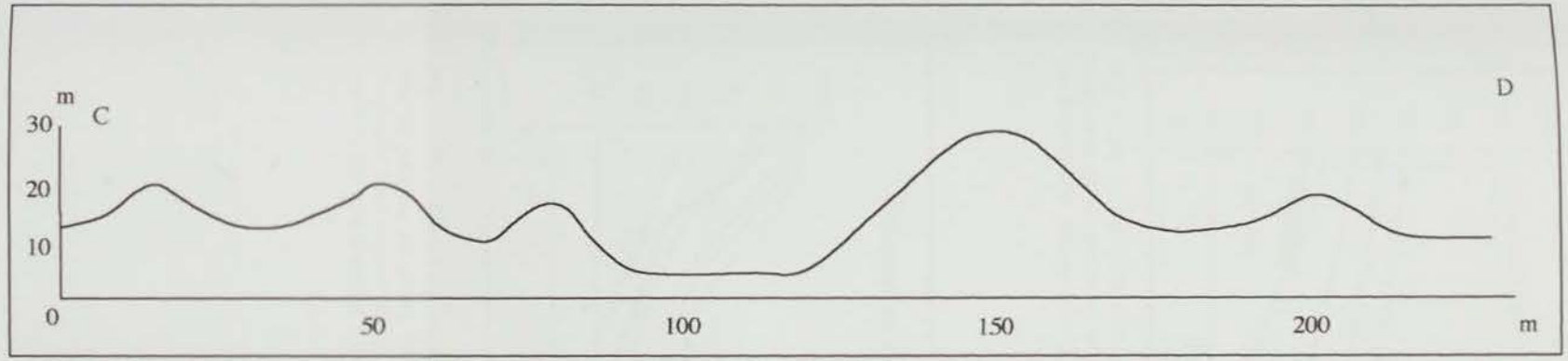

Fig. 3.18. A long profile of moraine no. 48 showing several small ridges. They represent several advances or still stands and are similar as the pattern of moraine remnants between Virkisá and Falljökulskvísl. The zero level is the outwash plain. For location of profile see line marked CD on Fig. 3.15.

Fig. 3.17. The moraines on Sandfellsheiði (centre of photo) as observed from moraine no. 16 towards east (see Fig. 3.15). These lateral moraines indicate extensive advances of Virkisjökull (I, II and III).

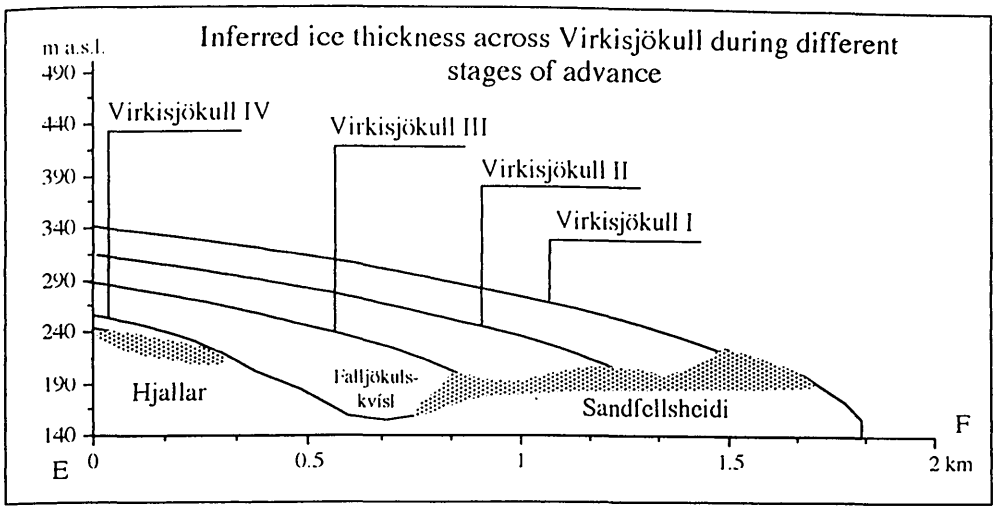

Fig. 3.19a. Inferred ice thickness across Virkisjökull depicted from geomorphic evidence. Note that the profiles are drawn with the same ice surface dip as the present glacier. It is highly probable that the profile was steeper during the advances. For location of transect see a line marked EF on Fig. 3.15.

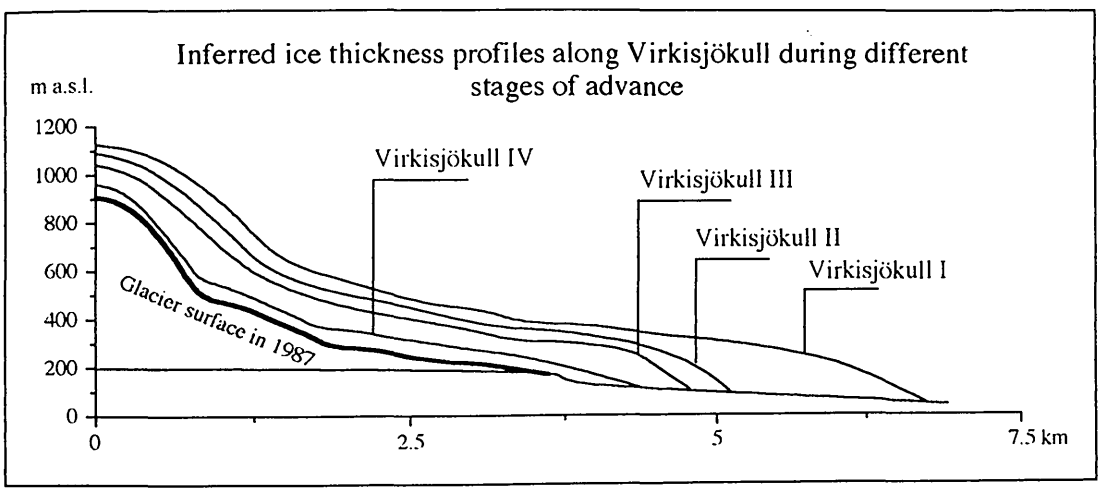

Fig. 3.19b. Inferred ice thickness profiles along Virkisjökull depicted from geomorphic evidence. Note that the profiles are drawn with the same ice surface dip as the present glacier. It is highly probable that the profile was steeper during the advances. The profile was drawn on top of Falljökull, the eastern outlet of the two forming Virkisjökull.

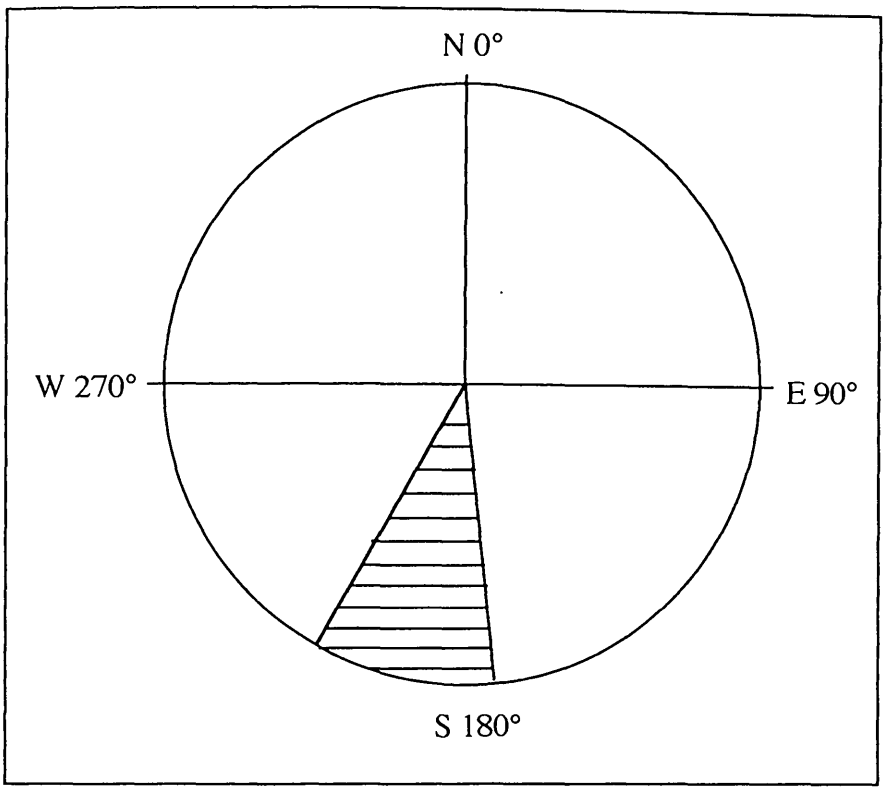

Fig. 3.20. The orientation of the long axis of moraines between Virkisjökull I and II. The horizontally lined area marks the distribution of the measurements which generally shows south by south west orientation. The mean is 208°S. The mean length/width ratio of these moraines is 3:1, the mean proximal slope is ca. 10° and the mean distal slope ca. 16°. The mean proximal/distal slope ratio is 1:1,6. For location of moraines see Fig. 3.15 where each feature measured is marked by its orientation.

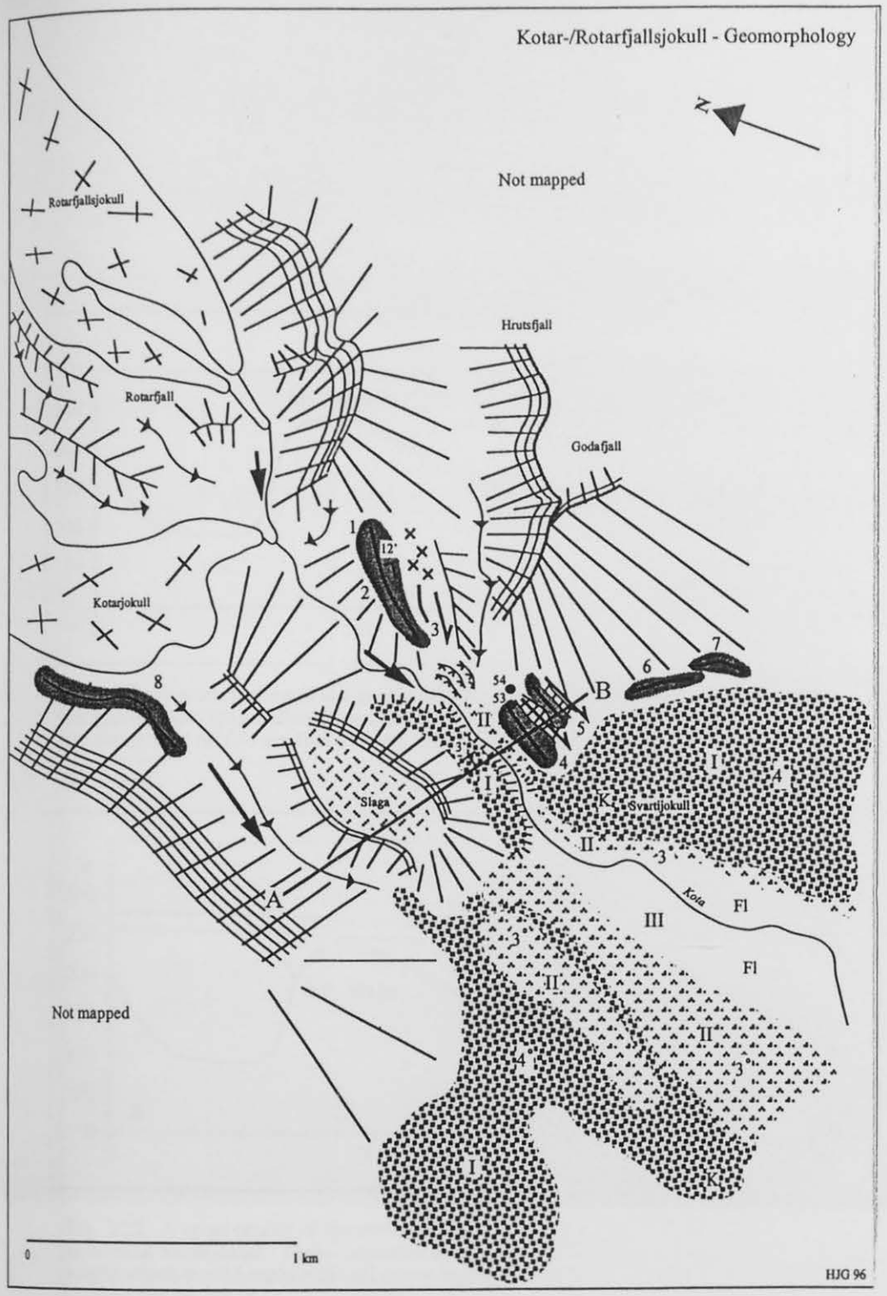

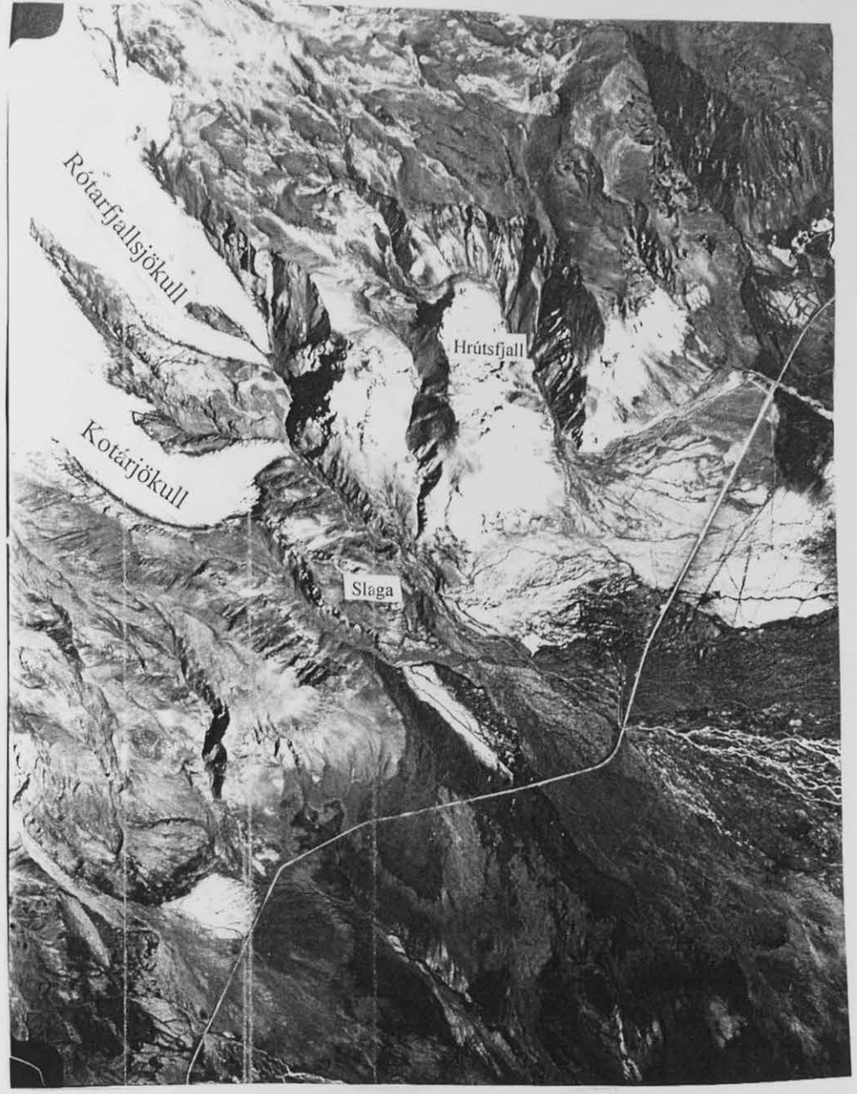

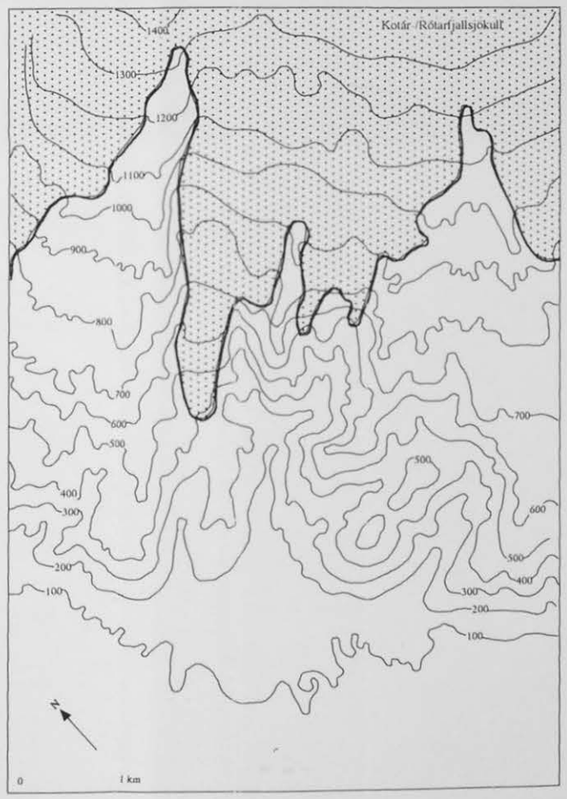

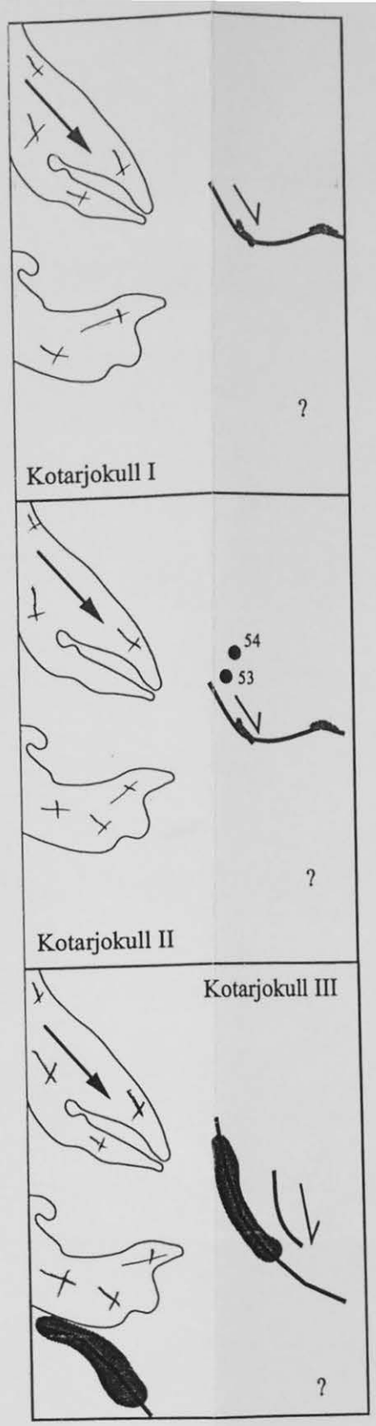

Fig. 3.21. The Geomorphology of the proglacier area of Kotárjökull. The small inse maps on the right show the reconstruction of the ice limits (bold curved black lines) i relation to the observed glacial geomorphology. The small inset maps on the rigl show single advances of the Kotárjökull outlet. The insets cover approximately th same area as the geomorphic map on the left. The letters in *italics* represent a specif number given to each moraine and black circles show the location of tephra profile Topography of the area is shown on the map below the aerial photo. Contour interv is 100 m. The geomorphology of the area is characterised by glacier erosio moraines and extensive jökulhlaup deposits.

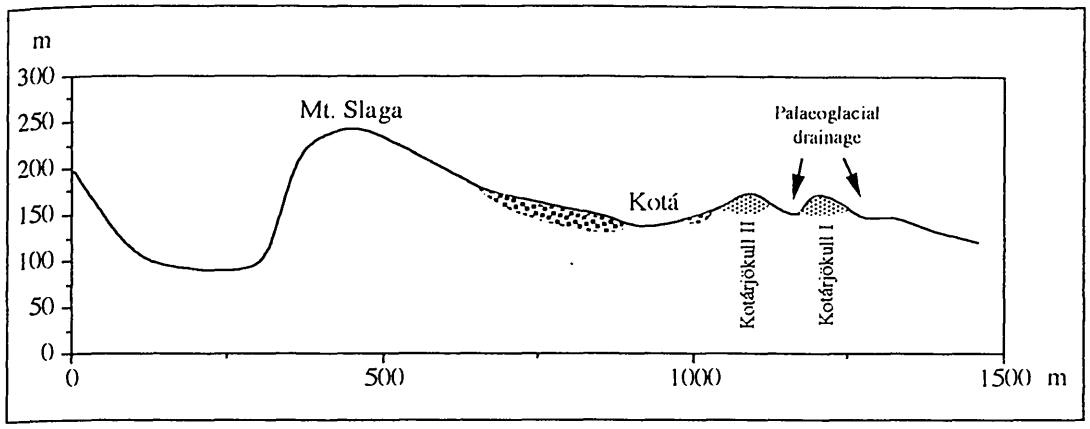

Fig. 3.22. A cross section of the proglacial area in front of Kotárjökull. The dark grey areas indicates the approximate spatial distribution of moraines and the black dotted areas the 1727 AD jökulhlaup deposits. For location of profile see line marked AB on Fig. 3.21.

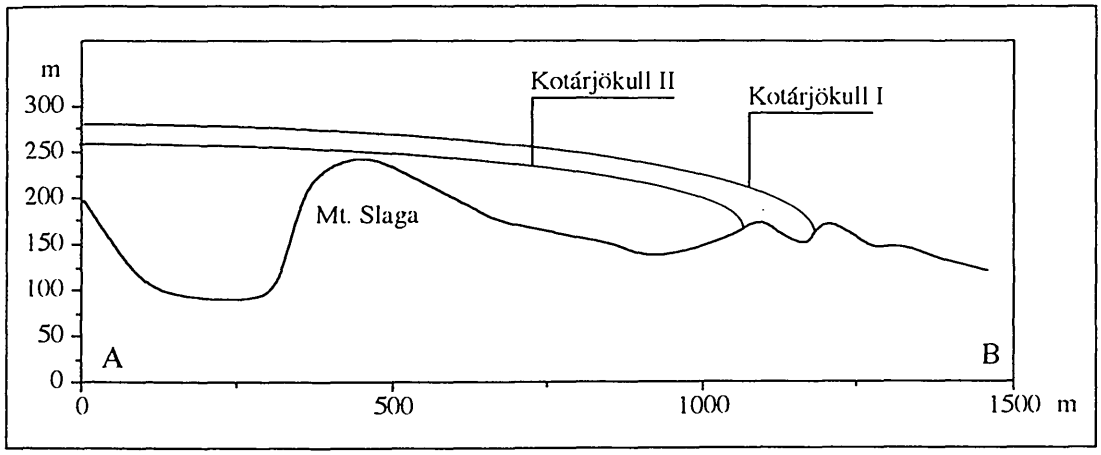

Fig. 3.23. A cross profile of the surface and estimated ice thickness during different stages of advance in front of Kotárjökull. These estimates indicate that Mt. Slaga was ice covered during these stages which would explain the till cover found on top of the mountain. For location of profile see line marked AB on Fig. 3.21.

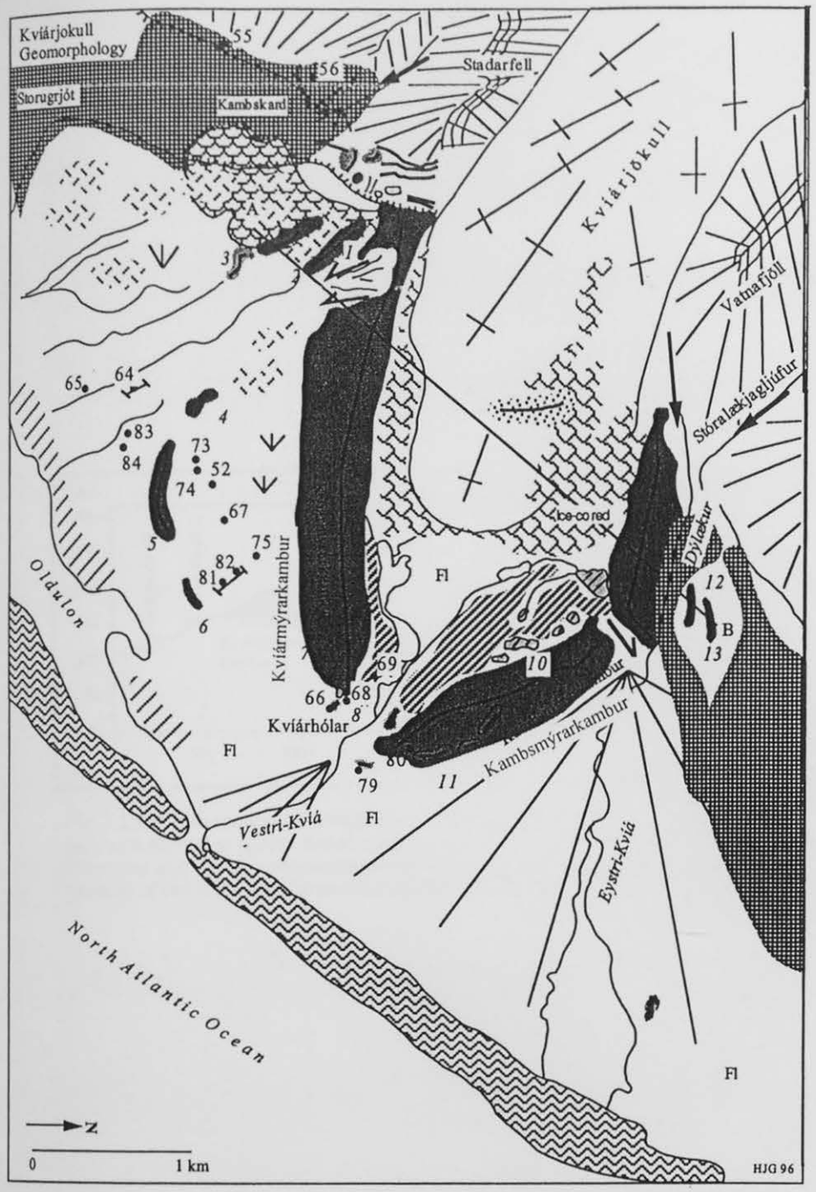

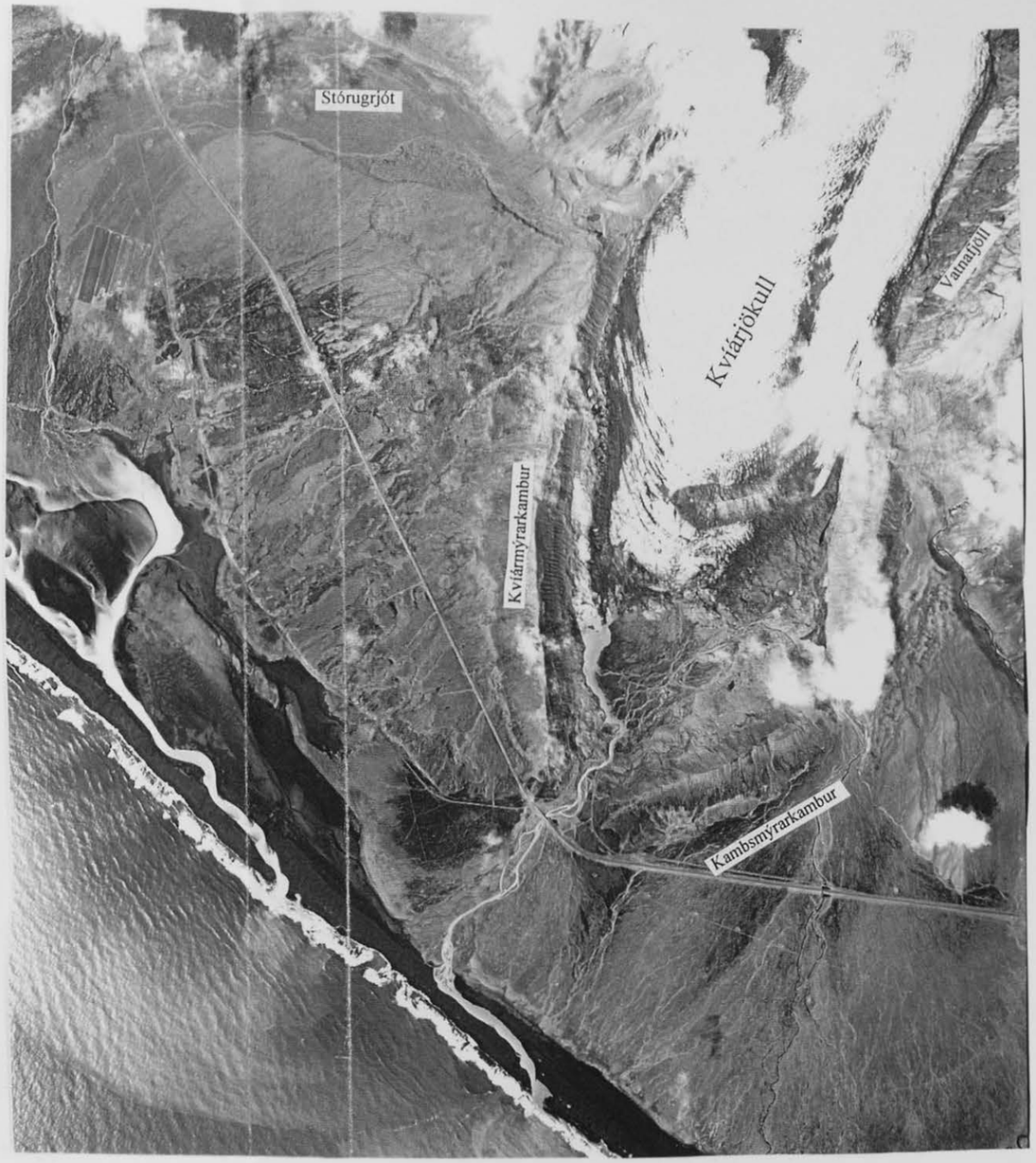

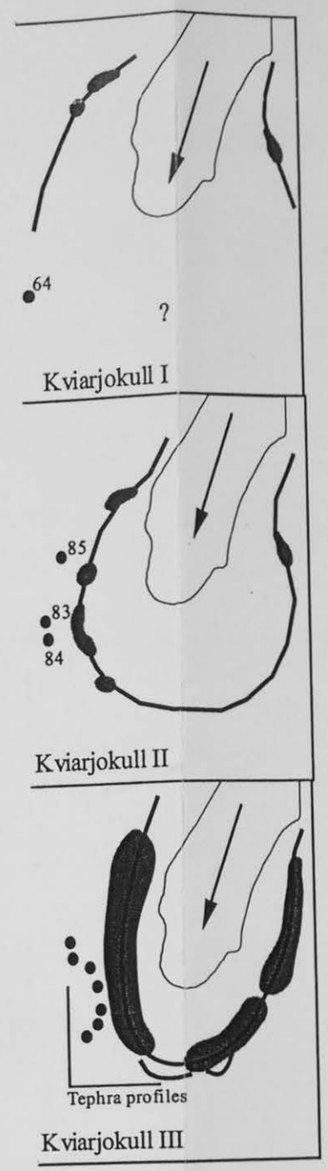

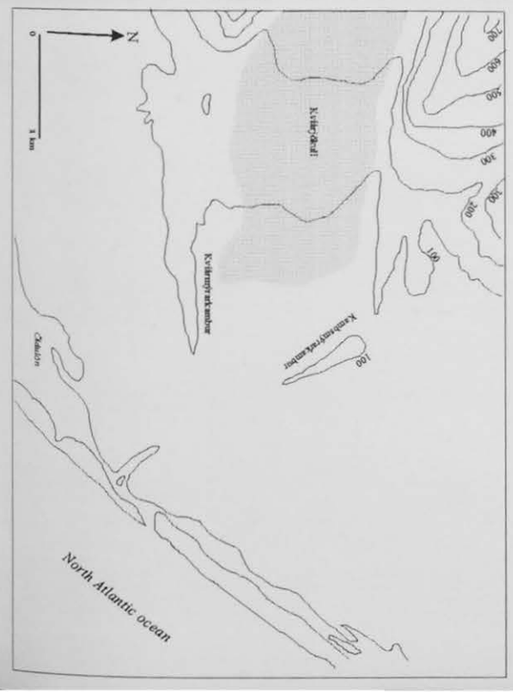

Fig. 3.24. The Geomorphology of the proglacier area of Kviárjökull. The small inset maps on the right show the reconstruction of the ice limits (bold curved black lines) in relation to the observed glacial geomorphology. The small inset maps on the right show single advances of the Kviárjökull outlet. The insets cover approximately the same area as the geomorphic map on the left. The letters in *italics* represent a specific number given to each moraine and black circles show the location of tephra profiles. Topography of the area is shown on the map below the geomorphology map. The geomorphology of the area is chararcterised by lateral moraines of different sizes, till cover and jökulhlaup deposits.

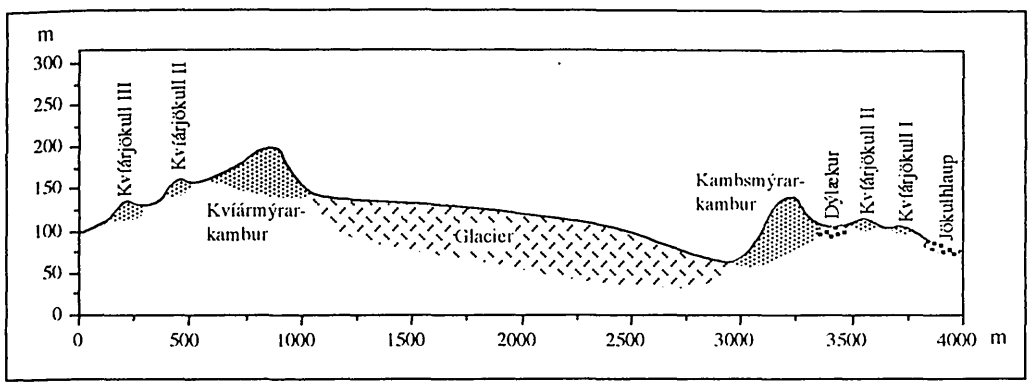

Fig. 3.25. Cross section of Kvíárjökull moraines showing different advances of the glacier. The dark grey area represent spatial distribution of moraines. Note the contrast in moraine size between the innermost and the two outermost ridges. The base of the moraines and the glacier is hypothetical. For location of the cross section see line marked AB on Fig. 3.24.

Glacier	*Limit*	*Moraine no.*	*Moraine height*	*Material*	*Type*	*Comments*
Table 3.1						
Morsárjökull	South		1-3m	Matrix supported gravel	Terminal	Boulders subangular
	North		4-6m	Matrix supported gravel	Terminal	Boulders subangular
Table 3.2						
Skaftafellsjökull	Vesturheidi	1,3,4,5	ca. 40m	Matrix supported gravel	Lateral	Boulders subangular and frost-shattered
	Midheidi	2,6,7,8	2-3m	Matrix supported gravel	Lateral	Boulders subangular
	Austurheidi	9-13,14-16	3-10m	Matrix supported gravel	Lateral	Boulders subangular and frost-shattered
Table 3.3						
Svínafellsjökull	Stóralda	1,2,3.5	2-5m	Matrix supported gravel	Terminal	
	Stóralda	4	25m	Matrix supported gravel	Terminal	Occasional boulders
	Breiðatorfa		3m	Matrix supported gravel	Terminal	No boulders
	Freysnes		2m	Matrix supported gravel	Terminal	No boulders
Table 3.4						
Virkisjökull	Virkisjökull I	8,9,10,46,47,53	5-9m	Matrix supported gravel	Lateral/Terminal	Gravel subangular
	Virkisjökull II	3,5,7,13(?),21,26,27,51,52	5-7m(52=26m)	Matrix supported gravel	Lateral/Terminal	Gravel subangular
	Virkisjökull III	4,6,20(?),23(?),24,25,50	7-12m	Matrix supported gravel	Lateral/Terminal	Gravel subangular
	Virkisjökull IV	1,2,14-18	20-30m)	Matrix supported gravel	Lateral/Terminal	Gravel subangular
	Unidentified	32-49	2-30m	Matrix supported gravel	Terminal	Gravel subangular
Table 3.5						
Kotárjökull	Kotárjökull I	5,7	5-17m	Gravel	Lateral	Subangular to angular. Material frost-shattered
	Kotárjökull II	4,6	15-20m	Gravel	Lateral	Subangular to angular. Material frost-shattered
	Kotárjökull III	1,2,3,8	3-20m	Sand supported gravel	Lateral	Subangular. Material frost-shattered
Table 3.6						
Kviárjökull	Kviárjökull I	2,3,13	ca.10m (13=4m)	Sand supported gravel	Lateral	Subangular. Material frost-shattered
	Kviárjökull II	1,4,5,6,12	ca.10m(12=4m)	Sand supported gravel	Lateral	Subangular. Material frost-shattered
	Kviárjökull IIIa	7,11,14	70-100m	Sand supported gravel	Lateral	Subangular - subrounded. Boulders
	Kviárjökull IIIb	7,10,11,14	70-100m (10=3-8m)	Sand supported gravel	Lateral	Subangular - subrouned. Material in no.10 frost-shattered
	Kviárjökull IIIc	7,8,11,14	70-100m(8=5-10m)	Sand supported gravel	Terminal	Subangular. Material frost-shattered

Tables 3.1-6. Characteristics of moraines in the study area. Note the great variability in moraine size. Moraine locations can be seen on the relevant geomorphic maps.

Chapter 4. The tephrochronology of the Öræfi district

4.1 Introduction

The aim of this chapter is to develop a local tephrochronology in order to date the observed glacier fluctuations.

The most precise dating control is obtained by using tephra layers coupled with historical dates, radiocarbon dating and calculation of sediment accumulation rates. The tephra layers form precise age-equivalent *isochrones* (marker horizons) that, when abundant, can be used to date effectively the intercalated geomorphological record. The age and origin of the tephras deposited in Öræfi is poorly known, especially the pre-historical part of the record before the settlement of Iceland around ca. 870 AD (Hallsdóttir, 1987; Grönvold *et al.*, 1995). This makes it necessary to construct a regional tephra stratigraphy and then link this with 'absolute' dating techniques in order to create an effective chronology. The first step was to create a stratigraphic framework, based on ca. 90 profiles recorded from open sections in soils, peat and lacustrine sediments. Stratigraphic connections were confirmed with geochemical fingerprinting of constituent tephra grains. This helped to determine the origin and subsequently the age of a tephra layer. If the age is unknown, it has to be determined by written sources (the historic period), radiocarbon dating and sediment accumulation rates.

Three absolute dating methods have been widely practised elsewhere in Iceland (e.g. Thórarinsson, 1961; Larsen and Thórarinsson, 1977; Larsen, 1981, 1982; Dugmore, 1989a; Dugmore *et al.*, 1995a). The first method is to analyse written sources, such as annals, to determine the age of the tephra falls. This has been widely adopted for historical eruptions e.g. Thórarinsson (1944, 1958, 1967, 1975) and Larsen (1978) but, as stressed by Ogilvie (1984), suitable caution has to be exercised because of the limitations of some parts of the annals in terms of both accuracy and completeness. The second method is to use radiocarbon dates, and the third is to use Soil

Accumulation Rates (SAR) to interpolate and extrapolate dates (Thórarinsson, 1958; Dugmore, 1987). Soil accumulation rates have been shown to be particularly effective in the pre-historic record in Iceland where specific profiles in a similar geomorphological settings can be determined within ±100 years.

No original annals investigations were attempted to trace the age and origin of tephra layers in Öræfi because a framework had already been established by Thórarinsson (1958) in Öræfi and in other parts of Iceland by Thórarinsson (1967, 1974, 1975) and Larsen (1978, 1984). However, the record reported by Thórarinsson (1958) needed refinement and revision because new tephra layers were identified in the study area. The pre-historical tephras of Öræfi have not been investigated to date and therefore had to be analysed in detail to determine the origin and subsequently the age. In addition, the tephras had to be locally and regionally correlated and linked with the well-established tephra record elsewhere in Iceland. Only one radiocarbon date existed in the area prior to this study (Black, 1990).

The following chapter is divided into three parts. The 1362 AD eruption of Öræfajökull (Thórarinsson, 1956) and the eruption of Hekla-4 about 3830 years BP (Larsen and Thórarinsson, 1977; Dugmore *et al.*, 1995a) will be used to distinguish three chronostratigraphical sections. In many ways it would have been more appropriate to use Vö ca. 900 tephra, or the Landnám layer (Thórarinsson, 1944, 1967; Larsen, 1984; Hallsdóttir, 1987; Grönvold *et al.*, 1995) for this purpose following Dugmore (1987) in Eyjafjallajökull, south Iceland. However, because this layer could not be identified with certainty in the majority of sections logged in the study area, the idea was abandoned and the Ö1362 tephra used instead because of its abundance and excellent potential as an isochrone. It has been detected in the GISP2 ice core (Palais *et al.*, 1991) which consequently creates an opportunity to link the chronologies of two geographically different regions in the North Atlantic. Additionally, a distinctive feature of much of Iceland is the profound environmental changes at Landnám with the first extensive human settlement (e.g. Hallsdóttir, 1987). In the Öræfi region, however, the impact of the Ö1362 AD eruption of Öræfajökull is

one of the most profound events of the late Holocene (Thórarinsson, 1958). Using this isochrone to divide major lithostratigraphical units does, therefore, identify a most significant local environmental change in the district.

The first part of this chapter describes the post-1362 stratigraphy. This has been studied by Thórarinsson (1956, 1958) but the record turned out to be more complicated than older investigations suggest. More tephra layers were identified and mapped in soil sections. Chemical analyses were conducted on the upper part of the stratigraphy and correlation with published data was used to identify tephra layers in the lower part. The second and third part of this chapter will describe the pre-1362 AD stratigraphy using the Hekla-4 tephra as a marker to split up the distinctive parts. The Hekla-4 tephra can be traced extensively in soils in the study area and is therefore an excellent principal marker horizon.

An idealised composite profile of the period from the Hekla-4 tephra to present is drawn in Fig. 4.1. This diagram is mainly based on the tephra stratigraphy from Skaftafellsheiði and Svínafellsheiði because of a lack of suitable sections from Kviárjökull. However, Ö1362, Hekla-4 and the Skaftafellsheiði tephra are clearly visible in most sections. It was impossible to build a definitive composite tephra stratigraphical profile of pre-Hekla-4 time in Öræfi due to the complexity of the record (Fig. 4.1). Because of high spatial variability, each tephra layer from this period is recognisable only over a limited area (Fig. 4.1). The regional stratigraphy will be discussed in a summary at the end of the chapter and put in the wider context of Iceland. All profiles are stored in a pocket attached to the inner side of the back cover of the thesis and are labelled according to the nearest glacier. These will be referred to as Sheets I-VI.

4.2 Analytical methods

The analytical methods of the geochemistry have been described in Chapter 2. Nine elements were analysed and the abundance listed in various tables referred to in the text. The tables are located in Appendix II. Dugmore *et al.*, (1995a) have shown that

replicable and consistent results can be obtained with element totals >95%, that are most effective for correlating tephras. With totals well below this figure changes in apparent abundance of elements can be influenced by the analytical total. In this study, totals exceeding 94% for silicic and 96% for basaltic grains are accepted as showing sufficient consistency for correlation. Inconsistent, low totals of all samples were rejected. All components are expressed as weighted total percentage (wt%) and total iron as FeO. Na is a potentially unstable element under x-ray analysis by electron microprobe. It is therefore analysed twice, at the beginning and at the end of each analysis. This is done to monitor the loss during the analysis process as a result of Na migration. If the Na loss is significant it leads to a slight increase in the SiO_2. This was always checked by looking at the Na wastage in the analysis.

In order to guard against bias caused by machine instability, andradite was used as a standard and analysed after every tenth analysis. In Table 4.1 (Appendix II), variation of the andradite standard readings are shown. They show consistency and relatively low standard deviation throughout. They match the values obtained by Dugmore *et al.*, (1992), and can be used as error estimates for the geochemical results.

The radiocarbon method was used to date tephras and important horizons. However, samples could only be extracted from the Kviárjökull proglacial area because of lack of organic material in profiles elsewhere in the study area. Four dates were obtained (Table 4.2; Appendix II). Samples of peat and tree stumps were extracted and cleaned before submission to SURRC. Selected organic material was hand-picked from a bulk peat sample extracted in the field. The sample was collected from no more than 1 cm below the horizon to be dated in the laboratory. Tree fragments were hand-picked and provisionally cleaned in the field. In the laboratory in Edinburgh, they were further cleaned before submission to SURRC. Cellulose from tree fragments was dated.

The key to stratigraphic symbols is shown on Fig. 4.2 and applies to all profiles in this study. The tephra grain size division and stratigraphic symbols are adopted from

Thórarinsson (1958). Coarse grains are defined as >2 mm, intermediate 0.2 - 2.0 mm and fine grains <0.2 mm. Soil classification is adopted from Arnalds (1990) where Icelandic soils are classified as andisols which are developed in volcanic ejecta. This soil type shows a distinctive combination of characteristics including high organic matter content, low bulk density, high water-holding capacity and mineralogy dominated by short-range order minerals.

4.3 Post-1362 AD tephra stratigraphy

4.3.1 Tephra layers formed since the eruption of Öræfajökull in 1727 AD

Five tephras are considered in this section (Fig. 4.1) which are best represented in profiles 6, 7, 10 and 11 on Skaftafellsheiði (Sheet II). Four of these layers can be identified with high certainty with the aid of geochemical analysis, namely K1918, G1786, K1755 and Ö1727. One of the tephras could not be identified with certainty. However, it probably originates from some of the 19th Century eruptions in Grímsvötn reported by Thórarinsson (1974).

Öræfajökull (Ö)1727.

The eruption of Öræfajökull in 1727 forms the first continuous isochrone in the Öræfi district and can be traced as a coarse-grained black tephra usually about 2 - 4 cm thick. When reworked it is up to 40 cm thick, for example on steep slopes and infills in small interfluves cut in the terrain. Thórarinsson (1958) has briefly described this eruption, mainly the consequent jökulhlaup, but did not study the tephra fall in any detail. The tephra from this eruption is thickest and coarsest in the western part of the area and finer on the eastern side, at Kviárjökull (cf. Sheet I profiles 1,2; Sheet II profiles 6, 7, 10; Sheet III profiles 14, 18, 19 - 22; Sheet IV profiles 33, 35; Sheet VI profiles 55, 56, 64). The implication is that the dispersal axis was orientated to south west. The tephra layer immediately above the Ö1727 layer is interpreted as a secondary deposition because it is a mixture of grains and other sediment, probably reworked by wind shortly after the eruption. The Ö1727 tephra layer was sampled from profile 21 on top of Stóralda at Svínafell (Sheet III) in order to analyse the geochemical characteristics. The results are shown in Table 4.3 and reveal an

andesitic composition according to the classification system of Le Maitre (1989) with silica and potassium content constant at about 58% and 1.6%, respectively.

Katla (K) 1755.

The first tephra layer above the Ö1727 tephra in the study area has been mapped by Thórarinsson (1956, 1958) as originating from the eruption of Katla in 1755. This eruption was the biggest Katla eruption in historical times where the main dispersal axis was to the north and north east and caused devastation in Skaftártunga, Álftaver and western part of Síða (Thórarinsson, 1974). These areas are about 50 - 70 km west of Öræfajökull. This tephra layer forms a band of fine to medium-grained black 1 - 2 cm thick tephra which can be traced in nearly all profiles logged at the western side of the study area (e.g. Sheet II profiles 7, 10, 11; Sheet II profiles 14, 18, 21, 22; Sheet IV profiles 33, 35). At Kviárjökull this layer could not be detected with certainty. The tephra layer was sampled from profile 22 (Sheet II) on Stóralda for geochemical analysis. The results are shown in Table 4.4 and compared with other volcanic systems to determine the origin on a FeO-TiO_2 plot in Fig. 4.3. The black colour indicates a basaltic layer from a system to the west; the thickness indicates a major tephra fall. The geochemical results confirm that this layer is derived from the Katla volcanic system. Combined with the stratigraphical position above the Ö1727 layer, the only realistic possibility is for this tephra layer to have been produced by the eruption of Katla in 1755.

Grímsvötn (G) 1784.

Several eruptions beneath the south west corner of the Vatnajökull ice cap have been reported by Thórarinsson (1974) most of which might be attributed to the Grímsvötn area. A thin band (<1 cm) of fine-grained greyish to blue-black tephra can be found in most historical profiles in the study area (e.g. Sheet II, profiles 6, 7, 10, 11; Sheet III, profile 19-22). Thórarinsson (1956, 1958) identified this layer as the tephra from the eruption of Lakagígar in 1783-1786 (L1783) which caused a major famine in Iceland. However, later studies of this layer conducted by Thórdarsson (1990) indicated that the tephra fall went no further than Skaftafell in the east where it was traced as being very patchy and therefore not likely to form a continuous layer in the Öræfi district. This tephra layer was sampled for geochemical analysis and the result is shown in

Table 4.5. It originates from the Grímsvötn volcanic system (Fig. 4.4). There are two grains with different chemical composition which can be explained by being secondary deposition, or 'stray' grains, but the bulk of the analysis shows a Grímsvötn origin. The age of the layer can be estimated from soil accumulation. Comparisons between various profiles where the layer was found shows that it usually occurs proportionally at the same distance above K1755 as the soil thickness between Ö1727 and K1755. This means that about 28 years elapsed between the Grímsvötn layer and the K1755 tephra. Given this estimate the deposition of this particular Grímsvötn layer occurred around 1783. The closest possible Grímsvötn eruption to this date would be that of 1784 as reported by Thórarinsson's (1974) historical Katla eruption and Steinthórsson (1977) in an ice core from Bárðarbunga. This eruption is thought to have accompanied the Laki eruption (L1783).

K1918.

The uppermost tephra layer in the Öræfi district is a 0.5 - 1 cm thin band of fine grained black ash, usually about at 10 - 12 cm depth in loessial soil (most historical profiles on Sheet I - VI) This tephra has been identified by Thórarinsson (1956, 1958) as the eruption of Katla in 1918. The bulk of the ash from this eruption went due north by north east according to Thórarinsson (1974). The tephra layer was sampled for chemical analysis (Table 4.6) in a section in front of Skaftafellsjökull close to the meltwater river Skaftafellsá which drains Skaftafellsjökull (Fig. 3.7). It is basaltic and can be best distinguished by a FeO/TiO2 plot (Fig. 4.5) which reveals a good overlap with the chemistry of Katla eruptions in historical time (Haflidason *et al.*, 1992). As there is no record of tephra fall in the Öræfi district from the Katla eruptions of 1860 or 1823, the stratigraphical position, combined with the chemical composition, would strongly suggest that this tephra is from the eruption of Katla in 1918.

4.3.2 Tephras deposited between the eruptions of Öræfajökull in 1727 and 1362 AD

There are 10 tephra layers to be considered in this time interval based on profile 7 where the highest number of tephras occur (Fig. 4.1). These tephras vary considerably in colour from blue-black to grey, the particle size varies from fine to

coarse, and layer thicknesses range from traces to a few centimetres. These characteristics can be used to effectively determine the source (Thórarinsson, 1981). The discussion of the origin and age of the 10 tephras is based on the field-based observations of layer thickness, colour, particle size and shape, correlation with published data, stratigraphical position and soil accumulation date. In Öræfi the tephras are from Katla, Hekla, Veiðivötn, Bárðarbunga, Kverkfjöll and Grímsvötn. In a few cases, the systems can be distinguished in the field by colour. For example, Katla layers are usually solid black (reflecting the low silica content) while eruptions from Veiðivötn are normally green or olive green (reflecting a more silicic tephra). The Grímsvötn volcanic system ejects a green/grey or greyish/black tephra which is also relatively easy to identify in Öræfi.

The eruption of Öræfajökull in 1362.

The catastrophic eruption of Öræfajökull in 1362 was studied in some detail by Thórarinsson (1958) who describes the rationale of the dating evidence from various annals, dispersal of the tephra fall in Iceland and the eruption mechanisms. The eruption is thought to have begun in the middle of June in 1362 causing devastation of Litlahérað ('The small district'), a name associated with prosperity and success in Iceland at that time. After the eruption, the province was renamed and called Öræfi ('Wasteland') because it was completely uninhabitable at least until the beginning of the 15th Century (Thórarinsson, 1958). A Jökulhlaup from this eruption has already been described in Chapter 3. Combined with a powerful and devastating flood, it is generally thought that the direct impact of the eruption caused a very heavy loss of human life (Thórarinsson, 1958). The tephra can be seen in all sections logged in Öræfi (Sheets I - VI). This tephra layer forms a distinctive continuous horizon of coarse-grained white pumice intercalated with finer material. It is usually about 15 - 20 cm thick *in situ* but can be much thicker where locally accumulated, particularly on slopes and in small gullies. The tephra layer fulfils every condition set out to form a principal isochrone in the Öræfi district. It is stratigraphically discrete, well dated and can be found in all sections in the study area.

The Eystriheiði and Kvíármýri 0 tephras.

Above the 1362 layer, two silicic tephra deposits have been found, one in a single profile on Skaftafellsheiði (Sheet II, profile 11) and one in front of Kvíárjökull (Sheet VI, profile 64). The name Kvíármýri 0 was selected because silicic tephra layers older than this particular layer had already been named Kvíármýri 1, 2, 3, 5 and 6 where Kvíármýri 1 was the youngest. These silicic tephra layers (Eystriheiði and Kvíármýri 0) are in a similar stratigraphical position but can not be detected in any other profiles logged in the study area. Both layers were sampled and chemically analysed. The results (Table 4.7 and 4.8) show two distinct geochemistries. The chemistry of the Eystriheiði tephra indicates an Hekla origin while that of Kvíármýri 0 tephra has an Öræfajökull affinity. This shows that these tephra layers are from two separate events and are patchy in distribution. The Eystriheiði tephra has a silica and potassium content which is the same as in the Hekla-4 eruption (Dugmore *et al.*, 1995a; Fig. 4.6). This shows it can not be a reworking of Ö1362 tephra. Possible Hekla candidates in the 14th and 16th Century are somewhat limited. A correlation between Eystriheiði and H1510 can be ruled out on chemical grounds as H1510 has not been found with higher silica content than 64% (Dugmore *et al.*, 1995a) while the same element in the Eystriheiði tephra is about 72 - 74% of the total (Table 4.7). The Eystriheiði tephra can be defined as a medium K-glass on the SiO_2/K_2O diagram of Le Maitre (1989). According to Thórarinsson (1967) an eruption of Hekla occurred in the year 1389 and produced a large fall of tephra, which was probably carried chiefly to the south east. It is therefore possible that this silicic tephra found only in profile 11 (Sheet II) is from a highly silicic part of this eruption. However, the colour of this layer logged by Thórarinsson (1958) is dark, suggesting a lower silicic content. Furthermore, Thórarinsson (1967) notes that a short fissure opened sometime later in the eruption about 5 km to the south west from the main fissure. This fissure produced a large lava flow which was andesitic. This would cast doubt on the correlation of the Eystriheiði tephra with the H1389 eruption because of the latter's high silica content. However, a decrease in the amount of silica as the eruption progresses is known to characterise Hekla eruptions (Thórarinsson, 1967) and it is possible that the Eystriheiði tephra might be the initial phase of the eruption or a

minor silicic component that travelled somewhat farther due to its more explosive eruption mechanism. Such a highly silicic but very minor component is known from recent Hekla eruptions (Sigvaldason, 1974) and, for example, has been tentatively associated with the H1510 tephra found in Scotland (Dugmore *et al.*, 1995a).

The Kviármýri 0 tephra reveals chemical characteristics of Ö1362 (Table 4.8; Fig. 7a,b,c). Since there is no eruption of Öræfajökull known to follow the big eruption in 1362 the best estimate of the origin of this tephra is as secondary deposition from the 1362 event. This can be understood by envisaging the landscape in the first decades after the big eruption. The tephra would have covered large areas in a layer 10 - 30 cm deep and the tephra must have been very unstable and damaged vegetation. It would have been transported by fluvial and aeolian activity for many years, mixing with the andisol and occasionally forming bands of concentrated tephra.

Unknown tephra (a).
The first tephra layer above Ö1362 on Fig. 4.1 is a fine-grained black tephra never exceeding 1 cm in thickness. According to rates of soil accumulation in the same profile this layer was deposited ca. 1377±10. This date is not far from the eruption of Hekla in 1389 which produced heavy tephra fall which was carried south east (Thórarinsson, 1967). It could be the less silicic component of the tephra and equivalent in age to the Eystriheiði tephra in profile 11.

Kx.
Lenses of fine-grained black tephra, not exceeding 1 cm in thickness, can be detected about 12 cm above the Ö1362 tephra (Fig.4.1). Extrapolating soil accumulation rates, this layer was deposited in 1430±10. The colour indicates a basaltic composition and the stratigraphic position would suggest an origin from an eruption occurring in the early 15th Century. Thórarinsson (1967) reports an eruption from Hekla in 1436 but states that annals and other written sources are rare and unreliable. Another possibility is that of the eruption of Katla in 1416 (Thórarinsson, 1975; Larsen, 1978). Tephra from this eruption is found in profiles about 40 - 50 km west of the study area but is thinning rapidly towards the east (Larsen, 1978).

K1440.

A medium-grained black tephra about 2.5 cm thick can be found above the Kx tephra. The date according to the extrapolation of soil accumulation rates, is 1447±10. Larsen (1984) mapped a tephra from a Katla eruption occurring around 1440. A bulk character of the layer is indicative of a Katla eruption. Therefore, the best present estimate for this layer is this particular eruption.

Veiðivötn (V)1477 (layer "a").

In profile 7 (Fig. 4.1) lenses of medium-grained black tephra can be found as the fourth basic tephra above Ö1362. According to rates of soil accumulation the layer should have been deposited in 1456±10. No Katla, Hekla or Grímsvötn eruptions are known from the middle of the 15th Century. Thórarinsson (1956, 1975) mentions an eruption in the Kverkfjöll area at the northern side of Vatnajökull sometime late in the 15th Century. This eruption is though to have been big and produced considerable amount of tephra. Stratigraphically, there is an outside possibility that this tephra layer is from that eruption but this can not be sustained with certainty. This tephra layer is more likely to have come from a big eruption in the Veiðivötn fissure swarm which occurred ca. 1480 and is usually referred to as layer "a" (Larsen, 1984). The bulk of the tephra produced is basaltic and was carried eastwards over Öræfi.

K1490.

The fifth layer above Ö1362 is a medium-grained tephra ca. 1 cm thick which is dated to the end of the 15th Century, using rates of soil accumulation. The colour indicates basaltic composition and the particle size either a nearby eruption, or a major, more distant event. Thórarinsson (1975) reports a major eruption in Katla dated to around 1490 which is also dated by Larsen (1984) to 1485. According to Thórarinsson (1975) tephra from this eruption was dispersed widely around the lowlands of the southern part of Iceland and although a major component fell to the west, sufficient was also carried eastward to make deposition in Öræfi possible.

Unknown tephra (b).

The sixth layer above Ö1362 is a 1 cm thick fine-grained black tephra that is also about 36 cm below the Ö1727 tephra. According to soil accumulation rates, it would

have been deposited around 1515±10. The origin can not be traced but the colour of the tephra would indicate a Katla source.

Unknown tephra (c).

A 3 cm-thick fine-grained black tephra can be detected about 33 cm below the Ö1727 tephra which, according to soil accumulation rates in profile 7 should date from 1532±10. As this tephra occurs only in this profile, it suggests that the 3 cm thickness results from a localised concentration of fallout. Historical records for the 15th Century are not abundant, and thus contain few references to possible candidates. It may be concluded that a basaltic, tephra-producing eruption did occur in the early 16th Century and resulted in detectable, but somewhat patchy fallout in Öræfi.

G1540s.

A 2 cm thick dark green/greyish tephra occurs about 2 cm above the unknown tephra (c). The colour indicates an origin from either the Grímsvötn or Veiðivötn volcanic systems. The latter can be ruled out because detailed work around the Veiðivötn system by Larsen (1984) has not found any tephra layer originating from around this time. There are no contemporary annals or written sources recording volcanic activity in Grímsvötn between 1341 and 1598 (Thórarinsson, 1974). However, this does not necessarily mean that volcanic activity was low in Grímsvötn because the written descriptions are very scant for this period. It is therefore inferred that an eruption took place in Grímsvötn sometime in the 1540s.

G1619.

A fine-grained green/greyish tephra about 2 cm thick is located approximately 18 cm below the Ö1727 tephra (Fig. 4.1). This tephra is nearly identical in terms of bulk characteristics of colour, particle size and shape to the layer 13 cm below it. Consequently, it is likely to be from the same source. According to rates of soil accumulation the deposition of this tephra occurred ca. 1621±10. On the 29 of July 1619 an eruption started in Grímsvötn (Thórarinsson, 1974) and produced a tephra reported to have reached Norway and the Faeroe Islands (Thórarinsson, 1974). A ship located about 600 km south east of Iceland reported that tephra fell on it shortly after the beginning of the eruption (Thoroddsen, 1911). Given the characteristics of

this eruption, it must be present in the study area. This ash is the best candidate, given its bulk characteristics, stratigraphic location and estimated age. It reinforces the interpretation of the underlying tephras as also being from Grímsvötn.

K1625.
A fine to medium-grained black tephra is located ca. 15 cm below the Ö1727 tephra (Fig. 1). Soil accumulation rates put deposition to 1638±10. On 15 September in the year 1625 written sources describe in detail a big eruption in Katla (Thórarinsson, 1975). The tephra was mainly carried due east and spread over Öræfi causing serious problems as sheep had to be taken off fields due to the tephra blanket and the danger of fluorosis pollution of the grass. The best estimate of this tephra layer, based on its bulk characteristics, would therefore be that from the eruption of Katla in 1625.

4.4 1362 AD to Hekla-4 (ca. 3830 BP) tephra stratigraphy

4.4.1 Tephras from Hekla-4 to Vö ca. 900 AD

All of the silicic layers over this time interval were sampled and prepared for chemical analysis. To synthesise the results a composite stratigraphical profile (Fig. 4.1) was assembled, building on two profiles logged in Skaftafell (profile 6 and 7, Sheet II) and a third profile from Svínafell (profile 14, Sheet III). These sections show the maximum number of tephras, both basaltic and silicic, for this particular chronostratigraphical unit.

The Hekla-4 tephra (ca. 3830 BP).
A fine-grained yellow white tephra can be found in nearly all pre-historical profiles in the study area (Sheet I, II, III, IV, V, VI; Fig. 4.1). The tephra is usually about 3 - 4 cm thick and forms a continuous chronostratigraphical marker easily identified in the Öræfi district. The tephra layer was sampled for chemical analysis from profile 6 (Sheet II). The results show a Hekla chemical fingerprint, mainly deduced from the potassium content (Table 4.9; Dugmore *et al.*, 1995a). On an SiO_2/K_2O diagram the tephra can be defined as medium-K glass according to Le Maitre (1989; Fig. 4.8) and corresponds to the chemical analysis of the Hekla-4 tephra layer in Iceland and Scotland (Dugmore *et al.*, 1992; 1995a). If the Hekla-4 link is accepted, the SiO_2

component is very constant, lying between 72 and 73%. This means that the range of the silica reported by Larsen and Thórarinsson (1977) and Dugmore *et al.* (1992, 1995a) is not found in the Öræfi samples. The reason could be that the sample was taken at the base of the tephra layer, thus representing the initial phase of the eruption which in turn would correspond to the white pumice sub-unit c and d of Hekla-4 (Larsen and Thórarinsson, 1977). In the Öræfi data set of this particular tephra, a range of variables can be offered to differentiate the Hekla-4 from other tephras. For example, based on TiO_2/FeO and K_2O/Na_2O diagrams it is clear that the source is not Öræfajökull since K_2O, TiO_2 and FeO are normally much higher compared with Hekla-4 (Fig. 4.8b,c).

Larsen and Thórarinsson (1977) have studied the eruption that created this tephra layer both in terms of progress and the dispersal pattern of the tephra. Furthermore, the Hekla-4 tephra has recently been identified in Scotland and Ireland (Dugmore, 1989b; Dugmore *et al.*, 1995a; Pilcher and Hall, 1992) which underlines the potentially vast extent of tephras originating in explosive eruptions (see also Dugmore *et al.*, 1995a; Pilcher and Hall, 1992). This is the first time the Hekla-4 tephra has been mapped and identified in the Öræfi district where previously it has been confused with a putative eruption of Öræfajökull (Thórarinsson, 1958). As Hekla-4 is one of the best dated pre-historic tephras in Iceland (Dugmore *et al.*, 1995b), the identification of Hekla-4 represents a significant addition to the chronology of the key area.

The Hs tephra.

A mixture of fine-grained black basaltic tephra and fine-grained white silicic tephra is usually located about 10 cm above Hekla-4 in soil sections in Öræfi. The white tephra band is typically <1 cm thick and has been found in various places inside the normally ca. 4 - 6 cm thick basaltic tephra (most profiles on Sheets I - VI; Fig. 1). The tephra layer is in most cases reworked; the difference in thickness and the various positions of the silicic band probably indicate that the deposition occurred when snow covered the ground (Larsen and Thórarinsson, 1977). According to rates of soil accumulation, the layer is dated to 3520±30 BP.

Chemical analysis was conducted on the silicic part of the layer sampled from profile 6 (Sheet II) in Skaftafellsheiði and from profile 14 in Svínafellsheiði (Sheet III). The results are shown in Table 4.10. The SiO_2 content is similar to that of Hekla-4, ranging from 64% to 73%. However, most of the analyses show SiO_2 typically about 65% - 66% (Table 4.10; Fig. 4.9a). The tephra can be defined as medium-K glass according to Le Maitre (1989). The potassium content suggests an origin from Hekla and this together with the estimated age and silica content, suggests that this particular tephra layer is the Selsund tephra (Larsen and Thórarinsson, 1977) also called 'Hs' layer. When compared with chemical data of the Hs tephra analysed by Dugmore *et al.* (1992) the match is acceptable (Fig. 4.9). The correlation is shown clearly on the FeO/TiO_2 diagram (Fig. 9c) where the two data sets show the same trend.

Initially this layer was called Hekla-2 because it was thought to be younger than Hekla-3 but later it was found to lie between Hekla-3 and Hekla-4 (Larsen and Thórarinsson, 1977) and so was renamed Hs. As a result of its stratigraphic and spatial distribution it is thought that the Selsund tephra was presumably erupted in calm weather during winter time and the silicic airfall deposit was thin (Larsen and Thórarinsson, 1977). This concurs with the characteristics of the thin silicic tephra band found in Öræfi. The dispersal pattern has yet to be published, but it has been mapped eastwards from Hekla (Larsen, pers. com). This is the first time this layer has been detected in Öræfi. In most cases it occurs along with Hekla-4, forming a couplet easily traced throughout the study area. Therefore, this pair of Hekla tephras, i.e. Hekla-4 and Hs, form significant marker horizons in Öræfi.

The Miðheiði tephra.

This silicic tephra layer is found in two profiles on Skaftafellsheiði (6 and 7, Sheet II) and in a single profile on Svínafellsheiði (14, Sheet III; Fig. 4.1). In profile 81 in front of Kviárjökull a tephra layer can be found which is probably the Miðheiði tephra, although it was not chemically confirmed. The Miðheiði unit is fine-grained airfall tephra and seems to get thinner towards the north west. Its thickness falls from 1 cm in profile 14 on Svínafellsheiði to thinner or ca. 0.5 cm in profile 7 on Skaftafellsheiði.

According to mean rates of soil accumulation on Svínafellsheiði and Skaftafellsheiði, this layer dates back to 2860±160 years BP.

The tephra layer was sampled for chemical analysis from profile 14 (Sheet III) on Svínafellsheiði (Table 4.11). The SiO_2 content is always >70% and the tephra may be described as a medium-K glass (Le Maitre, 1989). The K_2O is typically >3% while MgO never exceeds 1% of the total volume. FeO and TiO_2 components are usually >3% and ca. 1%, respectively. These chemical characteristics are typical of the Öræfajökull 1362 eruption (Fig. 4.11; Pilcher *et al.*, 1995) and it is therefore also inferred to be an eruption from Öræfajökull. The low TiO_2, FeO, MgO and CaO are all characteristics which can be used to discriminate between Hekla and Öræfajökull tephras.

It is likely that the eruption was a relatively small event in comparison with the Öræfajökull eruption in 1362 AD. The tephra found in profiles west of the mountain was probably deposited at the fringe of the dispersal area. Consequently, the general wind direction during the eruption was probably from the west, implying that most of the tephra was deposited in the sea. Because of this localised distribution on land and difficulties in tracing the layer, it is not a significant isochrone in the study area.

The Svínafellsheiði tephra.

This tephra layer is a fine-grained airfall deposit, white in colour and ca. 1 cm thick (profile 14, Sheet III; Fig. 4.1). According to rates of soil accumulation the tephra is dated to 2390±240 years BP. The layer was sampled for chemical analysis and reveals two groups (Table 4.12). Group A has SiO_2 content >70% and K_2O always <2%. The low K_2O means that the tephra can be defined as low-K glass based on Le Maitre (1989). In turn, this rules out an origin from Hekla and Öræfajökull (Fig. 4.11) where K_2O is typically >2.5%. This view is supported by the amounts of TiO_2, FeO, MgO and CaO which are usually higher than those of Hekla and Öræfajökull (Fig. 4.11c,d). If data from the Askja 1875 AD eruption (Sigvaldason, 1982) is compared with the Svínafellsheiði tephra, certain similarities become apparent, especially in the MgO/CaO plot (Fig. 4.11d) and the FeO/TiO_2 diagram (Fig. 4.11c).

The data seem to follow a similar linear trend which tentatively suggests an origin from Askja or the Dyngjufjöll volcanic system. The group B tephra shows >70% SiO_2 content and can be defined as high-K glass according to Le Maitre (1989). The K_2O is always >4% and the MgO, CaO, TiO_2 and FeO components are all lower than for group A. The chemistry indicates an origin from the Torfajökull volcanic system (Grönvold, 1972; McGarvie *et al.*, 1990; MacDonald *et al.*, 1990).

If the group A tephra is compared with the Glenn Garry tephra found in northern Scotland (Dugmore *et al.*, 1995a) strong similarities become apparent, notably values of MgO and CaO (Fig. 4.11d). Furthermore, the dates match relatively well because the Glenn Gary tephra has been radiocarbon dated to ca. 2100 years BP (Dugmore *et al.*, 1995a) which agrees with the age estimates made here from soil accumulation rates.

The Skerhóll tephra.

About 4 cm above the inferred Askja and Torfajökull layers a 0.5 cm thick fine silicic tephra can be found (Sheet III; profile 14; Fig. 4.1). According to soil accumulation rates, the tephra band dates back to 1940±30 years BP. The tephra layer was sampled for chemical analysis and the results are presented in Table 4.13. The SiO_2 content is typically >70% with one exception where it was measured at ca. 68%. In addition to the SiO_2 values, K_2O is >3.5% and <4%, values which hint at an origin from Öræfajökull. According to Le Maitre (1989) the tephra can be classified as medium-K glass (Fig. 4.12a,b). The Öræfajökull affinity is less clear if TiO_2/FeO and MgO/CaO contents are compared with other possible origins (Fig. 4.12c,d). Two out of four of the analyses fit with values for the Öræfajökull 1362 eruption. A characteristic of the silicic tephras from Öræfi is their very high visicularity which makes the glass of the bubble wall very thin and difficult to analyse. This tephra was characterised by grains of this type. Despite the difficulties of obtaining good analytical results, the pumice characteristics make a strong case for an Öræfajökull source.

The Skaftafellsheiði tephra.

A fine-grained silicic tephra, about 1.5 cm thick, which is overlain by a 1 cm-thick coarse grained black tephra, is the last white tephra in profile 14 before the eruption of Öræfajökull in 1362 AD. This sandwich layer can also be found in profiles 6 and 7 on Skaftafellsheiði (Sheet II). Additionally, this tephra can be seen in profiles in front of Kviárjökull (profiles 52, 67, 81; Sheet VI). Profile 6 indicates that at least 7 tephras were deposited between the Skaftafellsheiði tephra and the Vö ca. 900 tephra layer which was identified in the profile with high certainty. The Skaftafellsheiði tephra was dated with the radiocarbon methods in front of Kviárjökull (profile 67; Sheet VI) and revealed an age of 1540±50 (GU-4914).

The layer was sampled for chemical analysis from profile 14. The results are presented in Table 4.10. The silica content is always >70% and K_2O is around 3.5%. Furthermore, the MgO is <0.1%. The tephra can be classified as medium-K glass according to Le Maitre (1989; Fig. 4.13a). These chemical characteristics are common in the silicic part of Öræfajökull eruptions as can be seen in the Ö1362 tephra (Pilcher *et al.*, 1995) and in the Miðheiði tephra. Diagrams comparing different components in different eruptions are shown in Figs 4.13a,b,c. These plots emphasise the Öræfajökull source.

Black (1990) mapped a fine grained silicic layer immediately underlying a coarse, black tephra in front of Kviárjökull. He interpreted the tephra as an eruption from Öræfajökull and called the layer 'Ö4'. He applied the radiocarbon method to date the layer using peat sampled immediately under the tephra. The sample turned out to be 1720±195 years BP old (GX 15180). This date is statistically indistinguishable from GU 4914 at 1σ. It is most likely that the Skaftafellsheiði tephra and Black's 'Ö4' tephra are the same. This can be further substantiated with chemical analysis of what is stratigraphically interpreted as the same layer in profile 67 on Sheet VI, here called the Skaftafellsheiði tephra. The results of the analyses are presented in Table 4.15 show strong Öræfajökull characteristics. K_2O is between 3.5 to 4% and MgO and CaO is low compared with other possible sources. Furthermore, both layers are of

similar texture and colour and of the same sandwich character, with a coarse, black tephra underlying a fine-grained white tephra.

This particular eruption of Öræfajökull was substantial but smaller than the eruption in 1362. The dispersion of the tephra on land, probably all around the mountain, would suggest that it occurred over a brief period of calm weather. An extensive jökulhlaup, called Stórugrjót, can be traced to this eruption and flowed from the eastern part of the caldera and rushed down the Kviárjökull valley to spread out south and north of the big moraine amphitheatre (Thórarinsson, 1958; Fig. 3.24). According to the geomorphological relationships, the jökulhlaup deposit occurred after the initial formation of the composite Kviármýrarkambur moraine.

The Vö ca. 900 AD tephra.

One of the most significant marker horizons in the Icelandic tephra stratigraphy is the Settlement (landnám) layer. It is a distinct and extensive tephra layer which effectively marks the beginning of the Norse Settlement of Iceland (Thórarinsson, 1944; Larsen, 1984; Hallsdóttir, 1987). The sandwich layer was deposited in two separate eruptions that took place at the same time in the Vatnaöldur fissure swarm, generating the olive brown basaltic tephra from the main fissure and ejecting the white silicic part from the Hrafntinnuhraun crater row. The tephra layer was initially referred to as VII a+b by Thórarinsson (1944) but Larsen (1984) chose to abbreviate it to Vö ca. 900 (Larsen, 1984) because of its origin and age (Hallsdóttir, 1987). Recent studies of the GRIP2 ice core, where this layer has been identified, suggests that the layer is 871±2 ice core years old (Grönvold *et al.*, 1995). During the early stages of the eruption the winds blew from the south, but later changed in a counter-clockwise direction, allowing the silicic tephra to be deposited prior to the basaltic tephra in most localities to the north west and west of the eruption fissure (Larsen, 1984). Therefore, only the basaltic olive-brown part of the tephra can be identified in the Öræfi district. A caveat has to be introduced here because the tephra layer can be confused with other eruptions from the Veiðivötn volcanic system; therefore the layer was constantly checked in sections to confirm that characteristic white plagioclase crystals were present (Larsen, 1979).

Vö ca. 900 was identified with certainty on Skaftafellsheiði (profiles 6 and 7, Sheet II) and in front of Virkisjökull (profile 31, Sheet IV). The layer was sampled for chemical analysis from a section in Skaftafellsheiði (profile 6; Sheet II). The results are presented in Table 4.16 and Fig. 4.14. and match well with other Vö ca. 900 samples (Haflidason *et al.*, 1992). However, care is required when using the chemistry alone to pinpoint the Vö ca. 900 tephra because all tephra layers from the Veiðivötn volcanic system are similar in major element composition (Larsen, pers. com.) and the only way to identify Vö ca. 900 is by using the plagioclase crystals in field inspection, a unique product of the simultaneous eruption from Hrafntinnuhraun.

4.4.2 The tephras formed between Vö ca. 900 and Ö1362.

There is one white silicic tephra found in this part of the stratigraphy. However, it is only found as a patchy trace in profile 6 on Skaftafellsheiði (Sheet II) and is therefore not a continuous distinct layer in the area. It was sampled for chemical analysis and the results are presented in Table 17. The SiO_2 content is >70% and the K_2O volume is around 2.6% on average. The tephra can be classified as medium-K glass according to Le Maitre (1989). The overall chemistry is similar to that of the eruption of Hekla in 1104 AD (Thórarinsson, 1967; Pilcher *et al.*, 1995; Fig. 4.15). The FeO content is slightly lower in the patchy tephra. This eruption was the first from Hekla in historical times and was highly explosive, producing great quantities of tephra, The dispersal axis is towards the north but the 0.2 mm isopach line in the east crosses the centre of Vatnajökull from south west to north east (Thórarinsson, 1967). This would imply that some patchy air fall deposits could have fallen on the western part of the study area. However, an Hekla eruption occurred in 1158 and the tephra travelled north east (Larsen, pers. com.). This would imply that this particular patchy white tephra could be Hekla 1158. Little is known about the Hekla 1158 eruption and the consequent tephra fall and therefore, it is concluded that the eruption of Hekla in 1104 AD is the best match of this patchy discontinuous tephra band.

4.4.3 The Kviármýri tephras

The tephras described in this section come from profile 52 (Sheet VI) in front of Kviárjökull. This is the only peat section in the study area apart from profile 67 (Sheet VI) and is about 100 m north-north west from profile 52. These profiles do not show the same tephra stratigraphy and most of the tephras in profile 52 seem to be absent in profile 67. The missing tephras are very thin (<1 cm) which makes them very vulnerable to any local environmental disturbance, or variation due to uneven surface condition.

It is likely that the dates of the Kviármýri 5, 3 and 2, calculated from sediment accumulation rates, are underestimated here. This is because rates were deduced from rates between Ö1362 AD and the eruption of Öræfajökull dated to 1540±50 BP (Skaftafellsheiði tephra). To do this, it was necessary to convert the BP date to AD to standardise the units. This was done by using the calibrated age of the BP dates under 2δ and then calculating the mean. This could cause an error firstly because the span of the date is 430 - 610 AD (2δ) and secondly the rate of sediment accumulation increased when the country was settled in the 9th Century and anthropogenic soil erosion began (Thórarinsson, 1958, 1961; Dugmore and Buckland, 1991).

The Kviármýri 7 tephra.

This tephra is a 1 cm-thick fine-grained white airfall and is deposited in peat. It was sampled for chemical analysis and the results are listed in Table 18. The chemistry reveal two groups of tephra, Kviármýri 7 A and B, belonging to distinct volcanic systems.

Tephra A is typically >70% SiO_2 and can be defined as medium-K glass according to Le Maitre (1989; Fig. 4.16a). Out of 12 analyses, 9 belong to group A where K_2O ranges between 1.8 and 2.2% (Fig. 16b). The tephra can be best distinguished by MgO, CaO, TiO_2 and FeO. In all cases, it shows higher volumes of these components compared to group B (Fig.16c,d). The chemical composition is close to the chemistry of Askja (Sigvaldason, 1982). The B tephra shows >70% SiO_2 content and can be

defined as high-K glass according to Le Maitre (1989). As above, 3 out of 12 analyses belong to this group which can be best distinguished by the same components as group B. The K_2O is always >4% while MgO, CaO, TiO_2 and FeO components are in all cases lower compared with the values in group A. The chemistry indicates an origin from the Torfajökull volcanic system (Grönvold, 1972; McGarvie *et al.*, 1990; MacDonald *et al.*, 1990).

The overall chemistry and stratigraphic location of the Kvíármýri 7 tephra suggests that it has the same dual source as the Svínafellsheiði tephra. Therefore, the A group is probably from an eruption in Askja and the B group from an eruption in the Torfajökull volcanic system. The tephra has been dated to 2115±20 years BP from combination of radiocarbon dates (Dugmore *et al.*, 1995a) and soil accumulation rates. The Askja eruption (group A) has recently been detected in Scotland and called the Glenn Garry tephra (Dugmore *et al.*, 1995a) as mentioned earlier.

The Kvíármýri 6 tephra.
The tephra is composed of a 0.5 cm thick, fine and white-grained unit overlain by a 2 cm-thick fine-grained black band. The chemistry and the stratigraphic position shows that this tephra is the same as the Skaftafellsheiði tephra (Table 4.19; Fig. 4.17a,b,c,d).

The Kvíármýri 5 tephra.
This white tephra could only be found as a very fine grained white trace and sampling for chemical analysis was unsuccessful. However, the colour of the tephra suggests a highly silicic chemical composition. Soil accumulation rates suggests that the tephra was deposited ca. 1330±120 years BP.

The Kvíármýri 3 tephra. This tephra is a 1 cm thick fine-grained white airfall deposit underlying a 2.5 cm thick-fine grained black tephra (profile 52; Sheet VI). The tephra is deposited in peat and is dated to 1108±85 years BP according to soil accumulation rates. The white layer was sampled for chemical analysis and the results are presented in Table 4.20. The SiO_2 content is always >70% and potassium levels are high. Out of five analyses, four showed K_2O >4% which means that the tephra can be defined as

high-K glass according to Le Maitre (1989; Fig. 4.18a). The tephra is best discriminated by its K_2O, MgO and CaO content. Using these components both Hekla and Öræfajökull can be ruled out as possible sources (Fig. 18b,c). The high K_2O volume is known from the Torfajökull volcanic system (Grönvold, 1972; MacGarvie *et al.*, 1990; MacDonald *et al.*, 1990), the most likely source of the tephra.

The Kvíármýri 2 tephra.

A layer of approximately 0.5 cm of fine-grained white airfall tephra is located at a depth of 13 cm in profile 52 (Sheet VI). The tephra is deposited in peat and can be dated to about 1088±80 BP according to soil accumulation rates. The tephra was sampled for chemical analyses (Table 4.21). Most of the analysis show high silica (>70%) and potassium (>4%) contents hence defining the tephra as high-K glass according to Le Maitre (1989; Fig. 4.19a). Like the Kvíármýri 3 tephra it is best discriminated by the K_2O, MgO and CaO contents thus confirming the Torfajökull volcanic system (Fig. 4.19b,c).

The Kvíármýri 1 tephra.

At a depth of 25 cm in profile 52 (Sheet VI) is a 1.5 cm thick fine-grained white tephra. The tephra is interpreted as the airfall deposit from the 1362 AD eruption of Öræfajökull because this particular tephra can be found reworked about 8 cm above. The thickness and the structure of the reworked Ö1362 tephra indicates that the tephra was carried by water, which in turn suggests the site was a small basin filled with the water-laid tephra. The soil between the two deposits might therefore be explained as a rapid infill of sediments. The layer was sampled for chemical analysis which confirms that the source is Öræfajökull (Table 4.22; Fig. 4.20). The tephra reveals typical K_2O, MgO and CaO contents as seen in other Öræfajökull tephras.

4.5 Pre-Hekla-4 tephra stratigraphy

Most of the silicic layers found in profiles covering this time period were sampled for chemical analysis to determine their source. A discrepancy between sites became apparent, thus inhibiting correlation of tephras of similar stratigraphic position, colour and texture between sites (Fig. 4.1). In most cases the tephra layers were unique for a single profile. Consequently, the tephras will be accounted for on a local scale rather than regional. Proglacial areas will be used as reference sites in order to put the tephra stratigraphy in context with the glacier fluctuations in the study area

4.5.1 Skaftafellsheiði

The most important profile in terms of tephrochronology on Skaftafellsheiði, and perhaps in the Öræfi district, is profile 6 (Sheet II). It is nearly 6 m long and is located in a corrie called Botn ideal for soil and tephra preservation (Fig. 3.7). It is difficult to estimate the basal date of the profile because the soil accumulation succession is interrupted by silt, sand and gravel units creating an unknown hiatus. On the other hand, the geomorphological evidence presented in Chapter 3 suggests that the basal date for this particular site is the early Holocene, since it is located in an area beyond the outermost Neoglacial limits but within limits of the last Termination.

The Botn tephras.

The first ca. 2 m of profile 6 (Sheet II) contains six silicic tephras called Botn 1-6. The Botn 1-5 tephras are older than the Hekla-4 tephra but younger than the last Termination, however, the Botn 6 tephra was dated to 4430±100 BP according to rates of soil accumulation. These tephras are deposited in silt indicating a small lake or a pond. Botn 6 is, however, deposited in andisol. In turn, this date would indicate the minimum age of the pond. These tephras are typically 1 - 4 cm thick white silicic units overlain by black basaltic or andesitic layers.

The chemical characteristics of these tephras are diverse and difficult to correlate with known volcanic systems in Iceland. Typically, the silicic analyses can be defined as high-K glass except for Botn 2 which is medium-K glass. Botn 1 does show certain

similarities to Öræfajökull eruptions in terms of potassium content but a clear link is difficult to establish (Table 4.23; Fig. 4.21). Botn 2 is composed of white and black tephra where the silicic units show some similarities with the Askja volcanic system (Sigvaldason, 1982; Table 4.24; Fig. 4.22). No successful analyses of the silicic unit of the Botn 3 tephra was obtained. However, basaltic analyses are listed in Table 4.25 and Fig. 4.23. These indicate an origin from Veiðivötn/Dyngjufjöll I/Dyngjuháls volcanic system (Jakobsson, 1979; Larsen, 1982). The Botn 4 tephra is composed of silicic and basaltic units hinting at an origin from Öræfajökull (Table 4.26; Fig. 4.24). Only two basaltic analyses were successful of the Botn 5 tephra. These results are consistent and suggest an origin from the Grímsvötn/Kverkfjöll volcanic system (Jakobsson, 1979; Larsen, 1982; Table 4.27; Fig. 4.25). The colour of the tephra and the geochemistry would suggest an origin from Kverkfjöll rather than Grímsvötn. The Botn 6 tephra is the top silicic tephra under the Hekla-4 layer in profile 6. Only one silicic analysis was satisfactory, and indicated an Öræfajökull source.

The Oddar tephra.

In profiles 57 and 58 (Sheet II; Fig. 3.7) a trace of 1 cm fine-grained silicic tephra can be detected below the Hekla-4 layer. It is deposited in andisol. Extrapolating from soil accumulation rates, this layer dates back to 5470±270 years BP. The layer was sampled for chemical analysis (Table 28). The silica content is >70% and the tephra can be defined as medium-K glass according to Le Maitre (1989; Fig. 4.26a). The sodium component is low in all of the analyses, given the high SiO_2, and is therefore underestimated. The sodium loss was checked and it revealed significant depletion during the analysis. In turn, the amount of SiO_2 is probably slightly overestimated. The tephra has similar characteristics to that of Hekla-4 in all elements analysed (Fig. 4.26). Furthermore, it resembles the Lairg A tephra, found in Scotland in all components except potassium and sodium (Dugmore *et al.*, 1995a). Additionally, it has a similar date not far from the age of the ca. 6000 BP for the Hekla-5 tephra (Larsen and Thórarinsson, 1977). The difference in sodium content can be explained by abnormal depletion during analysis.

4.5.2 Svínafellsheiði

Profile 14 (Sheet III) on Svínafellsheiði (Fig. 3.26) provides an insight into the pre-Hekla-4 tephra stratigraphy of the Öræfi district. The site is at the western edge of the active Öræfajökull stratovolcano and well clear of the Neoglaciation limits. The implication is that the site should preserve tephras formed in eruptions from Öræfajökull since it is very close to the active centre. Profile 14 (Sheet III) is not broken by major silt, sand or gravel units implying an opportunity to date the observed tephras by soil accumulation rates. However, only three silicic layers were found in this part of profile 14.

The Sv14-12 tephra.

The oldest silicic layer in profile 14 is a 1 cm thick fine-grained white silicic tephra deposited in andisol. According to soil accumulation rates the tephra dates to 9790±980 BP. The layer was sampled for chemical analysis (Table 4.29). Most of the grains analysed can be defined as medium K-glass according to Le Maitre (1989) but some show a tendency towards a high-K glass (Fig. 4.27a). The silica content is >72% and Na_2O component is underestimated because of wastage during the analysis which might, in turn, partly explain the high silica content . This tephra can be distinguished from other tephras by using K_2O/Na_2O and MgO/FeO (Fig. 4.27b,c). The diagrams show that Hekla can be ruled out as a possible source. By comparing K_2O/Na_2O and MgO/CaO of the Botn 1 and the Sv14-12 tephra, a close match appears. Furthermore, the Botn 4 tephra seems to have a similar chemical fingerprint (Fig. 4.27b,c). The analogy of the Botn 1 and the Sv14-12 tephra can be further substantiated by the comparable stratigraphic location of these two tephras. It is therefore likely that the Botn 1 and Sv14-12 tephras are the same layer and the Botn 4 tephra has the same source.

The Sv14-11 tephra.

This tephra layer is 1 cm thick and is mainly composed of fine black basaltic tephra but with some notable fine silicic white grains scattered throughout the thickness of the layer. According to soil accumulation rates the tephra dates to about 6430±140 years BP. The white silicic grains were sampled for chemical analysis (Table 4.30).

Out of six successful analyses, four were consistent but two showed a different chemistry. These two analyses are considered to represent either secondary deposition or another phase of the eruption. The other four results are consistent and show silica contents slightly under 65%, comprising a marginal high-K glass (Fig. 28a). The K_2O content, about 2.7%, is high when considering the relatively low silica content (Fig. 28b). However, the tephra can be best distinguished by using the MgO/CaO relationship (Fig. 22c). The MgO content is always >1% and CaO >3% which, combined with the high K_2O content, rules out an origin from Hekla. However, explicitly using the MgO/CaO diagram the analyses are on the same linear trend as the Botn 1, Botn 4 and SV14-12 tephras hinting at the same source (Fig. 4.28d).

The Sv14-9 (A and B) tephra.

In profile 14 (Sheet III) a 4 cm-thick coarse-grained white silicic tephra is located about 30 cm below the Hekla-4 tephra. According to soil accumulation rates this tephra is dated to 5030±200 years BP.

The tephra was sampled for chemical analysis and revealed mainly basaltic andesite values (Table 4.31). Only three out of eight successful analyses turned out to be rhyolitic with silica contents ranging from 67 - 69%. The tephra can be defined as medium-K glass according to Le Maitre (1989) showing a high potassium content, similar to the Sv14-11 tephra (Fig. 4.29a,b). The sodium level is relatively high, which might result in a slight underestimation of the silica. This tephra can be best distinguished from Hekla and possibly Öræfajökull by magnesium, calcium, iron and titanium contents (Fig. 4.29c,d). It resembles some of the tephras of unknown source in this study. Imsland (1978) has compiled a diagram showing trends of selected Icelandic rock suites. If the basaltic andesitic results are plotted on this graph, certain similarities begin to appear with Öræfajökull. Therefore, the Sv14-9 tephra shows two distinct chemical signatures. The silicic grains (group A) show some relation to many of the tephras of unknown origin in this study, the basaltic andesites show more similarities with the chemistry of Öræfajökull (group B).

The Sv14-7 tephra.

A 2 cm band of fine-grained white silicic tephra can be detected in between Hs and Hekla-4 in profile 14 on Svínafellsheiði. According to soil accumulation rates the tephra is 3630±30 BP years old. The layer was sampled for chemical analysis (Table 32). Out of four successful results, three showed Öræfajökull characteristics but a single grain revealed an origin from Hekla. Two possibilities could explain this result. Firstly, it might indicate a mixture of two tephras hinting at a secondary deposition, probably by aeolian transport. Therefore, the Sv14-7 tephra would probably not be an individual layer but a combination of Öræfajökull and Hekla tephra. Secondly, the layer could be an individual tephra, probably originating from Öræfajökull, since the majority of grains analysed show Öræfajökull characteristics. However, since this layer can not be detected in any other profile in the study area, the former explanation is more plausible.

The Sv61-1 (A and B) tephra.

A patchy 0.5 cm-thick white silicic tephra can be found near the base of profiles 61 and 62 (Sheet III; for location see Fig. 3.10). According to soil accumulation rates the age of the tephra is 8590±780 years BP. The tephra was sampled for chemical analysis and the results indicate two distinct populations of grains (Table 33). The range of silica in group A is between 72.5 and 73.5% and shows similar chemical characteristics as the Sv14-12 tephra in profile 14. However, group B contains a slightly wider silica range of 71 to 74%. The tephras can be best discriminated by FeO, TiO_2, MgO and CaO contents where these components are consistently lower in group A compared with group B. As to the source of group B grains, there are certain similarities with Öræfajökull if FeO and TiO_2 are considered. This relationship is not so clear if MgO and CaO are considered, but cannot be ruled out (Fig. 4.30).

The relationship between group A and the Sv14-12 tephras is only speculative at this stage. However, it is likely that the Botn 1, Sv14-12 and Sv61-1 (A and B) tephras are from the same eruption, perhaps from Öræfajökull in the early Holocene. These tephras will be collectively named the Botn-Svínafellsheiði (BS) tephra from here onwards.

4.5.3 Virkisjökull

The Virkisjökull tephra. In profile 31 (Sheet IV) a single white tephra can be found below the Hekla-4 tephra. It is 2 cm thick fine-grained white band with a grey stripe in the middle. The tephra is overlaid by a 1 cm-thick fine-grained black tephra. It is deposited in very indurated andisol. The tephra dates back to 4590±125 years BP according to the extrapolation of soil accumulation rates.

The tephra was sampled for chemical analysis (Table 4.34). The SiO_2 content ranges from 65 - 72% and can be defined as high K-glass according to Le Maitre (1989; Fig. 4.31a). The potassium ranges from 3.4 - 3.8% strongly indicating an origin from Öræfajökull (Fig. 4.31b). However, if MgO/CaO and TiO_2/FeO ratios are examined this link is not so clear (Fig. 4.31c,d). In all cases, these components have higher volumes in the Virkisjökull tephra compared with known Öræfajökull eruptions such as Ö1362 (Pilcher *et al.*, 1995). Nevertheless, the link cannot be excluded. There is no tephra in the study area with which it can be correlated with certainty but the stratigraphic location would suggest that some of the unknown tephras found on Skaftafellsheiði and Svínafellsheiði could be from the same eruption, probably Öræfajökull. The SV14-9 tephra is a plausible candidate because of its similar date and some similar chemical characteristics. For example, both can be defined as high-K glass and the silica content varies significantly. This would suggest that the Sv14-9/Virkisjökull tephras originate from an eruption in Öræfajökull in the mid-Holocene. However, a direct link can not be justified with the present data.

4.5.4 Kviárjökull

The Kviárjökull 64-1 tephra. The tephra is deposited in organic-rich loessial soil (Fig. 4.32). It is a 4 cm-thick fine-grained white airfall deposit. It dates back to 6120±375 BP according to extrapolation of soil accumulation rates. The layer was sampled for chemical analysis and the results are presented in Table 4.35. The SiO_2 content is >72% and the tephra can be defined as medium-K glass according to Le Maitre (1989; Fig. 4.32a). The potassium component varies little, 2.7 - 2.8% of the total

volume (Fig. 4.32a,b). The tephra matches known Hekla eruptions in all major components (Fig. 4.32). The Hekla-4 tephra can be ruled out because it can be detected higher in the profile combined with the Hs tephra. The tephra shows general similarities to Dugmore's *et al.*, (1995a) Lairg A tephra dated to ca. 6000 BP. This tephra will be called Hekla-Ö in this thesis.

The Kviárjökull 64-2 tephra.

The tephra is a 0.5 cm thick fine-grained airfall unit deposited in organic rich loessial soil. According to soil accumulation rates it dates back to 5560±105 years BP. The tephra was sampled for chemical analysis (Table 4.36) from which it can be defined as high-K glass according to Le Maitre (1989). The silica component is always >71% and the K_2O content is high, always >4.3% (Fig. 4.33a,b). A single analysis revealed different composition and is interpreted as a stray grain. The overall chemical composition, especially the high potassium content, is indicative of an eruption in the Torfajökull volcanic system (Grönvold, 1972; McGarvie *et al.*, 1990; MacDonald *et al.*, 1990). The chemistry (Fig. 4.33c,d) and the stratigraphical position of the Kviárjökull 64-2 tephra suggests that this is the same tephra as the Hoy tephra recently detected in Scotland dated to ca. 5600 BP (Dugmore *et al.*, 1995a).

The Kviárjökull 64-4 tephra.

This tephra is 0.5 cm-thick fine-grained white airfall. It is deposited in ca. 6 cm-thick organic rich loessial soil partly separating gravel units B and C in profile 64 (Fig. 4.34). The tephra is dated to between ca. 5000 and 4300 years BP according to soil accumulation rates. The mean is 4650 BP. The tephra was sampled for chemical analyses (Table 4.37) and has the same main characteristics as the Kviárjökull 64-2 tephra (Fig. 4.34). Therefore, it originated from an eruption in the Torfajökull volcanic system.

4.6 Tephrostratigraphy and its implication

4.6.1 Tephrostratigraphy: summary

Detailed study of the tephra stratigraphy of the Öræfi district, south east Iceland, revealed a more complicated record of tephras than previously known in the area (cf. Thórarinsson, 1956, 1958). 88 profiles were logged to reconstruct the regional tephra stratigraphy of the Öræfi district. In all, 22 silicic tephras were identified in the Holocene succession in the study area. The majority of these layers are dated to the latter part of the Holocene; three were deposited during historical time.

Between the eruption of Katla in 1918 AD and the eruption of Öræfajökull in 1362 AD the silicic layers identified include Ö1362 and possibly H1389. Some of the basaltic layers are distinguished for the first time in the area, namely G1783, K1625 and G1619 (Fig. 4.1).

The Hekla-4 tephra, dated to ca. 3830 BP (Dugmore *et al.*, 1995a) was identified in the area for the first time along with the Hs and H1104 tephras (Fig. 4.1). The silicic tephras erupted prior to Ö1362 were discovered for the first time in Öræfi and in Iceland. These include at least two eruptions of Öræfajökull dated to 2860±160 BP and 1540±50 BP and simultaneous eruptions in Askja and Torfajökull dated to ca. 2100 BP by Dugmore *et al.* (1995a). The two latter eruptions have recently been identified in Scotland by Dugmore *et al.* (1995a). A possibility exists that the Skerhóll tephra on Svínafellsheiði originated from Öræfajökull dated to 1940±30 years BP.

The tephras earlier than Hekla-4 are very localised and profile specific. Most of the tephras show geochemistry which currently cannot be correlated with any known eruptions in Iceland. However, the trend of some elements and components analysed in these tephras would suggest links with either the Öræfajökull or Askja volcanic systems. Two of the tephras found in a profile in front of Kviárjökull could be traced with reasonable certainty to Torfajökull, and this is the first time these layers have

been identified in Iceland. The rest of the silicic tephras covering this period have not been detected in Iceland so far.

4.6.2 The Öræfajökull eruptions in the Holocene

The data presented in this chapter suggest that Öræfajökull has erupted at least five times over the last ca. 3000 years BP. It is difficult to establish the eruption history preceding this date because the geochemical data are difficult to interpret. However, it is likely that some of the pre-Hekla-4 tephras originated from Öræfajökull such as the Botn 1 tephra (profile 6), Sv14-12 (profile 14), Sv61-1 (BS tephra) tephra (profile 61 and 62) and the Virkisjökull tephra (profile 31). The number of eruptions over the Holocene presented here is minimal because it is inferred from chemical analysis of only the white silicic tephras found in the study area. The black andesitic/basaltic eruptions are excluded with the exception of the Öræfajökull eruption in 1727 AD. Therefore, the implication is that there was a more frequent eruption history of Öræfajökull. Assuming the silicic tephras reflect the true number of eruptions over this period, an eruption occurred every ca. 600 BP years on average. The longest interval between eruptions was ca. 950 years BP between the deposition of the Skaftafellsheiði tephra (1540±50 BP) and the great eruption in 1362 AD (588 BP). The shortest interval was 365 years between the Ö1362 AD and Ö1727 AD eruptions.

It is not at present possible to deduce the frequency of eruption of Öræfajökull prior to 3000 years BP. However, the evidence would suggest that at least two eruptions occurred. It is likely that Öræfajökull erupted shortly after the last Termination, probably around 9000 BP as seen by the deposition of the BS tephra. The evidence suggests that at least one eruption took place in the mid-Holocene as shown by the Virkisjökull tephra (ca. 4600 BP) and Botn 6 tephra (ca. 4500 BP). It can be speculated that the Sv14-11 tephra (ca. 6400 BP), and with less certainty, the Botn 4 tephra (mid-Holocene), represent eruptions around a similar time. These may have been two eruptions, but this can not be verified since these tephras have not been

found together in a single profile. However, it can be assumed that at least one eruption of Öræfajökull took place around the mid-Holocene.

Table 4.38 summarises the eruption history of the Öræfajökull volcano during the Holocene according to the evidence presented in this study. There is evidence of jökulhlaups from the 1727 AD, 1362 AD and ca. 1540 BP eruptions of the mountain. This does not mean that jökulhlaups did not follow older eruptions. Most probably the geomorphological evidence for these events is not preserved. Since glaciers endured throughout the Holocene, the caldera would have been ice-filled and jökulhlaups were therefore probable. These eruptions were probably small, increasing the possibilities of their traces being destroyed around the ice cap by subsequent geomorphological activity.

The eruption in 1727 AD was perhaps of similar size as the eruption depositing the Skaftafellsheiði tephra. However, no silicic ash was produced in the 1727 AD eruption, probably because of the short dormant period between the two historical eruptions. Tephra from the 1727 AD eruption can be found in most of the historical profiles in the Öræfi district, hinting at a similar dispersal pattern as in the two prior eruptions. The question of preservation has to be raised in terms of explaining the observed dispersal patterns of older tephras. The lack of suitable profiles around the mountain covering the last 3000 years inhibits further interpretation of tephra distribution and might obscure the true pattern. However, it is fairly clear that most of the tephra produced in the pre-historical eruptions was transported over the sea to the south and south east or over the ice to the north. This can be seen from detailed investigations of profiles west, north and east of the study area where no traces of any other eruptions of Öræfajökull have been found except from that of 1362 AD. Despite initially going to the east, the Ö1362 tephra has recently been found in a Greenland ice core (Palais *et at.*, 1991).

4.6.3 Limitations in tephra correlation

As explained above, the pre-Hekla-4 tephra stratigraphy is elusive and it is difficult to correlate tephras between sites, even a short distance apart. This can be broadly explained by the factors controlling the preservation of tephras and the limitations in using geochemistry to correlate between tephras and volcanic systems in Iceland.

One of the most important conditions for tephra preservation in soils is the depositional environment. In the study area, thin tephra layers seem to be best preserved in peat aeolian andisol. This can be best shown by comparing the aeolian soil-based stratigraphy of profile 14 on Svínafellsheiði following the deposition of the Skaftafellsheiði tephra with that covering the same period in the peat profile 52. Very thin (usually <0.5 mm thick) tephras in the latter profiles can not be found on Svínafellsheiði or in any other profile in the study area. The wet and fine grained environment of the peat is most probably the reason for the better resolution of the tephras. Therefore, it is likely that the depositional environment controlled the preservation rather than the dispersion of the tephras. Other major factors controlling preservation is the time of the year of deposition. During the summer, the tephra is more likely to be conserved in various soil types if the substrate is snow free. Tephra which falls on heavily vegetated land in late summer time would have the best preservation potential because long grass inhibits wind erosion. On the other hand, if the tephra falls on a snow-covered surface, it will probably be washed off or at least be reworked. This was the case when the Hs tephra fell in calm weather in winter time (Larsen and Thórarinsson, 1977). In Öræfi this can be substantiated by the location of the white unit of this particular tephra. It varies greatly, sometimes being at the base or even at the top of the basaltic unit. What is typical for the white unit is that it is always rippled, indicating reworking by water.

Environmental activity during the deposition of various tephras also played a great role in tephra preservation. It is clear that the soil formed prior to the deposition of the Hekla-4 tephra has been stripped away by glacier activity in many places,

especially inside the inferred Neoglaciation limits. This occurred either physically through the action of ice or jökulhlaups or because of glacier meltwater activity. The best example is in front of Kotárjökull where slope and meltwater activities eroded the soil cover or inhibited its formation.

The weather at the time of an eruption might also play a vital role in preservation. Winds and rain can rework the tephra to the point that it is stripped in places. This would cause a patchy distribution. The patchy nature can also be linked with the dispersal pattern of the tephra fall. This was the case with the H1104 AD tephra in the Öræfi district. Some of the profiles on Skaftafellsheiði did not contain this tephra while others did, even if profiles were only a few metres apart.

Lack of knowledge of the geochemistry of some of the volcanic systems in Iceland limits tephra correlation prior to the deposition of the Hekla-4 tephra in the Öræfi district. It especially applies to the silicic part of some of the known volcanic centres. As seen from the data presented in this study many of them are hard to 'fit' with the known composition of individual volcanic systems in Iceland. Whether these tephras are from a source for which the geochemistry is not yet known is hard to evaluate.

As can be seen from the above, many factors could explain the problems of correlating tephras in the Öræfi district. The implication is that in areas of high environmental activity, like the Öræfi district, a caveat should be introduced when either stratigraphy or geochemistry is applied as a correlation method. Both methods have to be used in conjunction with each other to get reliable results.

4.6.4 The nature and rate of sediment accumulation

The main factors controlling the sediment accumulation are the rate of erosion and accretion. More specifically, the supply of transportable sediments would control the rate of accumulation at any give time. This suggests that a link exists between the destabilisation of the environment and the accumulation rates. Therefore, the sediment accumulation should be enhanced if glaciers advance, both in terms of

increased rate and sediment grain size distribution. However, other non-climatic factors might change the supply of transportable sediments for example major jökulhlaup events onto Skeiðarársandur. The relationship between jökulhlaups onto Skeiðarársandur and subglacial volcanic activity is not apparent in the present data. However, this relationship is by any means refused since the sandur environment is greatly destabilised when jökulhlaups occur. On the other hand, a good relationship occur between the composition of the sediments and enhanced environmental activity in the study area. The best example is profile 64 in front of Kvíárjökull. The clast orientation and striation of the different gravel units substantiate the glacial source.

Sediment accumulation rates were established by using the mean of several rates from profiles covering the whole study area. In this study, extrapolation produced meaningful results, implying that the effect of local instabilities averaged out over time. There are some long term changes as discussed below. Therefore, the mean soil accumulation rate (MSAR) was calculated in order to best depict the variations in the soil thickness and error bars placed on the final results.

The pre-1362 AD time.

The nature and pattern of sediment accumulation in the pre-1362 time is very different between sites in the study area because of local erosion and instability of the environment. Table 4.39 (Appendix II) shows the results of the calculations of the MSAR of selected sites in the study area. The foregoing dating of unknown tephra layers and important marker horizons covering the pre-historic period revealed a MSAR of 0.249±0,04 mm/a. The error bands are calculated as half of the range of the calculated MSAR in the study area. This calculated rate fits reasonably well with the radiocarbon dates conducted for this study. However, in some cases the MSAR seems to overestimate the dates if compared with the radiocarbon dates but the difference is considered negligible. This is because the error bars of the MSAR and the radiocarbon dates always overlap.

Three well-dated tephra layers were used to calculate the MSAR i.e. Hekla-4 (ca. 3830 BP), Vö ca. 900 AD (ca. 1050 BP) and the 1362 AD (588 BP) tephras.

Because the Vö ca. 900 tephra was sometimes difficult to distinguish with a high degree of certainty, profiles were selected where the author was confident that the layer was correctly identified, mainly from white plagioclase crystals normally found in the layer which makes it clearly distinguishable from other Veiðivötn or Grímsvötn eruptions of similar colour and texture (Larsen, 1979, 1984). Profiles where Vö ca. 900 AD was identified are exclusively on Skaftafellsheiði and in front of Virkisjökull. Because these two sites only represent a limited region of the study area the MSAR was also calculated between Hekla-4 and Ö1362 AD to better characterise the accumulation rate in the whole of the study area. This enabled the author to include Svínafellsheiði and Kviárjökull. The rationale of using the Ö1362 as the upper limit of the pre-historical MSAR is that there is no significant difference in the accumulation rate between Vö ca. 900 AD and the big eruption in 1362 AD. This can be seen, for example, in profile 70 on Skaftafellsheiði, where this was specifically tested. Therefore, it will not bias the results.

If the Oddar-Hekla-Ö (ca. 6000 BP) correlation is accepted, the soil accumulation rate between Hekla-4 (ca. 3800 BP) and Hekla-Ö on Skaftafellsheiði is 0.18 mm/a. A caveat has to be introduced here because this is only based on a single profile. Furthermore, given the uncertainties of geochemical correlation, the true source of most of the tephras could not be established for the majority of the tephras for the period between Hekla-4 and Hekla-Ö. Therefore, three arguments would strongly recommend using the rate of 0.249 mm/a to date deposits formed prior to the Hekla-4 tephra. Firstly, this is a mean rate of soil accumulation which would take into account every fluctuation in the MSAR. Secondly, if slower growth rates are used, the dates of older deposits are probably overestimated in terms of the presently known deglaciation history of Iceland. Thirdly, only the Hekla-Ö tephra could be identified with high precision prior to the deposition of the Hekla-4 tephra. Furthermore, the tephra was only found in three profiles, where only two were suitable for calculating the MSAR. The nature of the tephrochronology of the study area inhibits further deduction.

The MSAR calculated here is in accord with the results from Dugmore (1987) around Eyjafjallajökull but notably higher than Thórarinsson (1958) derived over a similar time interval from eastern Iceland. This observed difference can be explained by more frequent destabilisation of the sandur environment near the glaciated areas where, along with glacier fluctuations, jökulhlaup activity onto Skeiðarársandur and the Öræfajökull jökulhlaup, serve as a major factor of sandur destabilisation in the study area.

The accuracy of the MSAR was tested by using the MSAR during the pre-1362 AD time to date the Skaftafellsheiði tephra previously dated by radiocarbon analysis. A similar test was carried out by Dugmore (1987) around Eyjafjallajökull. This was the only site that on which this was possible because of the lack of organic material. The MSAR revealed a date of 1581±60 BP and the radiocarbon date gave 1540±50 BP. The results are in close agreement. This would suggest that the dates obtained by MSAR have similar reliability as the radiocarbon method in the Öræfi district.

Post-1362 AD time.

The soil accumulation rate was calculated from selected profiles covering the whole study area to be 0.587±0.02 mm/a over the period between 1362 and 1727 (Table 4.40; Appendix II). The error bars are calculated as a standard measurement error of 5 mm when a section is logged. Tephra layers were subtracted from the soil profile and not used in the calculations. The MSAR is much higher compared with the results of Thórarinsson (1958) who calculated the mean accumulation rate as 0.27 mm/a between 1362 and 1875. However, this latter figure is much lower than Dugmore (1987) calculated for the area around Eyjafjallajökull. Dugmore's results give 2.0 mm/a over a similar period of time. The reason for this difference is probably due to the huge wind drift from the extensive sandur plains in Öræfi and around Eyjafjallajökull unlike Thórarinsson's measurement sites which are located in less active erosional and deposition environments. Furthermore, the difference between the MSAR used in this study and used by Dugmore (1987) is probably because the sandur catchment area is much bigger in the latter study and more sediment was available.

Profile 7 shows the largest number of post-1362 tephras in the study area. Therefore, it was used to identify and date tephras of unknown origin for this part of the stratigraphy (Fig. 4.1). When the tephras had been identified, it was possible to estimate the SAR between individual tephras in order to depict patterns. Figure 4.35 shows the results of the calculated SAR of profile 7 on Skaftafellsheiði. This profile is thought to represent the situation in Öræfi quite well and reveals interesting patterns. It is clear that the big eruption in 1362 AD increased soil accumulation in the area greatly for the first decades after the event. The second biggest SAR is calculated for the LIA, presumably because of increased environmental activity due to climate deterioration. Enhanced slope activity and increased supply of sediments followed when glaciers advanced as a consequence. It is also interesting to note the generally higher SAR when big volcanic eruptions deposit tephra. Here, the eruptions of Katla in 1625 and 1755 and the Öræfajökull 1727 can be taken as examples.

The general pattern is also interesting. The lowest SAR occurs at the time of settlement in the 9th Century apart from the period between 1918 and 1995. The implication is that the environment has stabilised over the recent decades in comparison with the period just after the 1362 AD eruption and around the Little Ice Age. If the SAR is compared with available and reliable climatic data (Ogilvie, 1984, 1991; Bergthórsson, 1969) certain similarities become apparent. The SAR slightly increases between the Settlement and the 1362 AD eruption, especially in the 12th and 13th Century which could be explained by a colder climate causing increased slope activity. Ogilvie (1991) reports climatic deterioration in the late 12th and early 13th Century and in the latter part of the 13th Century which fit reasonably well with the present pattern (Fig. 4.35). Similar results have been reported from around Eyjafjallajökull, south Iceland, by Dugmore and Erskine (1994). However, there is a notable difference around the 1362 AD eruption which devastated the Öræfi region (Thórarinsson, 1958).

Generally, the pattern of SAR during the historical time seems to reflect the nature of environmental change related to climate and eruption activity rather than pressures of human settlement (Fig. 4.36). If so, the basis of the pattern is different from the rest of Iceland where Thórarinsson (1961) and in south Iceland, Dugmore and Erskine (1994) suggest that pressures from settlement caused significant breaching of the vegetation cover mainly because of grazing. Small population numbers after the eruption in 1362 AD (Thórarinsson, 1958) could explain the differences between Öræfi and the rest of Iceland. The implication is that the Öræfi district is important in identifying the natural signal of environmental change over historical time in Iceland.

Fig. 4. 1. The composite tephra stratigraphy of the Öræfi district, SE-Iceland

The stratigraphic succession reveals the limitations in correlating tephras deposited prior to the eruption of Hekla ca. 3830 BP (Hekla-4) in the study area. This is mainly due to the different geochemistry of what stratigraphically could be the same layer. For legends, see Fig. 4.2.

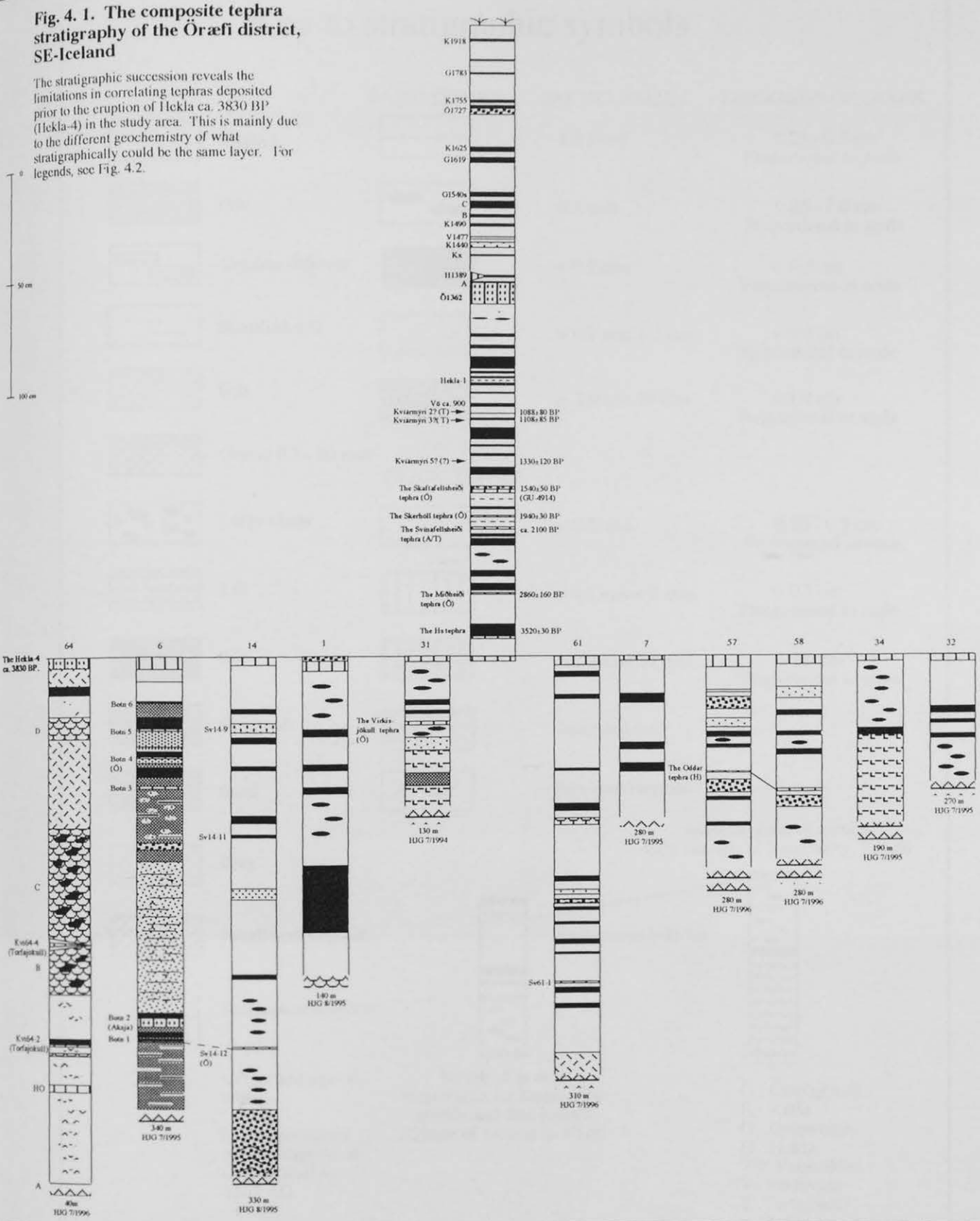

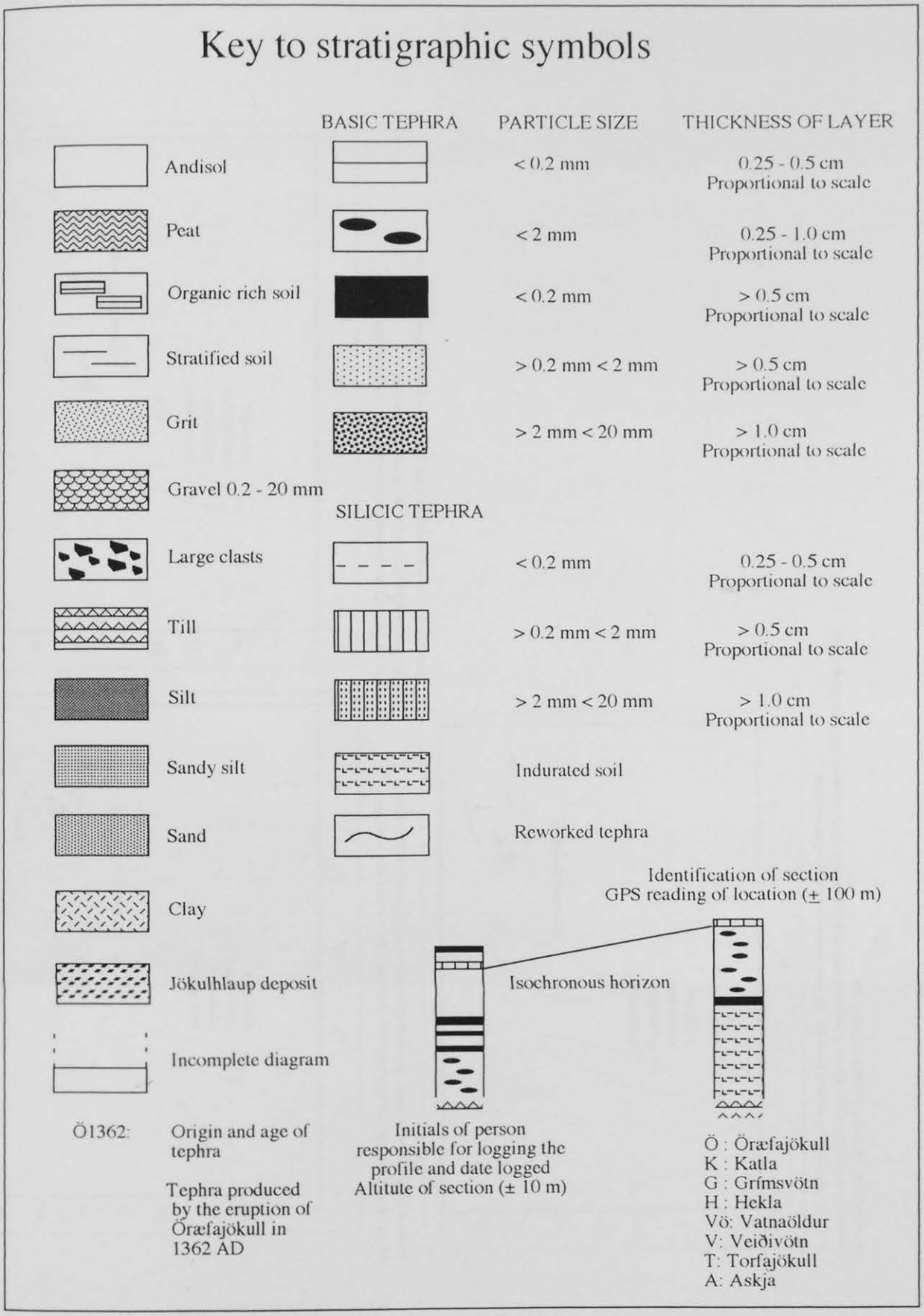

Fig. 4.2. Legends to all stratigraphic symbols used in the study.

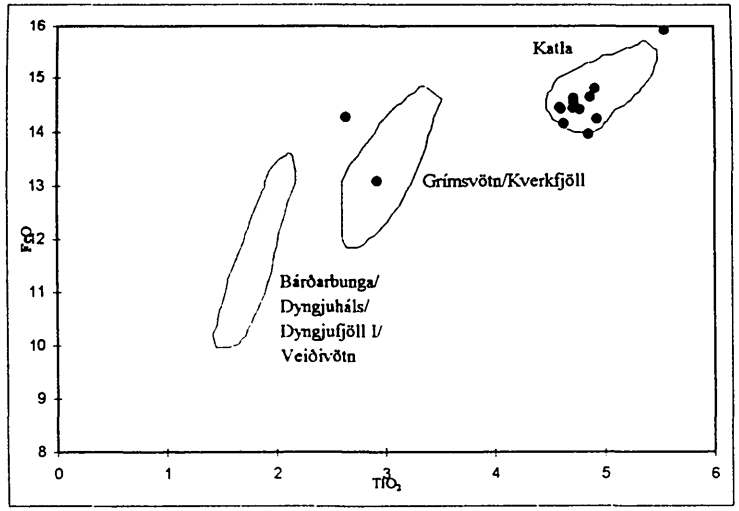

Fig. 4.3. FeO-TiO_2 plot showing the Katla origin. Comparison data is from Steinthórsson (1977), Jakobsson (1979) and Larsen (1982). The tephra shows high FeO/TiO_2 typical for Katla tephra.

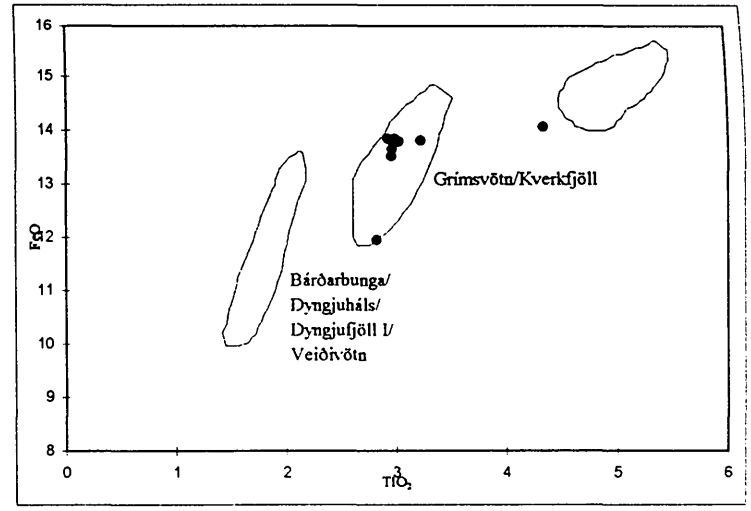

Fig. 4.4. FeO-TiO_2 plot showing the Grímsvötn origin. Comparison data is from Steinthórsson (1977), Jakobsson (1979) and Larsen (1982).
The tephra shows an intermediate FeO/TiO_2 composition typical for Grímsvötn tephra.

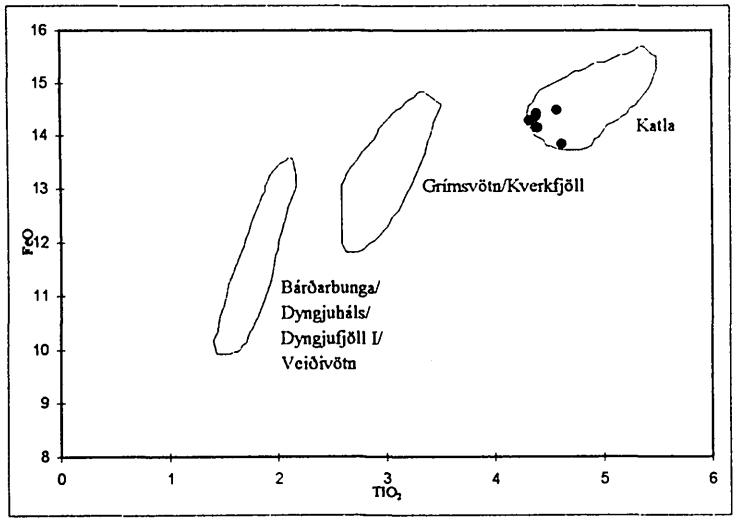

Fig. 4.5. FeO-TiO_2 plot showing the Katla origin. Enclosed areas show the range of known typical compositions of a distinct volcanic system. Comparison data isfrom Steinthórsson (1977), Jakobsson (1979) and Larsen (1982). The tephra shows high FeO/TiO_2 typical for Katla tephra.

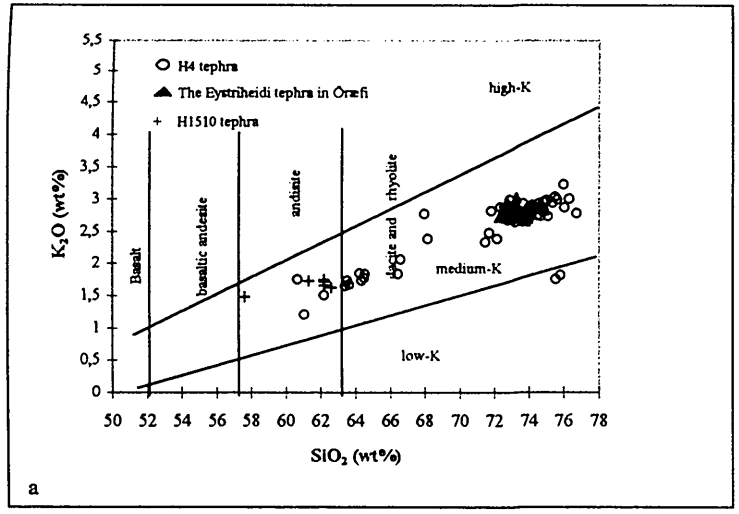

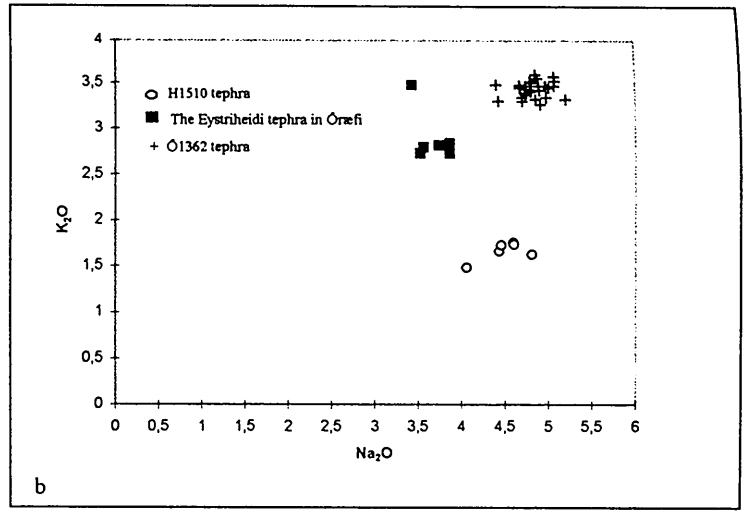

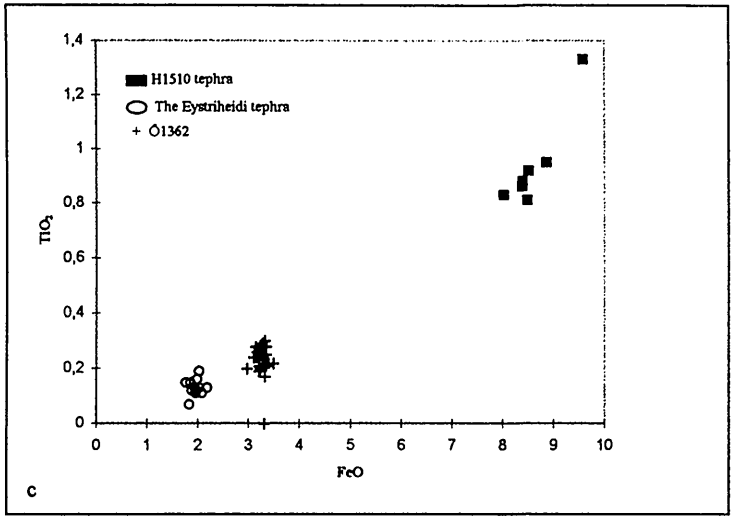

Fig. 4.6a,b,c. The Eystriheidi tephra. Reference data are from the Tephrabase at the department of Geography, University of Edinburgh (http://www.geo.ed.ac.uk).
The tephra shows a typical Hekla composition as seen by the silica and potassium content. Hekla 1510 can be ruled out as an origin since it shows different compostion in comparison with known H1510 chemistry. An origin from Öræfajökull volcanic system can also be ruled out based on the chemistry.

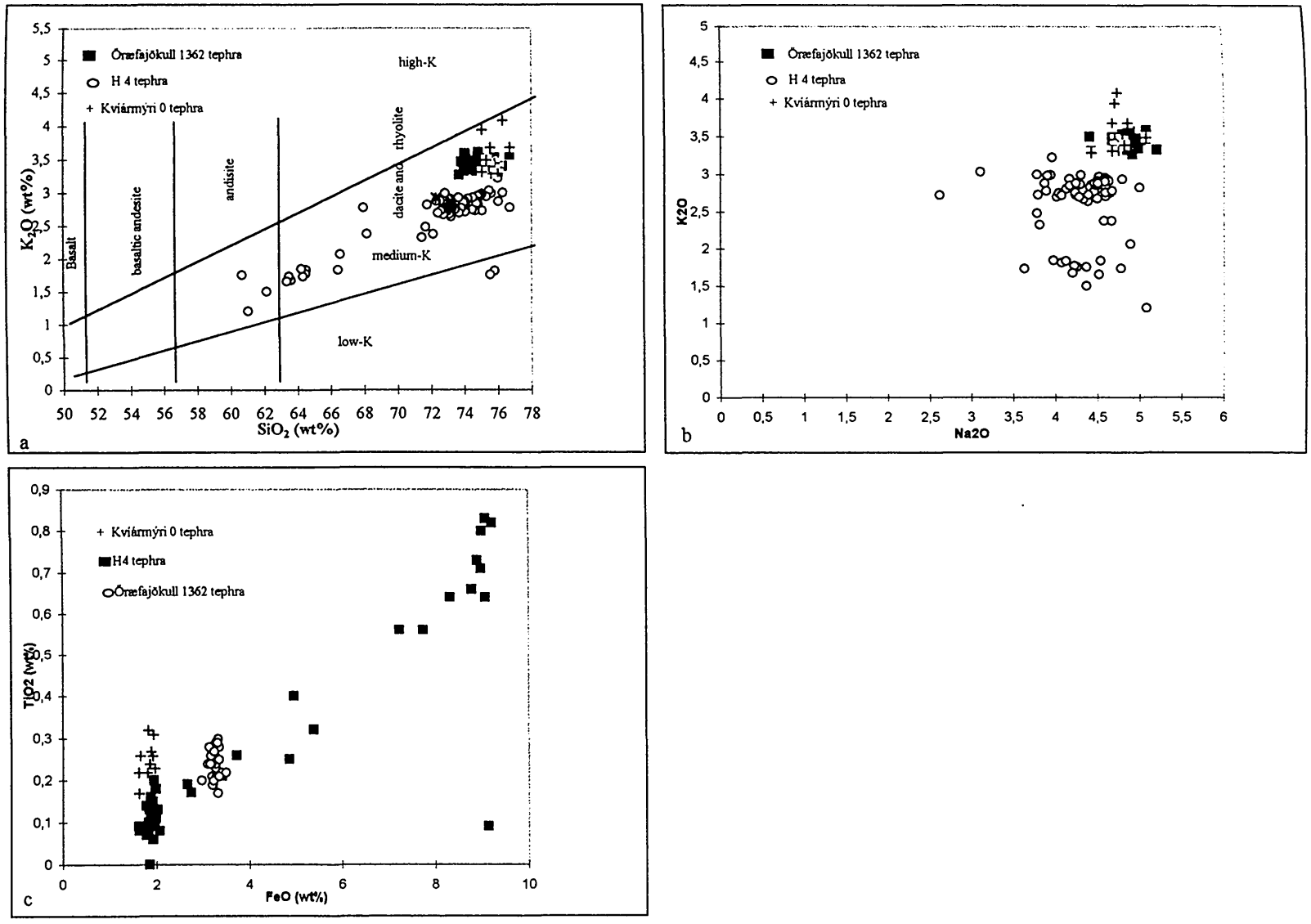

Fig. 4.7a,b,c. The Kviármýri 0 tephra. Reference data are from the Tephrabase at the department of Geography, University of Edinburgh (http://www.geo.ed.ac.uk). The Kviármýri 0 tephra shows similar chemical characteristics as the Öræfajökull tephra, particularily in terms of potassium, sodium and silica.

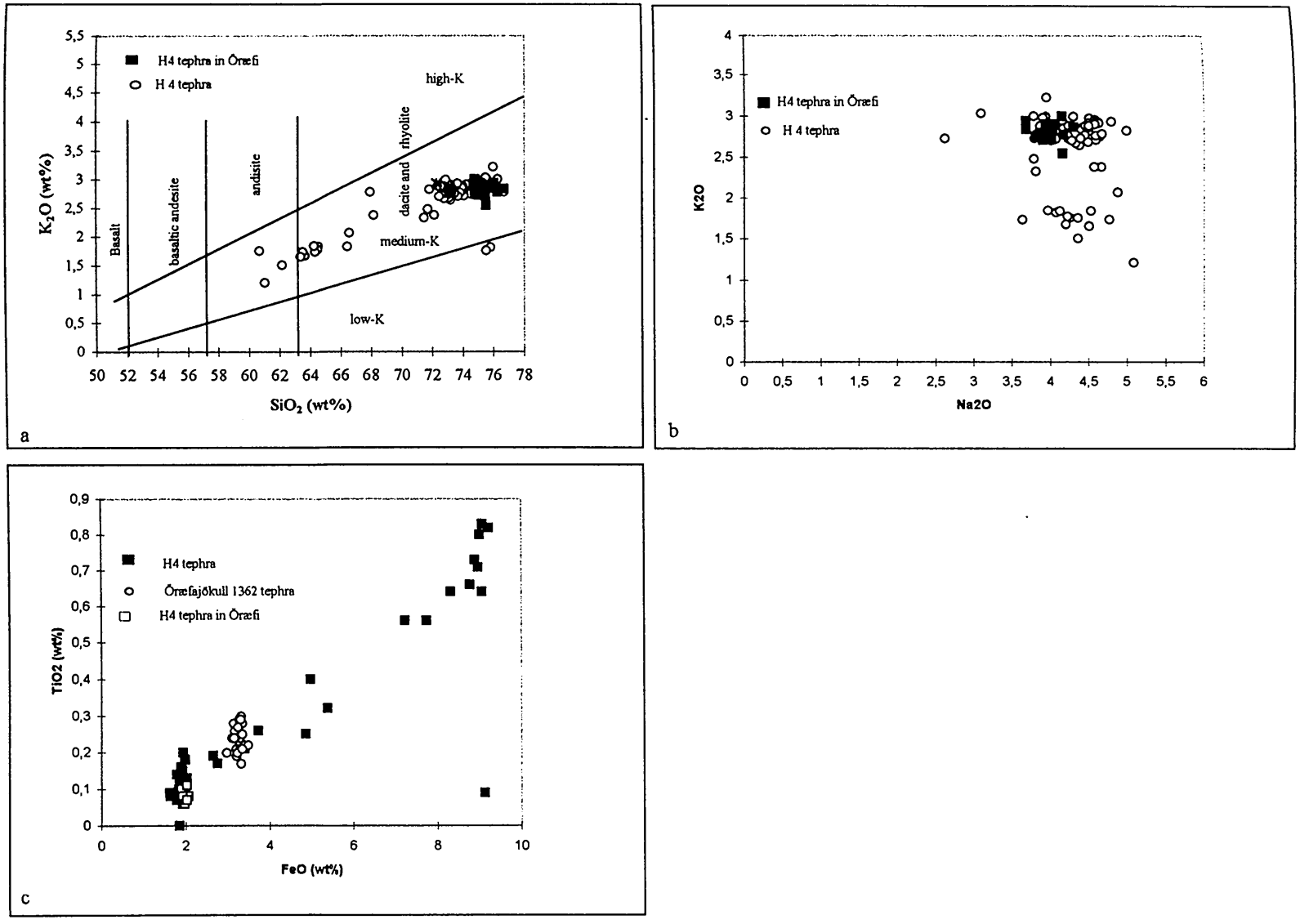

Fig. 4.8a,b,c. The Hekla-4 tephra. Reference data are from the Tephrabase at the department of Geography, University of Edinburgh (http://www.geo.ed.ac.uk). The tephra exhibits all major characteristics of the Hekla-4 tephra in the compared elements (silica, potassium, sodium, iron and titanium).

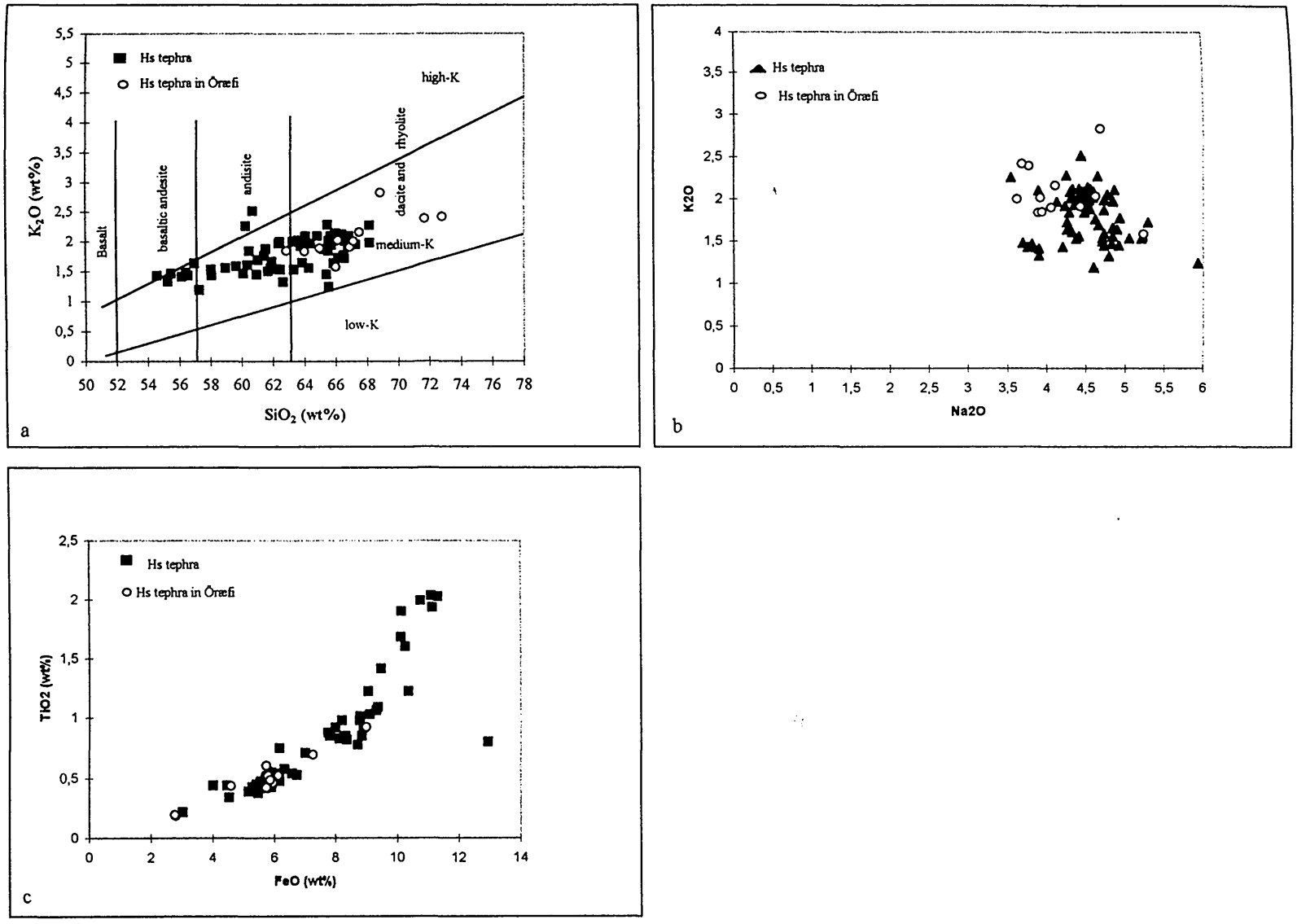

Fig. 4.9a,b,c. The Hekla-s tephra. Reference data are from the Tephrabase at the department of Geography, University of Edinburgh (http://www.geo.ed.ac.uk).
The tephra exhibits all major characteristics of the Hs tephra in the compared elements (silica, potassium, sodium, iron and titanium). Note the same chemical trend in Fig. a and c.

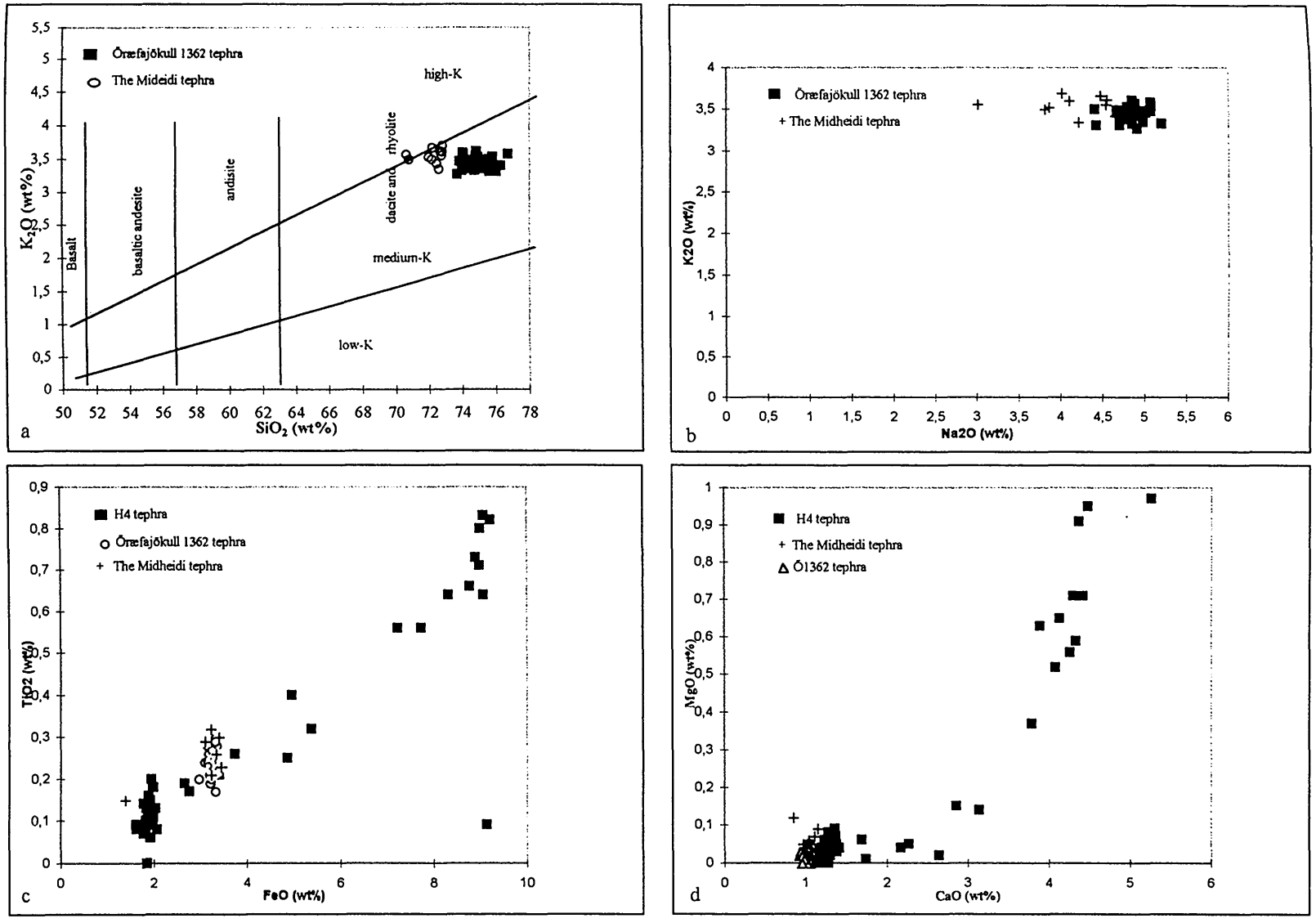

Fig. 4.10a,b,c,d. The Miðheiði tephra. Reference data are from the Tephrabase at the department of Geography, University of Edinburgh (http://www.geo.ed.ac.uk).
The tephra shows characteristics typical for the Öræfajökull volcanic system. Note the small deviation in sodium (Fig. a and b). This is probably due to sodium loss when analysed.

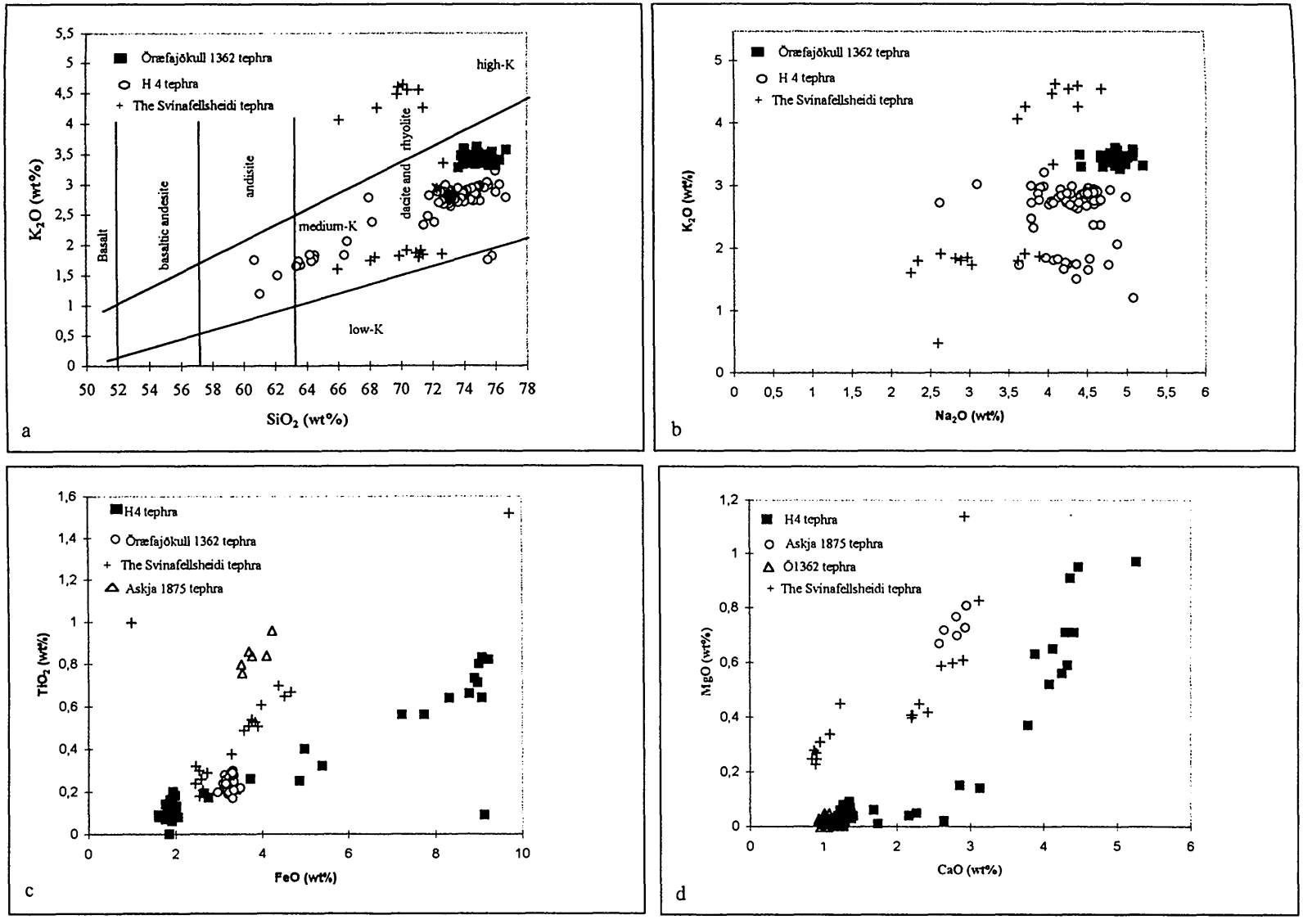

Fig. 4.11a,b,c,d. The Svínafellsheiði tephra. Reference data are from the Tephrabase at the department of Geography, University of Edinburgh (http://www.geo.ed.ac.uk). The tephra has two sources. Group A is low-K glass which rules out Hekla and Öræfajökull origin. Group B is high-K glass indicating an origin from Torfajökull.

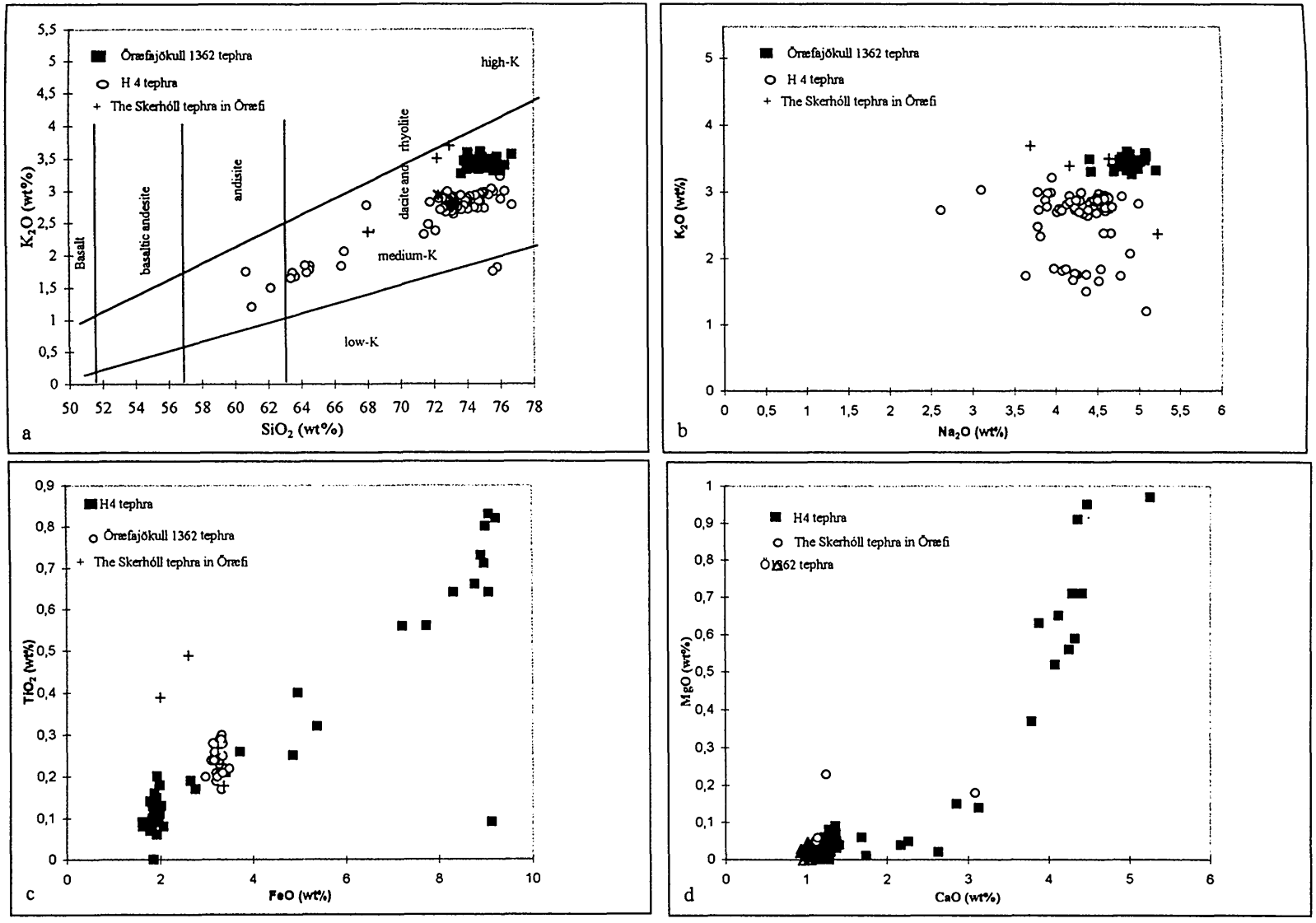

Fig. 4.12a,b,c,d. The Skerhóll tephra. Reference data is from the Tephrabase at the department of Geography, University of Edinburgh (http://www.geo.ed.ac.uk). The tephra shows similarities with Öræfajökull eruptions. This is best displayed in silica and potassium but titanium, iron, magnesium and calsium reflect more variation

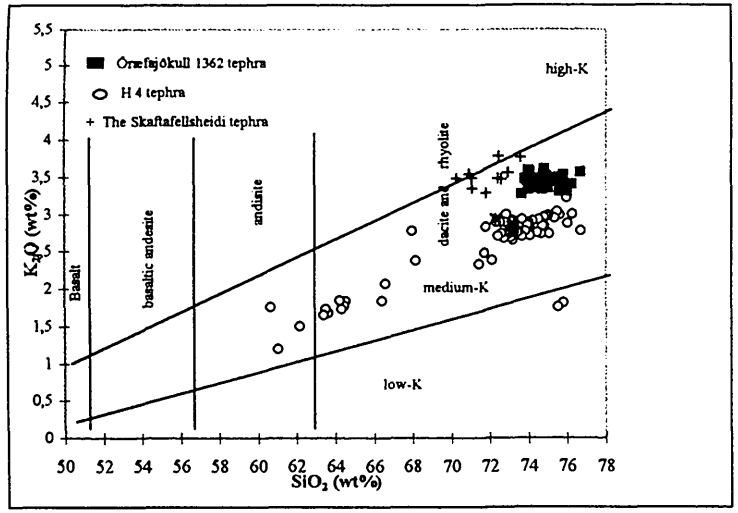

Fig. 4.13a. The Skaftafellsheiði tephra. Reference data are from the Tephrabase at the department of Geography, University of Edinburgh (http://www.geo.ed.ac.uk).

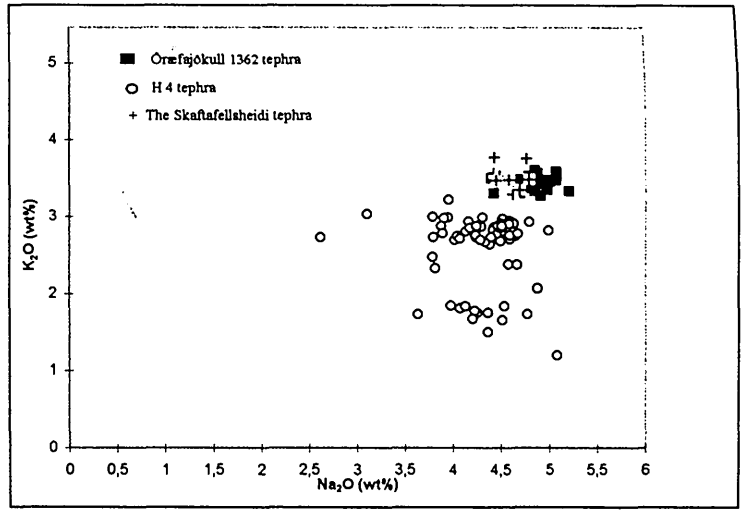

Fig. 4.13b. The Skaftafellsheiði tephra. Reference data are from the Tephrabase at the department of Geography, University of Edinburgh (http://www.geo.ed.ac.uk).

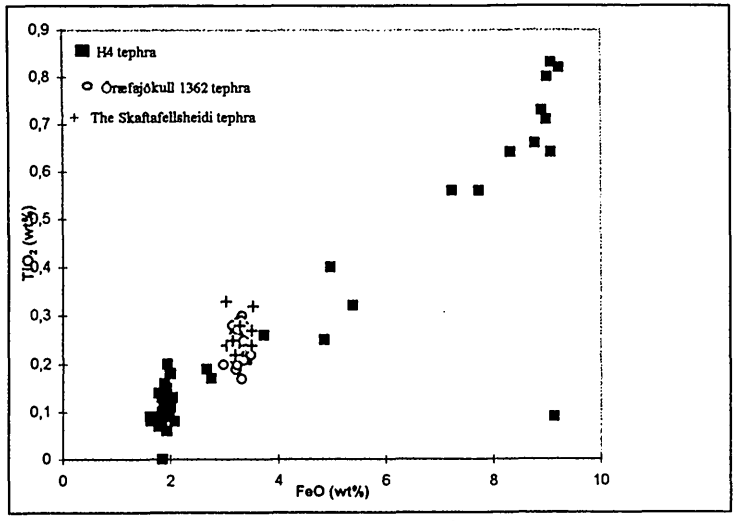

Fig. 4.13c. The Skaftafellsheidi tephra. Reference data are from the Tephrabase at the department of Geography, University of Edinburgh (http://www.geo.ed.ac.uk) . The Skaftafellsheiði tephra shows a strong Öræfajökull characteristics in all elements compared. It is a medium-K glass tephra with the same iron and titanium content as other Öræfajökull tephras.

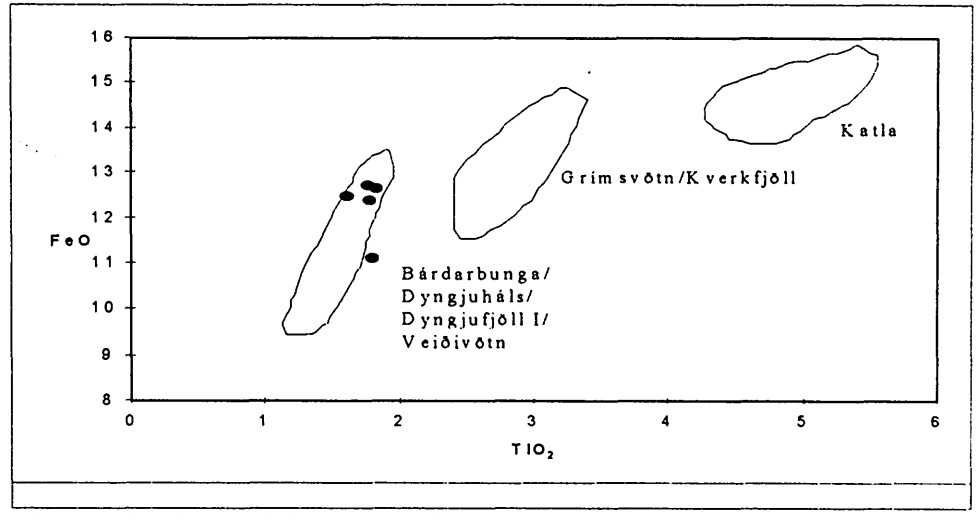

Fig. 4.14. The Vö ca. 900 tephra. FeO/TiO_2 plot showing a source from the Veidivötn volcanic system. Reference data are from Steinthórsson (1977), Jakobsson (1979) and Larsen (1982).

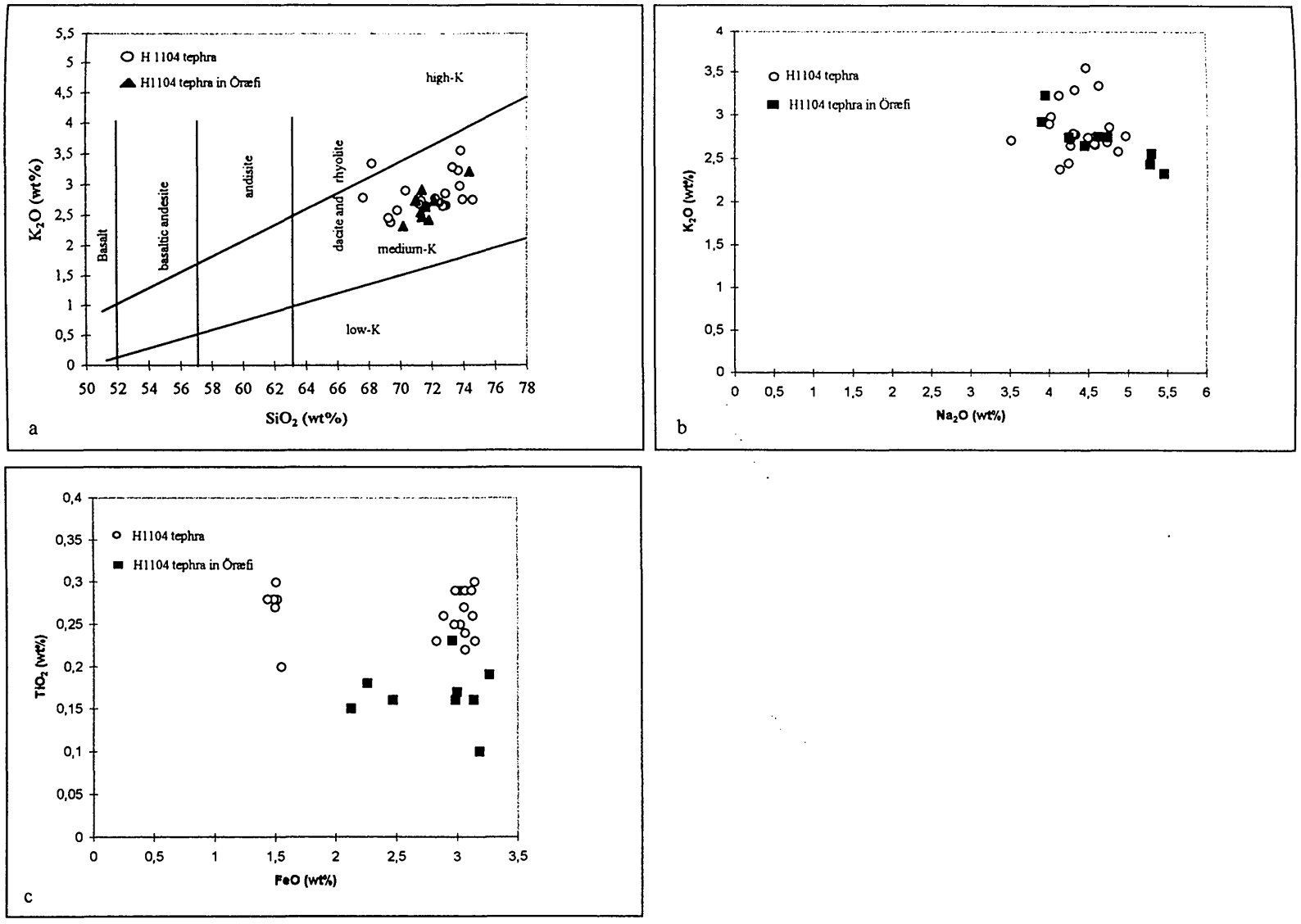

Fig. 4.15a,b,c. The Hekla-1104 (1) tephra. Reference data are from the Tephrabase at the department of Geography, University of Edinburgh (http://www.geo.ed.ac.uk).
The Hekla-1104 in Öræfi is a medium-K glass tephra showing similar chemical characteristics as Hekla-1104 elsewhere. However, titanium is slightly lower in the Öræfi samples (Fig. c).

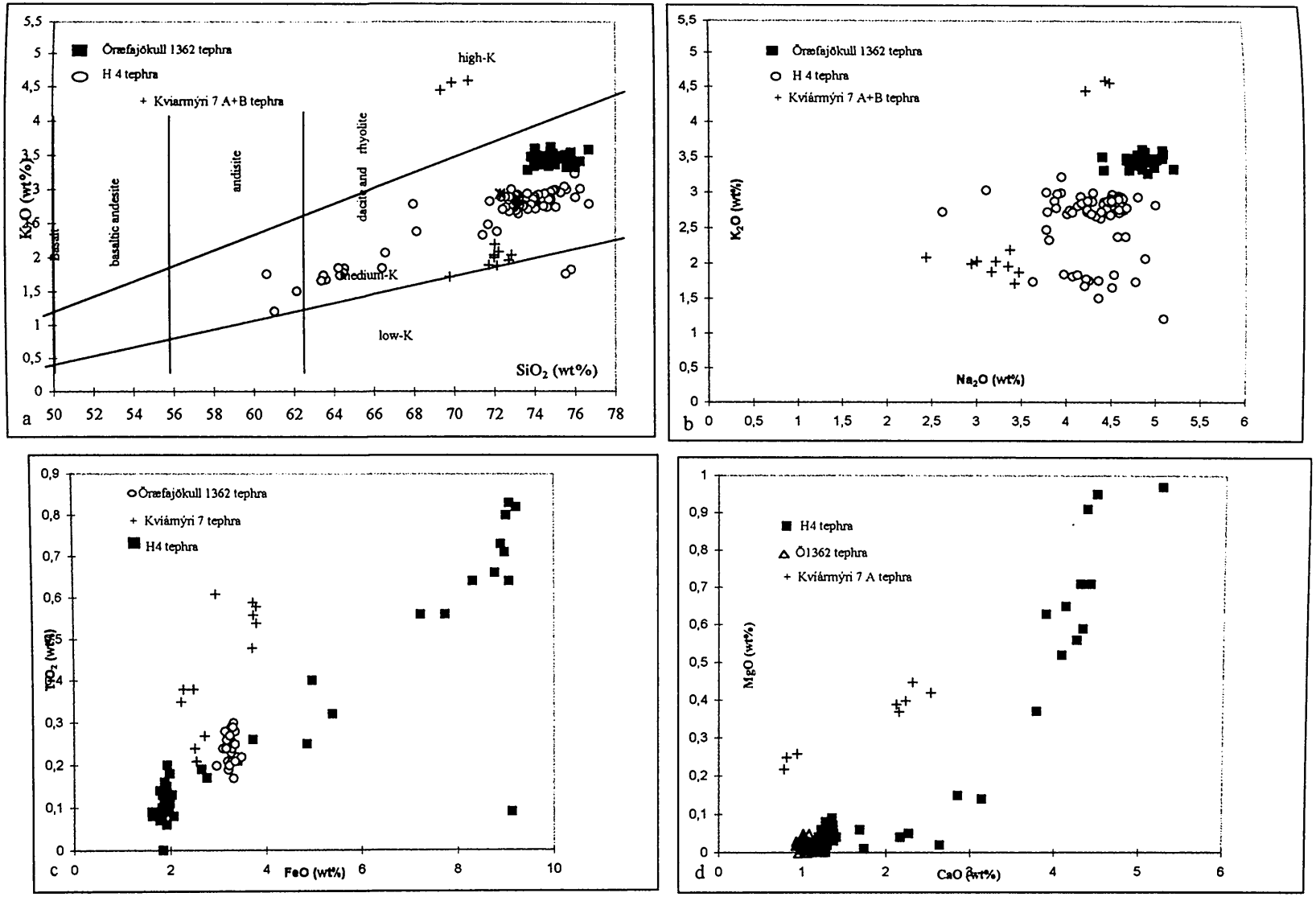

Fig. 4.16a,b,c,d. The Kvíármýri 7 tephra. Reference data are from the Tephrabase at the department of Geography, University of Edinburgh (http://www.geo.ed.ac.uk). The overall chemistry of Kvíármýri 7 tephra indicates the same dual origin as the Svínafellsheiði tephra, namely Askja and Torfajökull.

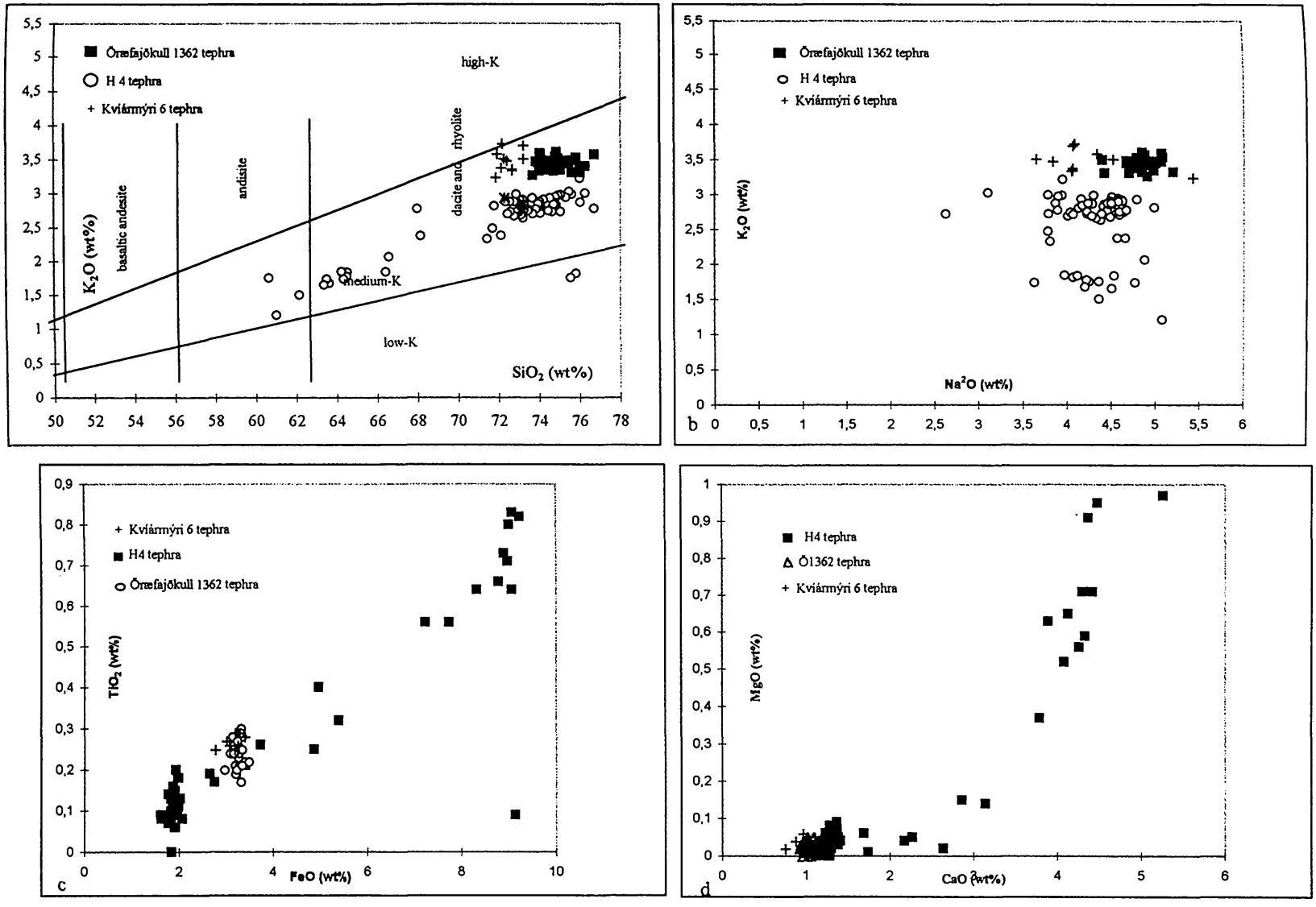

Fig. 4.17a,b,c,d. The Kviármýri 6 tephra. Reference data are from the Tephrabase at the department of Geography, University of Edinburgh (http://www.geo.ed.ac.uk). This tephra shows the same chemical characteristics as the Skaftafellsheiði tephra originating from the Öræfajökull volcanic system.

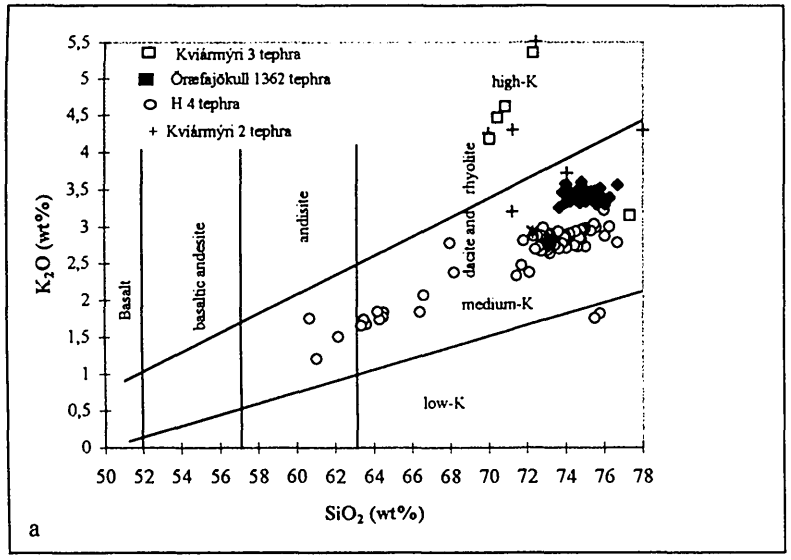

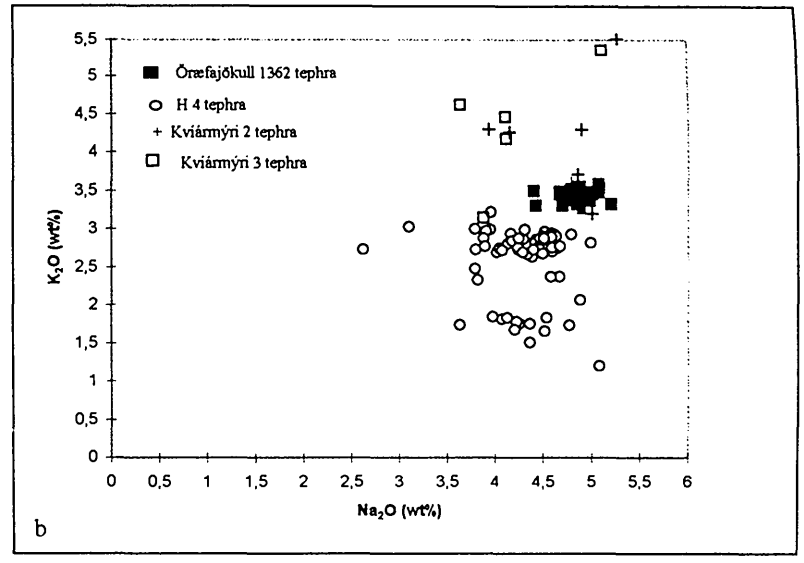

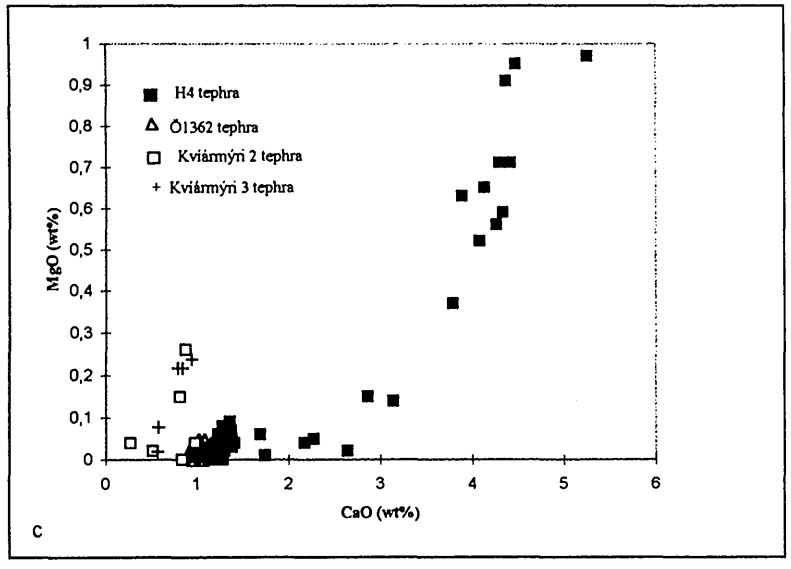

Fig. 4.18 and 19a,b,c. The Kviármýri 3 and 2 tephras. Reference data is from the Tephrabase at the department of Geography, University of Edinburgh (http://www.geo.ed.ac.uk). Note that Fig. 4.18 and 4.19 are shown together on the same diagram. Both Kviármýri 2 and 3 are high-K glass indicating a Torfajökull source.

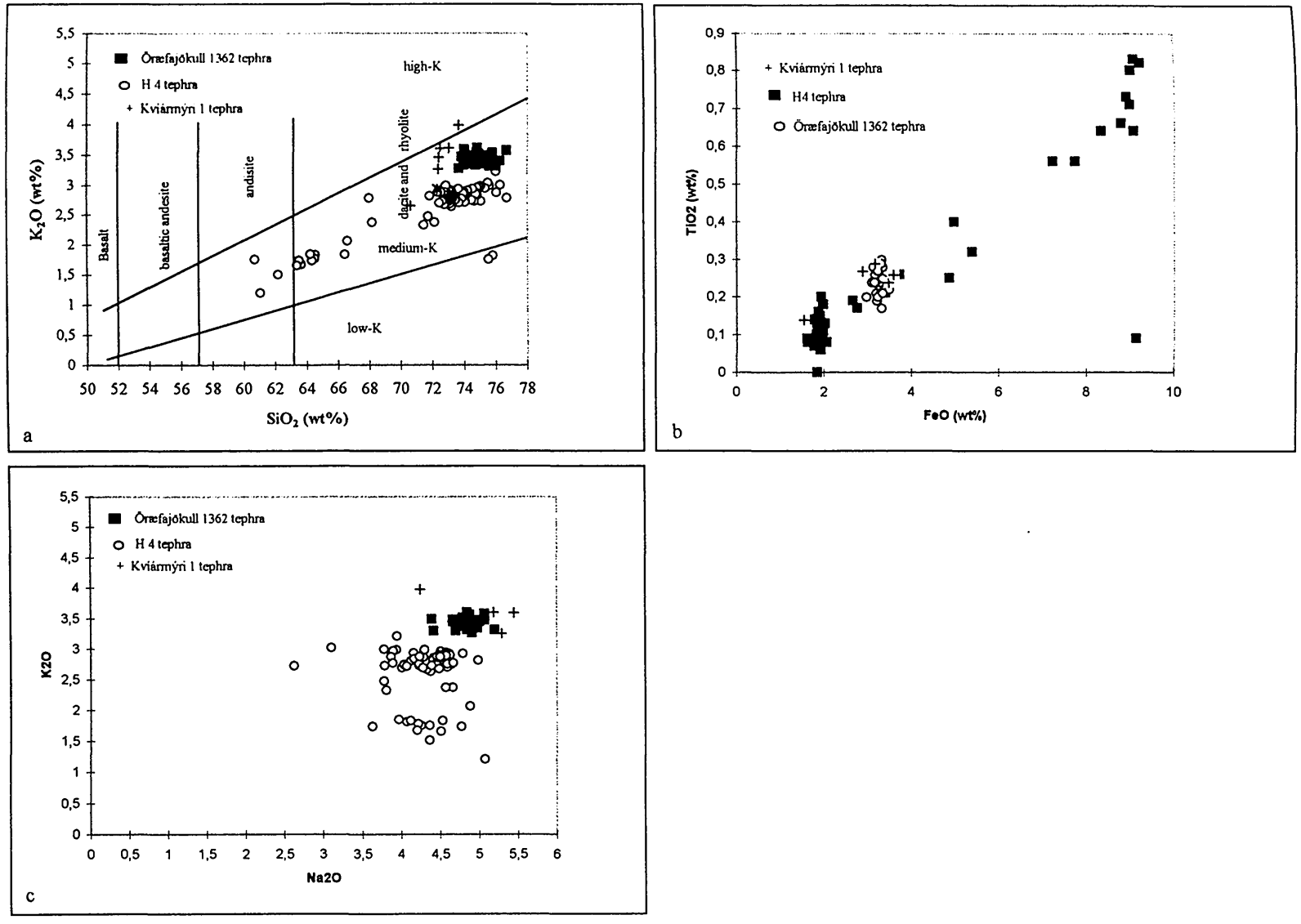

Fig. 4.20a,b,c. The Kviármýri 1 tephra. Reference data is from the Tephrabase at the department of Geography, University of Edinburgh (http://www.geo.ed.ac.uk). The tephra reveals typical K_2O, MgO and CaO contents as seen in known Öræfajökull tephras.

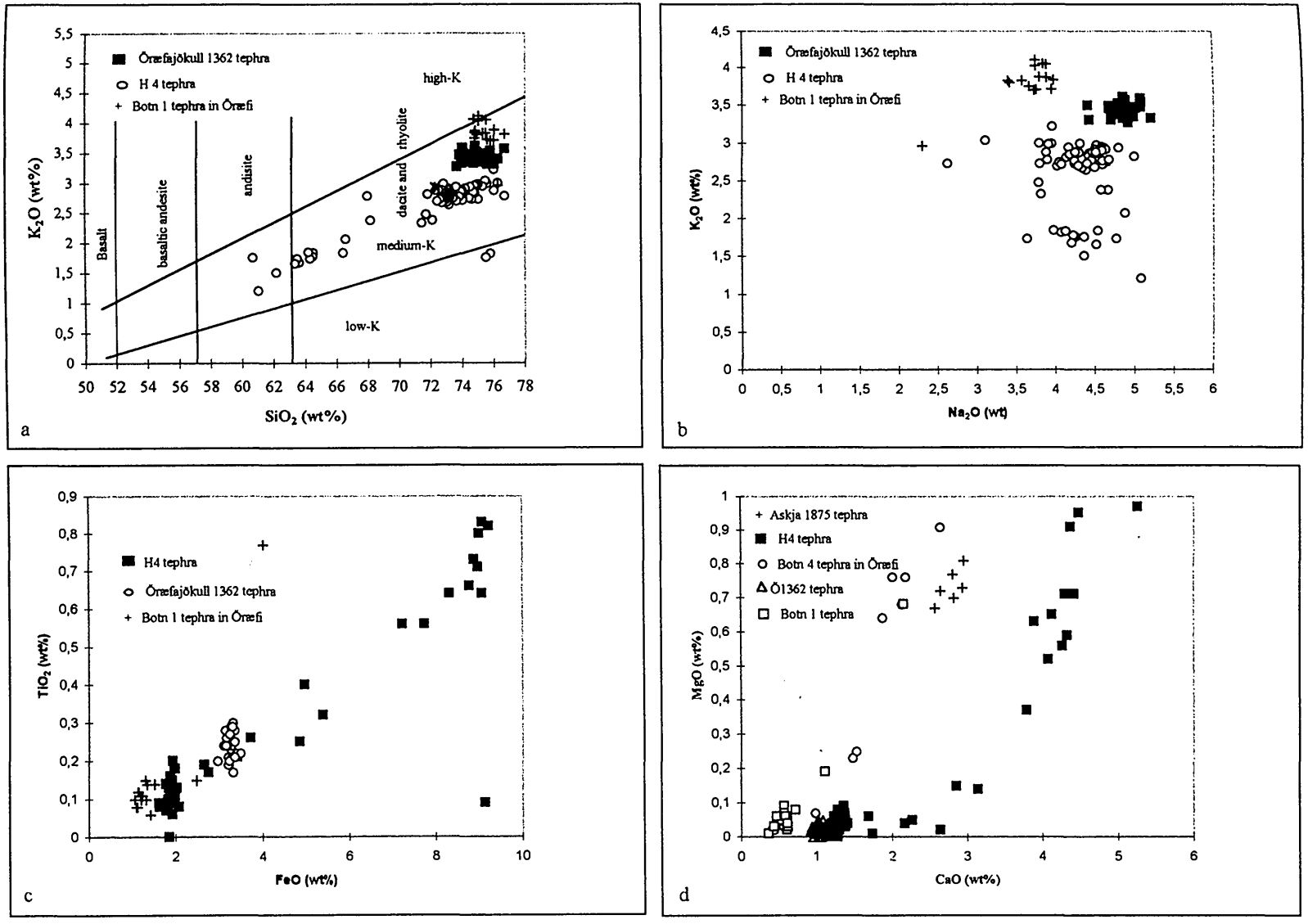

Fig. 4.21a,b,c,d. The Botn 1 tephra. Reference data are from the Tephrabase at the department of Geography, University of Edinburgh (http://www.geo.ed.ac.uk).
The tephra is difficult to correlate with known volcanic system in Iceland. The Botn 1 tephra is medium-K glass and shows certain similarities to Öræfajökull eruptions in terms of potassium.

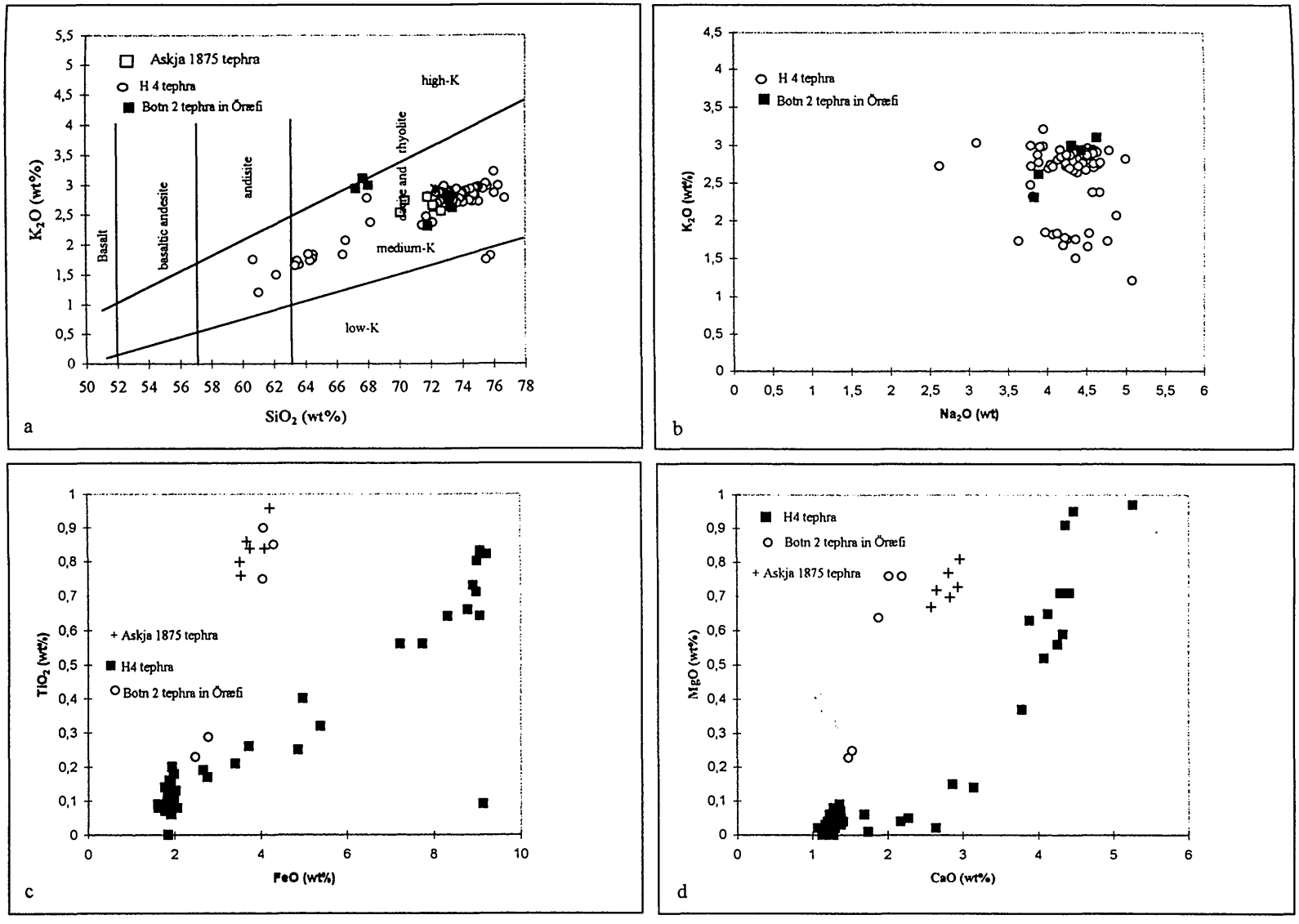

Fig. 4.22a,b,c,d. The Botn 2 tephra. Reference data are from the Tephrabase at the department of Geography, University of Edinburgh (http://www.geo.ed.ac.uk).
The tephra indicates some similarities with the Askja volcanic system and is defined as medium-K glass. The Askja affinity is most clearly indicated by looking at titanium and iron (Fig. c).

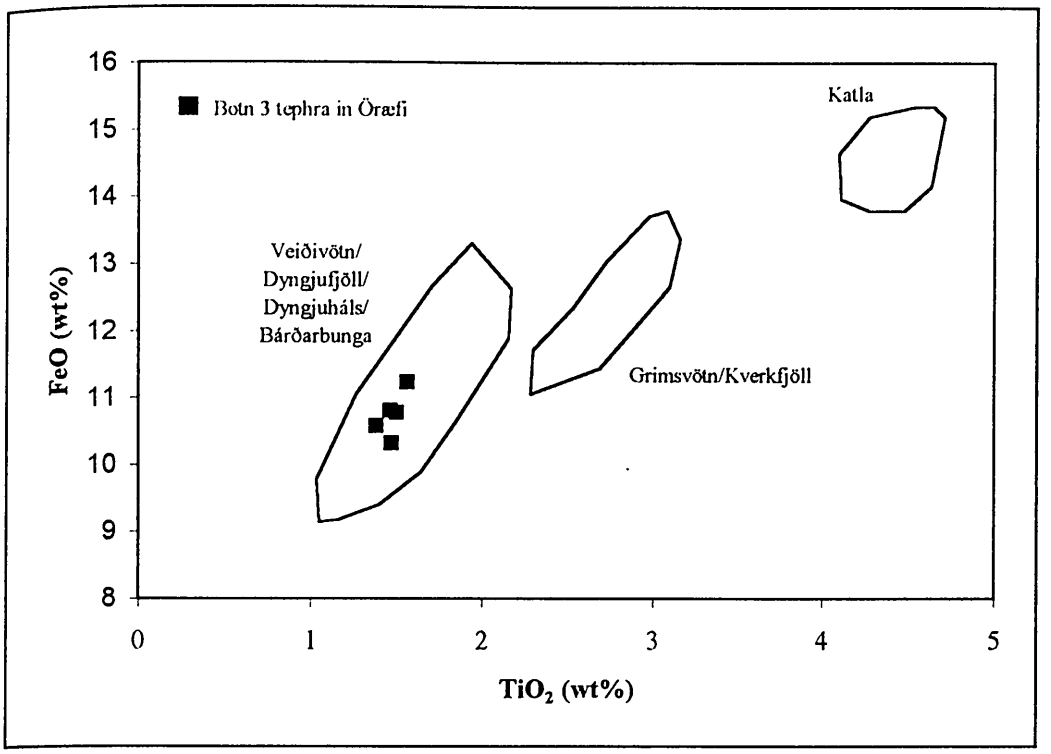

Fig. 4.23. The Botn 3 tephra. FeO/TiO_2 plot showing a source from the Veidivötn/Dyngjufjöll/Dyngjuháls/Bárdarbunga volcanic system. Reference data are from Steinthórsson (1977), Jakobsson (1979) and Larsen (1982).

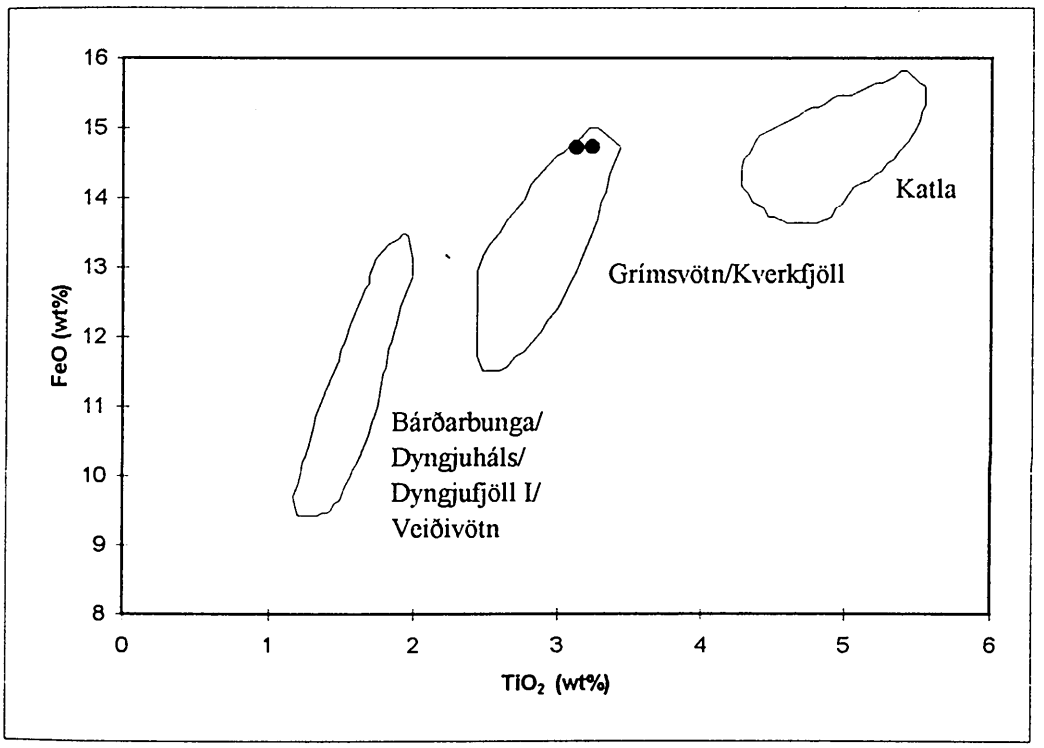

Fig. 4.25. The Botn 5 tephra. FeO/TiO_2 plot showing a source from the Grímsvötn/Kverkfjöll volcanic system. Reference data are from Steinthórsson (1977), Jakobsson (1979) and Larsen (1982). Enclosed areas show typical composition of each volcanic system.

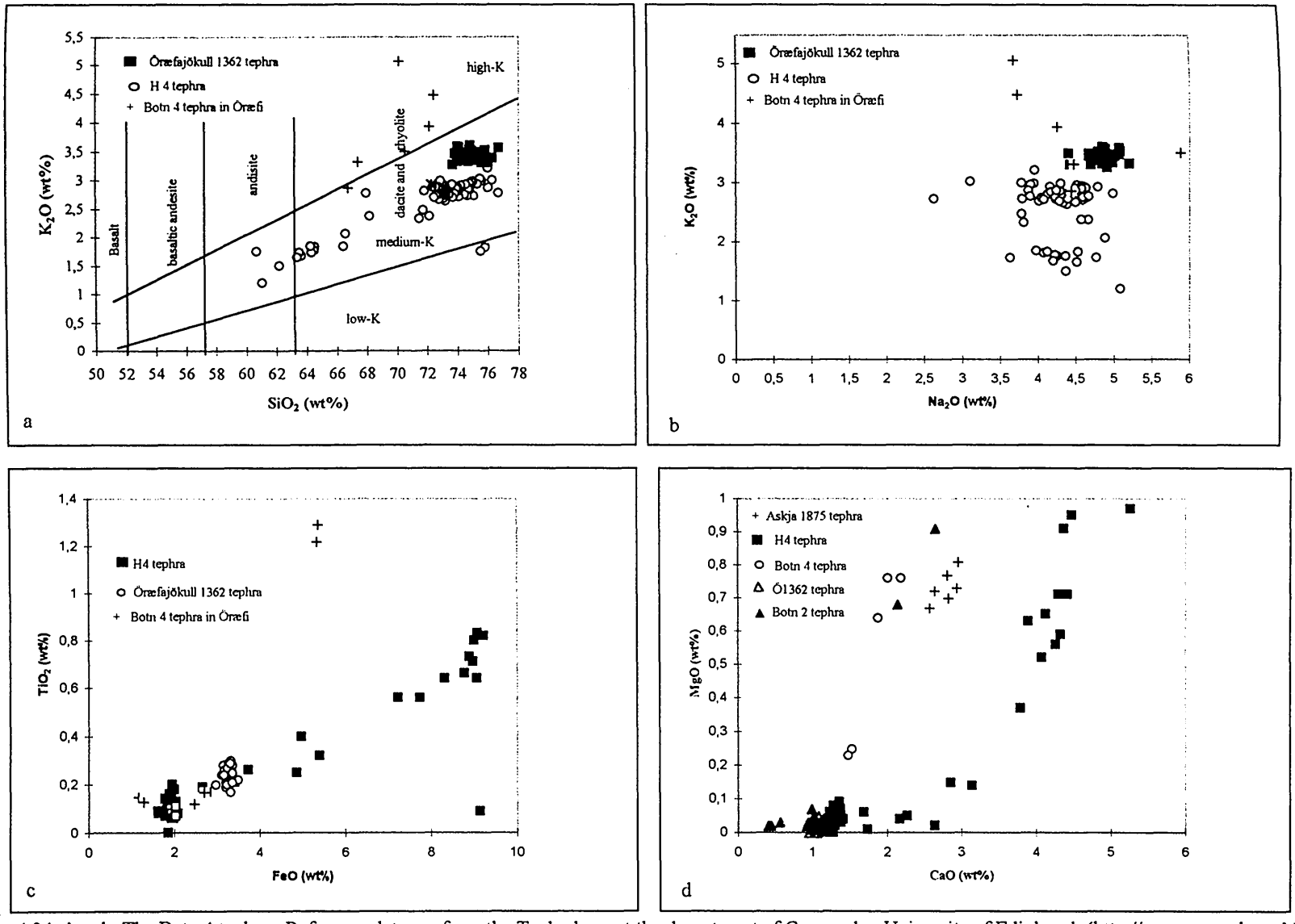

Fig. 4.24a,b,c,d. The Botn 4 tephra. Reference data are from the Tephrabase at the department of Geography, University of Edinburgh (http://www.geo.ed.ac.uk). The chemical composition hints at an origin from the Öræfajökull volcanic system. This is best derived from titianium and iron (Fig. c)

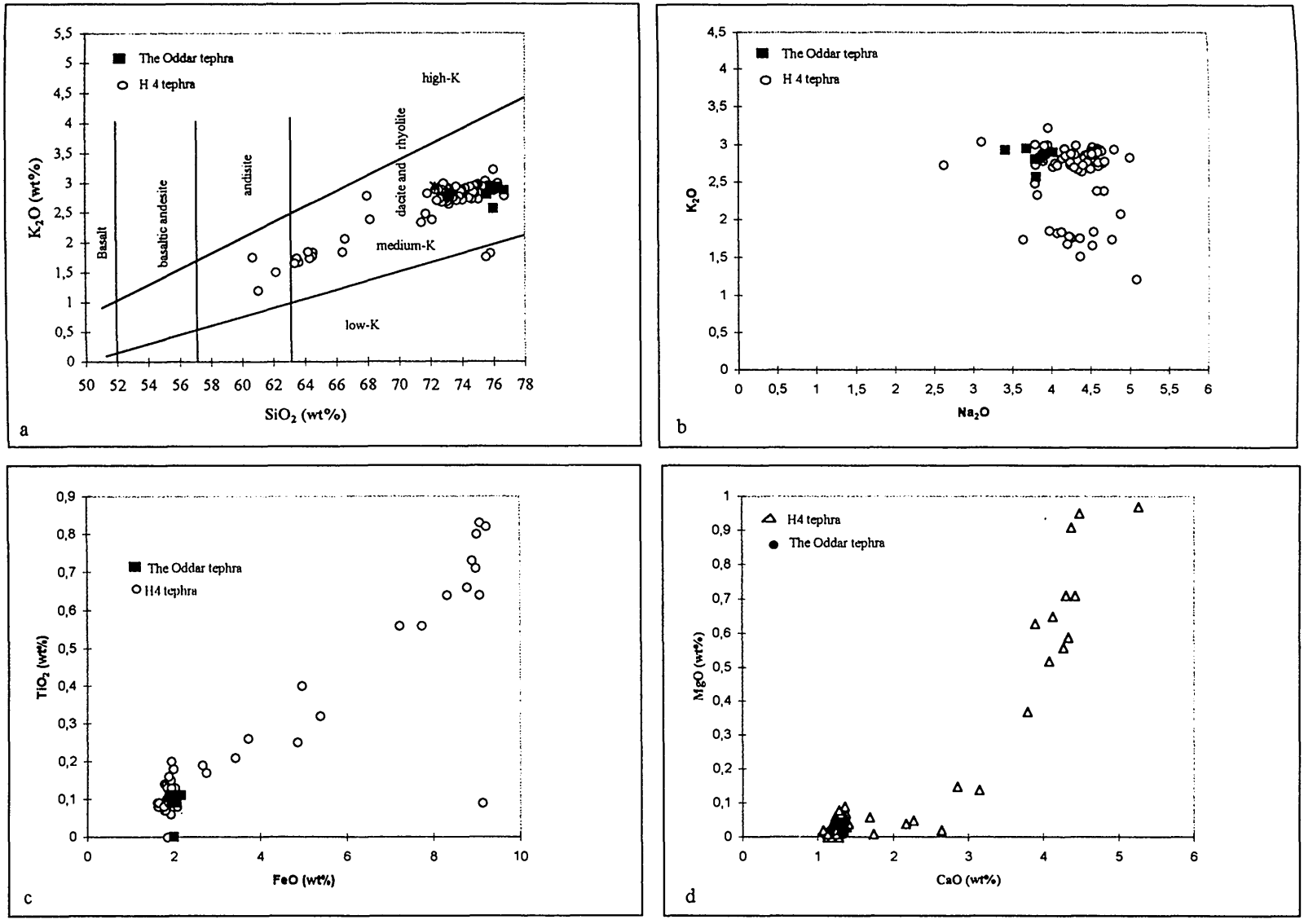

Fig. 4.26a,b,c,d. The Oddar tephra. Reference data are from the Tephrabase at the department of Geography, University of Edinburgh (http://www.geo.ed.ac.uk). The Oddar tephra is defined as medium-K glass and has a typical Hekla composition.

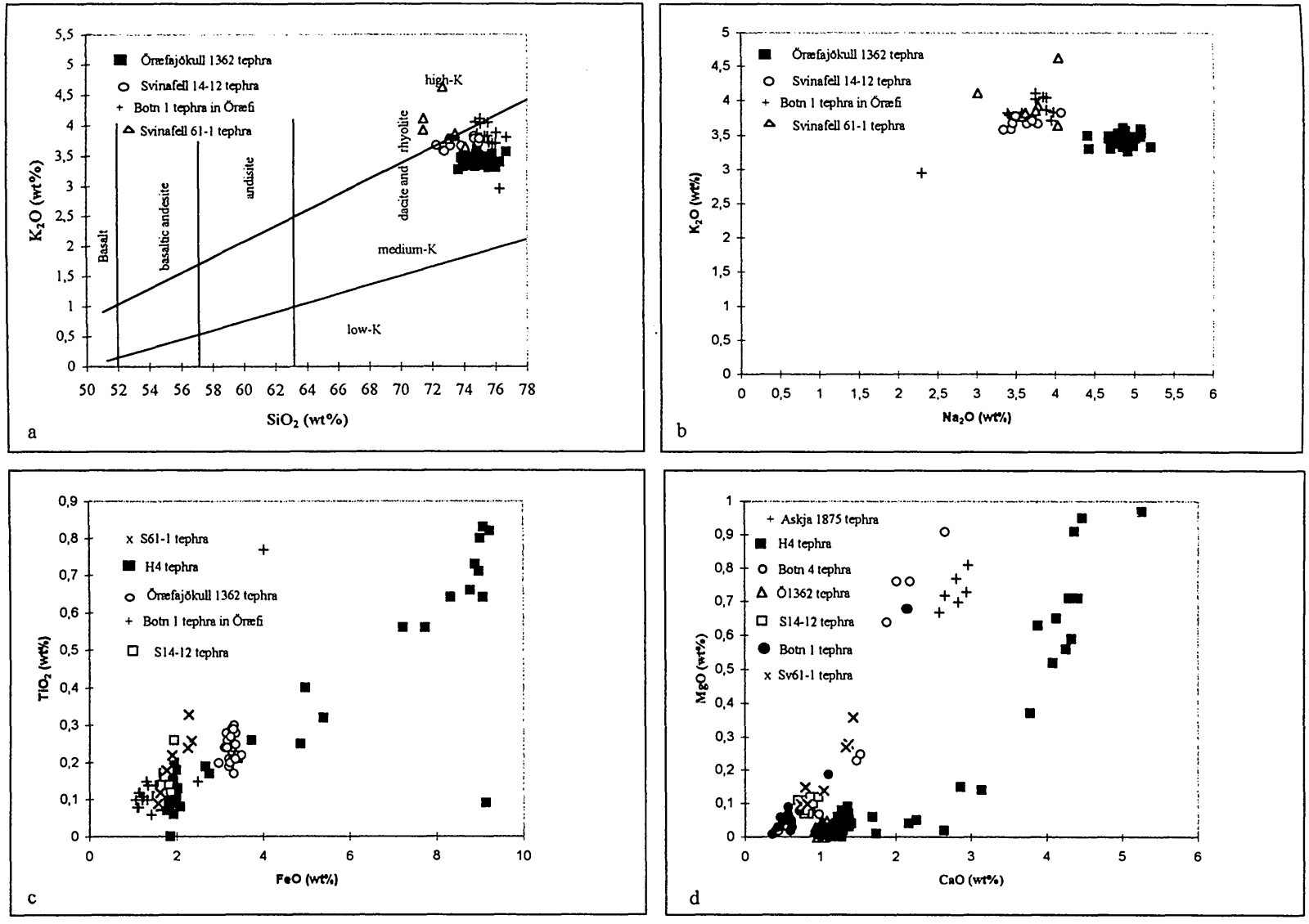

Fig. 4.27a,b,c,d. The Sv14-12 tephra. Reference data are from the Tephrabase at the department of Geography, University of Edinburgh (http://www.geo.ed.ac.uk). The tephra is medium-K glass and can be linked to Öræfajökull on the basis of potassium (Fig. a). The diagrams show that Botn 1 and Sv14-12 are the same tephra.

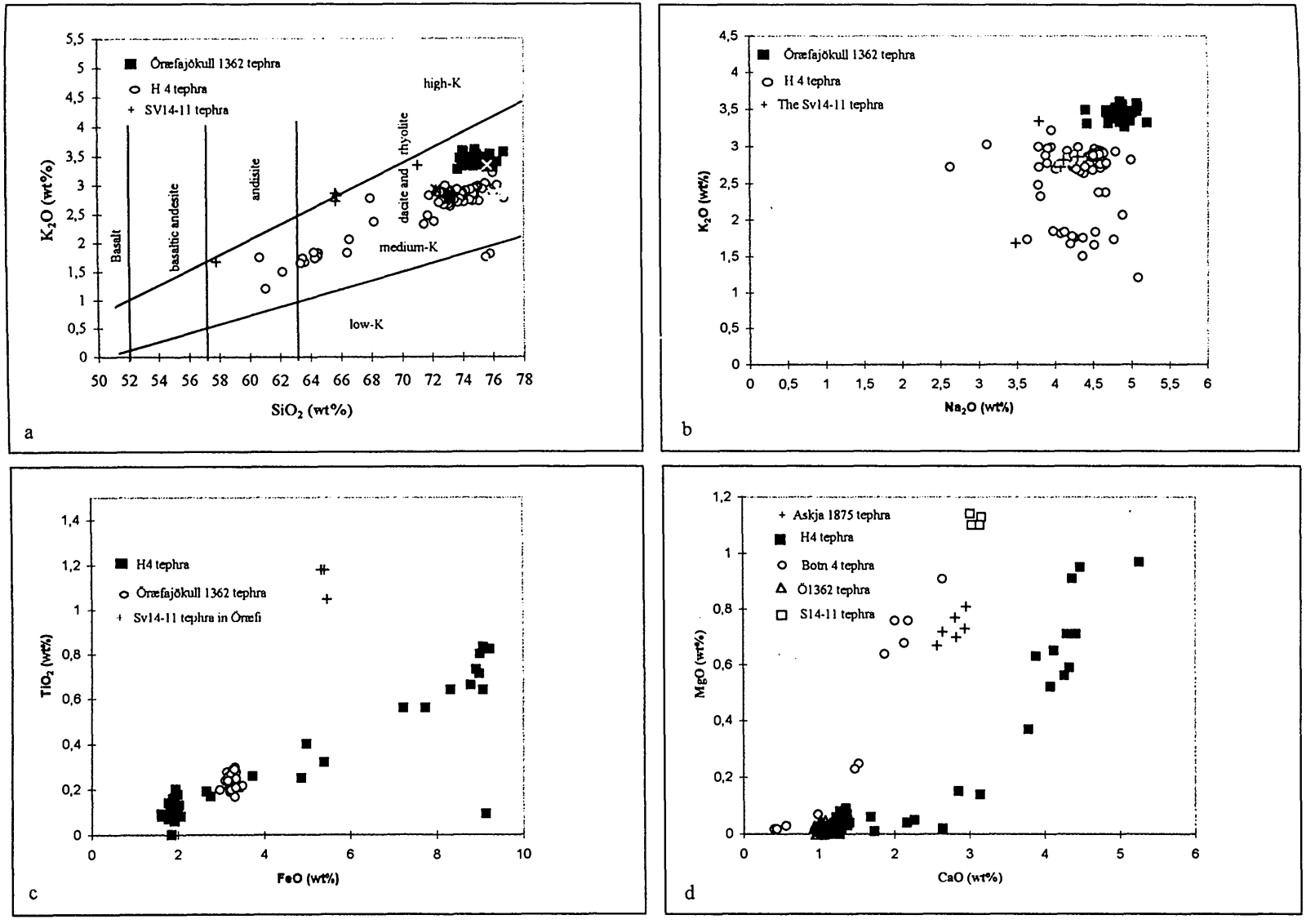

Fig. 4.28a,b,c,d. The Sv14-11 tephra. Reference data are from the Tephrabase at the department of Geography, University of Edinburgh (http://www.geo.ed.ac.uk).
The tephra shows similarities with the Öræfajökull volcanic system, especially in the MgO/CaO content which hints at the same linear trend as the Botn 1, Botn 4 and Sv14-12 tephras.

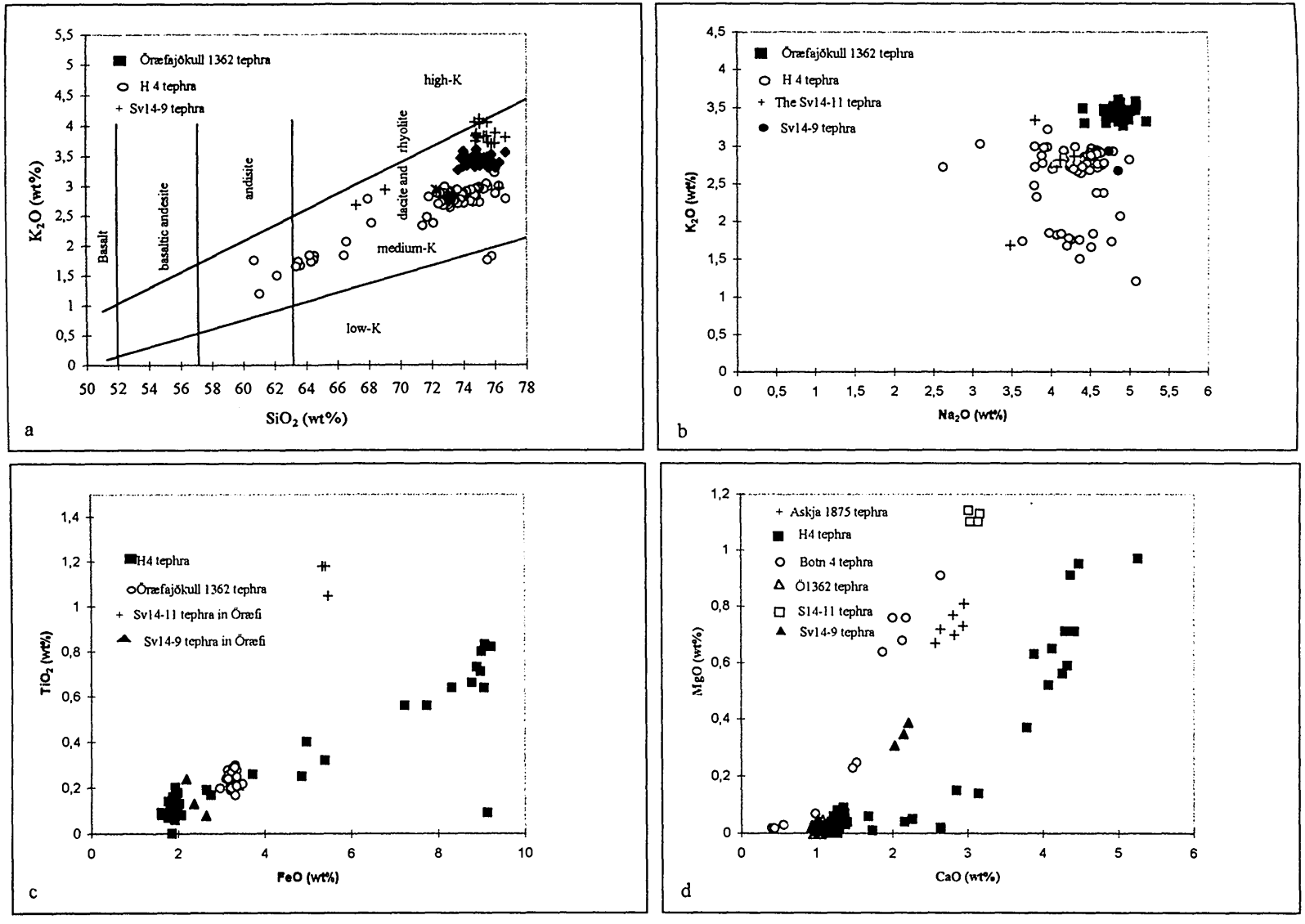

Fig. 4.29a,b,c,d. The Sv14-9 tephra. Reference data are from the Tephrabase at the department of Geography, University of Edinburgh (http://www.geo.ed.ac.uk). The tephra show two distinct chemical signatures. Group A has an unknown origin but group B shows similarities with the Öræfajökull volcanic system.

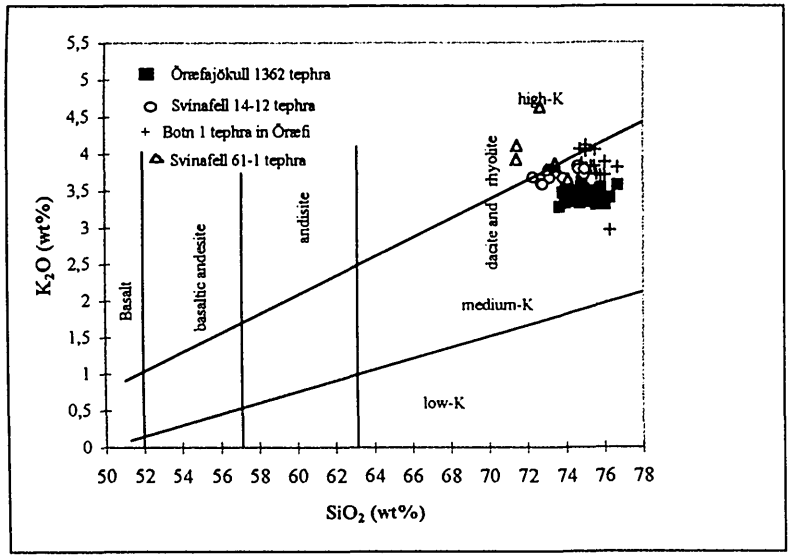

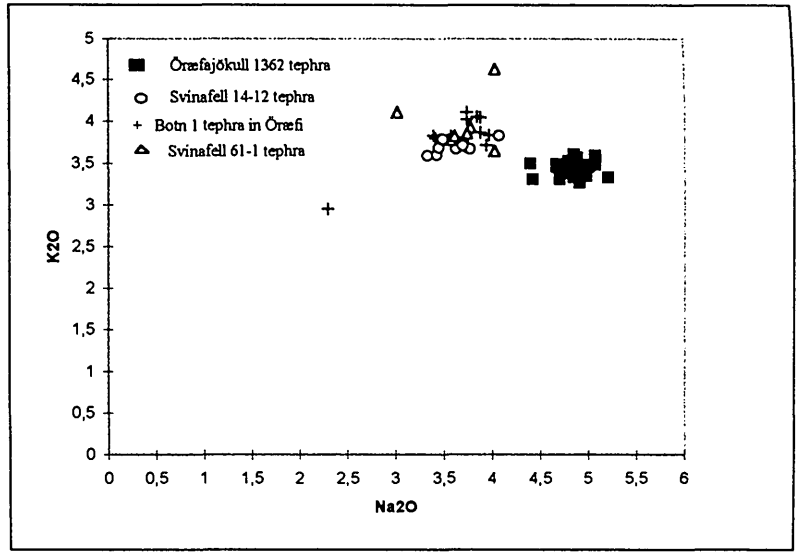

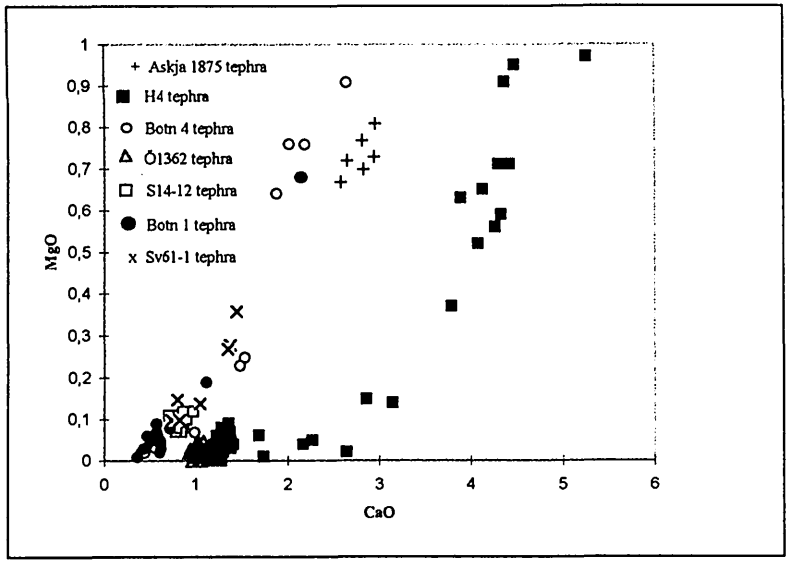

Fig. 4.30a,b,c,d. The Sv61-1 tephras. Reference data are from the Tephrabase at the department of Geography, University of Edinburgh (http://www.geo.ed.ac.uk). The diagrams show that the Sv14-12, Botn 1 and Sv61-1 are probably the same tephra most likely from the Öræfajökull volcanic system.

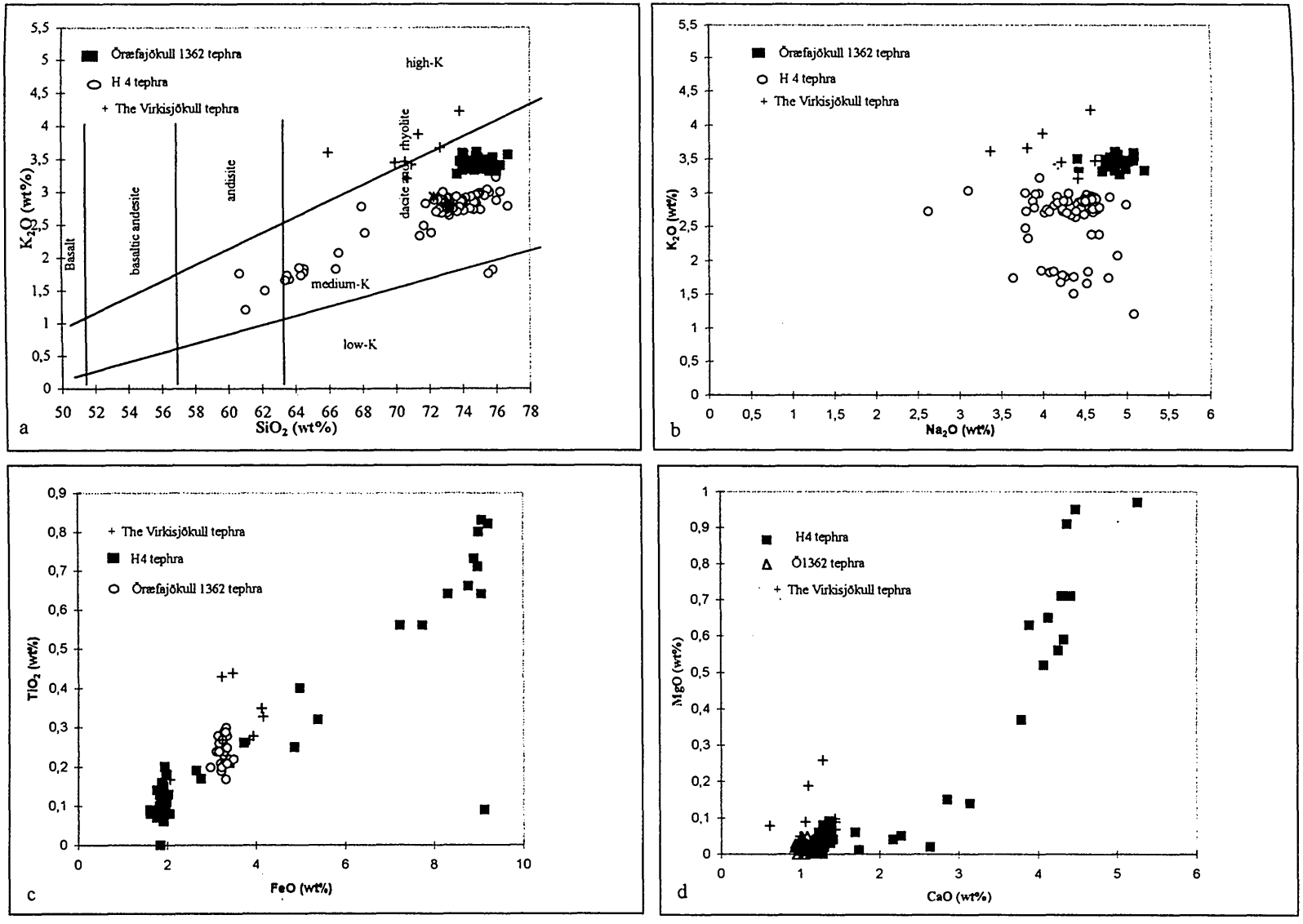

Fig. 4.31a,b,c,d. The Virkisjökull tephra. Reference data are from the Tephrabase at the department of Geography, University of Edinburgh (http://www.geo.ed.ac.uk).
The potassium range suggests an origin from Öræfajökull volcanic system for the Virkisjökull tephra (Fig. a,b). The link is not so clear looking at other chemical characteristics.

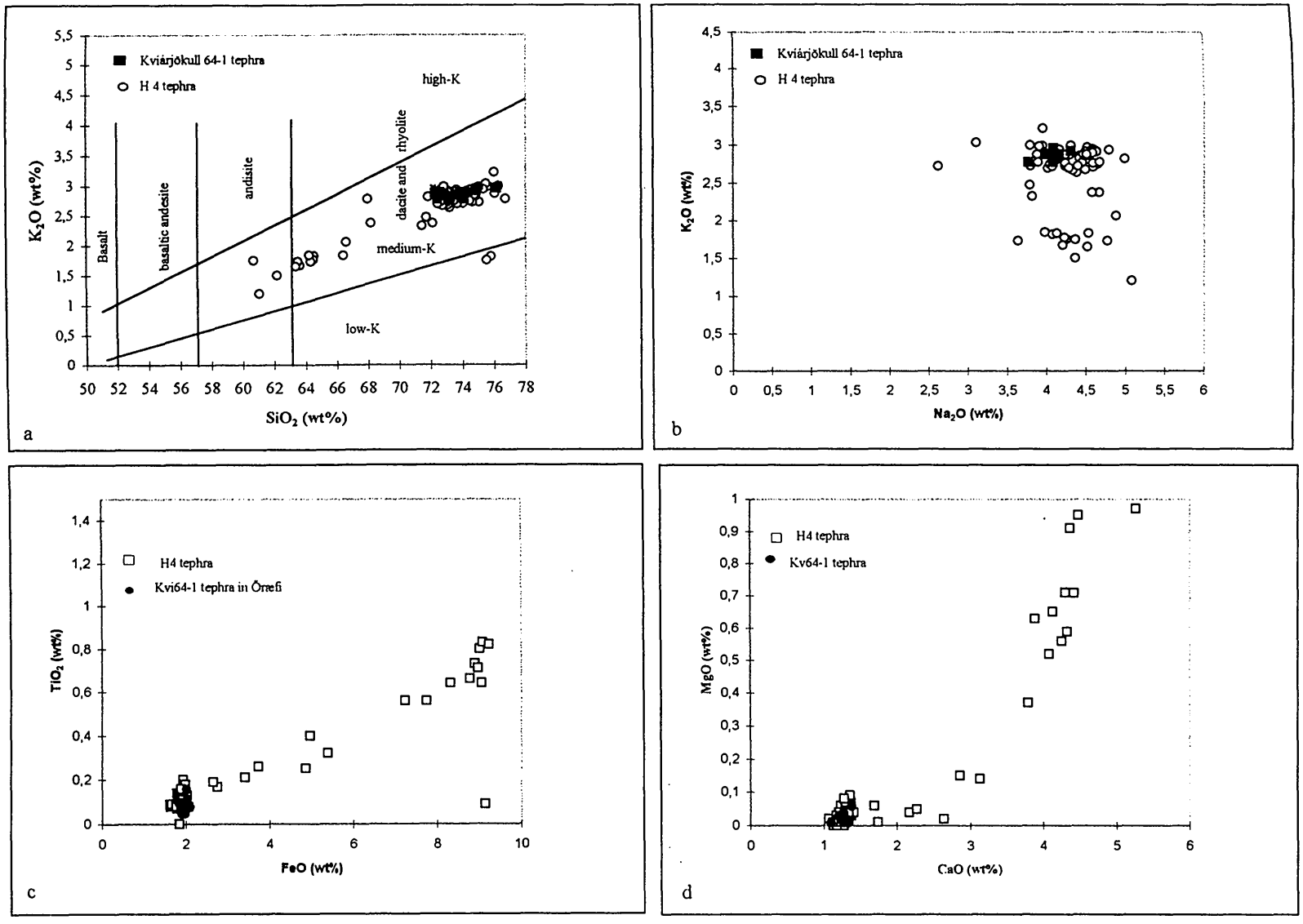

Fig. 4.32a,b,c,d. The Kví64-1 tephra. Reference data are from the Tephrabase at the department of Geography, University of Edinburgh (http://www.geo.ed.ac.uk). The tephra is medium-K glass and matches with the Hekla volcanic system in all major components.

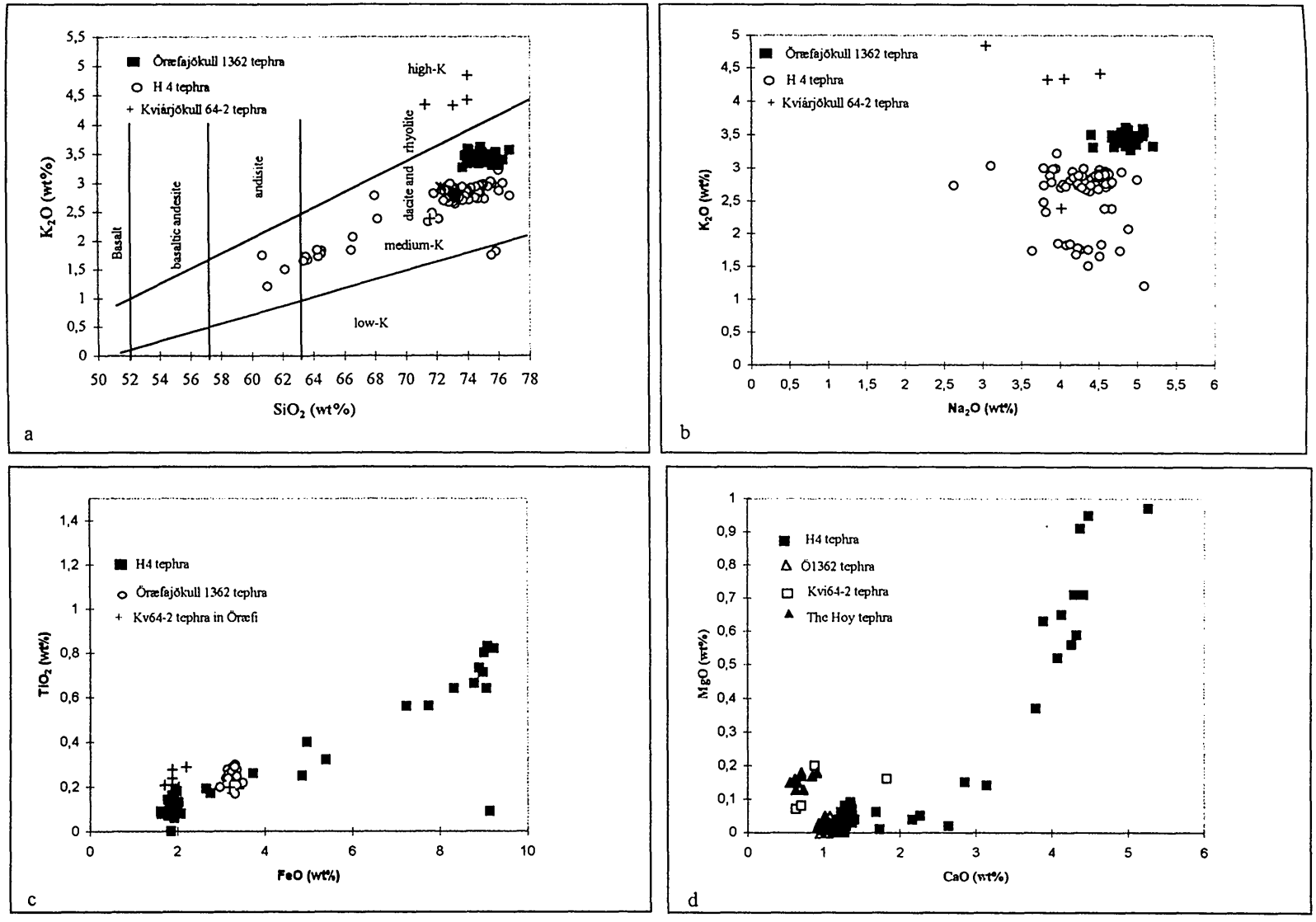

Fig. 4.33a,b,c,d. The Kví64-2 tephra. Reference data are from the Tephrabase at the department of Geography, University of Edinburgh (http://www.geo.ed.ac.uk). The tephra is high-K glass and its composition hints at an origin from the Torfajökull volcanic system especially if looked at the high potassium content. Note the similarities with the Hoy tephra found in Scotland (Fig. d).

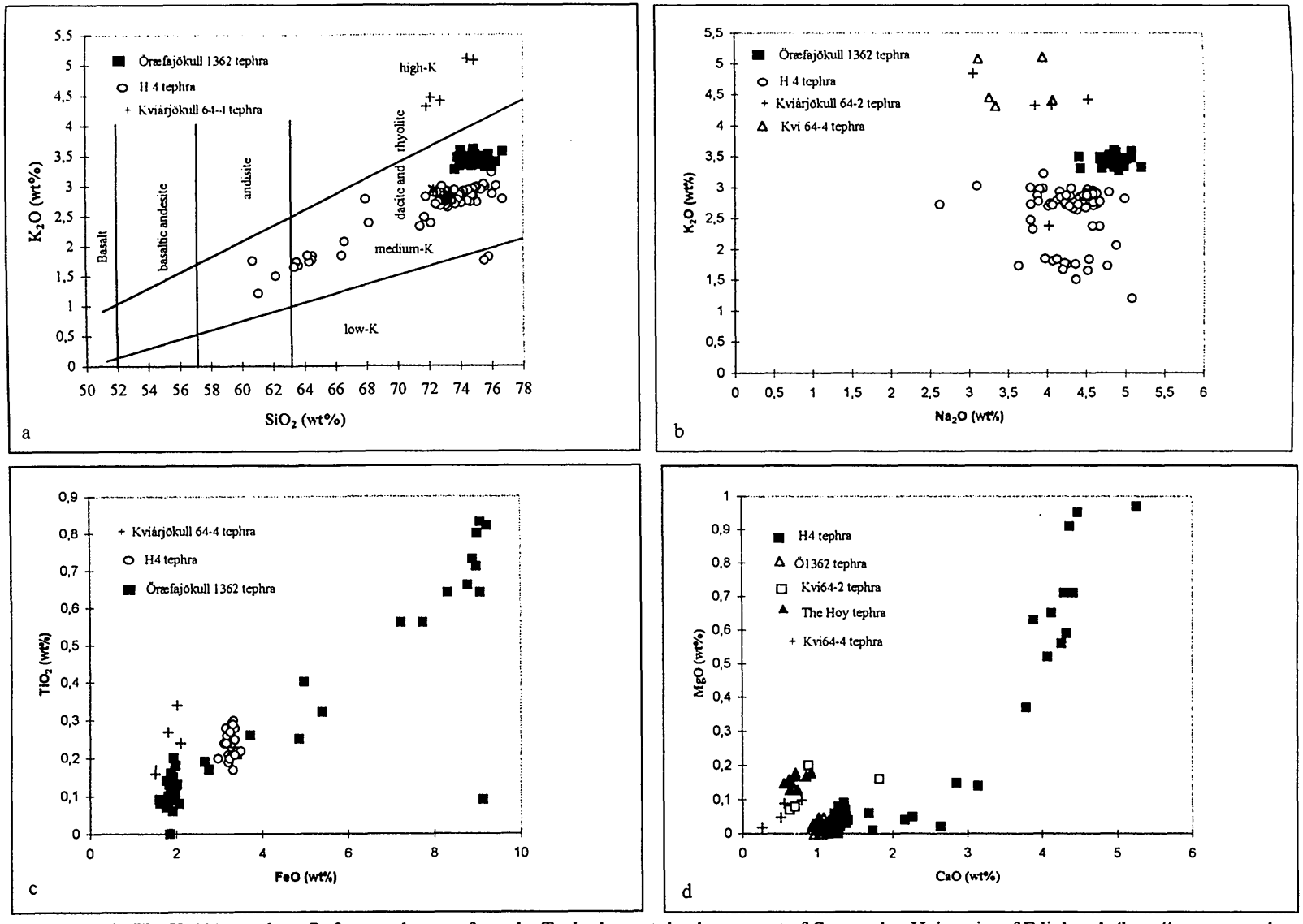

Fig. 4.34a,b,c,d. The Kví64-4 tephra. Reference data are from the Tephrabase at the department of Geography, University of Edinburgh (http://www.geo.ed.ac.uk). The tephra is high-K glass and the origin is the Torfajökull volcanic system. This is best shown by looking at the high potassium content.

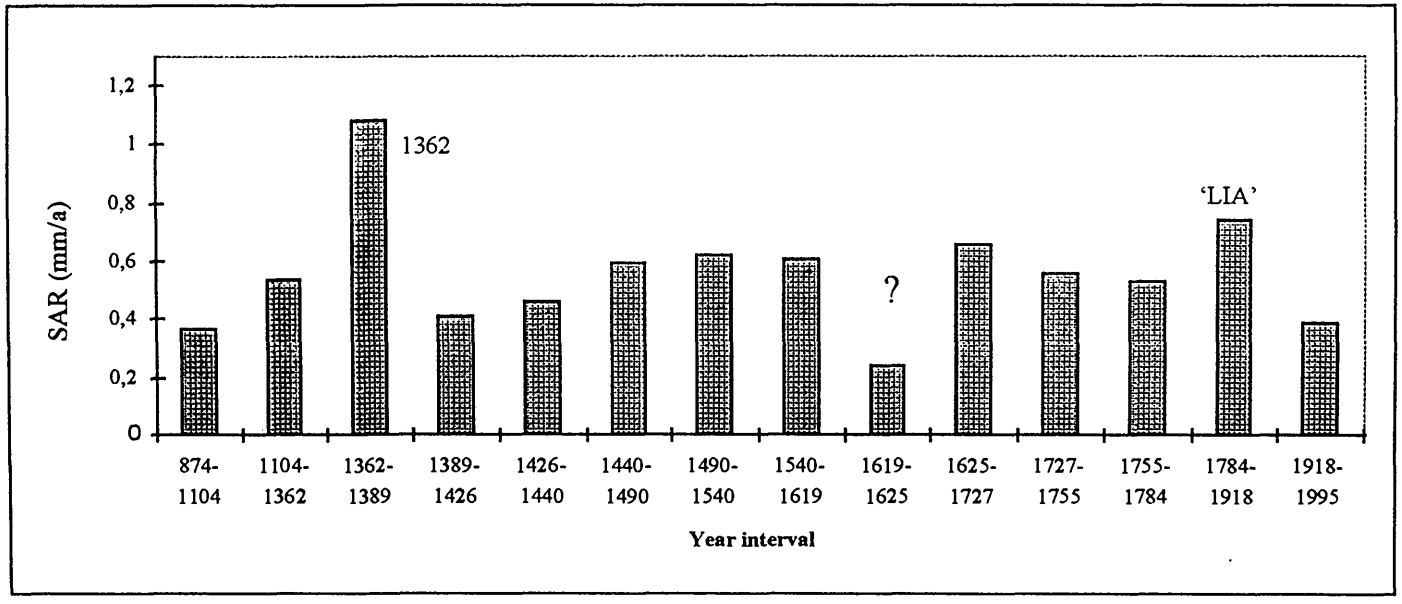

Fig. 4.35. Historical development of soil accumulation rates (SAR) on Skaftafellsheiði (ca. 280 m a.s.l. The pattern is thought to represent well the overall pattern of SAR in the Öræfi district. Note the increased rate of SAR immidietly after the eruption of Öræfajökull in 1362. High rates of soil accumulation are common in the LIA period (ca. 1250 - 1900). This could be linked with enhanced environmental activity.

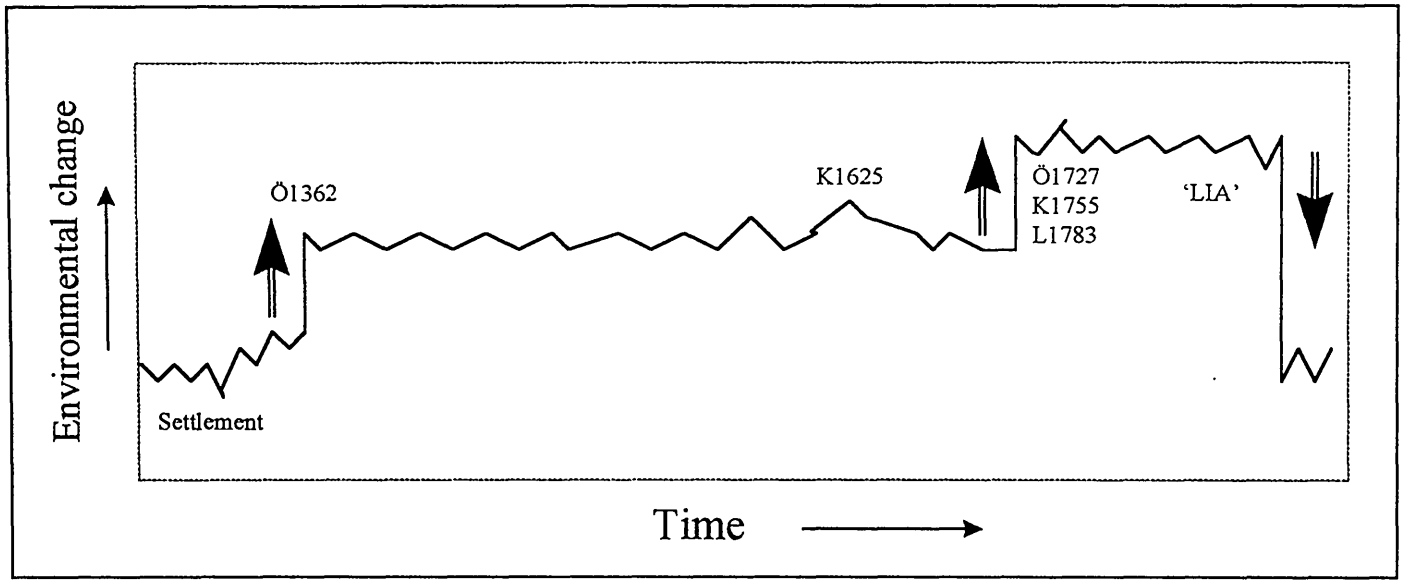

Fig. 4.36. Schematic model of environmental changes in the Öræfi district in the historical time. The model is depicted from the record of climate change in Iceland (sea ice), catastrophic volcanic eruptions affecting the Öræfi district and the soil accumulation rates on Skaftafellsheiði. Two periods of dramatic negative changes (feedbacks) are inferred; the first when climate deteriorated followed by the big eruption of Öræfajökull in1362 and the second following further cooling and three big eruptions devastating the Öræfi district in the 18th Century. Period of improved climate and lower volcanic activity had a positive feedback effect in the area decreasing soil accumulation rates in the beginning of the 20th Century.

Chapter 5. The timing and extent of glacier fluctuations

5.1 Introduction

The aim of this chapter is to analyse the temporal and spatial pattern of glacier fluctuations in the study area. This will be done by combining geomorphological mapping and tephrochronology. Well-dated tephra layers with extensive geographical distribution and clear stratigraphic resolution will be used as principal *isochrones*. Three tephra horizons are particularly important, Hekla-4, Hs (3520±30 BP) and Ö1362 AD. Additionally, the Miðheiði tephra (2860±160 BP), the Skaftafellsheiði tephra (1540±50 BP) and the Hekla-Ö (ca. 6000 BP) are considered crucial in the dating process.

The chapter is organised in a similar fashion as Chapter 3. Each outlet glacier studied will be examined beginning with Morsárjökull and ending with Kviárjökull (Fig. 3.1). Results are briefly summarised for each outlet glacier. The final part contains an overall synthesis of the glacier fluctuations in the study area. The overall implications of the observed pattern of glacier fluctuations are assessed in Chapter 6.

5.2 Criteria

The tephrochronological dating in the present study is based on the assumption that the oldest tephra in the stratigraphical column represents the minimal age for the underlying substrate or surface. The resolution can be increased by estimating the Mean Soil Accumulation Rates (MSAR) from the oldest tephra to the base of the stratigraphical column so improving the dates of the substrate. The age could be underestimated if the oldest overlying tephra is not found, if it was not preserved or if MSAR has changed. The possibility of finding a tephra was maximised by extensive search in possible sediment traps between moraines. Reference sites outside Holocene glacier limits were selected to include the maximum number of tephras for each glacier foreland.

The lichenometric dates are based on a mean growth curve from the south and south-eastern outlets of Vatnajökull and Öræfajökull (Gudmundsson, 1992: based on Gordon and Sharp, 1983; Thompson and Jones, 1986; Thompson, 1988; Snorrason, 1984). The calibration curve is based on the measurements of the lichen *Rhizocarpon geographicum* aggr. Comparable environmental conditions, such as temperature, precipitation and altitude above sea level (ca. 100 m) exist between the study area (Öræfajökull) and measurement sites of the lichen curve used (south east coast). Any climate and topographic differences that occur are very small and hence considered negligible in terms of lichen growth. Using this approach the mean of the five largest lichens was used to calculate the relative age of the substrates (Innes, 1985). The growth rate of 0,64mm/year and a 5 year colonisation lag time is applied in all cases. An important caveat has to be introduced because comparatively recent environmental limits to lichenometry dating have been identified in southern Iceland potentially restricting the application of the lichenometry method to ca. 150 - 160 years from the present time (Maizels and Dugmore, 1985; Gudmundsson, 1992). Therefore, all dates obtained by lichenometry, older than ca. 1850 AD reflect the minimum age of the surface.

5.3 Morsárjökull

The outermost advance of Morsárjökull is ca. 1.5 km from the 1995 position of the snout. The Bæjarstaðarskógur moraines are not from an advance of Morsárjökull as explained in Chapter 3. Trimlines show that during this outermost advance of Morsárjökull, the ice was about 100 m thicker than the 1990 profile (Fig. 3.4). Inside this limit there are series of arcuate terminal moraines. An extensive search revealed three soil sections containing the K1918 tephra within the moraine series in the south (Fig. 5.1a) indicating that the moraines outside the present drainage from Kjós are older than the K1918 tephra. The consistency of the section and the lack of the G1783 tephra suggests that the moraines are younger than 1783. As the tephrochronology suggests a recent age for these landforms, lichenometry was also applied. The outermost moraine of Morsárjökull is dated to 1816±13 AD and the youngest moraine west of the present drainage from Kjós to 1924±5 AD. On other

moraines, lichens were absent or too few to give a reasonable dating precision (marked n/a on Fig. 5.1). The glacier retreated rapidly in the beginning of the 20th Century as can be seen on the closely spaced dates on Fig. 5.1a. Due to limitations of lichenometry, the oldest date is interpreted as a minimum age of the outermost moraine. The northern moraine series could not be properly dated due to the scarcity of soils containing tephras, but some traces of reworked K1918 tephra were found in shallow soil on the proximal side of the third advance (Fig. 5.1b). This was the only moraine with sufficient lichens growing on the proximal side for dating purposes (Fig. 5.1b). The lichens suggest a moraine date of >1933±5 AD which is probably an underestimate when compared with the dates from the moraine series south of the site (Fig. 5.1a).

Neither lichens nor tephra layers could be located on top of the inferred ice contact deposit on the slope about 1.5 km south west of Morsárjökull. Part of this deposit is a fan which is highly unstable, inhibiting soil formation and lichen colonisation of surfaces. However, this possible ice limit can be assumed to be Holocene in age but older than the outermost moraine in front of Morsárjökull dated to 1816±13 AD.

The two areas of hummocky moraines west of Bæjarstaðarskógur, interpreted as an advance of Skeiðarárjökull, were dated with the aid of tephras. However, the age difference between the two advances could not be determined because the area between the moraines is stripped of soil. Profile 1, which is logged in Bæjarstaðarskógur inside the limits, gives the minimal age of the two advances (Fig. 5.2). The profile contains the Hs and the Hekla-4 tephras underlain by thick indurated andisol. Near the base is a thick black tephra of unknown age and origin. Consequently, the minimal date of the two advances is >3830 BP. However, this date can be broadly constrained with the aid of MSAR in the study area. This would give the minimal date of 9000±850 BP years. Nevertheless, the tephra record below the Hekla-4 layer is scant. More tephras can be expected to have been deposited over this long period of time as can be observed in other profiles, covering the same time period, in the area. This would suggest that some of the tephras might be missing.

Therefore, the minimal date of ca. 9000 BP might be overestimated. This can be tested by using the MSAR to estimate the age of Hs and Hekla-4 which are both of known age (ca. 3500 BP and 3800 BP, respectively). The Hs turned out to be roughly 3400 yrs BP old or ca. 100 BP years younger than the known date. Therefore, the basal date of ca. 9000 BP is very likely to represent a good estimate. Thus, from the evidence, the minimal date is inferred to be somewhat older than the mid-Holocene. The maximal date is therefore after the end of the late glacial maximum ca. 11.000 - 10.000 BP when the ice reached to or beyond the present coastline (Ingólfsson and Norddahl, 1994) but sometime significantly older than the Hekla-4 tephra. These bracketing dates would suggest at least a mid-Holocene date of the Bæjarstaðarskógur moraine series.

Summary.

Morsárjökull shows a limited record of Holocene fluctuations (Fig. 5.3). The moraine series in front of the glacier suggests that Morsárjökull reached a LIA maximum position in the early 19th Century in contrast to the nearby glaciers Skaftafellsjökull, Kviárjökull and Breiðamerkurjökull (Thórarinsson, 1943; Thórarinsson, 1956; Thompson, 1988). The oldest moraine date of >1816±13 implies that the advance of Morsárjökull culminated at least half a Century earlier than the date generally assumed for other glaciers in the area (Thórarinsson, 1943). The ice limit near Bæjarstaðarskógur, about 5 km from the 1990 position of Morsárjökull, was formed by Skeiðarárjökull, and dates from at least the mid-Holocene. The most probable date is Preboreal when the melting of the last inland ice sheet stood still or exhibited a small readvance in Iceland (Ingólfsson and Norddahl, 1994).

5.4 Skaftafellsjökull

Evidence of extensive glaciation outside the Neoglaciation limits of Skaftafellsjökull can be seen in Gimludalur and Botn in the form of trimlines and striations (Fig. 3.7). The glacial features in Gimludalur corrie are of unknown age. However, a minimum date can be obtained from profile 6 (Fig. 5.4). Although it was not possible to date the base of this profile directly, a early Holocene age may be inferred. The oldest dateable silicic tephra in profile 6, located just below the Hekla-4, is Botn 5 with a

possible MSAR age of 4400±100 BP. There are at least four other older tephras but their ages are unknown. According to geochemistry and stratigraphical position, the Botn 1, Sv14-12 and Sv61-1 tephras are the same layer (The BS tephra) and according to MSAR, its combined age estimate is 9200±880 BP. This would indicate a minimum early Holocene date (9200±880 BP) of the base of profile 6. Therefore, glaciation of Gimludalur and Botn could be related to the decay of the last inland ice sheet in Iceland when glaciers reached as far or beyond the present coastline (Ingólfsson and Norddahl, 1994).

Three distinct advances have been identified on Skaftafellsheiði, namely the Vesturheiði, Miðheiði and Austurheiði stages. These stages represent the Neoglaciation of Skaftafellsjökull. From the geomorphic evidence, the west lateral margin of Skaftafellsjökull has retreated 2 km from the oldest Vesturheiði advance, 1 km from the Miðheiði advance and 0.5 km from the Austurheiði advance. During these stages the ice, measured along a cross section marked A-B on Fig. 3.7, was probably between 200 - 150 m thicker than today.

The second oldest advance found on Skaftafellsheiði is the Vesturheiði stage represented by the Sjónarsker moraine (no. 3 on Fig. 3.7). Two other moraines mark this advance (no. 4 and 5) which have been separated from the Sjónarsker moraine by later meltwater activity. The base of profiles 7, 57 and 58 indicate the minimal age of this stage and were logged about 50 m east of the proximal slope of the Sjónarsker moraine (Fig. 5.5). Profiles 57 and 58 contain the oldest basal sections. The Hekla-Ö tephra dated to ca. 6000 BP was found in both profiles underlain by thick (30 - 40cm) indurated andisol. The mean basal date of these profiles, according to MSAR, is 7230±220 BP and the maximum basal date is 7850±270 BP. In profile 7 the basal MSAR date is 6160±380 BP, which is consistent with the lack of the Hekla-Ö tephra from this profile. The most likely date of the Vesturheiði stage is the Preboreal still-stand/advance (ca. 9800 BP), well known elsewhere in Iceland (Hjartarson and Ingólfsson, 1988). This is because the climatic deterioration needed to sustain an advance of the magnitude of the Vesturheiði stage has only been found in the early

Preboreal (Meese, *et al.*, 1994; Ingólfsson and Norddahl, 1994). Furthermore, the MSAR date might be underestimated because rates of soil accumulation may have been slower in the early Holocene. Alternatively the profile may have missed the best preserved sediment trap in the area, and may thus lack the very oldest part. In either case the advance may be ca. 9800 BP years old.

A second advance on Skaftafellsheiði is marked by a series of subdued arcuate moraine fragments here called the Miðheiði stage. This moraine sequence indicates at least two advances/still-stands, but it was not possible to distinguish the age difference. In general, the crests are separated by only a few metres, and no evidence of buried soil could be found between the crests. Profiles 8, 9 and 60 date this particular stage (Fig. 3.7). All profiles (8, 9 and 60) contained the Hekla-4 tephra; but the Hekla-Ö tephra was absent, therefore suggesting that moraines formed after the Hekla-Ö tephra fall (found in profiles 57 and 58 outside the Miðheiði stage) and before the Hekla-4 tephra fall (deposited inside the same advances)(Fig. 5.6). This indicates an age between ca. 4000 BP and ca. 6000 BP. Profiles 8, 9 and 60, located inside the Miðheiði stage, are underlain by indurated andisol varying in thickness. The average basal MSAR of these profiles is 6580±450 BP and the maximum date is ca. 6800 BP. The dating evidence therefore suggests that the Miðheiði advances represent the outermost Neoglacial advances of Skaftafellsjökull and they probably occurred between 6000 BP and 7000 BP. However, MSARs are exaggerated according to the bracketing tephra dates. This can be explained by local slope activity increasing the thickness of the older soil because the pre-Hekla-4 stratigraphy is sharply dipping, especially in profiles 8 and 9. This would suggest that the date is probably closer to between 5000 BP and 6000 BP, perhaps closer to the latter date.

A third advance of Skaftafellsjökull is here called the Austurheiði stage. It is marked by concentric moraines located on Austurheiði (Fig. 3.7). The minimum age of this stage is given by profiles 10 and 11 (Fig. 5.7). Soils are very rare inside this limit. The Hekla-4 tephra was not found in profile 11 and the basal date, indicated by MSAR, is 3125±335 BP suggesting a minimum date for the moraines on both Austurheiði and

Skaftafellsheiði. The Vö ca. 900 AD (Landnám) tephra, which is the best marker horizon inside the limit, was also identified in profile 10. In both profiles (10 and 11) the Vö ca. 900 tephra is underlain by thick (ca. 50 cm) andisol containing traces of tephra. Therefore, the tephra evidence would suggest that the Austurheiði stage dates back to around 3100 BP. Thompson (1988) has mapped glacier fluctuations on the sandur plain in front of the outlet. His results indicate a maximum position on the sandur plain in the late 19th Century. Since then the glacier has retreated about 1.5 km to its present position (Fig. 5.8).

Summary.

The moraine record of Skaftafellsheiði reveals a long history of Holocene fluctuations of Skaftafellsjökull (Fig. 5.8). The oldest glacial evidence is from the last Termination between 13000 BP and 9200±880 BP when ice covered the area east of the Sjónarsker moraine and occupied the Gimludalur corrie. This stage is called the Vesturheiði stage, and may correlate with other glacier fluctuations of this age identified elsewhere in Iceland (Ingólfsson and Norddahl, 1994). At this time the glacier margin was about 2 km outside the 1990 west lateral position, and the glacier was about 200 m thicker. A second advance is dated to the mid-Holocene and called the Miðheiði stage. At this time, two moraine crests were formed close together. The glacier margin was about 1 km from the 1990 position and was about 170 m thicker. This advance might correlate to other events identified in South Iceland (Dugmore, 1987; 1989a; Rose *et al.*, 1997) and North Iceland (Stötter, 1991). A third, and the most restricted advance of Skaftafellsjökull on Skaftafellsheiði, is called the Austurheiði advance. At this stage the glacier margin stood about 500 m from the 1990 lateral position and was about 150 m thicker. This advance is dated to around 3100 BP and forms the youngest moraine series on Skaftafellsheiði highlands west of the lateral margin. Advances at ca. 3100 BP have also been identified at Sólheimajökull (Dugmore, 1987; 1989a) and in the north of Iceland (Stötter, 1991). Within the historic period, fluctuations have been identified in the proglacial area by Thompson (1988), mainly covering the last 150 years.

5.5 Svínafellsjökull

Two extensive glacial advances have been identified on Svínafellsheiði, the highland east of Svínafellsjökull (Fig. 3.10). These are here named the Svínafellsheiði and Skerhóll stages, and they predate the Stóralda moraine complex in front of Svínafellsjökull. The Stóralda moraine complex indicates at least five stages of glacier advance prior to the Little Ice Age. The recent LIA limits have been mapped by Thompson (1988) and the outermost limit is shown on Fig. 3.10. The Svínafellsheiði stage was the most extensive covering the whole area east of the glacier (Svínafellsheiði); the Skerhóll stage margin stood ca. 500 m east from the 1987 lateral position of the modern glacier where the ice was ca. 150 m thicker. The terminal position is not known, but based on the morphology of present glaciers in the region, it was probably about 2 km in front of the 1987 terminus. The Stóralda stage culminated about 1 km from the 1987 terminal position. Only a few metres separate the different crests of the Stóralda moraines indicating a similar terminal position of several distinct phases. The ice thickness when the glacier formed the Stóralda terminal positions was <100 m thicker then in 1987.

The minimum date of the Svínafellsheiði stage is shown by profile 14 which includes the oldest and the most complete tephra record in the area (Fig. 5.9). It is located outside both the Skerhóll stage and the moraines of the Svínafellsheiði corrie (Fig. 3.26). Three other profiles, number 15, 16 and 17 (sheet III, chapter 4), were logged inside the limit but did not reveal as complete a record. In the profile 14 the oldest tephra is BS which has a mean date of 9200±880 BP, indicating that the Svínafellsheiði stage is at least this old. In addition, a MSAR basal date of the profile 14 of 11060±1200 BP reinforces the idea of a late glacial age for this stage.

The Skerhóll stage on Svínafellsheiði is dated by profiles 61 and 62 (Fig. 5.10). The mean basal date of the profiles is 9700±960 BP according to MSAR. The maximum date of 13000 BP can be inferred from the presence of ice free areas on Svínafellsheiði, suggesting a stage after the maximum of the last inland ice sheet. It is

very likely that the Skerhóll stage marks the early Preboreal still-stand or readvance of the last inland ice sheet.

The Stóralda moraine complex preserves a record of at least four separate marginal positions (Stóralda stage). These advances are younger than the record on Svínafellsheiði and thus the Stóralda moraine complex characterises the Holocene glacial record of Svínafellsjökull. The tephra record on top of the Stóralda moraine complex provides the minimum date of its formation (Fig. 5.11). Profiles 19 - 22 indicate that the moraine complex is older than 1362 AD. However, the basal part of profiles 19 and 20 contain undisturbed Ö1362 tephra whereas in profile 22, on the proximal side of the biggest moraine, the tephra is highly reworked and sometimes only found as a constituent of the underlying till. Therefore, it is likely that the glacier stood at or very close to crest no. 4 during the deposition of the Ö1362 AD tephra. A continuation of moraine crest no. 4 can be observed in Breiðatorfa (Fig. 3.26; chapter 3). These moraines show a similar distance from the 1987 position as the proximal side of moraine crest no. 4 (Figs. 3.11). The tephra stratigraphy of these moraine segments is shown in Fig. 5.12 and indicates a similar sequence to that of the Stóralda moraine complex. The minimum date is constrained by the Ö1362 AD tephra. Therefore, the evidence would suggest that the most likely date of these moraines (Stóralda moraine complex and the Breiðatorfa moraines) is the cold periods in the 13th and 14th Century (Ogilvie, 1991). The Ö1362 tephra is deposited on top of the proximal and distal slopes of the moraines with little or no soil between the surface of the till and the tephra layer. This would suggest an age not much older than the Ö1362 AD tephra.

There is a moraine segment (no. 5) located between the moraine crest no. 4 and the LIA limits identified by Thompson (1988) and in a similar spatial position just north west of the Stóralda moraine complex, here named the Freysnes moraines. These moraines can be dated by using tephrochronology (Fig. 5.11 and 5.12). The Freysnes moraines can be bracketed between the Ö1727 AD and the K1918 AD tephras (Fig. 5.13) but moraine no. 5 can be dated in more detail. Moraine no 5 was formed

sometime between the deposition of the Ö1727 AD and K1755 AD tephras. Given their similar spatial location, it is very likely that both moraine no. 5 and the Freysnes moraines were formed between ca. 1730 and 1750 AD. One implication of this pattern of glacier fluctuations is that all of the possible pre-1362 AD advances during the Holocene were within the Skerhóll stage.

Summary.

The oldest evidence of glacier activity can be found on Svínafellsheiði, and is dated to the late glacial or later, and is here called the Svínafellsheiði stage. The second oldest glacial advance is bracketed between 13000 BP and 9700±960 BP and is named the Skerhóll stage. This stage represents the early Preboreal still-stand or readvance in the area. The Stóralda stage moraine complex is dated to a Medieval advance of Svínafellsjökull ca. 1200 - 1350 AD, and a further moraine complex is dated to between 1727 AD and 1755 AD. Inside this 18th Century limit lie the late 19th Century advances mapped by Thompson (1988).

5.6 Virkisjökull

Three advances have been identified in front of Virkisjökull. The maximum extent is called the Virkisjökull I stage, and was formed when the glacier advanced about 3 km from its 1987 position. During this stage the glacier was about 200 m thicker. A second advance is called the Virkisjökull II stage. The glacier extended about 1.2 km onto the sandur plain and was about 150 m thicker compared with the 1987 position. A third advance is called the Virkisjökull III stage and the glacier advanced about 0.9 km onto the sandur plain. The ice was about 100 m thicker than in 1987. A fourth advance is called the Virkisjökull IV stage. It extended about 0.5 km onto the sandur plain and was probably similar in thickness to the preceding advance.

The first three stages can be dated on Sandfellsheiði using tephra sequences between lateral moraines. Fig. 5.14 shows a cross section of the lateral moraine record of Sandfellsheiði and the profiles logged between the distinct advances. The Virkisjökull IV stage was dated with lichenometry on the proglacial area.

The oldest tephra outside the maximum advance is the Virkisjökull tephra dated to 4590±125 BP. The tephra can be seen in profile 31 which has a basal date estimated by MSAR to 5640±300 BP. This date provides a maximum date for the Virkisjökull I advance (Fig. 5.14). Profiles 32, 33 and 34 reveal the minimum date of the Virkisjökull I advance and the maximum date of the Virkisjökull II stage (Fig. 5.14). The oldest tephra identified in these profiles is Hekla-4 underlain by thick (30 - 50 cm) indurated andisol with some poorly preserved tephras. The mean basal date of these profiles is 5960±350 BP. It is inferred that the Virkisjökull I stage is substantially older than the Hekla-4 tephra, as seen by the extensive soil formation beneath it, and is therefore concluded to date between 5000 - 6000 BP.

Profiles 32, 33 and 34 indicate a maximum mid-Holocene date for the Virkisjökull II stage and profiles 35, 36 and 37 the minimum date (Fig. 5.14). The oldest identified tephra in profiles 35, 36 and 37 is the Vö ca. 900 AD tephra, but it is underlain by andisol which hints at an older minimum date. The mean basal date of profiles 35, 36 and 37 is 1700±180 BP. Therefore, this stage occurred between 5000 - 1700 BP. A date close to 1800 BP is concluded because of relatively thin soils underneath the Vö ca. 900 AD tephra. If an older date is to be inferred, a more extensive soil formation would have taken place. The soil formation was apparently continuous because an hiatus could not be observed in the soil profile below the Vö ca. 900 tephra.

The maximum date of the Virkisjökull III stage is probably ca. 1800 BP. Profiles 38, 39 and 40 represent minimum dates of the Virkisjökull III stage (Fig. 5.14). The oldest tephra identified is the Ö1362 AD isochrone; it is underlain by andisol but the Vö ca. 900 tephra is absent. This means that the bracketing dates of the Virkisjökull III stage is between early historic time (1300 AD/650 BP) and 1700±180 BP. Profile 39 strongly suggests an age towards the younger date, possibly 13th Century AD, because of a lack of soils below it. The lack of the Vö ca. 900 AD tephra in all profiles would also suggests the younger date.

Within Virkisjökull III lies Virkisjökull IV. No tephra was found inside this advance. Therefore, lichens were used to relatively date the moraines characterising this stage. The results indicate an advance in the late 19th Century, more specifically dated to 1871±7 AD which would be the minimum date of the Virkisjökull IV stage (Fig. 5.15). Multiple advances can not be ruled out. As in front of Svínafellsjökull, the moraines could be composite features representing various glacier advances, which in turn would explain the large size of these landforms.

Summary.

The oldest identified advance, called Virkisjökull I, occurred more than 6000 - 5000 years BP when the glacier advanced about 3 km and was perhaps ca. 200 m thicker than the 1987 position. The second advance, Virkisjökull II, occurred after around 5000 BP and before 1700 BP, probably close to 1800 BP, and went 1.2 km onto the sandur plain. It is likely that the ice was about 150 m thicker than the 1987 position. The third advance is dated to between ca. 1700 and 650 BP and is called the Virkisjökull III stage. It could be early historic in age. It reached about 0.9 km onto the sandur plain and was about 100 m thicker than in 1987. The fourth advance is called the Virkisjökull IV and stood at about 0.5 km from the 1987 terminal position. It is likely to be of similar thickness as the Virkisjökull III stage and has been dated to ≥1871±7 AD (Fig. 5.16).

5.7 Kotárjökull

The moraine record in front of Kotárjökull shows that at least three distinct advances of the glacier have occurred in recent times. These advances are called Kotárjökull I, II and III. Kotárjökull I marks the outermost position of the glacier, and has been inferred from ice thickness extrapolation to have extended about 3 km onto the outwash plain. During this stage, the ice was probably about 150 m thicker than in 1990. Kotárjökull II must have advanced slightly less onto the sandur plain, but this can not be verified due to the lack of terminal moraines. The Kotárjökull III stage represents a variable frontal advance of ca. 0.7 - 2 km but ice thicknesses could not be estimated.

The limits depicting different positions of the Kotárjökull stages were difficult to date due to a lack of soil profiles. Only two profiles were logged between moraines 4 and 5 delineating the Kotárjökull I and II stages (Fig.3.21). These profiles (51 and 52) disclose the minimum date of the Kvíárjökull I stage and consequently, the maximum date of the Kvíárjökull II stage (Fig. 5.17). Both of the profiles contain the Hekla-4 tephra underlain by andisol, usually indurated and including at least three unidentified tephras. The basal date of profile 54 is 6310±410 BP. The presence of the Hekla-4 tephra and the basal date would suggest a post mid-Holocene advance of the Kvíárjökull II stage and an older date for the Kotárjökull I stage. On the moraines defining the Kotárjökull III limit, lichens were absent on moraine surfaces and the soil entirely stripped.

Summary.
According to two profiles, the most likely date of the Kotárjökull I stage is older than mid-Holocene. Kotárjökull II is probably younger than ca. 4000 BP with the Kvotárjökull III stage probably representing a recent historic age (Fig. 5.18).

5.8 Kvíárjökull

At least three series of moraines can be identified in front of Kvíárjökull and are called Kvíárjökull I, II and III. The most prominent moraine is the Kambsmýrarkambur and Kvíármýrarkambur theatre delineating the Kvíárjökull III stage. The Kvíárjökull I and II moraines are much smaller features representing two older advances outside the big moraine.

Stratigraphic sequences in the Kvíárjökull proglacial area include deep deposits of tephras, peat, organic-rich andisols and gravel units (Sheet VI). A composite stratigraphic column is presented in Fig. 5.19 and covers the Holocene period for the Kvíárjökull proglacial area. It allows the shorter stratigraphic units elsewhere in the proglacial area to be correlated. The oldest glacial gravel layer (A) in front of Kvíárjökull is exposed at the base of profile 64 (profile 64; Sheet VI; Fig. 5.20) and is older than 9410±525 BP as depicted from extrapolation of MSAR. It consists of subrounded to subangular striated gravel. No moraines can be correlated with this

stage. It is interpreted as representing a Preboreal glacial event of Kviárjökull and is consistent with other similar advances found elsewhere in the study area. The outermost advance is called Kviárjökull I and is defined by lateral moraines on the southern and northern side of the glacier (Fig. 3.24). The maximum and minimum bracketing dates can be inferred by using profiles 83, 84, 85 and 64, respectively (Figs. 5.20; 5.21). All the profiles contain the Hekla-4 tephra underlain by andisol. The mean basal date of profiles 83 and 85 is 5400±325 BP. Profile 64 contains the Hekla-Ö tephra dated to ca. 6000 BP and is located outside the Kviárjökull I stage. Thus the Kviárjökull I stage can be bracketed between Hekla-Ö (6000 BP) and Hekla-4 (ca. 3800 BP), and perhaps, using the mean basal dates of profiles 83 and 85, the date may lie close to ca. 6000 BP.

These moraines can be linked with gravel units B and C in profile 64 (Fig. 5.19; Sheet VI). The B unit is ca 30 cm thick and consists of striated subrounded pebbles. The C unit is ca. 70 cm thick and made of similar material as unit B. According to MSAR, these units can be dated to between 4750±240 BP and 4550±120 BP. The dates for the related stratigraphic units suggest that the dates of moraines are closer to 3800 BP. This suggests that two glacier advances may have occurred over a period of ca. 1000 years BP. Between these advances, soil was beginning to accumulate as can be seen by the deposition of the Kv64-4 tephra preserved in thin organic-rich soil in profile 64 (Fig. 5.20).

The C unit is overlain by a silty clay unit. The clay layer could be traced a little bit further south (profile 65) from the location of profile 64 where it terminates. To clarify the stratigraphy succeeding the C unit a long profile was drawn from an exposure in a small gully cut by meltwater activity where profile 64 was logged (Fig. 5.22). The altitude difference between profiles 64 and 65 is not more than 3-5 m. The clay layer exposed in profile 65 represents the minimal altitude of the base of the clay layer. On top of the clay, a gravel layer called unit D has been deposited (see profile 64, Fig. 5.20). No moraines can be correlated to this event. The implication could be that the clay layer and gravel unit D represents migrating channels on the outwash

plain. The bracketing dates of this event would be ca. 4600 and 5000 BP calculated from MSAR in profile 64 (Fig. 5.20). This would further sustain that gravel units B, C and D characterise a multiple advance sequence of the glacier around 4600 BP.

The next glacier advance is marked by the E gravel unit which is underlain by the Hs tephra. This gravel unit can be linked with the composite moraine theatre (Kvíármýrarkambur and Kambsmýrarkambur) hence delineating the Kvíárjökull IIIa stage (Fig. 5.23). This stage marks the initial formation of the big moraine. The E unit is made of subrounded sand-supported cobbles and, in some cases, large pebbles (15-20 cm in diameter). The maximum date of the big moraine theatre is therefore the Hs tephra dated to ca. 3500 BP. The gravel unit E is overlain by clay and peat units containing known tephras (Fig.5.23). The best exposure of this part of the stratigraphy is found in a gully located a short distance from the road 1 (Fig. 5.24). The gravel unit E lies in between the Hs tephra (ca. 3500 BP) and the Miðheiði tephra (ca. 2800 BP), indicating a glacier advance between these two dates. The minimum date of the clay layer deposited on top of the E unit is 3275±190 BP according to MSAR. This would be consistent with a mean date of the E unit, marking the initial advance that formed the big moraine theatre, of around 3300 BP.

The stratigraphy succeeding unit E is complicated, indicating cycles of clay and soil formation (profile 81, 67, 73, 75; Sheet VI). The clay formation hints at glacially-fed lagoon formation probably dammed up by a barrier further to the south east. In the upper part of the clay unit, containing the Miðheiði tephra (profile 81), some birch branches, usually about 4 cm in diameter, can be found. A second layer of birch branches is interfingered with a peat layer just below the Skaftafellsheiði tephra (profile 67; Sheet VI). These birch branches have been dated to 1830±70 years BP (GU-4915). Below the clay unit in profile 67 a layer of birch remains of similar size was detected. They were dated to 2240±50 years BP (GU-4917). It can not be verified whether this layer of birch fragments is of similar age to those interbedded in the clay layer above the Miðheiði tephra in profile 81. A soil accumulation date in profile 81 implies a minimum date of this clay layer of 2755±155 BP. The overall

implication of the birch and clay layers is that a glacier fed lagoon or migrating channel activity must have flooded a birch forest on at least two occasions between ca. 3200 and 2200 BP.

In profile 67 a clay layer has been dated between 1830±70 and 2080±60 BP (GU-4715 and GU-4716, respectively). This layer is in the same stratigraphical position as the upper clay layer at the base of profile 73. The lagoon was much smaller than the previous ones because it can only be found in two profiles i.e. 67 and 73, logged in the drainage ditch of Kvíármýri in front of Kvíármýrarkambur (Fig.3.24). No lagoons have been formed in the area since the maximum of 1830±70 BP which is a period characterised by andisol and peat formation.

The gravel unit F marks the fourth major pre-historic advance of Kviárjökull (Fig. 5.19, 5.20). Profile 64 (Fig. 5.22) indicates a date of this unit of around 1630±170 BP. Matching moraines can be found on the distal slope of Kambsmýrarkambur (Fig. 3.24,) showing that this advance extended a little bit further than the Kviárjökull III stage. It filled the big moraine theatre and went over the north east part of Kambsmýrarkambur. Profile 79 reveals the minimum date of the profile (Fig. 5.25). The Ö1362 AD tephra isochrone is found in the profile underlain by moderately thick (16cm) andisol. The basal date of the profile is 1710±180 BP according to extrapolation of MSAR. This is fairly consistent with the stratigraphic date. Therefore, the second advance forming the Kviárjökull III stage is inferred to have occurred around 1700 BP (Kviárjökull IIIb).

Unit G in profile 64 is interpreted as a response to increased slope instability, presumably as a consequence of enhanced environmental activity due to climate change and human impact (profile 64; Figs. 5.19; 5.20). The stratigraphic date of this unit can be bracketed to between the Kviármýri 2 tephra (1110±85 BP/840±85 AD) and the Ö1362 AD (588 BP) tephra. It was formed after the settlement of Iceland (ca. 1100 BP). The unit G represents the cooling of the climate in the 13th Century (Ogilvie, 1991). However, human impact on the environment can not be ruled out as

supplementary factor. It is highly likely that Kviárjökull advanced during this period and, again, extended to the limit of the big moraine theatre, perhaps slightly further. This can be inferred by looking at the tephra stratigraphy of the Kviárhólar moraines (Fig. 5.26) where the Ö1362 tephra is at the base of the profiles. This would suggest a late Medieval date of the Kviárhólar moraines similar to that of the Stóralda moraine and Virkisjökull III stage. If so, this advance would be the third advance forming the big moraine amphitheatre (Kviárjökull IIIc).

Thórarinsson (1956) has inferred that Kviárjökull filled up the area inside the big moraine theatre in the late 19th Century as a consequence of the climatic deterioration during the LIA in Iceland. This would be the fourth advance that shaped the Kviárjökull III (d) stage.

Summary.

A record of multiple Holocene glacier advances is preserved in front of the Kviárjökull outlet glacier (Fig. 5.19; 5.27). The oldest advance occurred between ca. 9400 BP and 13000 BP but has left no moraine record. The onset of the Neoglaciation in the area is marked by the Kviárjökull I and II stages dated to between 4600 BP and ca. 6000 BP, probably closer to the former date. The moraines from this stage can be mainly traced in front of Kviármýrarkambur but clear lateral limits are located on either side of the glacier. The third advance is delineated by the big moraine theatre comprising the Kviármýrarkambur and Kambsmýrarkambur lateral moraines. This limit is composed of multiple re-advances of the glacier. This advance is called the Kviárjökull III stage. The limit is dated between the Hs tephra (ca. 3500 BP) and an advance in the late 19th Century AD. This moraine amphitheatre is interpreted as representing four advances. This can be depicted from the stratigraphic evidence in the proglacial area. The initial advance took place around 3300 BP (Kviárjökull IIIa), the second around 1700 BP (Kviárjökull IIIb), the third in the 13th Century (Kviárjökull IIIc) and the final in the late 19th Century. The advance dated to around 1700 BP left a moraine record on the distal slope of the Kambsmýrarkambur moraine. The third advance (13th Century) is inferred to have

formed the Kvíárhólar moraine hillocks just to the east of the big Kvíármýrarkambur theatre.

5.9 Conclusion

All outlet glaciers studied, except Morsárjökull, show a long history of glacier fluctuations from the termination of the last inland ice sheet, beginning at ca. 13000 BP, to an advance in the late 19th Century (Table 5.1). The dates of the advances of different outlets seem to be consistent and contrasts are not identified between outlets of Vatnajökull and Öræfajökull outlets as reported by Thompson (1988) in the more recent recession from the LIA limits of Skaftafellsjökull and Svínafellsjökull. Thompson (1988) concluded that Svínafellsjökull recessed slower in comparison with the more rapidly retreating Skaftafellsjökull. In this study the difference, if any, might be hidden because the moraine and tephra record is not detailed enough to preserve the contrasting behaviour. The tentative correlation of glacier advances in the Öræfi district are displayed in Table 5.2. A close temporal match may exist where the time difference between different outlets can be explained by error margins in the MSAR dates. Differential soil accumulation is likely to occur between sites, even within the same stage as a consequence of contrasting depositional conditions. As a result, mean dates were always applied to minimise the error.

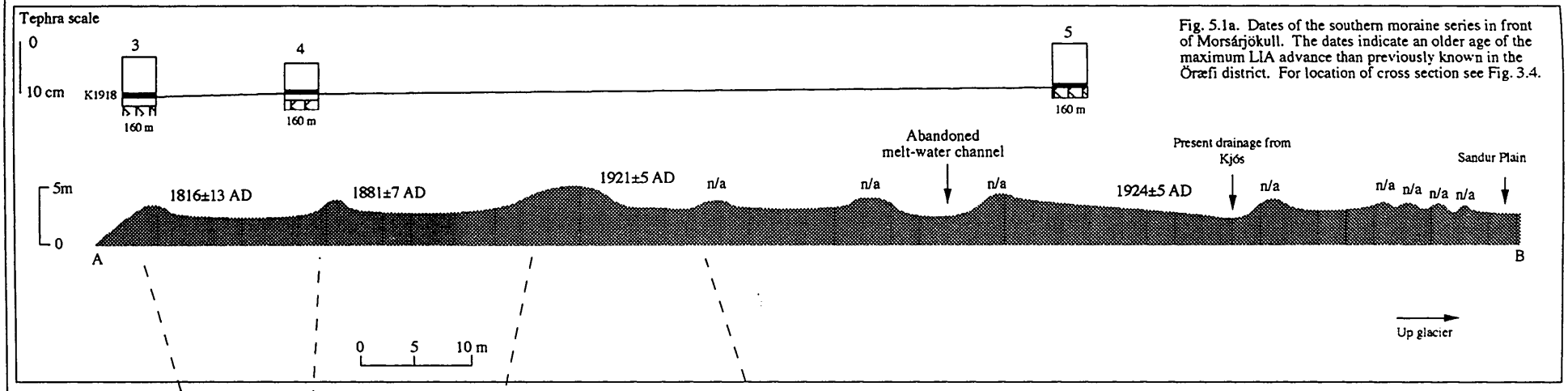

Fig. 5.1a. Dates of the southern moraine series in front of Morsárjökull. The dates indicate an older age of the maximum LIA advance than previously known in the Öræfi district. For location of cross section see Fig. 3.4.

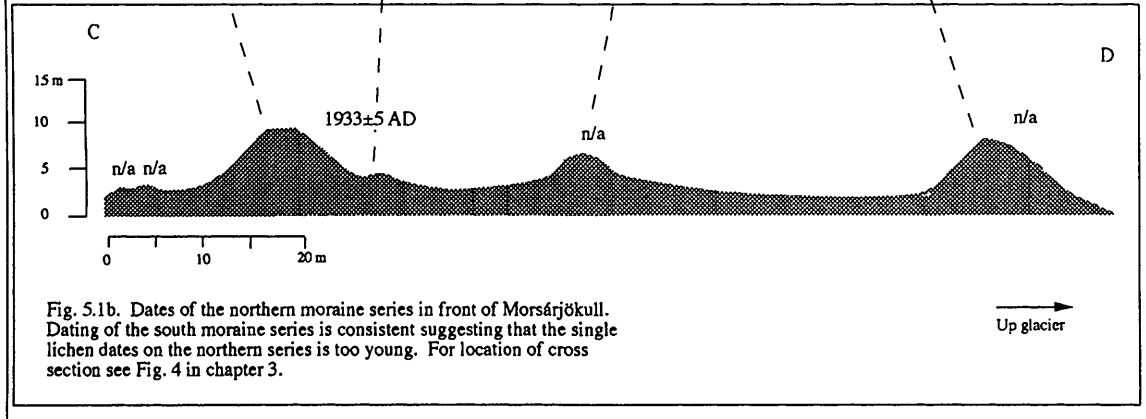

Fig. 5.1b. Dates of the northern moraine series in front of Morsárjökull. Dating of the south moraine series is consistent suggesting that the single lichen dates on the northern series is too young. For location of cross section see Fig. 4 in chapter 3.

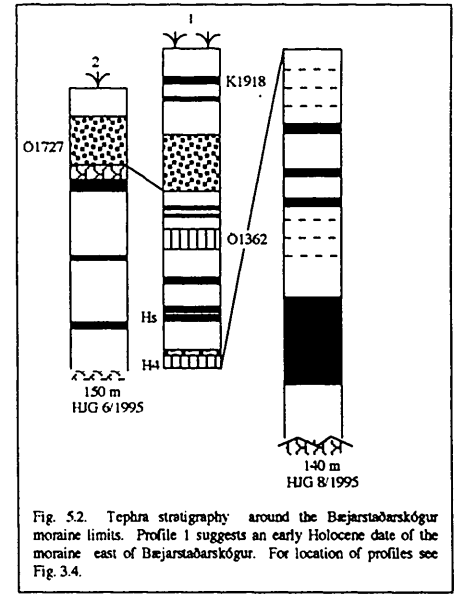

Fig. 5.2. Tephra stratigraphy around the Bæjarstaðarskógur moraine limits. Profile 1 suggests an early Holocene date of the moraine east of Bæjarstaðarskógur. For location of profiles see Fig. 3.4.

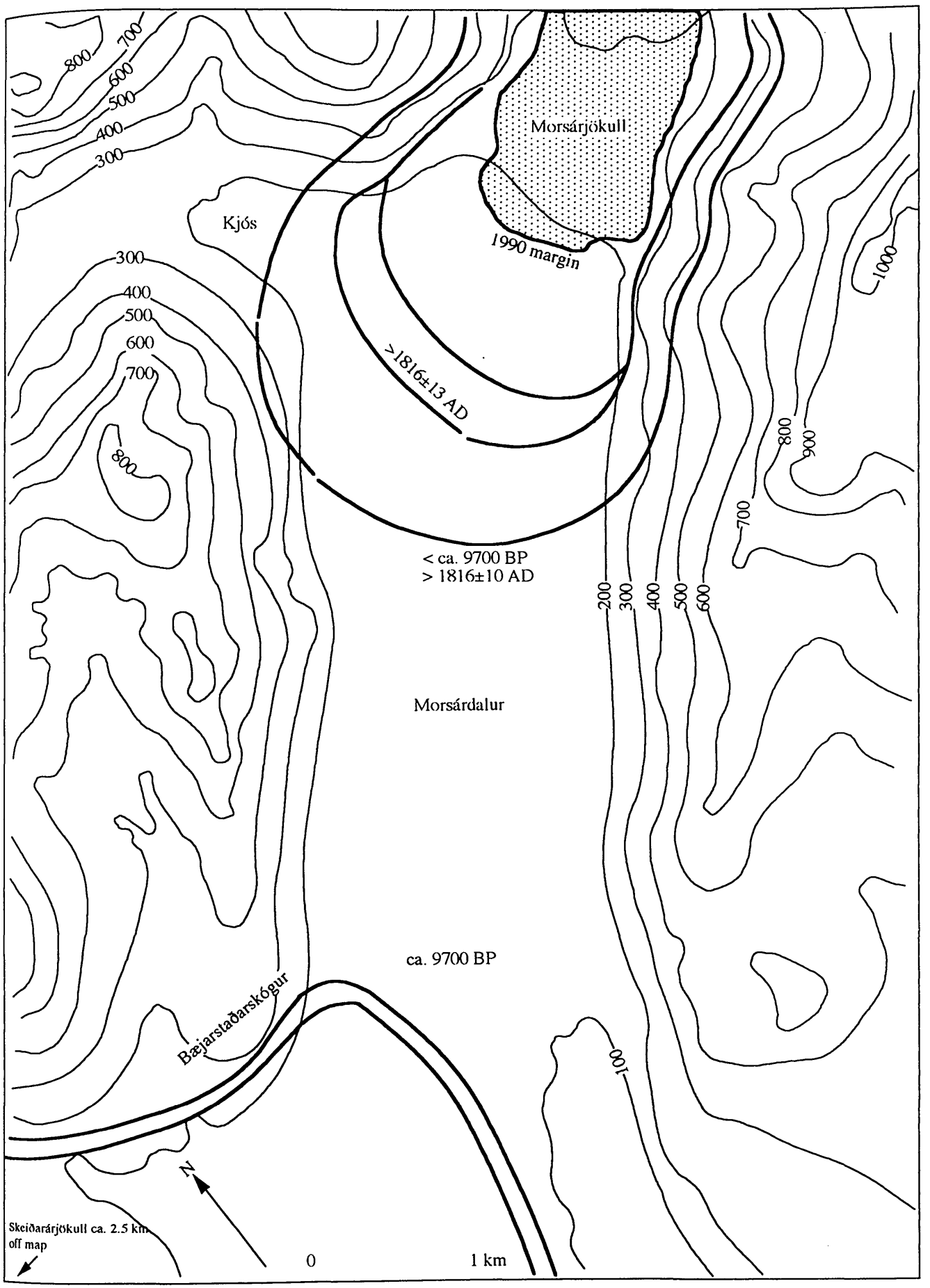

Fig. 5.3. Holocene ice margins found in Morsárdalur. The Bæjarstaðarskógur limits are orginated from Skeiðarárjökull in the south (ca. 2.5 km off map). Glacier advances older than LIA are most probably buried by younger advances in front of Morsárjökull.

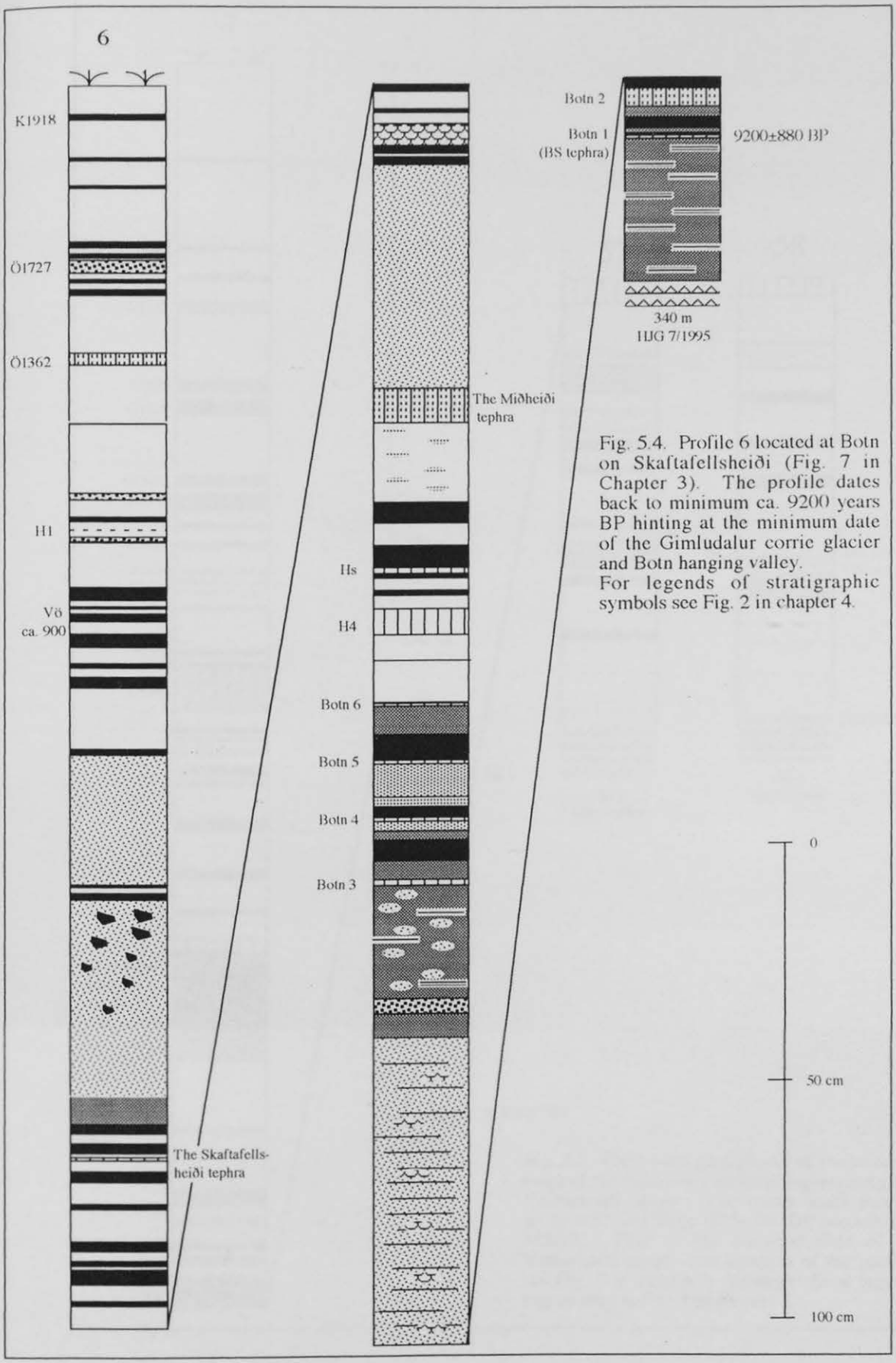

Fig. 5.4. Profile 6 located at Botn on Skaftafellsheiði (Fig. 7 in Chapter 3). The profile dates back to minimum ca. 9200 years BP hinting at the minimum date of the Gimludalur corrie glacier and Botn hanging valley.
For legends of stratigraphic symbols see Fig. 2 in chapter 4.

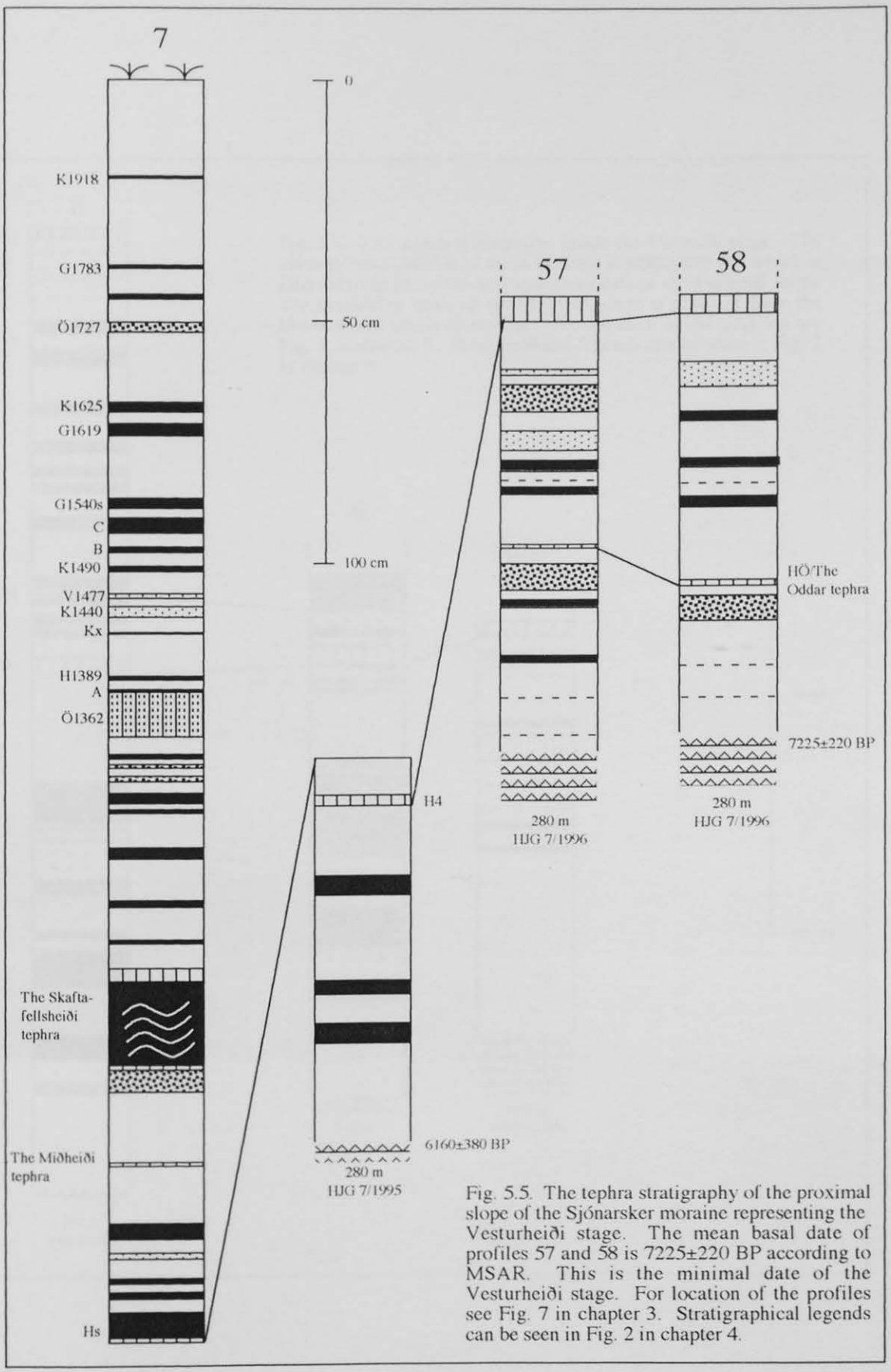

Fig. 5.5. The tephra stratigraphy of the proximal slope of the Sjónarsker moraine representing the Vesturheiði stage. The mean basal date of profiles 57 and 58 is 7225±220 BP according to MSAR. This is the minimal date of the Vesturheiði stage. For location of the profiles see Fig. 7 in chapter 3. Stratigraphical legends can be seen in Fig. 2 in chapter 4.

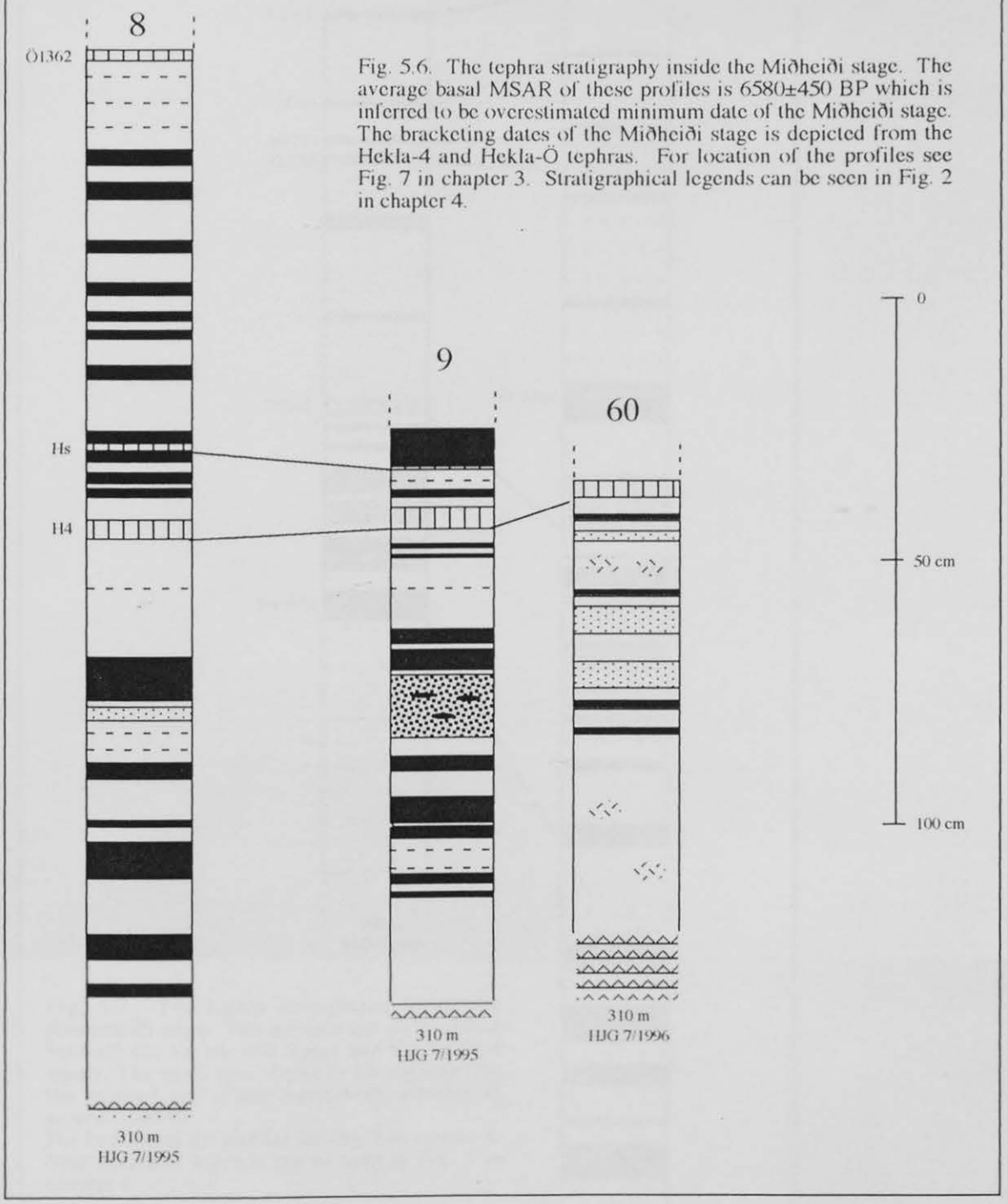

Fig. 5.6. The tephra stratigraphy inside the Miðheiði stage. The average basal MSAR of these profiles is 6580±450 BP which is inferred to be overestimated minimum date of the Miðheiði stage. The bracketing dates of the Miðheiði stage is depicted from the Hekla-4 and Hekla-Ö tephras. For location of the profiles see Fig. 7 in chapter 3. Stratigraphical legends can be seen in Fig. 2 in chapter 4.

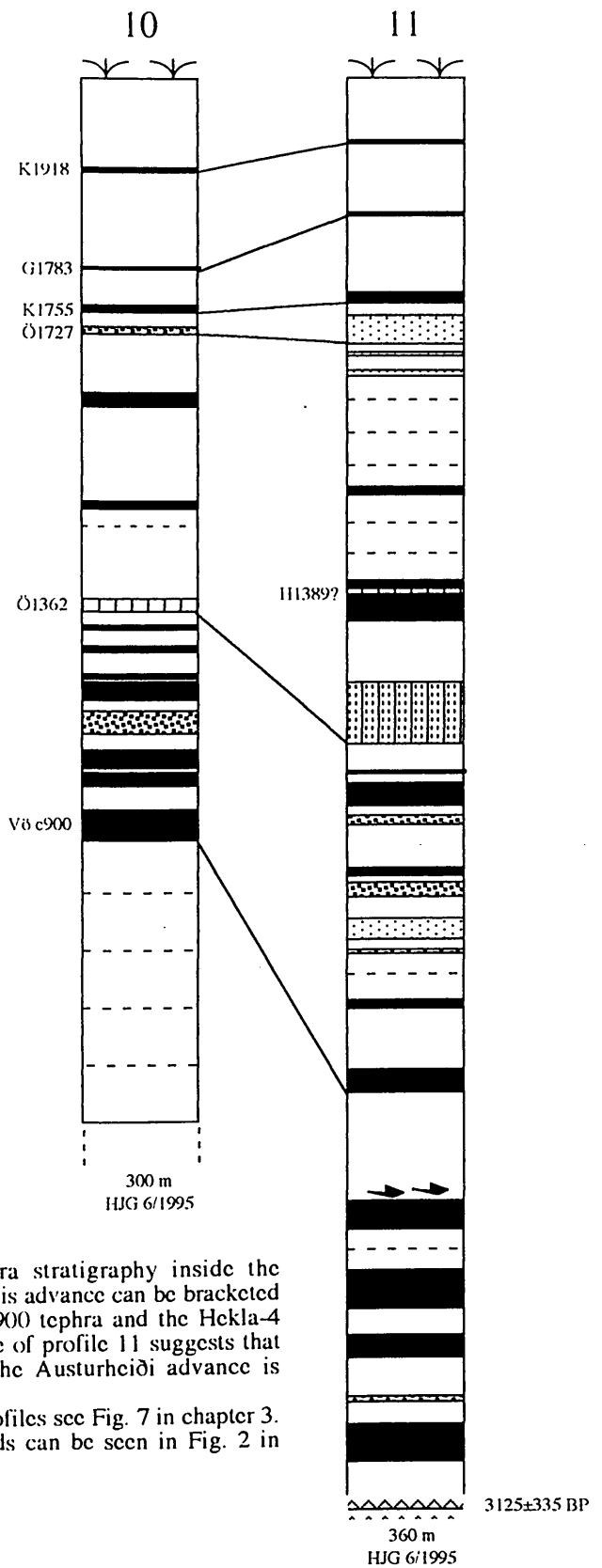

Fig. 5.7. The tephra stratigraphy inside the Austurheiði stage. This advance can be bracketed between the Vö ca. 900 tephra and the Hekla-4 tephra. The basal date of profile 11 suggests that the mininal age of the Austurheiði advance is around 3100 BP.
For location of the profiles see Fig. 7 in chapter 3. Stratigraphical legends can be seen in Fig. 2 in chapter 4.

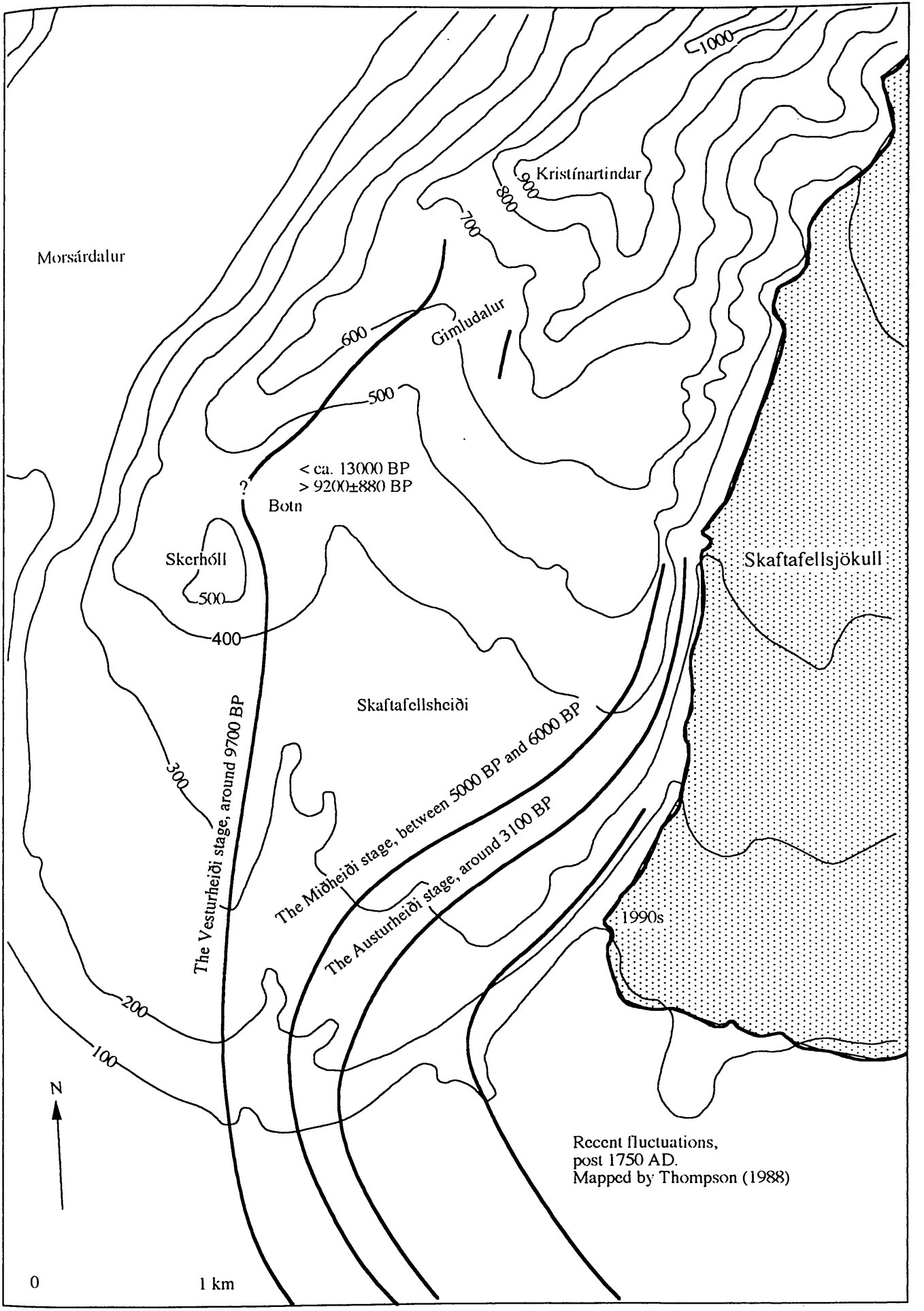

Fig. 5.8. The Holocene ice limits on Skaftafellsheiði. During the Preboreal, Skaftafellsheiði was covered by ice. The Miðheiði stage represents the Neoglaciation in the mid Holocene.

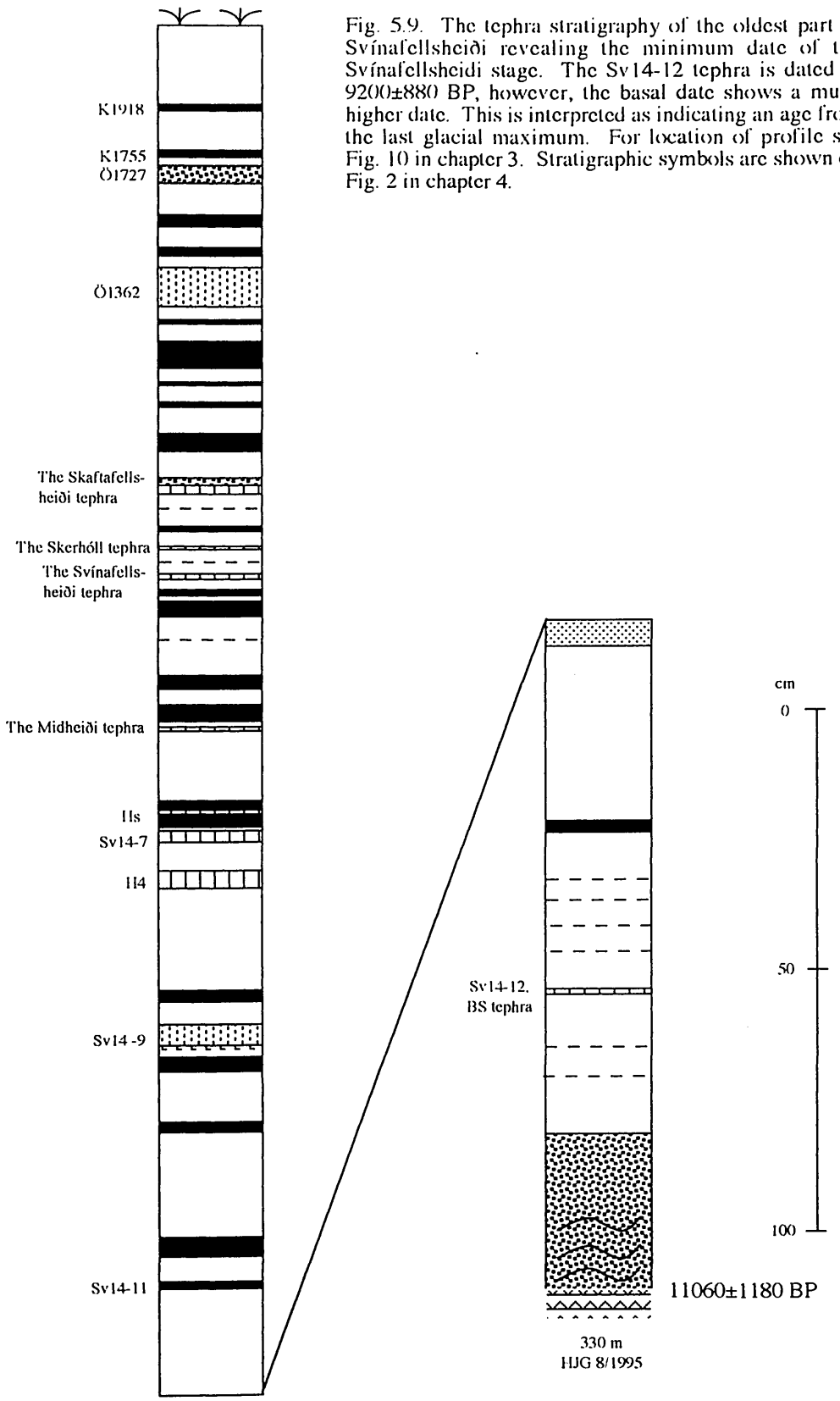

Fig. 5.9. The tephra stratigraphy of the oldest part of Svínafellsheiði revealing the minimum date of the Svínafellsheidi stage. The Sv14-12 tephra is dated to 9200±880 BP, however, the basal date shows a much higher date. This is interpreted as indicating an age from the last glacial maximum. For location of profile see Fig. 10 in chapter 3. Stratigraphic symbols are shown on Fig. 2 in chapter 4.

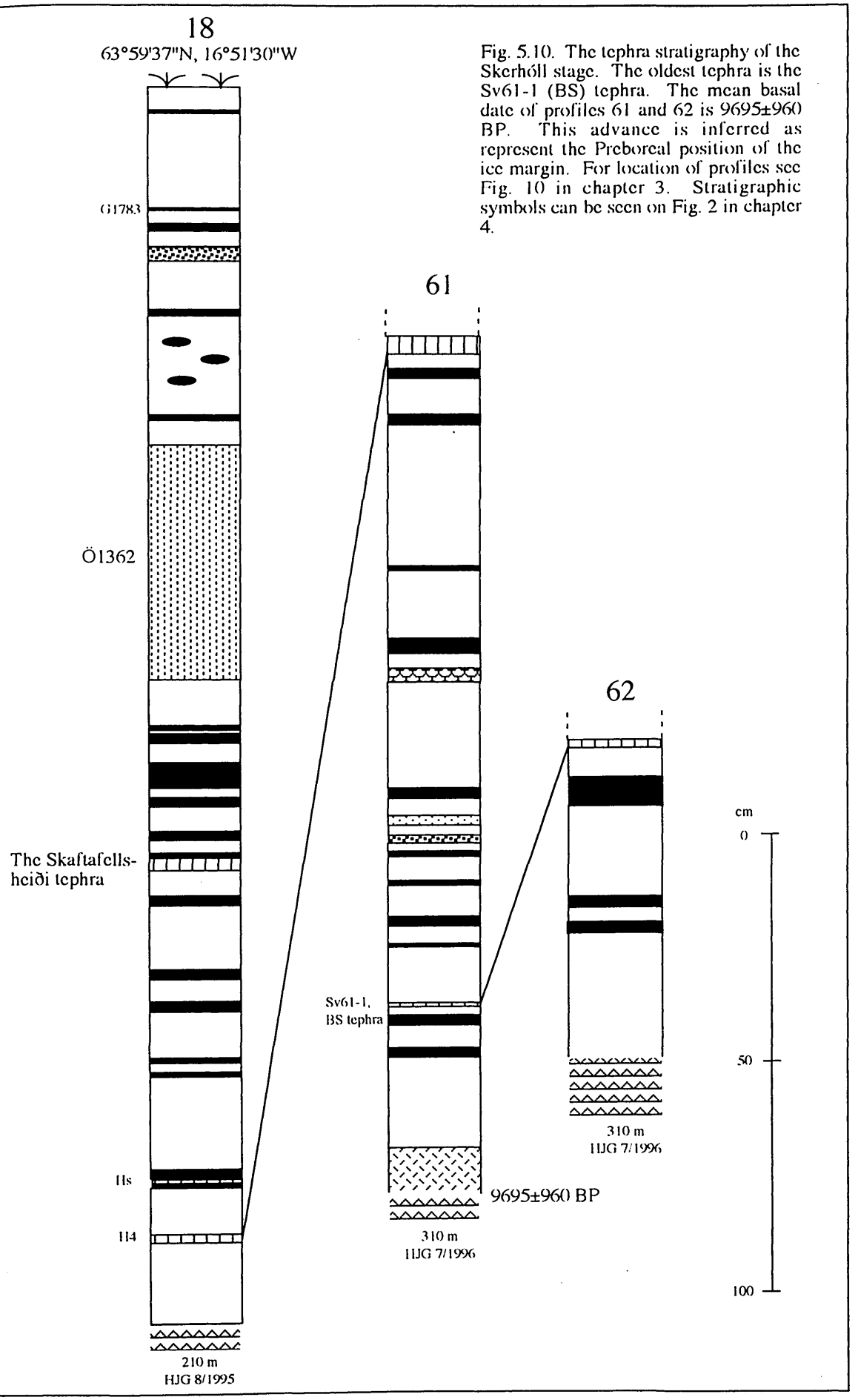

Fig. 5.10. The tephra stratigraphy of the Skerhóll stage. The oldest tephra is the Sv61-1 (BS) tephra. The mean basal date of profiles 61 and 62 is 9695±960 BP. This advance is inferred as represent the Preboreal position of the ice margin. For location of profiles see Fig. 10 in chapter 3. Stratigraphic symbols can be seen on Fig. 2 in chapter 4.

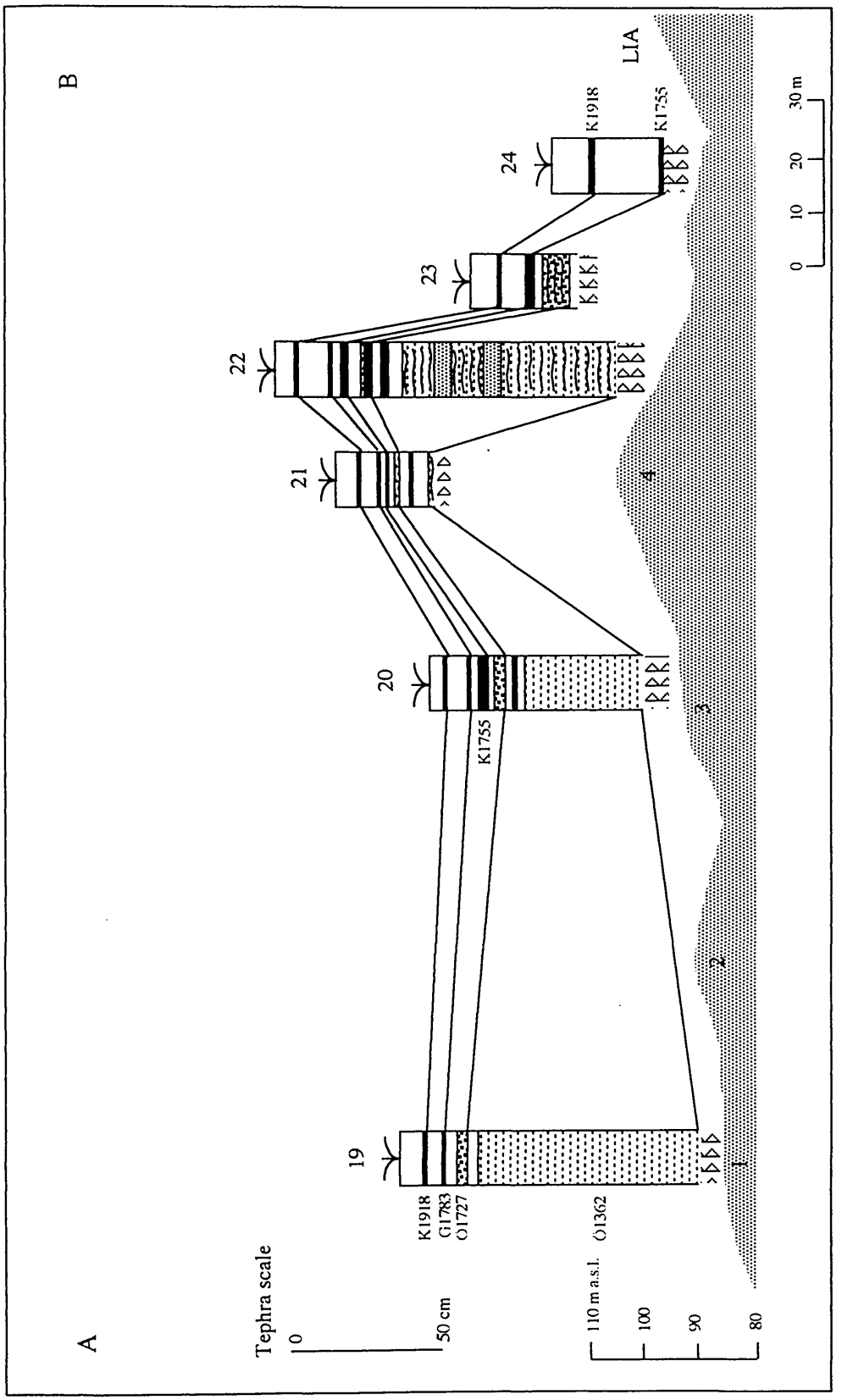

Fig. 5.11. The tephra stratigraphy of the Stóralda moraine complex. The tephra stratigraphy suggests a Medieval date of the Stóralda moraine complex. For location of section see line AB on Fig. 5.13.

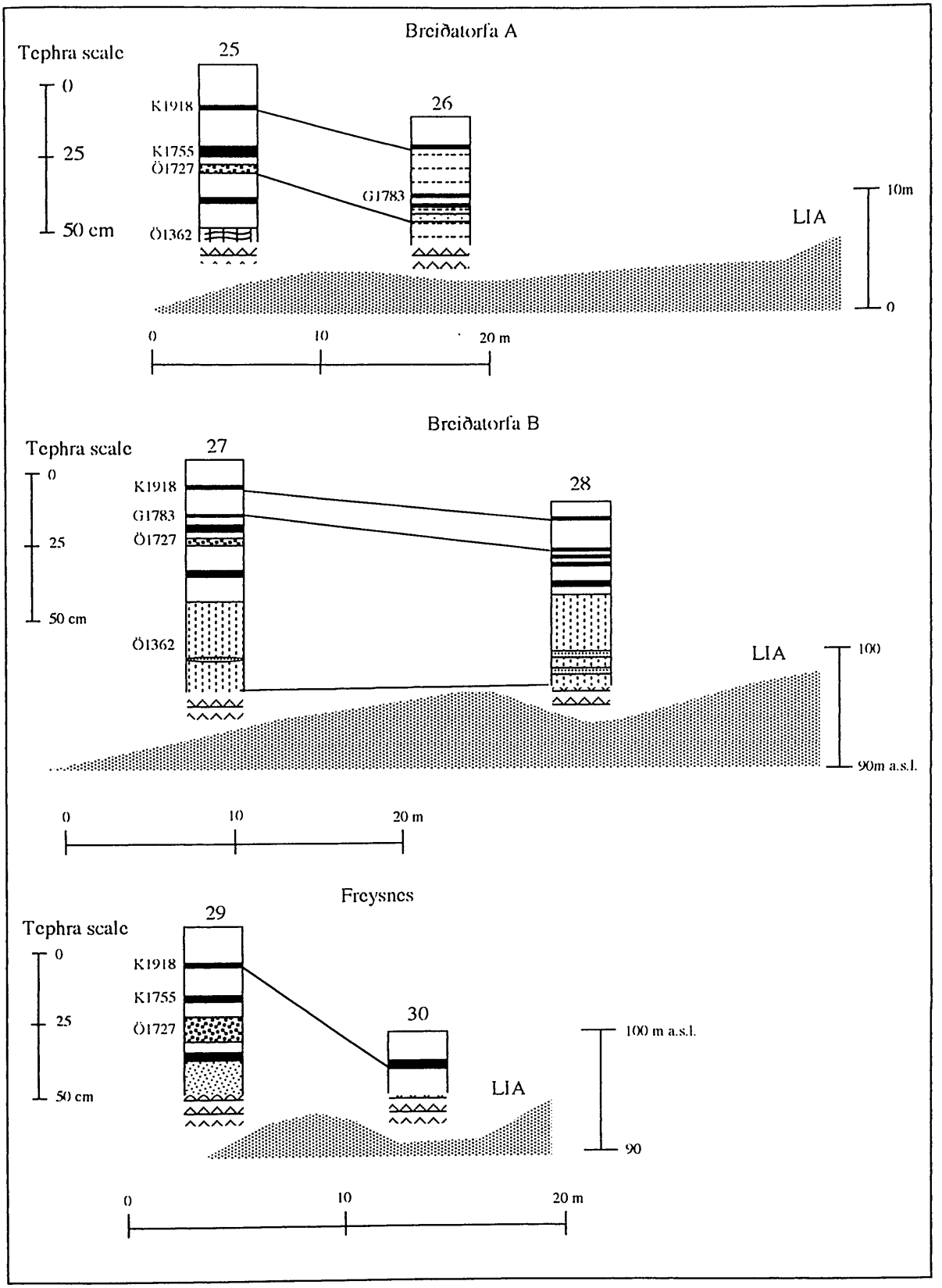

Fig. 5.12. The tephra stratigraphy of the Breiðatorfa and Freysnes moraines. The Breiðatorfa moraines are of Medieval age and the Freysnes moraines are dated to between 1727 and 1755 AD. The Freysnes morains morphologically correlates with crest no. 5 of the Stóralda moraine complex. For location of moraines see Fig. 10 in chapter 3.

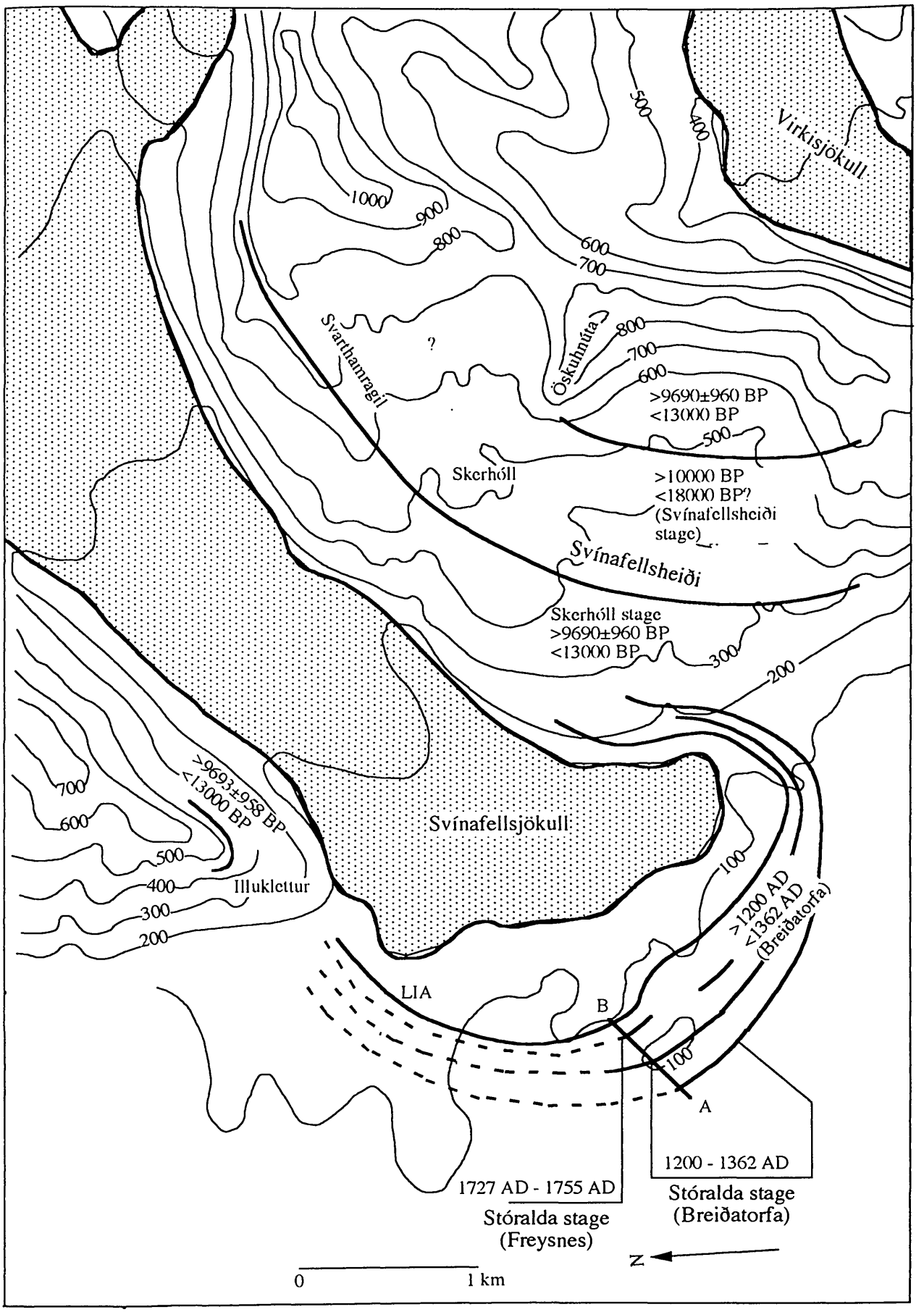

Fig. 5. 13. Ice limits around Svínafellsjökull. The Stóralda moraine complex in front of the glacier dates back to Medieval times. Ice limits on Svínafellsheiði, which is the highland to the west of the ice margin, are dated to the last Termination. Transect A - B in Fig. 5.11.

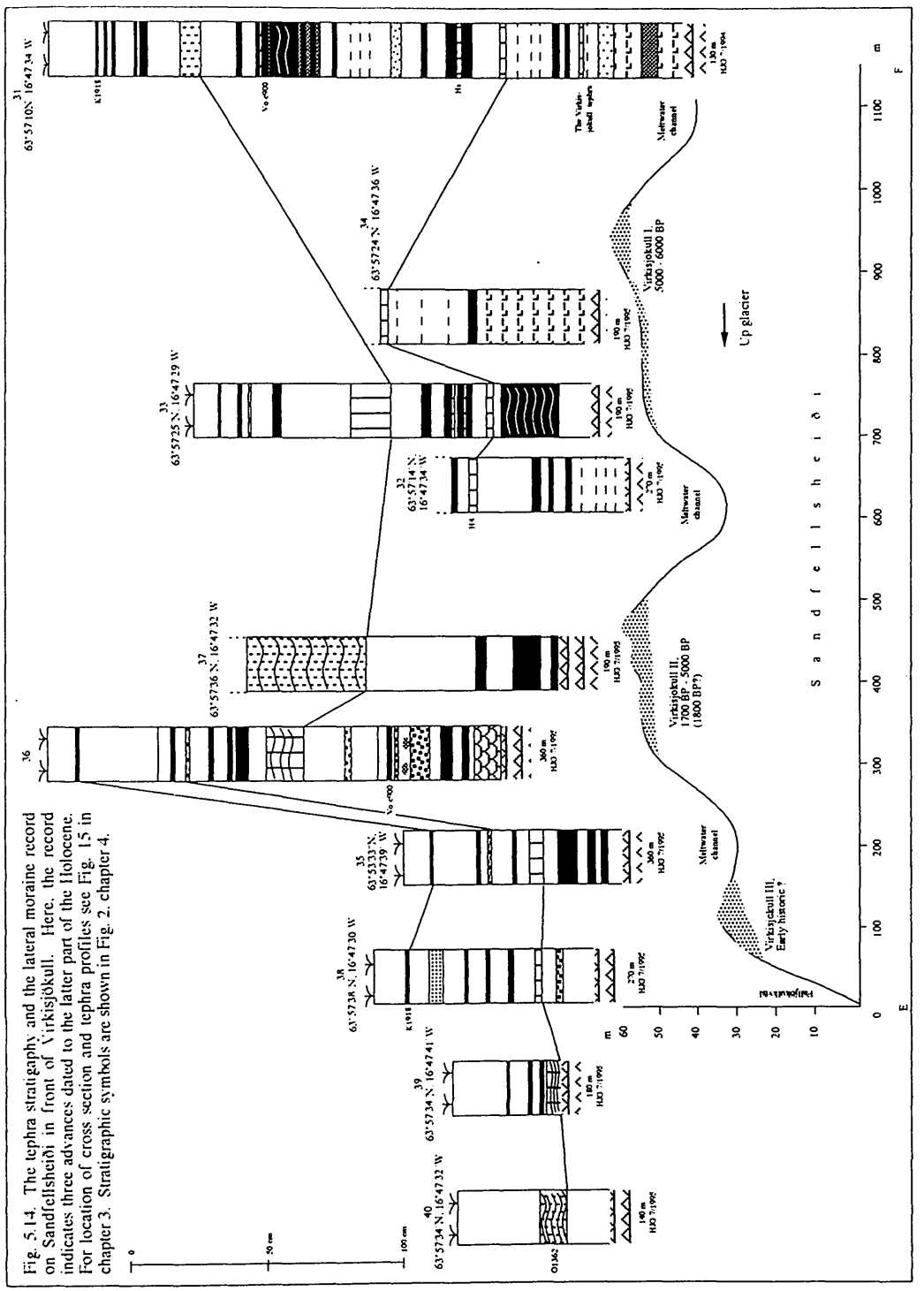

Fig. 5.14. The tephra stratigaphy and the lateral moraine record on Sandfellsheiði in front of Virkisjökull. Here, the record indicates three advances dated to the latter part of the Holocene. For location of cross section and tephra profiles see Fig. 1.5 in chapter 3. Stratigraphic symbols are shown in Fig. 2. chapter 4.

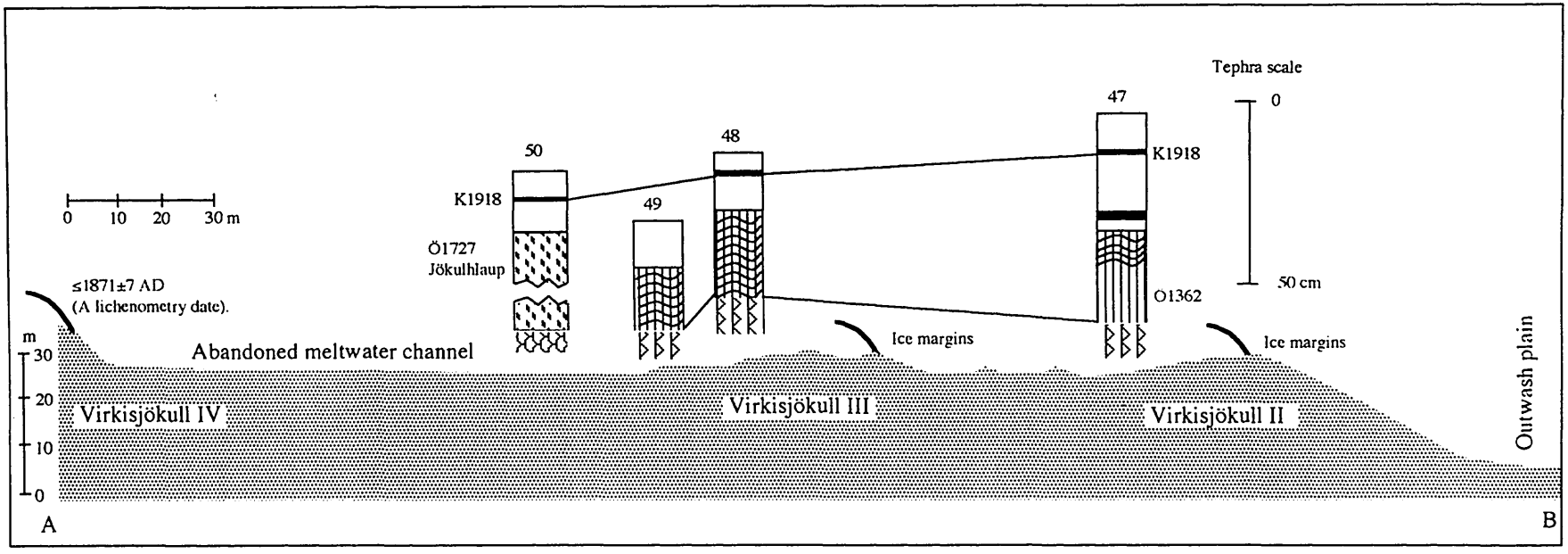

Fig. 5.15. The tephra stratigraphy and the moraine record in front of Virkisjökull. The tephra stratigraphy suggests Medieval dates for Virkisjökull II and III advances, however, these moraines geomorphologically correlate with moraines on Sandfellsheiði which indicate older dates for these advances. For location of the cross section see line AB on Fig. 3.15.

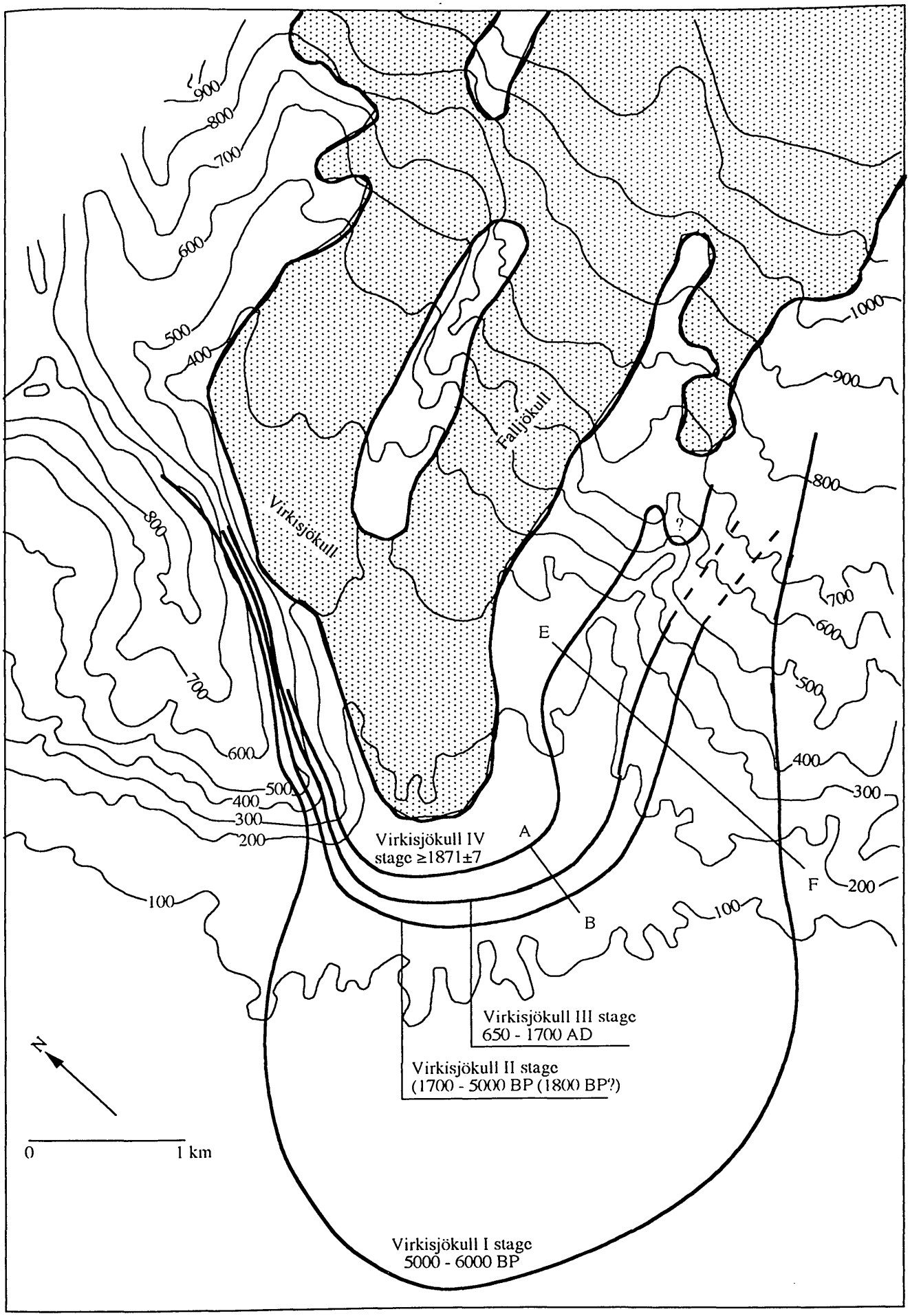

Fig. 5.16. The Holocene ice limits around Virkisjökull. Virkisjökull I is the biggest mid Holocene advance of the outlets studied. Transect A-B and E-F, see Figs. 5.15 and 5.14, respectively.

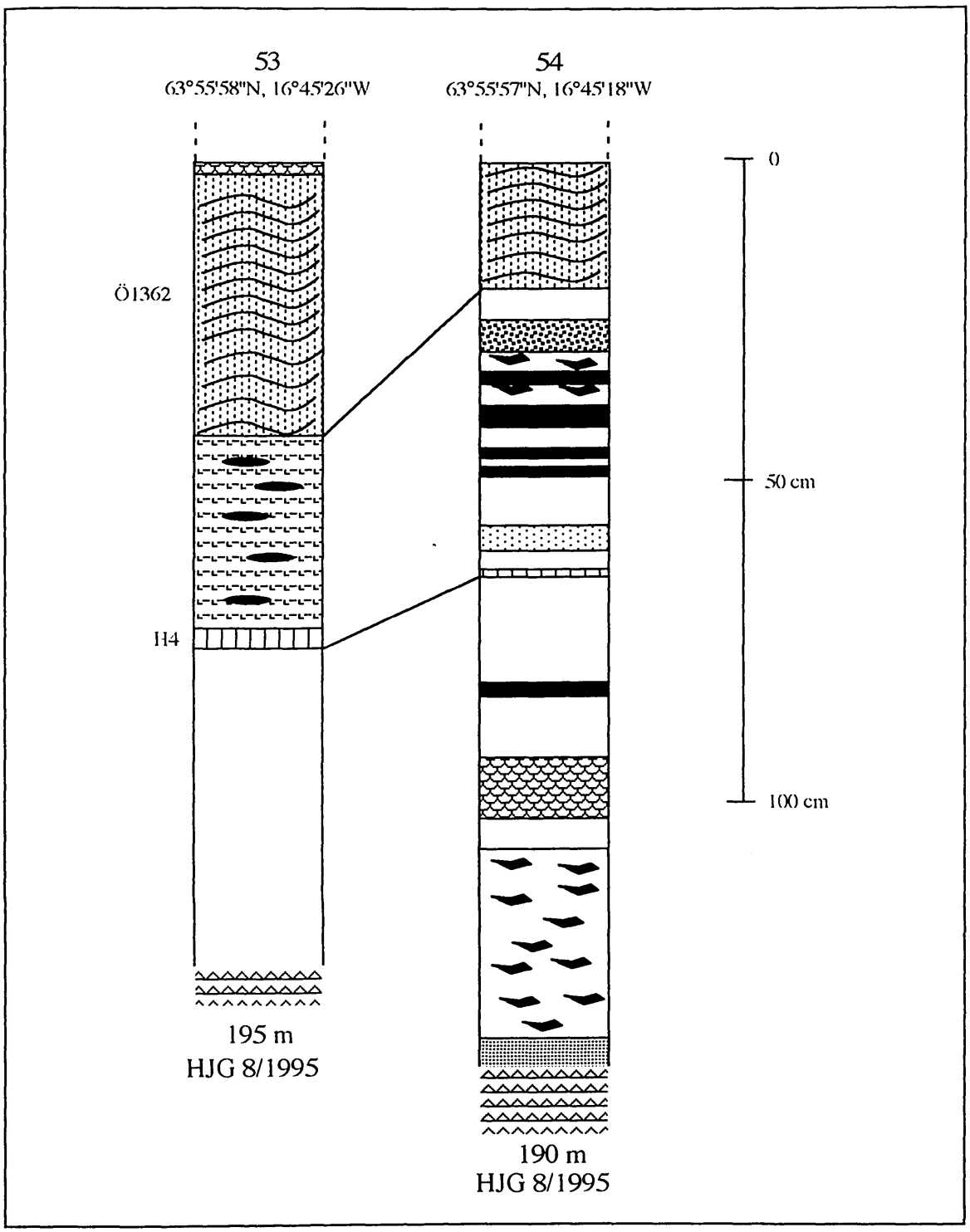

Fig. 5.17. The tephra stratigraphy between Kotárjökull II and I stages in front of Kotárjökull. The dating evidence are interpreted as depicting advances in the mid and late Holocene.

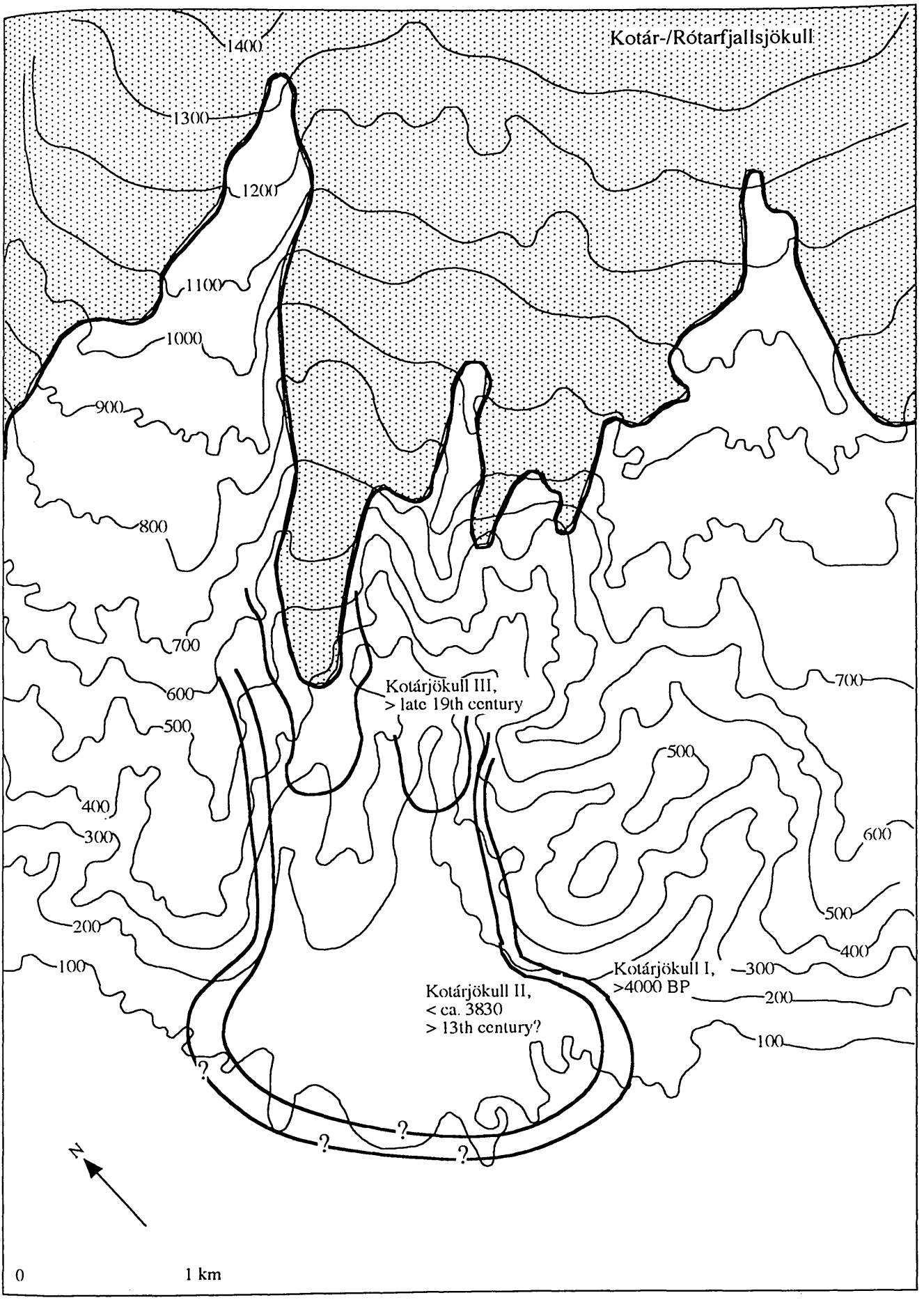

Fig. 5.18. Holocene ice limits in front of Kotárjökull. The extension of Kotárjökull I and II on the sandur plain is unknown due to lack of evidence. The evidence are most likely buried under jökulhlaups from Öræfajökull eruptions.

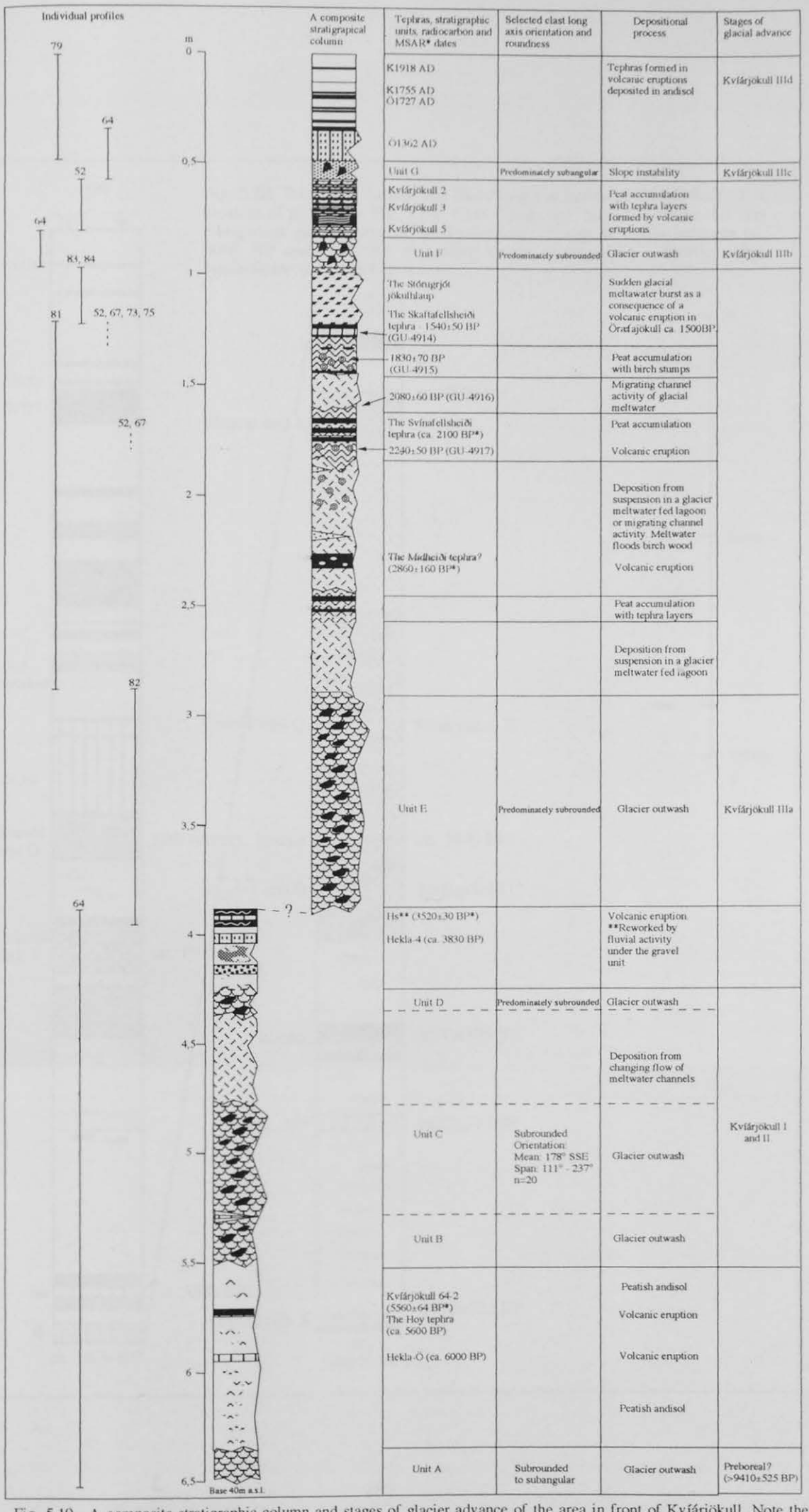

Fig. 5.19. A composite stratigraphic column and stages of glacier advance of the area in front of Kvíárjökull. Note the high environmental activity represented by different soil types ranging from gravel (high environmental activity) to peat (low environmental activity) Soils in the area preserve diverse tephra record covering the last 6000 BP years.

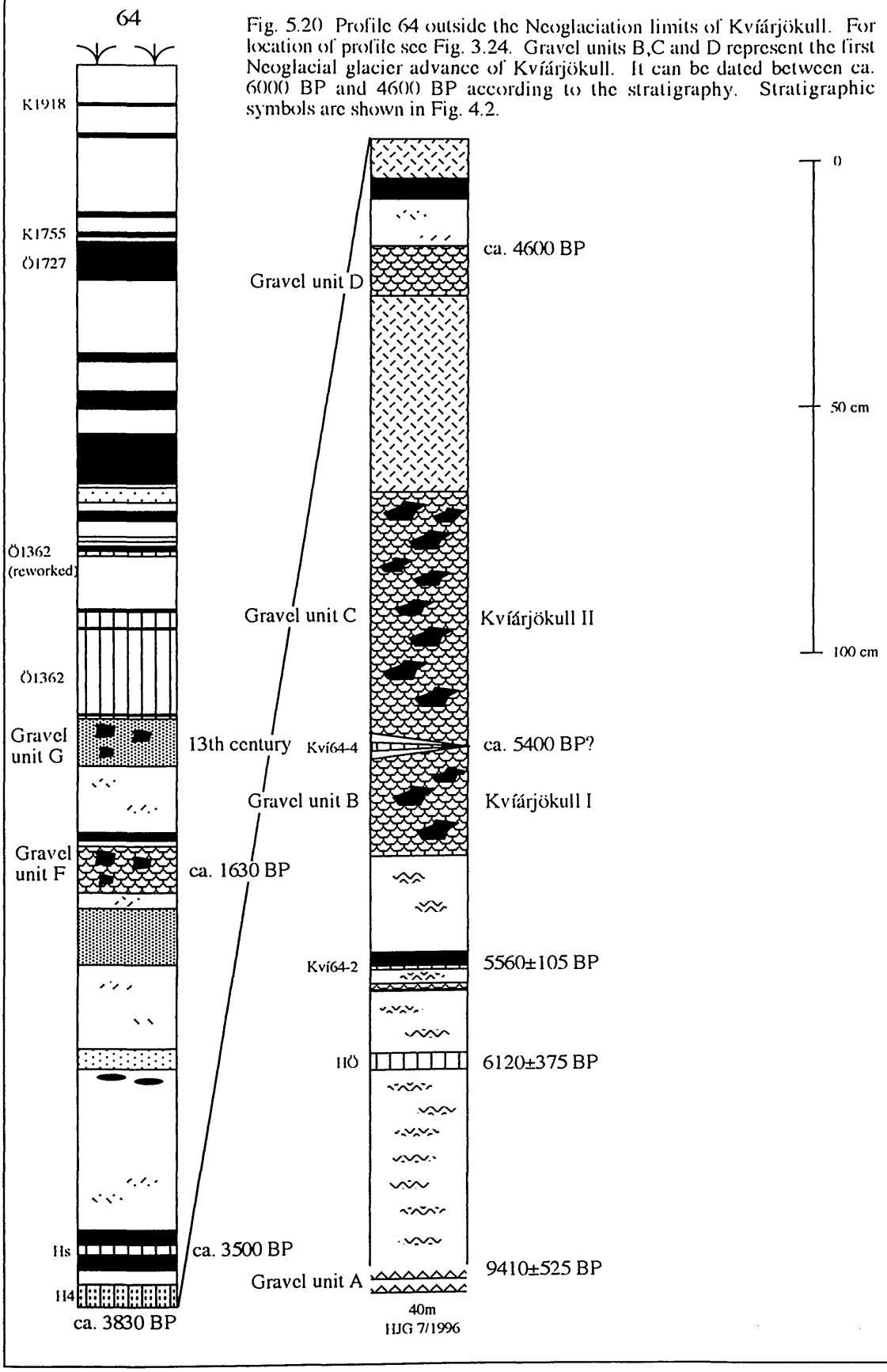

Fig. 5.20 Profile 64 outside the Neoglaciation limits of Kvíárjökull. For location of profile see Fig. 3.24. Gravel units B,C and D represent the first Neoglacial glacier advance of Kvíárjökull. It can be dated between ca. 6000 BP and 4600 BP according to the stratigraphy. Stratigraphic symbols are shown in Fig. 4.2.

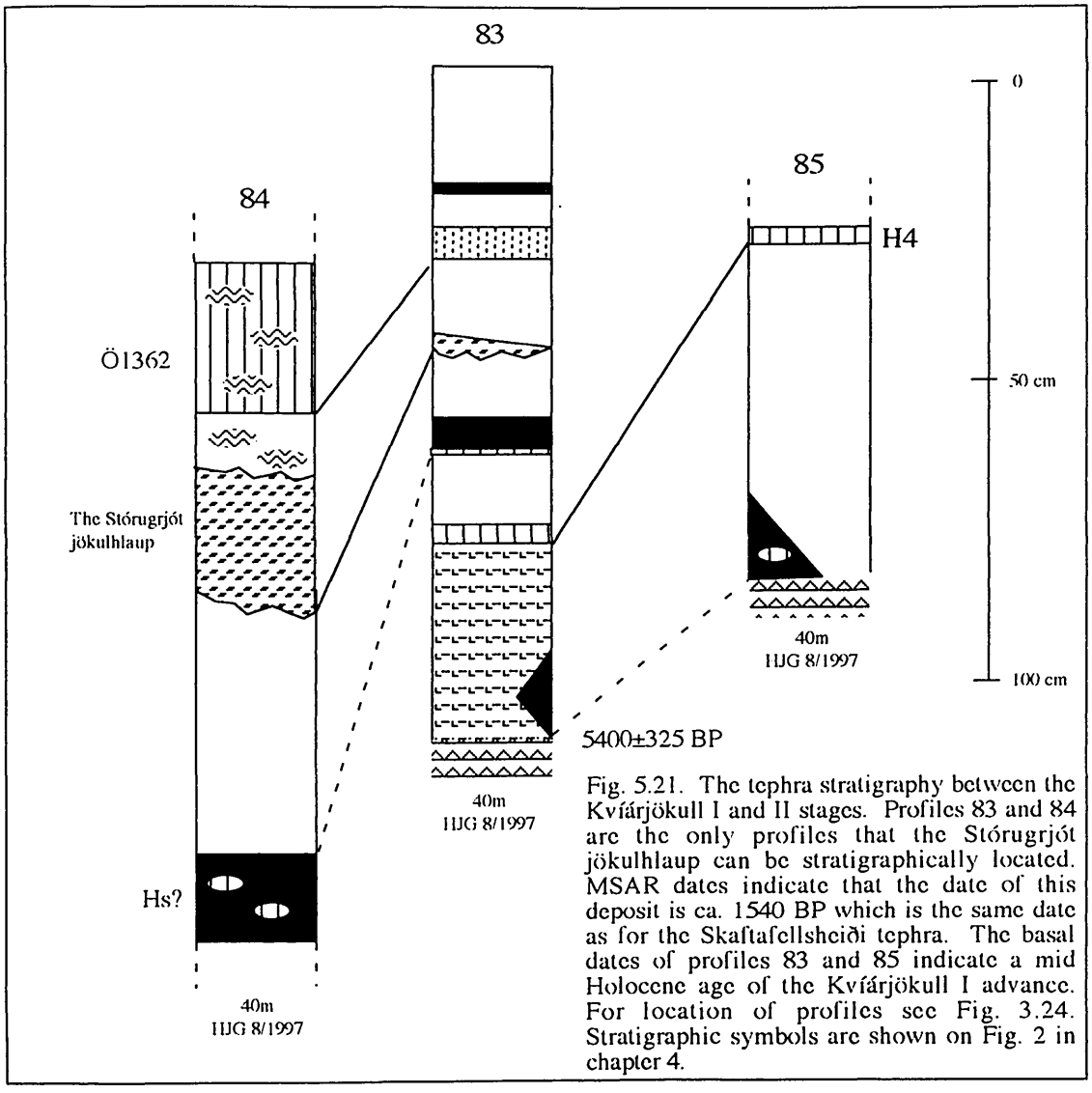

Fig. 5.21. The tephra stratigraphy between the Kvíárjökull I and II stages. Profiles 83 and 84 are the only profiles that the Stórugrjót jökulhlaup can be stratigraphically located. MSAR dates indicate that the date of this deposit is ca. 1540 BP which is the same date as for the Skaftafellsheiði tephra. The basal dates of profiles 83 and 85 indicate a mid Holocene age of the Kvíárjökull I advance. For location of profiles see Fig. 3.24. Stratigraphic symbols are shown on Fig. 2 in chapter 4.

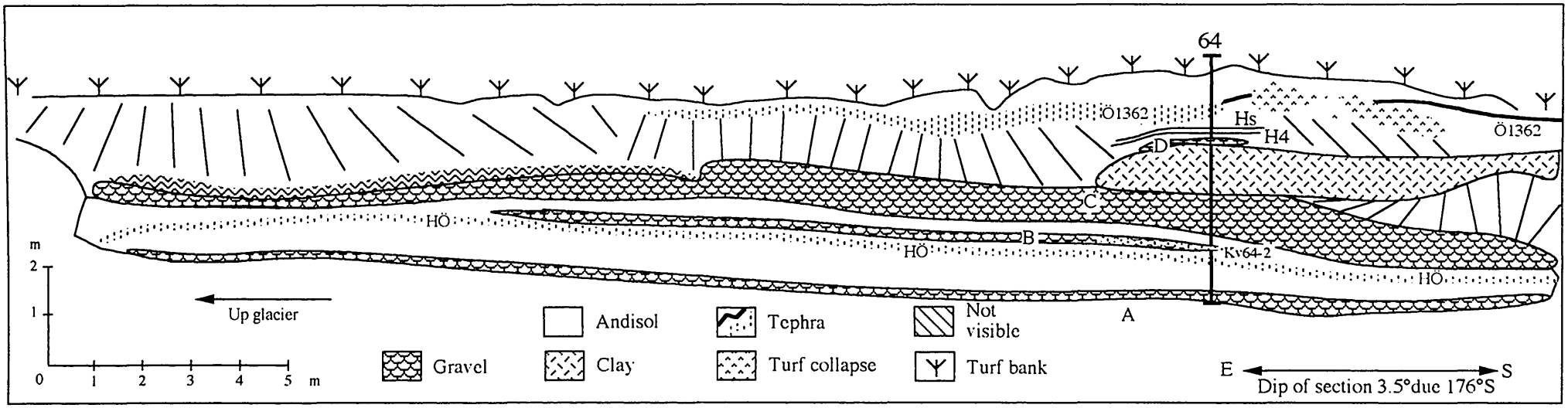

Fig. 5.22. A long section of the oldest stratigraphic section in front of Kviárjökull. The outwash deposit from the first major advance of the glacier in the mid Holocene is very clear as gravel unit B, C and D. For location of the profile, see Fig. 24 in chapter 3.

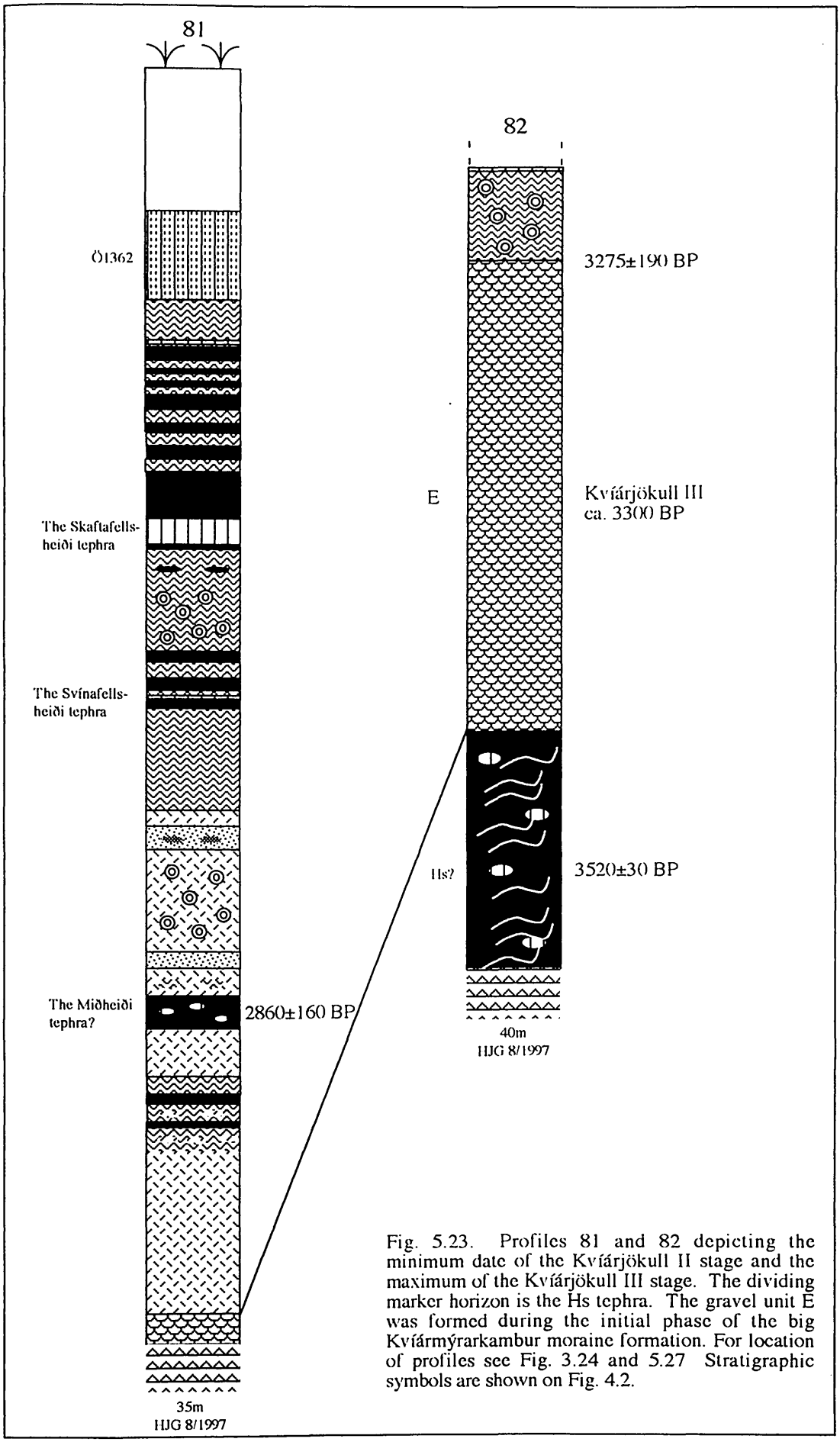

Fig. 5.23. Profiles 81 and 82 depicting the minimum date of the Kvíárjökull II stage and the maximum of the Kvíárjökull III stage. The dividing marker horizon is the Hs tephra. The gravel unit E was formed during the initial phase of the big Kvíármýrarkambur moraine formation. For location of profiles see Fig. 3.24 and 5.27 Stratigraphic symbols are shown on Fig. 4.2.

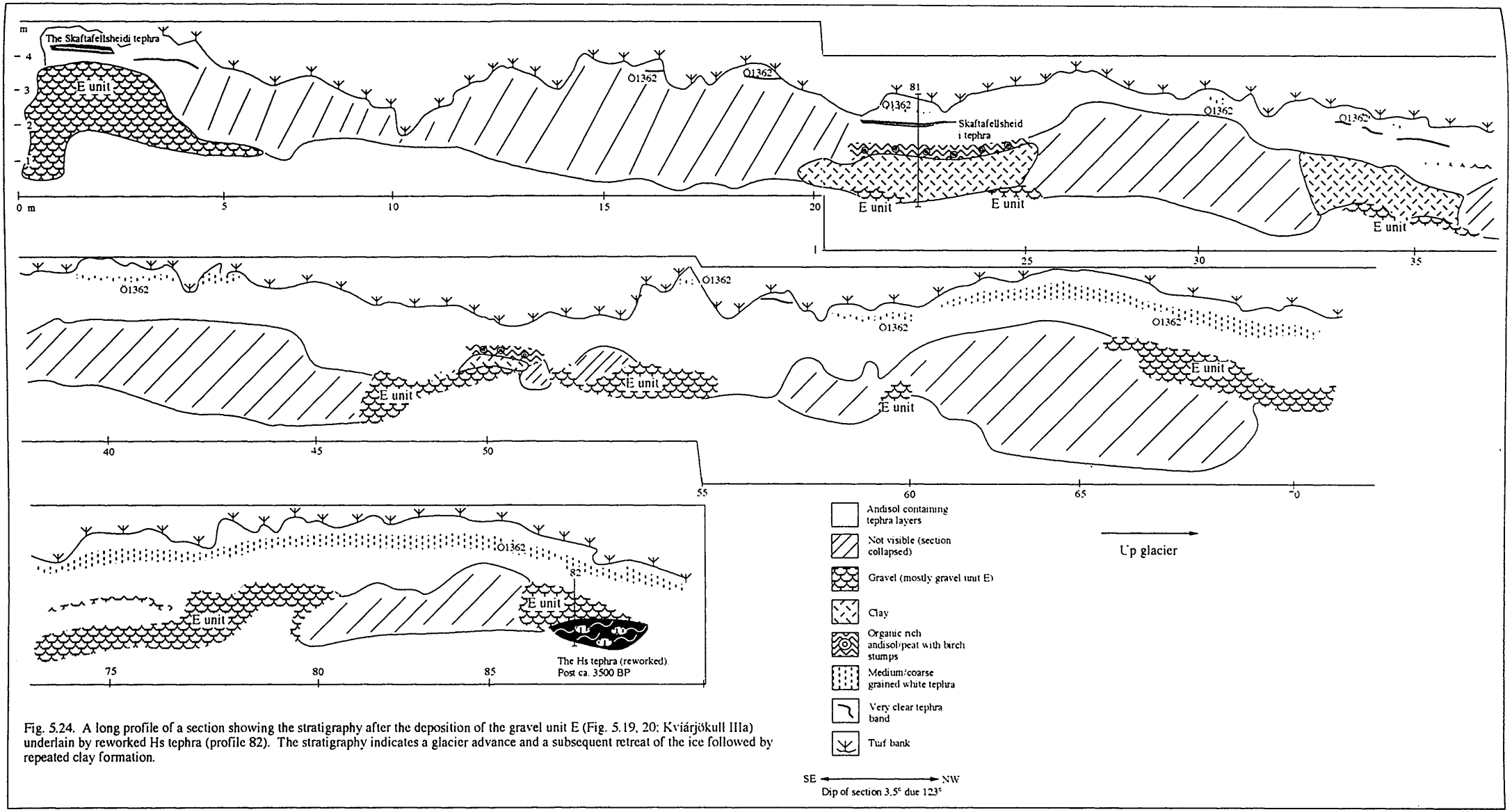

Fig. 5.24. A long profile of a section showing the stratigraphy after the deposition of the gravel unit E (Fig. 5.19, 20; Kviárjökull IIIa) underlain by reworked Hs tephra (profile 82). The stratigraphy indicates a glacier advance and a subsequent retreat of the ice followed by repeated clay formation.

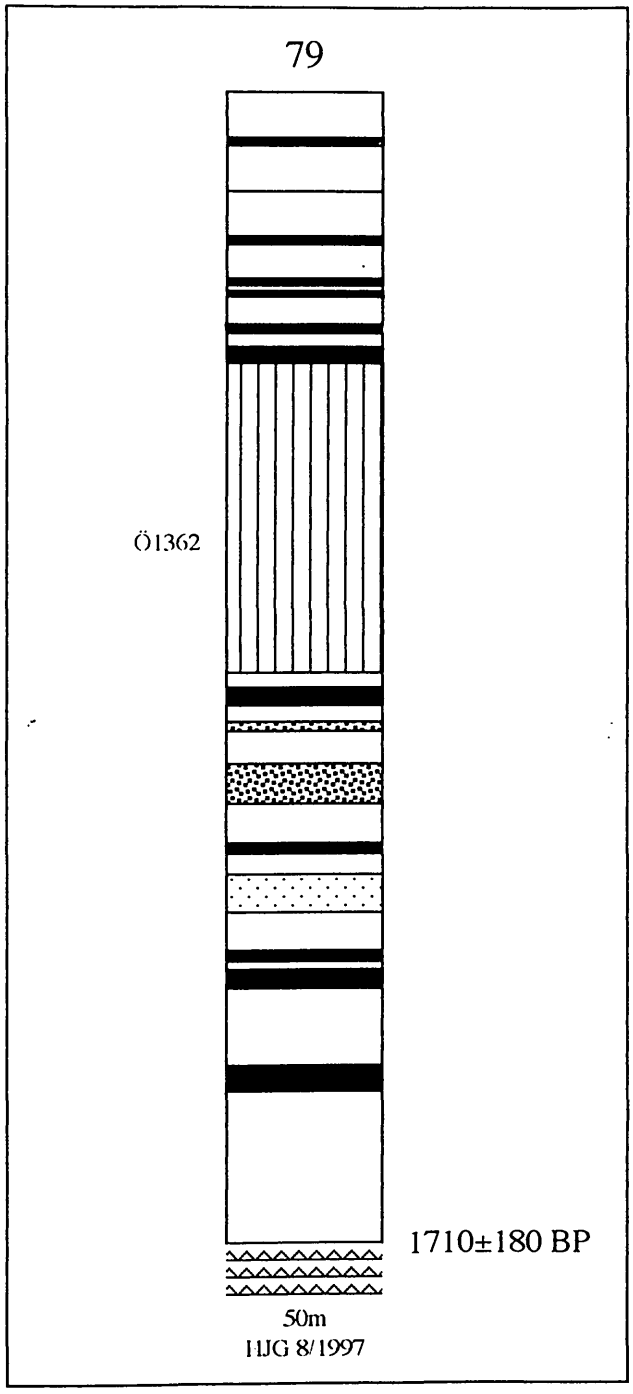

Fig. 5.25. The tephra stratigraphy inside the moraine loop on the distal slope of Kambsmýrarkambur. The moraine limit is interpreted as represent an advance around 1700 BP.

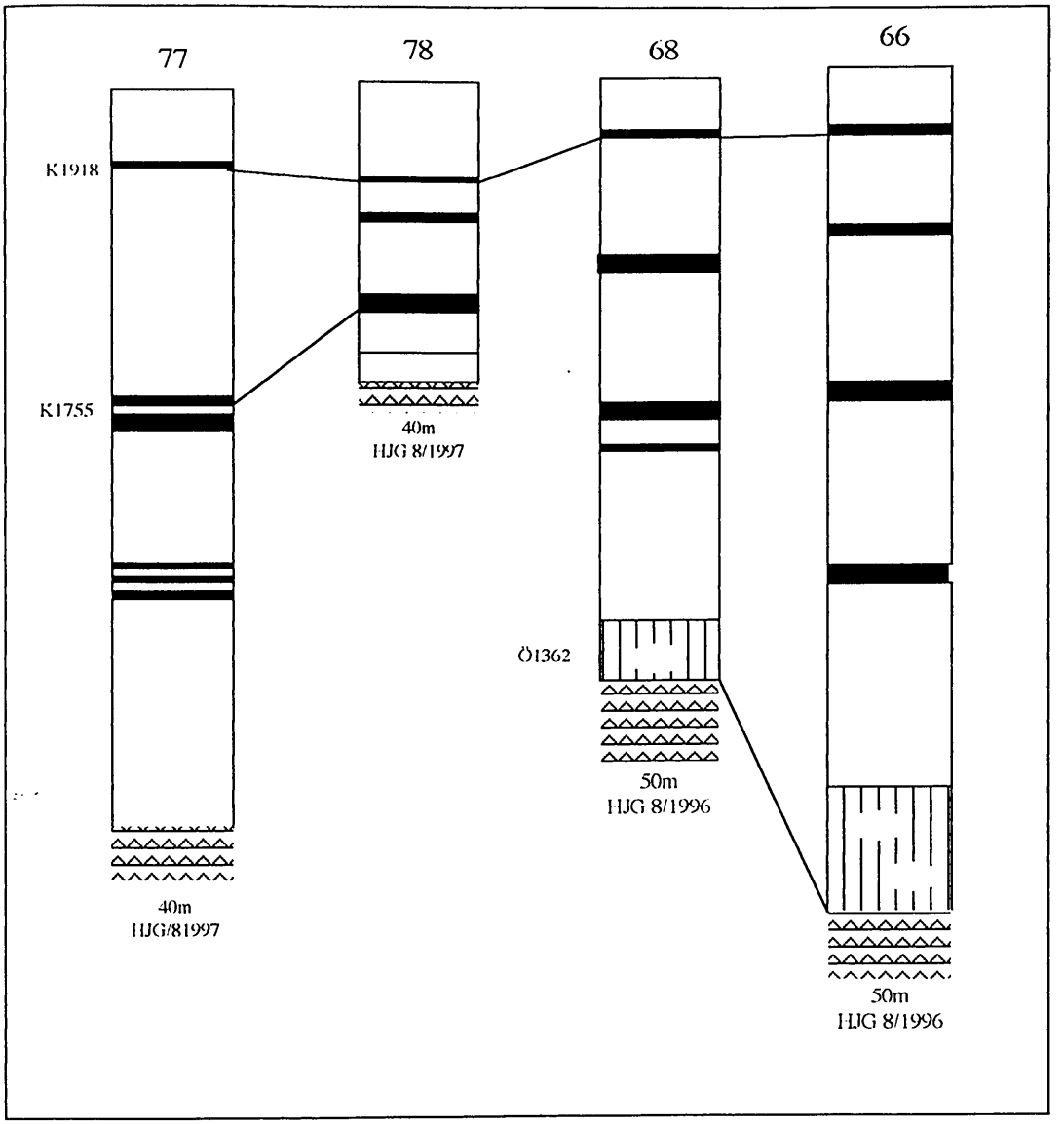

Fig. 5.26. The tephra stratigraphy of the Kviárhólar moraines. Profiles 66, 68 and 77 are located on top of the moraines but profile 78 on the distal slope. These moraine series are likely to represent a Medieval advance. For location of profiles see Fig. 24, chapter 3, and stratigraphic symbols can be seen on Fig. 2 in chapter 4.

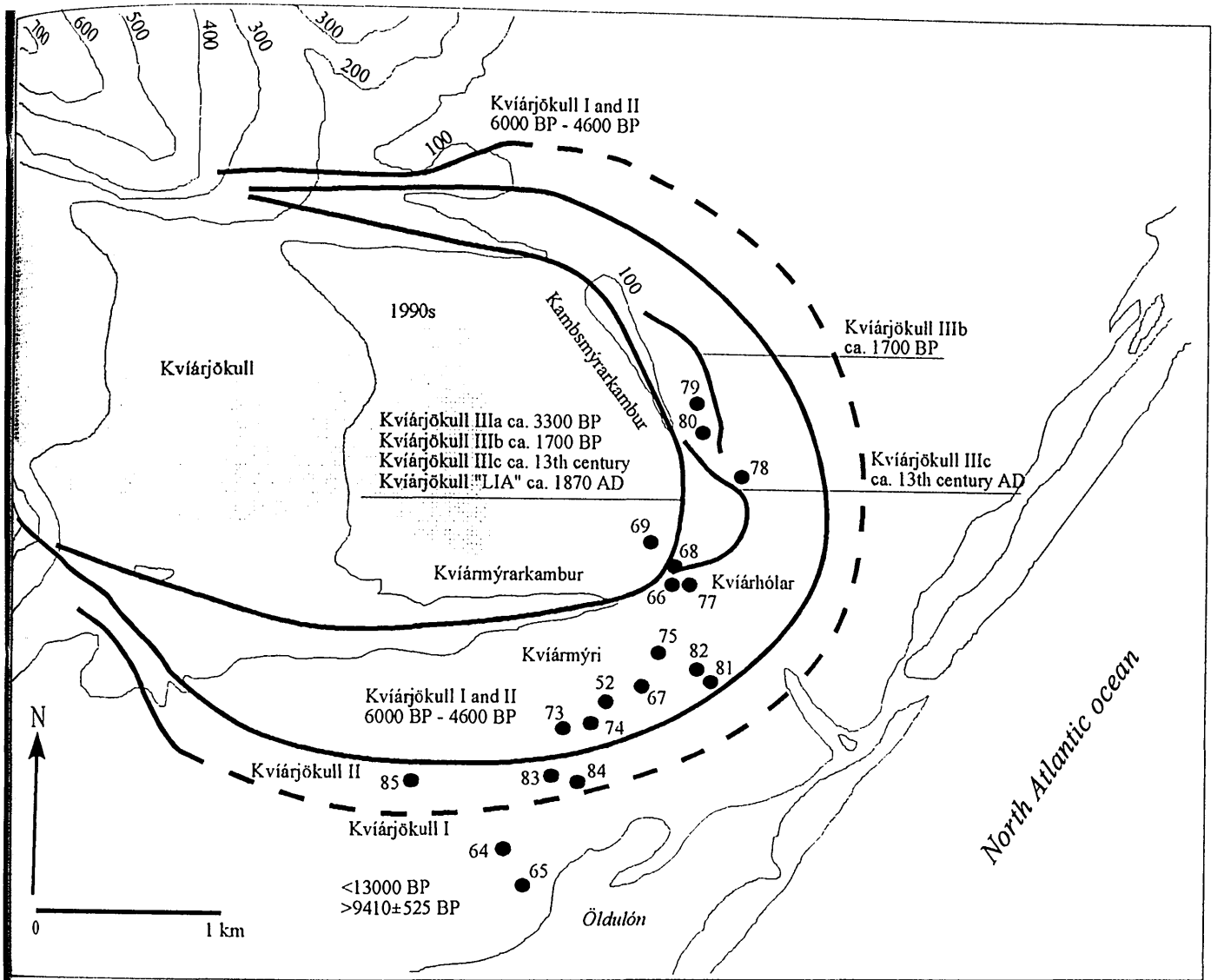

Fig. 5.27. Holocene ice limits around Kvíárjökull. Kvíárjökull III represents the big moraine theatre. The extension of Kvíárjökull I advance is not known.
Filled black circles are tephra sections. The extent of the outermost advance of the glacier is unknown. The base of profile 64 depicts the oldest gravel layer in the area. It is dated to the end of the last Termination.

Outlet name	*Origin*	*Advance*	*Bracketing dates*
Skeiðarárjökull	Vatnajökull	Preboreal	>8930±835 BP <13000 BP
Morsárjökull	Vatnajökull	Holocene	>1816±13 AD <9000±850 BP
		"LIA"	>1816±13 AD
Skaftafellsjökull	Vatnajökull	Gimludalur (Preboreal)	>9200±880 BP <13000 BP
		Vesturheiði (Preboreal)	>7230±220 BP <9200±880 BP
		Miðheiði	Hekla-Ö* - Hekla-4**
		Austurheiði	Hekla-4** - 3125±335 BP
		"LIA"	>1904 AD
Svínafellsjökull	Öræfajökull	Svínafellsheiði	<18000 BP? >11060±1180 BP
		Skerhóll	<13000 BP >9200±880 BP
		Stóralda/ Breiðatorfa	<1362 AD >1200 AD
		Stóralda/Freysnes	1727 AD - 1755 AD
		"LIA"	ca. 1870 AD
Virkisjökull	Öræfajökull	Virkisjökull I	<6000 BP >5000 BP
		Virkisjökull II	<5000 BP/>1700±180 BP (ca. 1800 BP)
		Virkisjökull III	<1700±180 BP >650 BP (ca. 1300 AD)
		Virkisjökull IV	>1871±7 AD
Kotárjökull	Öræfajökull	Kotárjökull I	>6310±410 BP
		Kotárjökull II	<Hekla-4** >13th century AD?
		Kotárjökull III	>19th century?
Kvíárjökull	Öræfajökull	Kvíárjökull (outermost)	<13000 BP >9410±525 BP
		Kvíárjökull I Kvíárjökull II	<Hekla-Ö* ca. 4600 BP
		Kvíárjökull IIIa	<Hs*** >Miðheiði tephra**** (ca. 3300 BP)
		Kvíárjökull IIIb	ca. 1700 BP
		Kvíárjökull IIIc	<840±85 AD >1362 AD
		"LIA"	ca. 1870 BP

*Hekla-Ö tephra ca. 6000 BP
**Hekla-4 tephra ca. 3830 BP
***Hs tephra ca. 3500 BP
****The Miðheiði tephra ca. 2800 BP

Table 5.1. Bracketing dates of glacier fluctuations of selected outlet glaciers of Öræfajökull and Vatnajökull ice caps, SE Iceland. The results indicate high glacier activity at the end of the last Termination. The onset of the Neoglaciation is around mid Holocene and since then, glacier activity has been relatively high in the study area.

Stages of advance	*Inferred date*
Svínafellsheiði	Last Glacial maximum?
Skeiðarárjökull, Gimludalur/Vesturheiði, Skerhóll, Kvíárjökull	ca. 9700 BP. Preboreal?
Miðheiði, Virkisjökull I, Kotárjökull I?, Kvíárjökull I and II	6000 - 4600 BP Onset of Neoglaciation
Austurheiði, Kotárjökull II?, Kvíárjökull IIIa	ca. 3200 BP
Virkisjökull II, Kvíárjökull IIIb	1700 - 1800 BP
Stóralda/Breiðatorfa, Kvíárjökull IIIc, Virkisjökull III	13th century AD
Stóralda/Freysnes	Early 18th century AD
Morsárjökull, Skaftafellsjökull ("LIA"), Virkisjökull IV, Svínafellsjökull ("LIA"), Kotárjökull III?, Kvíárjökull ("LIA")	19th century AD

Table 5.2. Inferred correlation and consequent mean dates of the glacier advances in the Öræfi district, SE Iceland. The Medieval glacier advance is detected for the first time in Iceland in the study area. The observed glacier fluctuation history in the Öræfi district spans at least the last 10.000 BP years. Evidence of the last Termination can be found in the western part of the study area where it has not been destroyed by later glacier advances or other environmental activities.

Chapter 6. Discussion, implications and conclusion

Part I Discussion and implication

6.1 Introduction

The implications of the Öræfajökull glacier fluctuations record are great. The ice cap shows a long history of glacier fluctuations stretching back to the last Termination. This would suggest that the Öræfajökull and Vatnajökull ice caps survived through much, if not all, the Holocene which is in contrast to the model of Björnsson (1979) but echoes Dugmore's (1989a) results indicating long periods of Neoglaciation around Eyjafjallajökull and Mýrdalsjökull. Björnsson proposed that after the last Termination all of the major glaciers in Iceland disappeared for a long period (between ca. 10.000 and 2500 BP years) of the climatic optimum except for small ice caps restricted to the highest mountains. Thus the present ice cap configuration was not established again until about 2500 BP during a climatic deterioration. This scenario appears unlikely given the evidence presented here of a long period of Neoglaciation beginning sometime after the deposition of the Hekla-Ö tephra dated at ca. 6000 BP. Furthermore, the presence of an early Preboreal still-stand or readvance around 9700 BP (Ingólfsson and Norddahl, 1994) narrows the proposed hypsothermal period to a maximum of 3000 years, i.e. 9800 to 6000 BP. According to modelling experiments of ice mass accumulation elsewhere (e.g. Payne and Sugden, 1990) the process of regional ice cap formation takes about 10^3 years which is inconsistent with glacier disappearance and reformation during the 3000 years of "warm" climate (Gudmundsson, 1997). It has to be considered very unlikely that the major ice caps vanished although they might have been dramatically smaller during "warmer" climatic periods.

The Medieval and the early 18th Century glacier advance has not been reported in Iceland so far. The implications are important for the climatic history of the LIA and especially the question of when it began. According to Grove and Switsur (1994) the Medieval Warm Period was a global event occurring between about 900 and 1250

AD, possibly interrupted by a minor readvance of ice between about 1050 and 1150 AD. Since episodes of glacier advances have been identified elsewhere (Grove, 1988; Grove and Switsur, 1994) these events should be present in a climatically sensitive region like Iceland.

It has been puzzling that equivalent advances have not been formerly recognised in Iceland. The present work suggests that the LIA commenced ca. 1250 in Iceland and terminated ca. 1890 AD. This can be deduced from advances of Svínafellsjökull, Virkisjökull and Kviárjökull outlets in the 13th Century. However, this period was interrupted by warm spells in Iceland (Bergthórsson, 1969; Ogilvie, 1991, 1992) as well as in Europe (Grove, 1988) hinting at variability of ice growth and decay during the period between ca. 1250 and 1890 AD in Iceland.

6.2 Asymmetrical glacier extension

The extent of Holocene advances of the Öræfajökull ice cap shows significant regional variability. A different pattern of extension can be observed depending on the timing of fluctuations, location, and origin of the outlets (see chapter 5). This is especially pronounced during the mid-Holocene. Morsárjökull and Skaftafellsjökull (originating from the Vatnajökull ice cap) and Svínafellsjökull (from Öræfajökull) show comparatively limited extension. However, during the same climatic and chronological period (e.g. mid-Holocene), Virkisjökull, Kotárjökull and Kviárjökull which originate in the Öræfajökull caldera, advanced farther onto the sandur plain. The difference is in some cases 1 - 2 km (Table 6.1).

Several factors could explain the differential glacier fluctuations of the Öræfajökull and Vatnajökull ice cap, which will be discussed below. Anomalous glacier extents with similar timings have been reported by Dugmore and Sugden (1991) around Mýrdalsjökull and Eyjafjallajökull, south Iceland. They explained the pattern by ice divide migration where the catchment area is asymmetric and there is a strong regional precipitation gradient. In the case of Öræfajökull, it is unlikely that a single

factor is sufficient to explain the pattern, but rather a combination of factors are most probably involved.

The main precipitation source is from the south east which results in a rain shadow west of the mountain. Measurements show that precipitation at Kvísker, east of rhe Kviárjökull outlet, is 3300 mm per year. At Fagurhólsmýri, south of Öræfajökull, the precipitation is 1800 mm per year and in Skaftafell, east of the ice cap, the mean annual precipitation is about 1500 mm (Icelandic Meteorological Office, pers. com.) (Fig. 6.1). Assuming that the Equilibrium Line Altitudes (ELA) are approximately equivalent to the regional snow line of 1100 m, the Accumulation Area Ratios (AAR) of all of the outlets studied show that between 60% and 70% of the total area belongs to the accumulation zone (see chapter 3). It is probable that this ratio has not changed dramatically during the ice cap growth and decay in the Holocene (Björnsson, 1979). Thus the more restrictive advances of Morsárjökull, Skaftafellsjökull and Svínafellsjökull could simply be related more to precipitation variations rather than temperature fluctuations alone. This would be in concordance with a recent study of Mackintosh *et al.* (in press) interpreting the recent fluctuation pattern of Sólheimajökull as a dynamic response to changing mass balance and climatic change rather than to ice divide migration.

One of the key factors controlling the extent of the outlet glaciers studied is topography and glacier shape. The subglacial topography causes big ice-falls to form where the ice flows out of the Öræfajökull caldera (Fig. 6.2). The ELA of some of the outlets is located close to the top of an ice-fall that is generally narrower than other sectors of the accumulation area. These ice-falls typically have a larger altitude range than Holocene ELA changes caused by climate. Hence the vertical migration of the ELA has usually taken place within a short horizontal distance. This topographic effect will moderate fluctuations of the glacier front by limiting mass balance changes caused by a falling ELA (Furbish and Andrews, 1984; Kerr, 1993; Paterson, 1994). This can be demonstrated by looking at the hypsometric curves for each of the outlets studied and comparing them (Furbish and Andrews, 1984)(Fig. 6.3). The outlet

glaciers which advance least (Svínafellsjökull and Morsárjökull) seem to exhibit a U-shaped hypsometric curve. These are outlets where the ELA is located very close to the top of a steep, narrow ice-fall. This is very clear in the case of Svínafellsjökull which shows the most restricted advances during the Holocene of all of the outlet glaciers studied. On the other hand, Virkisjökull and Kotárjökull do not have a U-shaped hypsometric curve and their response to a falling ELA is more pronounced, as can be seen from the moraine record. Other glaciers like Skaftafellsjökull and Kviárjökull show similar shaped but more subdued hypsometric curves as Svínafellsjökull (Fig. 6.3). In these cases there is a less pronounced topographic effect.

6.3 Moraine formation

The contrasts in the size and continuity of the moraine record in front of various outlets of Öræfajökull and Vatnajökull ice caps at different times in the Holocene suggests a change in the glaciological processes of the ice (Tables 3.1-6). The most recent work on the geomorphological interaction with processes in terms of glacial geomorphology has been reported by Spedding (1997). He explores the influence that glacial meltwater exerts on styles of ice-marginal sedimentation, using past and present examples from Sólheimajökull, Gígjökull and Steinholtsjökull, south Iceland. The principal argument is that meltwater controls ice-marginal sedimentation. This involves two basic themes. One is that an aggressive subglacial drainage network captures and evacuates the bulk of debris generated by erosion by flushing it onto the sandur plain. This produces small moraines. The second case is where there is an overdeepened basin near the glacier snout. In this case, englacial debris bands are preserved because the meltwater takes up a new englacial route due to higher water pressures in the overdeepened basin. The debris carried up in these englacial channels is swiftly abandoned within the ice because of the rapid channel switching within the englacial drainage network. These debris bands, combined with basal ice that has not been "flushed" clean of debris by basal meltwater, are carried to the ice margin under the influence of a strong compressive terminal flow regime. This debris supply results

in the formation of big overlapping moraine ridges that can produce large moraine complexes.

The moraine record of the Öræfajökull and Vatnajökull ice caps can be used to further explore the ideas of Spedding (1997). These moraines satisfy all major conditions of the model, firstly being formed by a temperate glacier in a maritime climate, and secondly showing geometric contrasts within the same glacier foreland. Thirdly, the moraine sequences are temporally distinct. The moraine record of two outlet glaciers of Öræfajökull ice cap are of special interest, namely Svínafellsjökull and Kviárjökull. The moraine record in front of these glaciers show contrasts on a larger scale compared with other outlets studied.

The moraine record in front of Svínafellsjökull has been interpreted to show historical advances commencing in the Medieval times and terminating in the late 19th century. During this time, the glacier advanced ca. 1 km onto the sandur plain and formed several different sizes of moraines. The largest crest (Stóralda no. 4) is much bigger compared with the subdued ridges in front of it. If the moraine record is interpreted according to the work of Spedding (1997) the implication is that the Svínafellsjökull outlet normally flushed out debris by meltwater because the meltwater was free to flow unhindered beneath the ice. Consequently, limited moraine formation took place. A big moraine (no. 4) began to form just prior to 1362 AD. This would suggest, according to Spedding's ideas (1997), that the subglacial drainage system changed just prior to this date. A basin could have formed under the snout area and basal meltwater could have been forced away from the bed. As a result Svínafellsjökull could have created a big moraine. Some 600 years later, it is still building big moraines. This would also suggest that the base of it is still overdeepened. One principal implication of the pattern of glacier fluctuations of Svínafellsjökull is that two factors could modify the ice extension. Firstly, the subglacial topography and secondly, changes in the sub- and englacial drainage system. The relative dominance of each factor may vary through time.

The Kviárjökull outlet is surrounded by a big moraine theatre (for further description see Chapter 3) which has been forming in repeated advances of the glacier since ca. 3200 BP. Conversely, smaller moraines can be found in front of the big moraine which, according to Spedding (1997), again suggests that a change in the ice geometry and subglacial drainage system occurred, in this case, around 3200 BP. This can be argued as a dominant process since the hypsometric curve of this glacier shows a subdued version of the U-shaped form, suggesting relative sensitivity to ELA variation. Recent ice radar investigations of Kviárjökull subglacial landscape revealed that the base is overdeepened close to the ice-fall (Spedding, pers. com.) creating the necessary snout conditions for big moraine formation. The big moraine in front of Kviárjökull has been developing over the last 3000 years BP in contrast to ca. 600 years in front of Svínafellsjökull. Therefore, the size of these moraines could reflect the age difference since the Stóralda moraine complex (ca. 45 m) is a smaller feature than the big moraine amphitheatre in front of Kviárjökull (70 - 100 m).

An additional factor in contrasting moraine size could be differences in ice marginal topography. It is clear from aerial photographs that a huge amount of avalanche material is carried onto Kviárjökull but the ratio between significant supra- (rockfall) and englacial (fluvial/basal ice) debris is unknown. Therefore, it could be argued that the size of the big moraine amphitheatre is not only due to a change in the drainage system but also an anomalously large input of supraglacial debris is carried down the glacier as a consequence of landslides and other avalanche debris.

The formation of a large moraine amphitheatre had an effect on the extension pattern of Kviárjökull, as it inhibited the extent of later glacier advances. Similar circumstances have been identified in the middle Canadian Rocky Mountains (Luckman and Osborn, 1979). As the debris in front of Kviárjökull began to pile up, forming a big composite moraine, it created a threshold point where the ice was pinned thus restricting a further advance. Consequently, as a response to cool and/or wetter climate the ice gets thicker thus piling up more material and therefore increasing the height of the threshold (moraine). If the climate deteriorates beyond

the capability of the big moraine (threshold) to retain the ice, it will flow over the crest where it is lowest. This happened around 1700 BP as indicated by the moraine loop located on the northern slope of Kambsmýrarkambur. Later (historical) advances have not been able to sustain an ice flow of this magnitude. The overall implication is that the Kviárjökull outlet should be considered an inhibited indicator of climate deterioration over the last 3000 years BP.

6.4 The climatic implications

The overall evidence indicates an identifiable relationship between climate and the fluctuations of outlet glaciers of the Öræfajökull ice cap. Climate change inferences can be made from calculations of the lowering of the ELA and comparisons of AAR. It is assumed that the present AAR is 1.7:1 (Björnsson, 1979) and the present ELA of south eastern Iceland is at ca. 1100 m a.s.l. The proglacial area of the Virkisjökull outlet shows the best terminal moraine record in Öræfi of the outermost Holocene advance. Other outlets do not have terminal geomorphological records with sufficient spatial detail to permit the precise calculations of the AAR for the outermost advance. The result of this calculation is that an ELA lowering of no more than 450 m is sufficient to sustain the outermost advance in front of Virkisjökull. Given a lapse rate of 0,6°C/100m (Einarsson, 1975) in moist air and constant precipitation, the mean annual temperature was between 2.1°C and 2.4°C colder compared with the present time during the mid-Holocene advance. A constant precipitation can be assumed since glacier in Iceland are dominantly temperature sensitive (Björnsson, 1979). This agrees with the results of Dugmore and Sugden (1991) of 2°C cooling and Einarsson (1961) of a temperature between 2°C and 3°C colder during bog (colder) periods in the Holocene. The mean annual cooling during the latter part of the 19th century in Iceland has been estimated about 1°C to 1.5°C colder than at present (cf. Bergthórsson, 1969). This means that the mean annual temperature in the colder periods in the latter part of Holocene were ca. 1.5°C to 2.4°C lower than at present. This would agree with the temperature estimations from the GISP2 indicating cooling of 1.8° during the winter months in the 14th century (Barlow *et al.*, 1997). Additionally, Rousseau *et al.* (1994) reconstructed February and August average

temperature in France according to terrestrial molluscs. The results indicate similar temperature fluctuations during the Holocene as indicated in this study. The colder periods were 2° - 3°C colder than at present and the coldest period was in the mid Holocene.

The catchment areas of Morsárjökull and Skaftafellsjökull lie within the Vatnajökull ice cap. The subglacial topography is not known. However, the simple geometry of the glacier surfaces of these two outlets would suggest that they are sensitive to climate change. This includes a wide flat accumulation area and a long narrow confined snout (Oerlemans, 1989). The surface of the glaciers indicates a gently inclining bed that has no significant undulations. This would suggest that Morsárjökull and Skaftafellsjökull are sensitive to climatic signals. Whether the climatic signal is modified can be assessed by simple calculations of the ELA variations and a comparison with the results of the Virkisjökull outlet. The ELA of Skaftafellsjökull was discerned using the same method as described above for Virkisjökull. An ELA lowering of roughly 400 m, as calculated for the Virkisjökull outlet, is sufficient to sustain the Miðheiði advance in front of Skaftafellsjökull based on the most likely terminal position during the advance. This supports the view of the proposed climatic sensitivity for the Öræfajökull outlets.

A wider importance for the glacier fluctuations record in Öræfi, lies in its implications for circulation pattern changes and the movements of the boundary between the warm and the cold ocean currents around Iceland. This is because the marine and atmospheric Polar fronts are located close to Iceland, where the North Atlantic Deep Water is formed (Aagaard and Carmack, 1989; Dickson *et al.*, 1996). Major changes in the position of the ocean Polar Front are known to have occurred in Greenland/Iceland/Norwegian Sea throughout the Holocene (Kroç, 1993). Furthermore, it has been suggested that freshwater fluxes from the Laurentide ice sheet had a significant effect on the North Atlantic circulation at the final stages of the deglaciation (ca. 8200 cal. BP) (Klitgaard-Kristensen *et al.*, 1998). As the big North American ice-sheet melted the freshwater input to the North Atlantic circulation was a

major factor in causing a 2°C temperature reduction in north west Europe (Klitgaard-Kristensen *et al.*, 1998). These results further underline the strong relationship between glaciers, oceans and climate. According to the pattern of glacier fluctuations discussed in this study, it is likely that the Polar Fronts migrated to a more southerly position at least four times in the latter part of the Holocene, compared with the current position. The dates of these events are likely to be ca. 5000 BP, ca. 3300 BP, ca. 1800 BP?, ca. 700 BP and ca. 80 BP. These changes are likely to have been part of more general global change. They could have resulted in a cooler maritime climate affecting Iceland and the intensity and frequency of storm tracks south of Iceland could have changed. One of the results could have been that more of the total precipitation fell as snow and the summer temperature was lower. This would greatly affect the high altitude glacier accumulation areas such as those of the Öræfajökull outlets where precipitation gradients are very high. Given a strong link to climate change in general and changes in north Atlantic circulation in particular, Icelandic glacier fluctuations should show a similar pattern to glaciers elsewhere in the northern Hemisphere in a similar location relative to the major global circulation patterns. This does seem to be the case as shown by comparisons in Fig. 6.7. This is particularly evident around 5000 and 3000 BP. However, this pattern is interesting in terms of the long-term stability of the Greenland ice core records. In general, the contrast between Iceland and Greenland might reflect the geographical differences of the two regions. Iceland is a maritime island greatly climatically influenced by the surrounding oceans and therefore the North Atlantic circulation. Conversely, Greenland is a continent generating a more stable, perhaps local climate more receptive to changes in the general atmospheric factors. It can consequently be suggested that Iceland is located in more climatically sensitive position, especially when studying short term climate change.

6.5 The Holocene Öræfajökull eruptions and pattern of glacier fluctuations

In Iceland, studies of how volcanic and geothermal activity influence ice behaviour have been conducted by Björnsson (1974; 1988) and Björnsson and Kristmannsdóttir (1984). They studied the highly active Grímsvötn volcanic area (Thórarinsson, 1974;

Jóhannesson, 1983, 1984) located under the western Vatnajökull ice cap. These studies include the effect of geothermal and volcanic activity upon jökulhlaups and upon the drainage of ice into the Grímsvötn subglacial lake. Furthermore, they have dealt with the influence of subglacial melting caused by geothermal activity and volcanic eruptions on the filling of the Grímsvötn caldera with meltwater. These events have affected ice dams, consequently inhibiting or triggering jökulhlaups onto Skeiðarársandur outwash plain in south (cf. Gudmundsson *et al.*, 1997). However, these studies do not comment on the relationship between volcanic eruptions and the pattern of glacier margin fluctuations. The literature on this relationship is scarce of studies. Kjartansson (1964) suggested, that during the wastage of the last inland ice sheet, volcanic activity in Iceland was enhanced due to the unloading of the ice mass. As an example, Kjartansson (1964) mentioned the huge eruption of Leggjabrjótur on Kjölur in the central highlands of Iceland. This eruption is thought to have contributed to the catastrophic floods occurring at the end of the last deglaciation that formed the impressive Hvítá canyons (Tómasson, 1993).

The history of glacier fluctuations and volcanic activity of the Öræfajökull ice cap offers a unique opportunity to study the relationship between "ice and fire". The ice cap fills a well-constrained caldera and the present study has revealed the pattern of fluctuations of key outlet glaciers originating within the caldera. Additionally, the volcanic eruptions occurring in the Holocene have been dated with tephrochronology. Table 6.2 shows the tephra layers traced to Öræfajökull eruptions compared with glacier advances deduced from the moraine record around the ice cap. A strong association can be inferred as can be seen on Fig. 6.4. showing the simple regression calculations of the relationship. According to the statistical calculation, the r-squared value (r^2) is +0,99 under the 95% significance level indicating a very strong positive correlation. In statistical terms this means that 99% of the observed variation in the volcanic eruptions can be "explained" by variation in the pattern of glacier fluctuations. Table 6.2. shows that the eruptions generally lag behind the glacier retreat. The mean lag time is ca. 330 BP years during the prehistoric time except in

the LIA. It is possible that the 1727 eruption was a somewhat delayed response to medieval ice loading rather than an anticipation of later events.

As a result, there is a strong possibility that the volcanic history of the Öræfajökull ice cap may have a close relationship to climatic change since the last Termination. As the climate deteriorates, ice accumulates in the caldera increasing the local glacial load on the underlying crust. This would increase the pressure on the underlying magma chamber depending on the viscosity and to a lesser extent, the thickness of the overlying crust. As the ice melts in the caldera the pressure on the crust, and therefore the magma chamber, is reduced. During this uplift, magma is likely to escape to the surface as a consequence of pressure release thus causing a volcanic eruption. The pathway of the magma to the surface (base of the ice) is likely to be newly formed or older active fissures and fractures in the crust as it is reaching a new equilibrium with the overlying ice. These kind of glacio-isostatic linkage are known in Iceland and have been measured south east of the Vatnajökull ice cap as a consequence of glacier growth and decay. The results indicate a rapid isostatic uplift of several mm per year (Sigmundsson and Einarsson, 1992, Einarsson, *et al.*, 1994). The mean lag between the maximum glacier advance and a subsequent eruption can be inferred as the minimum dynamic recovery time of the crustal uplift after each major glacier advance. This would mean that a dynamic stabilisation between local crustal movement and the ice load is reached minimally ca. 330 BP years after each major glacier advance.

The alternative explanation would be that the volcanic activity follows an eruption cycle primarily driven by mantle processes. This would mean that the correlation between glacier advances and volcanic eruption is coincidental. In a tectonic setting like Iceland volcanoes will erupt sooner or later but the final trigger, however, may be external rather than internal.

If the strong relationship between the volcanic eruptions and glacier fluctuations is accepted, the results would indicate that the volcanic activity in Iceland is greatly

influenced by glacial activity and hence by climatic change. All the ice caps in the Neovolcanic zone (Mýrdalsjökull, Eyjafjallajökull, Tungnafellsjökull, Torfajökull, Hofsjökull, Langjökull and the western part of Vatnajökull) lie over volcanic systems. The crust under these ice caps is thin and has high viscosity (Sigmundsson, 1990). This would imply that major changes in the mass balance of these ice caps could result in pressure changes and alterations of the underlying magma chamber conditions that could trigger eruptions. The implications are important. A warmer climate due to the release of greenhouse gases could affect the mass balance of ice caps in Iceland. Predictions indicate that for example two of the outlets of Hofsjökull, an ice cap in west central Iceland, will disappear within the next 200 years (Jóhannesson, 1997). Applying similar predictions to the glaciers within the Neovolcanic zone would suggest an increased frequency of eruptions of glaciated volcanoes within the same area. This would greatly affect the population of Iceland as most of the hydroelectric power plants are located within the Neovolcanic zone and harness glacial meltwater. Volcanic eruptions could damage the reservoirs and the hydroelectric plants resulting in major economic costs.

6.6 Glacio-isostatic crustal movements caused by Neoglacial ice volume change

The study of glacio-isostatic crustal movements in recent times in Iceland was pioneered by Sigmundsson (1990) followed by two publications on the influence of the ice volume change of the Vatnajökull ice cap in historical times (Sigmundsson and Einarsson, 1992; Einarsson *et al.*, 1994). The results imply that the reduction in ice volume following the LIA caused a rebound of ca. 1 m at the glacier termini. The volume of the Vatnajökull ice cap is assumed to have decreased by 180 km^3 in this century (Einarsson *et al.*, 1994). This indicates a crustal uplift in the area around the glacier at a rate of 2 cm/year after 50 years. A 10 km thick elastic crust and $1x10^{19}$ Pa s sub-crustal viscosity is assumed. Furthermore, the marine transgression in south east Iceland in historical times is anomalously rapid. Based on the tephra from the 1362 eruption of Öræfajökull found within submarine freshwater peat in Ósland, south east Iceland, the relative sea level rise has been estimated as ≥3 m between 1362 and 1951 (≥5 mm/year). Sigmundsson and Einarsson (1992) have estimated that the

unexplained rate of relative sea level change in Ósland is ≥2.65 mm/year, cumulating to ≥ 1.6 m in the last 600 years which in turn can be explained by unloading of ice.

The fluctuations of Icelandic glaciers before the LIA would have also had crustal effects. In the calculations introduced above, a mean glacier advance of ca. 1000 m is always used for the LIA. It has been calculated that a small increase in ice radius results in a big volume increase, for example an advance of 50 m means that the volume would increase by 10 km^3 (Sigmundsson, 1990). Let's assume a mean (Neoglacial) advance of the Vatnajökull ice cap of 2000 m (which according to field evidence in Öræfi would be a conservative estimate) thus increasing the radius from 52320 m (1990) to 54320 m (mid-Holocene?). This would mean that the volume of the Vatnajökull ice cap would increase by 412 km^3. Consequently, we could probably expect an uplift of ca. 2 m at the glacier termini in the first 50 years after instantaneous removal of the load. This is assuming that the removed LIA load was 182 km^3 (Sigmundsson, 1990) and therefore the mid-Holocene (?) load was roughly twice as big. The implications for local sea transgressions caused by the loading during these advances could be significant, perhaps in the order of 2 - 6 m, or even more on the south eastern coast during the maximum advance/subsidence. This would mean that some of the south eastern outlet glaciers of the Vatnajökull ice cap might have experienced rapid reworking of sediment in a high-energy marine (shoreline) environment. Perhaps this is the key factor in explaining the lack of a terminal moraine record in front of the LIA advances, for example, in front of Breiðamerkurjökull. Recent studies of Holocene strandlines containing seashells in Hrútafjörður, north Iceland, suggests a sea level rise of 3.5 m compared with the present. The highest strandline was dated to around 5000 BP. By 3000 BP the sea level fell rapidly and progressively formed the present shoreline. This is explained by climatic deterioration and consequent ice growth after 5000 BP, especially post 3000 BP (Eiríksson *et al.*, 1998a). This is in reasonable accordance with the calculated sea level fluctuations presented above for south east Iceland, ranging from 2 - 6 m a.p.s.l. and the history of glacier fluctuations in Öræfi. The implication is that a sea transgression is likely to have followed each principal glacier advance of the Öræfajökull ice cap at or around 5000 BP, ca. 3300 BP, 700 BP and ca. 80 BP.

Part II Summary and conclusions

6.7 Pattern of glacier fluctuations

The geomorphology of the Öræfi district contains glacial and volcanic data. The glacial geomorphology indicates a history of glacial fluctuations covering at least the last 10.000 years BP and including at least eight advances. The oldest glacial evidence can be found on Svínafellsheidi indicating ice flow to the south west from the summit of Öræfajökull ice cap. The first advance in the Holocene is thought to have occurred around 9700 BP and is found in front of Skaftafellsjökull, Svínafellsjökull and in the Kviárjökull stratigraphical succession. The record for the succeeding 3000 years BP shows no indications of glacier fluctuations although they cannot be ruled out. Advances occurring between 9000 BP and 6000 BP could be hidden inside the limits of subsequent advances.

The onset of the Neoglaciation is assumed to have taken place around 5000 BP with a major advance of all of the outlets extending up to ca. 3 km onto the sandur plain. Smaller advances culminated ca. 3200 BP, 1700 BP, 700 BP, 200 BP and 70 BP. The two latest advances are taken to represent the LIA, thus indicating the onset of this cold period in the Medieval times. This Medieval advance extended to a similar position as the 70 BP advance which is usually referred to as the maximum position of the Icelandic glaciers in the historical time.

Different glaciers in the study area show a different pattern of extension. This can be explained by ice gradients, precipitation pattern, different accumulation area ratios, different glaciological processes and the role of topographic thresholds such as moraines. Despite such local effects, the outlet glaciers are still good indicators of climatic change and temperature oscillations can be deduced from the pattern of glacier fluctuations. It is inferred that the mean annual temperature, responsible for the onset of the Neoglaciation, was no more than 2.4°C lower than at present. These calculations assume a similar precipitation pattern. This agrees with other temperature estimates for the onset of the Neoglaciation in Iceland.

The glacier fluctuations of the Öræfajökull ice cap (Fig. 6.5, 6.6) are in reasonable accord with Icelandic glacial histories (Dugmore, 1987; Häberle, 1991; Stötter, 1991; Gudmundsson, 1992; 1997; in press; Gudmundsson and Norddahl, in press; Rose *et al.*, 1997). According to Eiríksson *et al.*, (1998b,c,d) and Knudsen *et al.*, (1998), recent biostratigraphical studies of deep sea sediment cores at Eyjafjarðaráll and Skjálfandadjúp on the north Icelandic shelf, indicate cold periods about 5000 BP and 3000 BP. This is also in concordance with recent studies of late Holocene strandline fluctuations in Hrútafjörður, north Iceland (Eiríksson, *et al.*, 1998a). If Iceland is compared with other glaciated areas of the world, some similarities can be inferred especially with that of Scandinavia and the European Alps (Osborn and Luckman, 1988; Davis, 1988; Calkin, 1988; Clapperton and Sugden, 1988; Karlén, 1988; Gellatly *et al.*, 1988, Hjort, *et al.*, 1997: Fig. 6.7). Correlation, however, can only be speculative at this stage. Nevertheless, the onset of Neoglaciation seems to occur globally around 5000 BP and glacial activity is generally more pronounced in the latter part of the Holocene compared with the former part. This would suggest a major global climatic change around mid-Holocene. One of the reasons for this might be a change in the thermohaline circulation system which is thought to be partly controlled by the ocean areas adjacent to Iceland (Broecker and Denton, 1989).

6.8 The tephrochronology of the Öræfi district

The tephrochronology of the Öræfi district and the related volcanic history of the Öræfajökull stratovolcano is complex. In a total of about 90 profiles, 22 silicic tephras were identified. Three of these tephras are dated to the historical times (post 900 AD) but the majority are dated to the latter part of the Holocene. All of these tephras are identified in the Öræfi district for the first time except the tephras deposited by the Öræfajökull eruption in 1362 AD (Thórarinsson, 1958). These include Hekla-Ö, Hekla-4, Hekla-S, Hekla-1 and Hekla-1389(?). Basaltic tephras located in Öræfi for the first time include Vö ca. 900 AD, G1619, K1625 and G1783.

The prehistoric eruptions of Öræfajökull identified for the first time include at least five eruptions. These eruptions were dated to BP 1540±50, 1940±30(?), 2860±160,

ca 4700, ca. 6700(?) and ca. 9200. Other tephras identified in Iceland for the first time include a simultaneous eruptions of Askja and Torfajökull at ca. 2100 BP. In addition, some tephras could not be traced with precision to any known volcanic system in Iceland, but chemical trends would suggest source in either the Öræfajökull or Askja volcanic systems.

Tephrochronology in the Öræfi district has a number of fundamental stratigraphic and geochemical limitations. These include the preservation of tephras pre-4000 BP, environmental activity that destroys the sedimentary record and the limitations in the use of geochemistry to correlate between tephras and volcanic systems.

A close relationship occurs between the pattern of glacier fluctuations and volcanic eruptions of the Öræfajökull ice cap. At a significance level of 95%, the correlation coefficient between these two factors is calculated +99%. The volcanic eruptions lag on average 330 years behind the glacier advances, suggesting that a small volcanic eruption occurs at the end of the period when the earth's crust reaches an equilibrium with the overlying glacier. This is the first time that this pattern is identified with a high degree of statistical significance and the implications are profound for both the glacier and volcanic history of Iceland. Other isostatic effects of glacier growth and decay suggest that some of the southern outlets of Vatnajökull ice cap might have calved into the sea during the latter part of the Holocene as a result of crustal loading by ice.

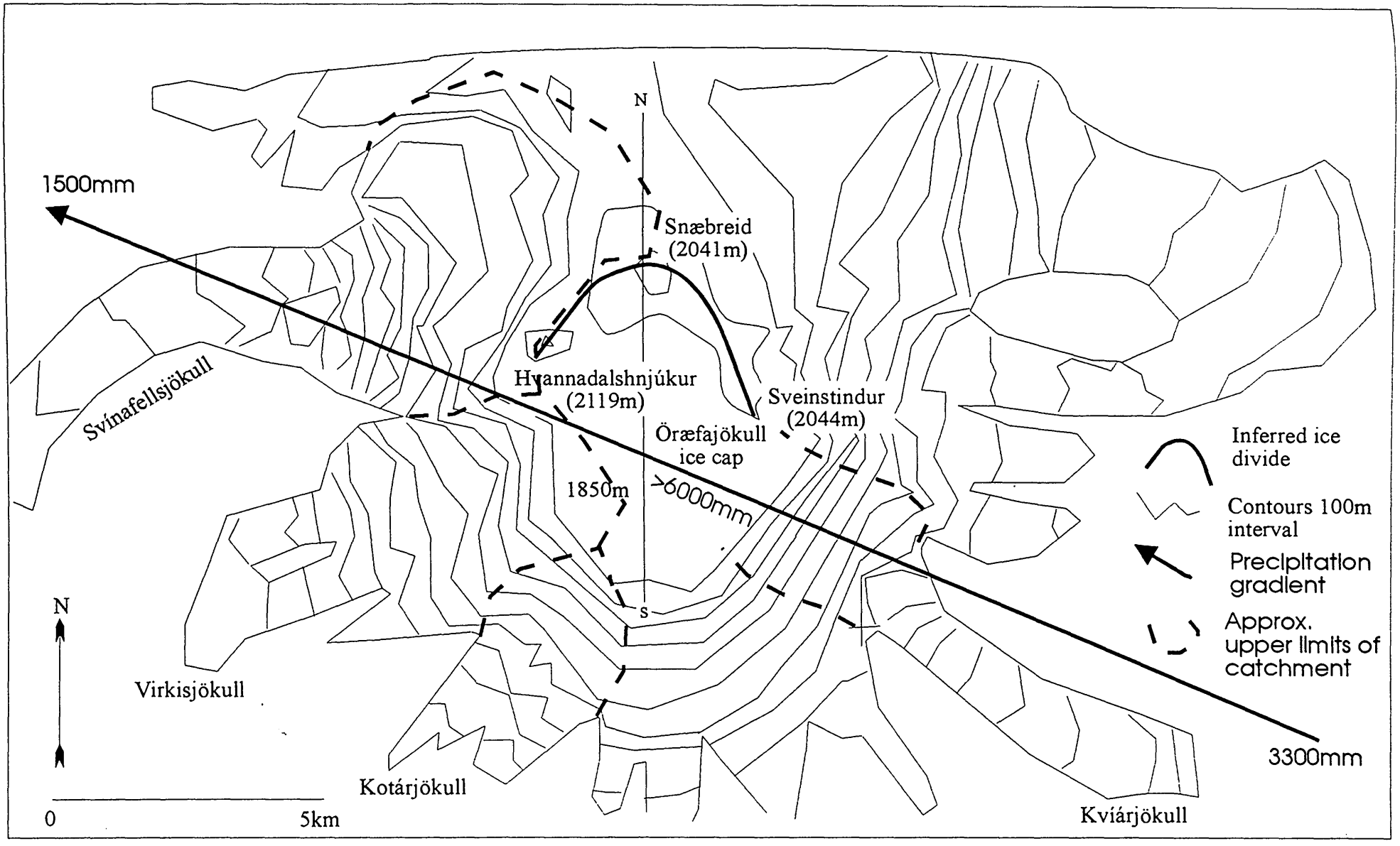

Fig. 6.1. Ice divides and the direction of the ppt. gradient of the Öræfajökull ice cap. The line marked N-S is the radio-echo sounding profile on Fig. 6.2 based on Björnsson (1988). The diagram shows the high ppt. gradient in the area.

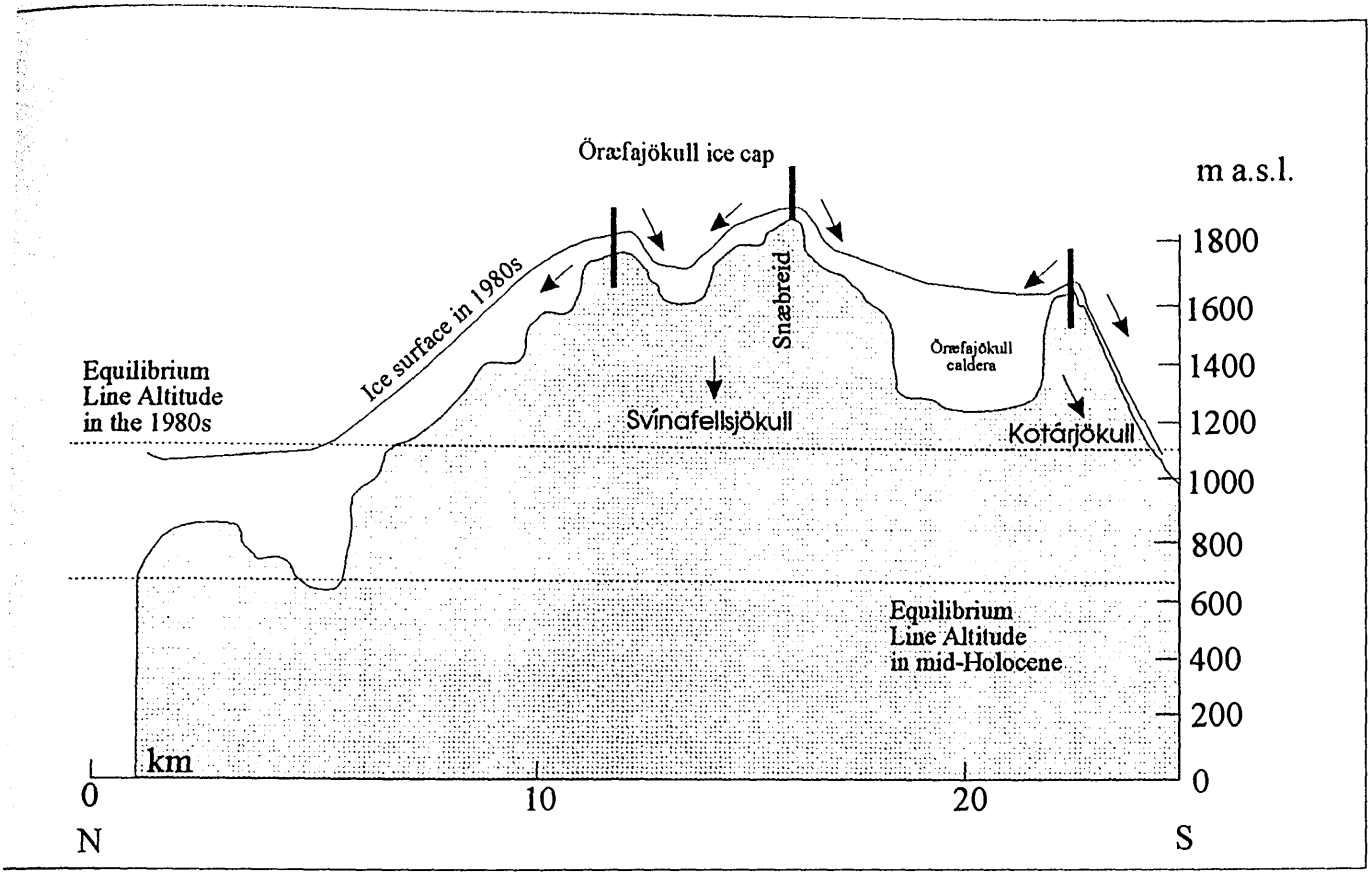

Fig. 6.2. Ice thickness and subglacier topography of the Öræfajökull ice cap. The maximum ice thickness inside the caldera is 500 m. The caldera rim is likely to affect the ice flow. Based on radio-echo soundings from Björnsson (1988).

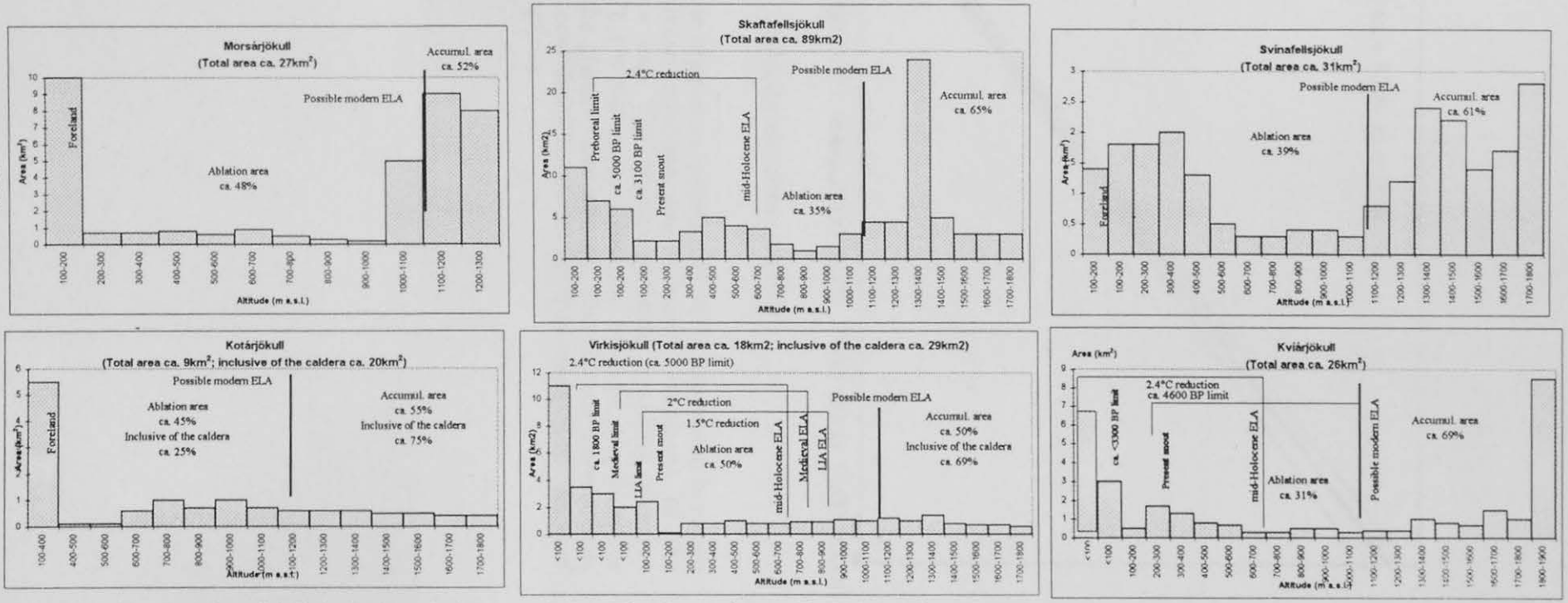

Fig. 6.3. Hypsometry of the outlet glaciers studied. Glaciers showing restricted advances tend to have U-shaped hypsometric curves. The ELA is always located close to the ELA, estimated at ca. 1100m (Björnsson, 1979). The caldera of Öræfajökull is likely to be a part of the accumulation area of Virkisjökull, Kotárjökull and Kviárjökull. Glaciers showing U-shaped hypsometric curves are displaying inhibited sensitivity to tepmerature change, for example Svínafellsjökull. On the other hand, glacier with a 'flat' hypsometric curve are very sensitive to temperature change, for example Virkisjökull.

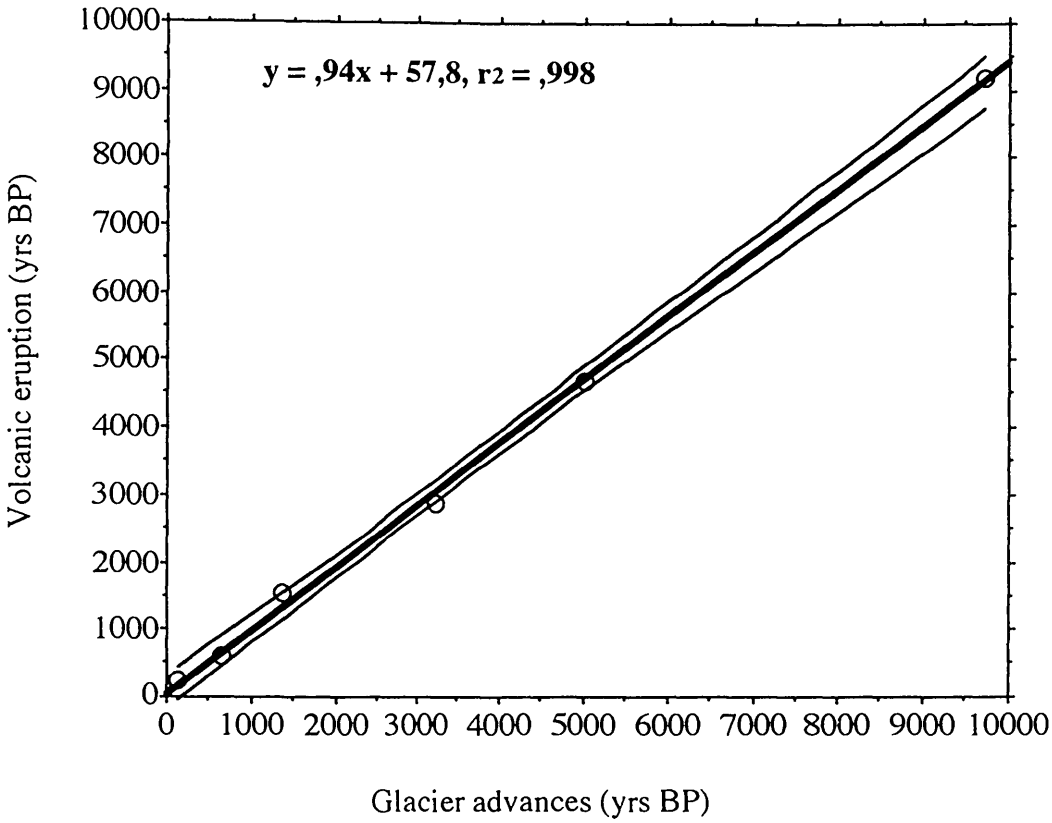

Fig. 6.4. Simple regression statistics of the relationship between culminating glacier advance and volcanic eruptions of the Öræfajökull ice cap. The results indicate a strong positive relationship. This would suggest that the volcanic eruptions are dependent on the glacier fluctuations. The thinner curved lines depict the 95% confidence bands for the true mean of the dates of the volcanic eruptions.

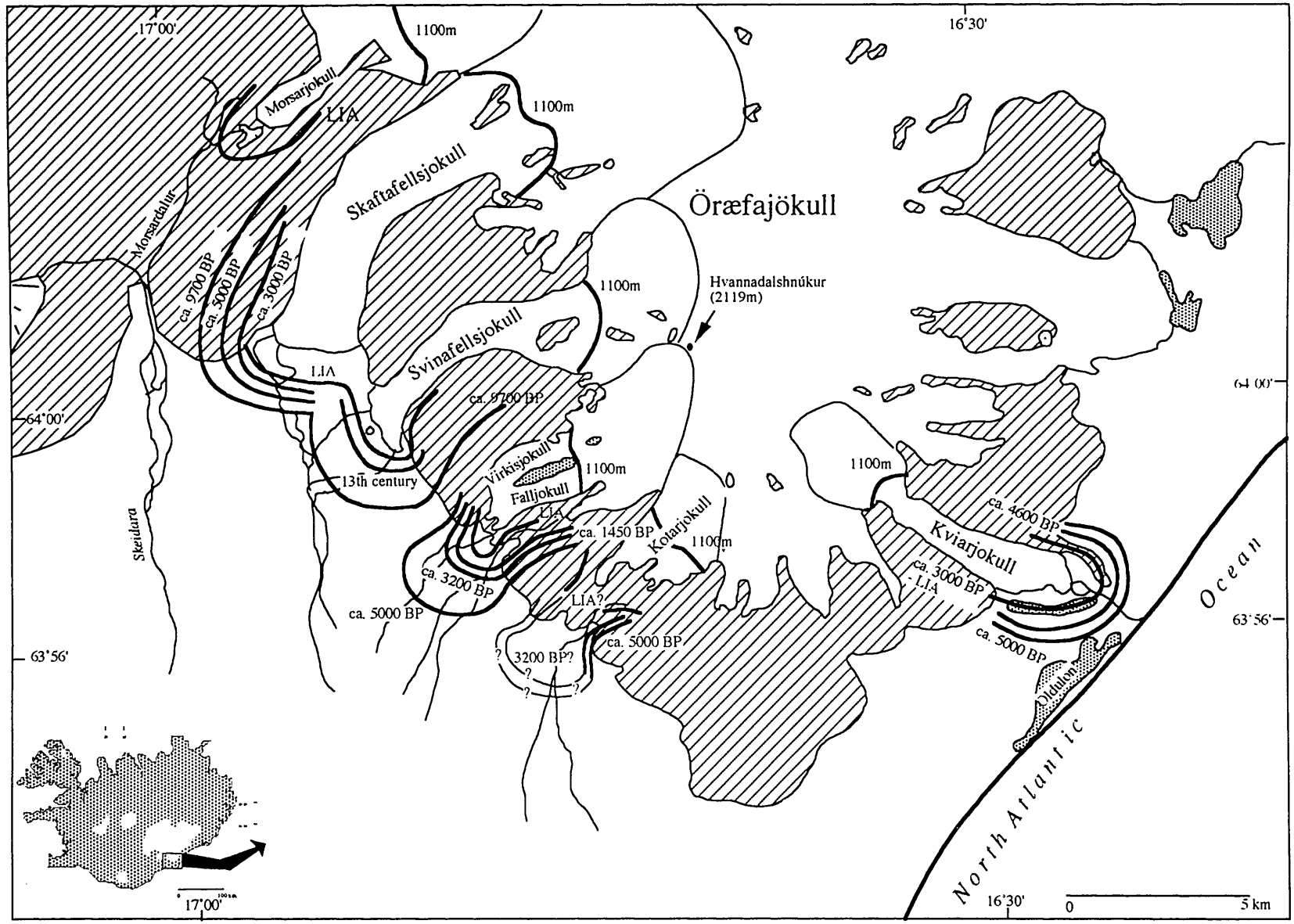

Fig. 6.5. Spatial pattern of the glacier fluctuations in the Öræfi district. Hatched lines mark the area above 100m a.s.l. Thin black lines on the ice cap indicate the catchment areas of individual outlets. Note the different spatial and temporal pattern of glacier fluctuations. This can be explained by local ppt. patterns, contrasting topography and change in glacier process. Unnamed glaciers not studied: pattern yet to be established.

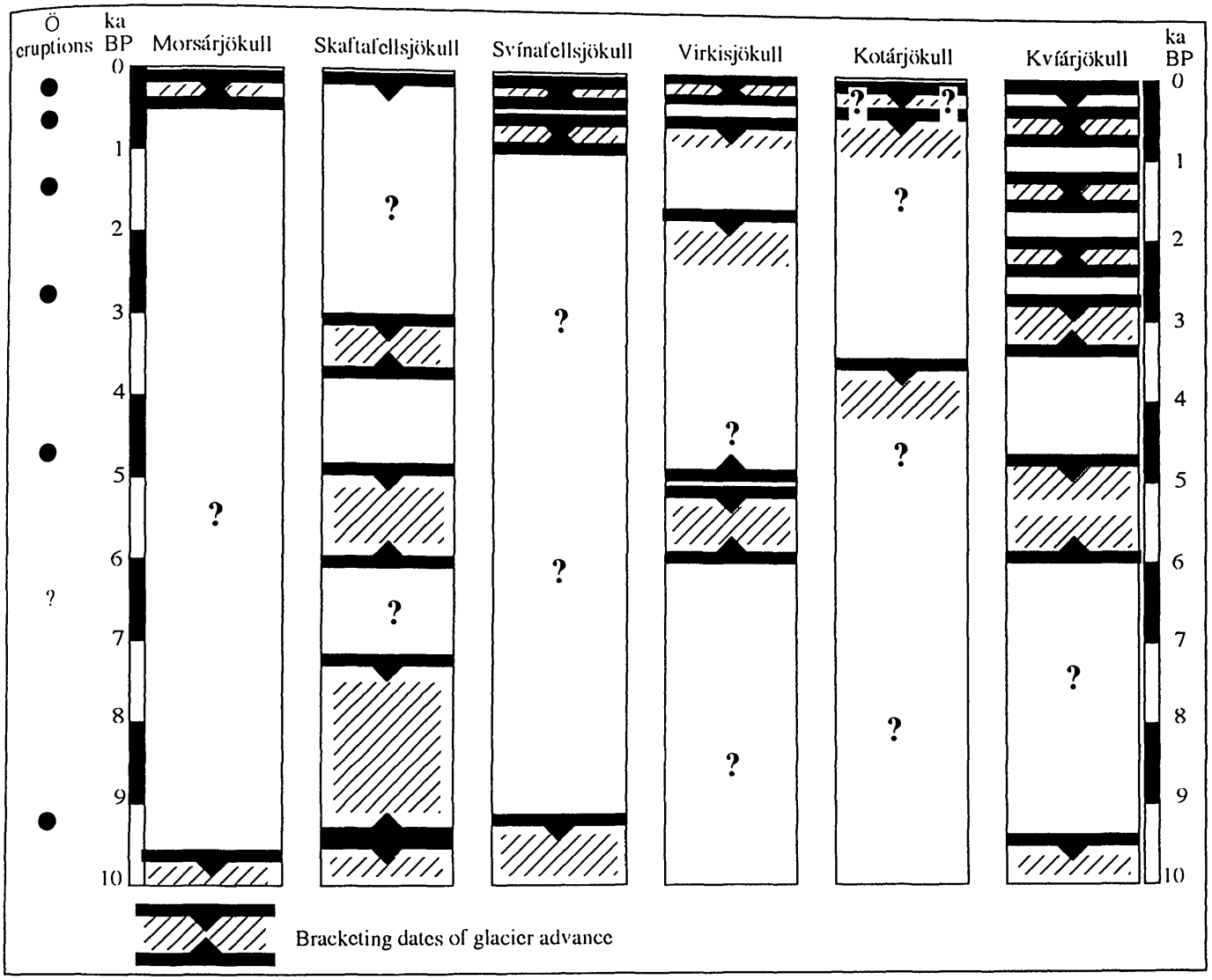

Fig. 6.6. Synthesis of glacier fluctuations of the Öræfajökull ice cap. The pattern indicates high glacier activity over the last ca. 5000 BP years. Öræfajökull eruptions are shown as solid black dots. Note the relationship between glacier advances and volcanic activity. The temporal pattern of glacier fluctuations is relatively consistent indicating climate change as the general cause for enhanced glacier activity. For precise dating, see table 5.1.

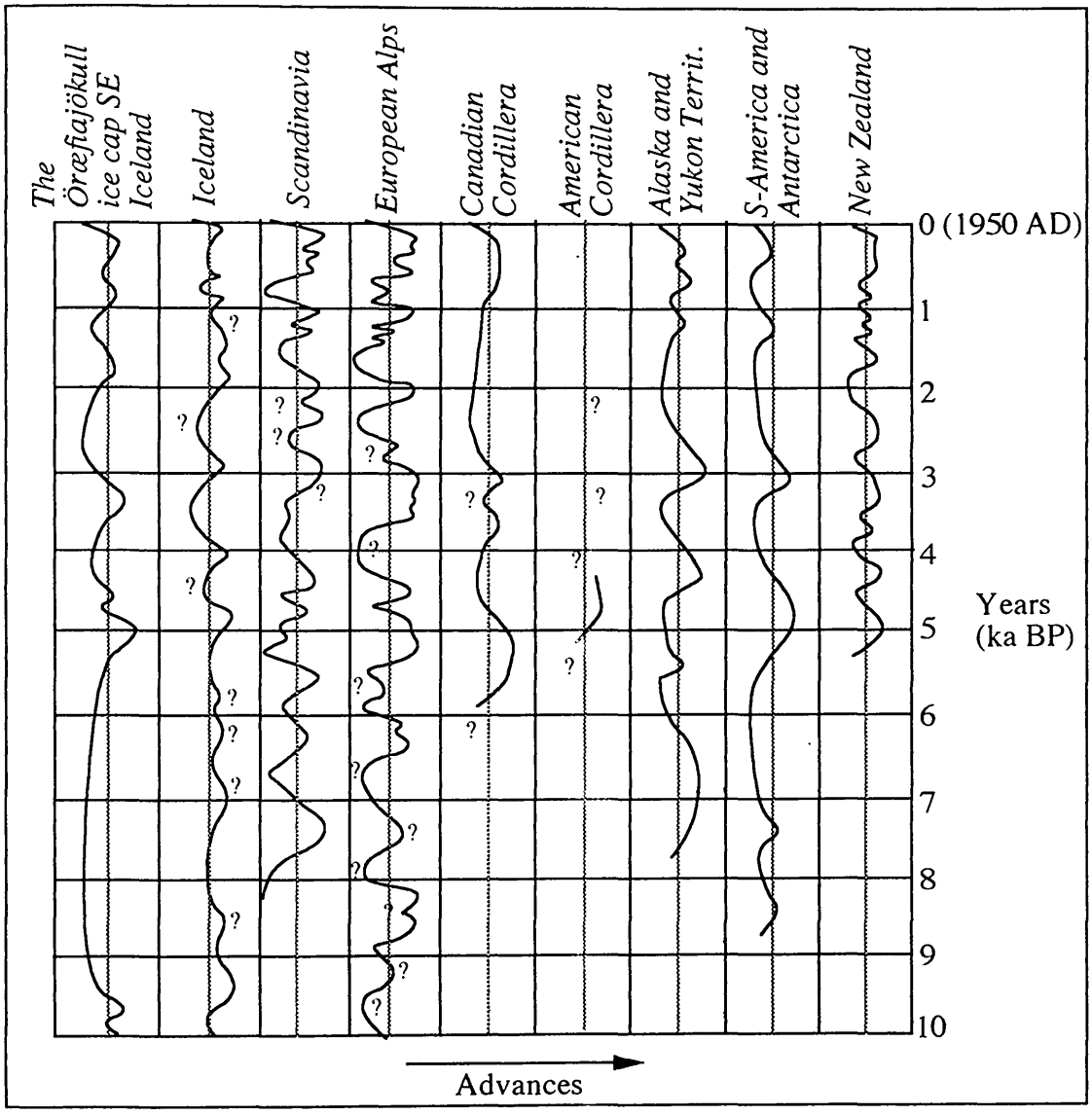

Fig. 6.7. The general pattern of Holocene glacier fluctuations of selected locations in the world compared with the Öræfajökull ice cap. Patterns show similarites but absolute correlations between sites can only be speculated. However, generally the Neoglaciation seems to occur around 5000 years BP. From Gudmundsson (1997), Hjort *et al.* (1997) and various papers in a special issue of *Quaternary Science Reviews*, Vol. 7, 1988 on Holocene glacier fluctuations.

Outlet glacier	Preboreal	6000-4600 BP	3200 BP	1800-1700 BP	700 BP	"LIA"
Skeiðarárjökull	2.5 km	n/a	n/a	n/a	n/a	n/a
Morsárjökull	n/a	<1.5 km	<1.5 km?	<1.5 km?	<1.5 km?	1.5 km
Skaftafellsjökull	3.0 km*	2.0 km*	1.8 km*	n/a	n/a	1.5 km
Svínafellsjökull	2.0 km*	<1.0 km?	<1.0 km?	<1.0 km?	1.0 km	0.7 km
Virkisjökull	n/a	3.0 km	n/a	1.2 km	0.9 km	0.5 km
Kotárjökull	n/a	3.0 km	n/a	n/a	n/a	0.7-1.5 km
Kviárjökull	n/a	2.5-3.0 km?	1.2 km	1.2 km	1.2 km	1.0 km

*An estimate according to the curvature of lateral moraines.

Table 6.1. Terminus extension of the outlet glaciers studied. The 1990 position of each snout is used as a reference. Note the different pattern of extension during the mid-Holocene advance. Overall, the table shows the great temporal and spatial variability of the glacier fluctuations of the outlet glaciers studied.

Tephra indicating eruption	Date of eruption	Er. prob.*	Glacial advances	Culmination of advances	Lead**	Lag**
Ö1727	1727AD	xxx	Stóralda/Freysnes, LIA maximum	1727AD - 1890AD	30-150 yrs	
Ö1362	1362AD	xxx	Stóralda/Breiðatorfa, Kvíárjökull IIIc, Virkisj. II	1200s AD		ca. 100 yrs
Skaftafellsheiði	1540±50 BP	xxx	Virkisjökull II, Kvíárjökull IIIb	ca. 1700 BP		ca. 200 yrs BP
Miðheiði	2860±160 BP	xxx	Austurheiði, Kotárjökull II?, Kvíárjökull IIIa	ca. 3200 BP		ca. 340 yrs BP
"Mid-Holocene"	ca. 4700 BP	xx	Miðheiði, Virkisjökull I, Kotárjökull I? Kvíárjökull I and II	ca. 5000 BP		ca. 300 yrs BP
"Early Holocene"	ca. 9200 BP	x	Skeiðarárjökull, Gimludalur/Vesturheiði, Skerhóll, Kvíárjökull	ca. 9700 BP		ca. 500 yrs BP

x Likely, xx Very likely, xxx Took place

** The time interval between culmination of glacier advance and eruption

Table 6.2. Comparison of volcanic eruptions and glacier fluctuations of the Öræfajökull ice cap, SE Iceland. The pattern indicates a strong relationship between the two where volcanic eruptions seem to lag behind glacial advances.

Reference list

A

Aagaard, K. and Carmack, E.C. (1989). The role of sea ice and other fresh water in the Arctic circulation, *Journal of Geophysical Research* **94**, 14485 - 14498.

Ahlmann, W.H. and Thórarinsson, S. (1937). Vatnajökull. Scientific Results of the Swedish - Icelandic Investigations, 1936, 37, 38, *Geogr. Annaler*, **19**:146 - 231, **20**:171 - 233, **21**:39 - 66, 171 - 242, **22**:188 - 205, **25**:1 - 54.

Albertsson, K. (1976). K/Ar ages of Pliocene-Pleistocene glaciation in Iceland with special reference to the Tjörnes sequence, Northern Iceland, Unpubl. PhD-thesis, University of Cambridge, 268p.

Arnalds, Ó. (1990). Characterisation and erosion of Andisols in Iceland, Unpubl. PhD-thesis, Texas A&M University, 179p.

B

Barlow, L.K., Sadler, J.P., Ogilvie, A.E.J., Buckland, P.C., Amorosi, T., Ingimundarson, J.H., Skidmore, P., Dugmore, A.J. and McGovern, T.H. (1997). Interdisciplinary Investigations of the end of the Norse Western Settlement in Greenland, *The Holocene* **7(4)**, 489 - 501.

Bentley, M. (1996). Moraines in the Chilean Lake District: form, process and chronology. Unpubl. PhD thesis, University of Edinburgh.

Bergthórsson, P. (1969). An estimate of ice drift temperature in Iceland in 1000 years, *Jökull*, **19**, 94 - 101.

Björck, S., Kramer, B. Johnsen, S., Bennike, O., Hammerlund, D., Lemdahl, G., Pessnert, G., Rassmusen, T.H., Wohlfarth, B., Hammer, C.U. and Spark, M. (1996). Synchronised terrestrial atmospheric deglacial records around the North Atlantic, *Science*, **274(5290)**, 1155 - 1160.

Björnsson, H. (1974). Explanations of Jökulhlaups from Grímsvötn, Vatnajökull, Iceland, *Jökull*, **24**, 1-26.

Björnsson, H. (1979). Glaciers in Iceland, *Jökull*, **29**, 74 - 80.

Björnsson, H. (1988). Hydrology of Ice Caps in Volcanic Regions. *Societas Scientarium Islandica* **XLV**. Reykjavík. Prentsmiðjan Oddi, 139p.

Björnsson, S. (1993). Hvað gerðist við Kviárjökul í lok ísaldar, *Náttúrufræðingurinn*, **62(1-2)**, 21 - 34.

Björnsson, H. and Kristmannsdóttir, H. (1984). The Grímsvötn geothermal reservoirs. *In*: Bear, J. and Corapcioglu, M.Y. (eds.). *Advances in transport phenomena in porous media*. Dortrecht, Martinus Nijhoff, 145-183.

Black, T.A. (1990). The Holocene Fluctuations of the Kviárjökull Glacier, South eastern Iceland. Unpubl. M.Sc-thesis, University of Colorado. 90p.

Broecker, W.S. and Denton, G.H. (1989). What drives glacial cycles? *Geochima et Cosmochima Acta*, **53(10)**, 2465-2510.

C

Calkin, P.E. (1988). Holocene glaciation of Alaska (and adjoining Yukon Territory, Canada), *Quaternary Science Reviews*, 7, 159-184.

Caseldine, C, and Baker, A. (1998). Frequency distribution of *Rhizocarbon geographicum* s.l., Modelling and climatic variation in Tröllaskagi, Northwest Iceland, *Arctic and Alpine Research*, **30(2)**, 175 - 183.

Clapperton, C.M. and Sugden, D.E. (1988). Holocene glacier fluctuations in south America and Antarctica, *Quaternary Science Reviews*, 7, 185-198.

D

Dansgaard, W., Johnsen, S.J., Clausen, H.B., Dahl-Jensen, D., Gundestrup, N.S., Hammer, C.U., Hvidberg, C.S, Stefensen, J.P., Sveinbjörnsdóttir, Á.E. Jouzel, J. and Bond, G. (1993). Evidence for general instability of past climate from a 250-kyr ice core record, *Nature*, **364**, 218 - 220.

Davis, P.T. (1988). Holocene glacier fluctuations in the American Cordillera, *Quaternary Science Reviews*, 7, 129-157.

Dickson, R., Lazier, J., Meincke, J. Rhines, P. and Swift, J. (1996). Long-term co-ordinated changes in the convective activity of the North Atlantic, *Progress in Oceanography* **38**, 241 - 295.

Douglas, T.D. and Harrison, S. (1996). Turf-banked Terraces in Öræfi, Southeast Iceland: Morphometry, Rates of Movement, and Environmental Controls, *Arctic and Alpine Research*, **28(2)**, 228 - 236.

Dugmore, A.J. (1987). Holocene glacier fluctuations around Eyjafjallajökull, south Iceland: A tephrochronological study. Unpubl. PhD. Thesis, University of Aberdeen.

Dugmore, A.J. (1989a). Tephrochronological studies of Holocene glacier fluctuations in south Iceland. *In*: Oerlemans, J. (ed.). *Glacier Fluctuations and Climatic Change*. Kluwer, Academic Publishers, 37 - 55.

Dugmore, A.J. (1989b). Icelandic volcanic ash in Scotland, *Scottish Geographical Magazine*, **105**, 168 - 172.

Dugmore, A.J. and Buckland, P.C. (1991). Tephrochronology and late Holocene soil erosion. In: Maizels, J.K. and Caseldine, C. (eds.), *Environmental change in Iceland: Past and Present*, Dordrecht, 37 - 55.

Dugmore, A.J. and Sugden, D.E. (1991). Do the anomalous glacier fluctuations of Sólheimajökull reflect ice-divide migration? *Boreas*, **20**, 105-113.

Dugmore, A.J., Larsen, G., Newton, A.J. and Sugden, D.E. (1992). Geochemical stability of fine-grained silicic tephra layers in Iceland and Scotland, *Journal of Quaternary Science*, **7**, 173 - 183.

Dugmore, A..J. and Erskine, C.C. (1994). Local and regional pattern of soil erosion in Southern Iceland. *In*: Stötter, J. and Wilhelm, F. (eds.), Environmental Change in Iceland. *Münchener Geogr. Abl.* **B12**, 41 - 63.

Dugmore, A.J., Larsen, G. and Newton, A.J. (1995a). Seven tephra isochrones in Scotland, *The Holocene*, **5(3)**, 257 - 266.

Dugmore, A.J., Cook, G.T., Shore, J.S., Newton, A.J., Edwards, K.J. and Larsen, G. (1995b). Radiocarbon dating tephra layers in Britain and Iceland, *Radiocabon*, **37(2)**, 379 - 388.

E

Einarsson, T. (1957). Magneto-Geological Mapping in Iceland, *Phil. Mag. Suppl.*, **6**, 232 - 239.

Einarsson, Th. (1961). Pollenanalytische Untersuchungen für spät- und Postglazialen Klimatgeschichte Islands. *Sönderveroffentichungen des Geologischen Institutes der Universitat Köln*, **6**.

Einarsson, Th. (1963). Pollen-analytical studies on vegetation and climate history of Iceland in late and post-glacial times, *In*: Löve, A. and Love, D. (eds.). *North Atlantic Biota and their history*, Pergamon, 255 - 365.

Einarsson, Th. and Albertsson, K.J. (1988). The glacial history of Iceland during the past three million years, *Philosophical Transactions of the Royal Scociety of London Series B*, **318**, 637 - 644.

Einarsson, M.Á. (1975). *Veðurfræði.* Reykjavík, Iðunn, 99p.

Einarsson, M.Á. (1976). *Veðurfar á Íslandi.* Iðunn. Reykjavík.

Einarsson, M.Á. (1984). Climate of Iceland. *In*: Van Loon (ed). Climates of the Oceans, *World Survey of Climaatology*, **15**, Elsevier Science Publ., 673 - 697.

Einarsson, M.Á. (1991). Temperature conditions in Iceland 1901 - 1990, *Jökull*, **41**, 1 - 20.

Einarsson, Th. (1994). *Jarðfræði. Myndun og mótun land.* Mál og Menning. Reykjavík.

Einarsson, P., Sigmundsson, F., Hofton, M.A. and Foulger, G.R. (1994). An Experiment in Glacio-Isostasy near Vatnajökull, Iceland, 1991, *Jökull*, **44**, 29-39.

Eiríksson, J., Símonarson, L. A. and Sveinbjarnardóttir, Á.E., (1998a). Heimsókn að Bæ í Hrútafirði: Ný tímasetning með kolefnisgreiningum og gjóskulagatímatali (in Icelandic), *Geoscience Society of Iceland, Spring meeting*, p20.

Eiríksson, J., Knudsen, L. and Haflidason, H. (1998b). 14.000 ára saga hafstrauma og loftslags á norðlenska landgrunninu, gögn frá setlagakjörnum (in Icelandic), *Geoscience Society of Iceland, Spring meeting*, p32.

Eiríksson, J.; Haflidason, H., Knudsen, K. L., Gudmundsson, B. Þ., Jónsdóttir, H. B. B. and Ófeigsson, Ó. (1998c). Holocene and Lateglacial sedimentation on the tectonically active shelf off North Iceland. In Wilson, J. R. and Plesner, S. (eds): 23rd Nordic Geological Winter Meeting Abstract Volume, p. 64. Århus, University of Aarhus.

Eiríksson, J., Knudsen, K. L. Haflidason, H., Jiang, H., Henriksen, P. and Rytter, F. (1998d). Palaeoenvironments on the North Icelandic shelf. In Wilson, J. R. and Plesner, S. (eds): 23rd Nordic Geological Winter Meeting Abstract Volume, p. 63. Århus, University of Aarhus.

Eyles, J. (1978). Facies of supraglacial sedimentation on temperate valley glaciers, Unpubl. PhD-thesis, University of East Anglia, UK.

Eyles, J. (1979). Facies of supraglacial sedimentation on Icelandic and Alpine temperate glaciers, *Canadian Journal of Earth Science*, **16**, 1341 - 1561.

Eyles, J. (1983). Modern Icelandic glaciers as a depositional model for hummocky moraines in the Scottish Highlands. *In*: Evenson, E.B., Schluster, C.S. and Rabussa, J. (eds). *Tills and related deposits*, AA Balkema Press, Rotterdam.

Eythórsson, J. and Sigtryggsson, H. (1971). The climate and weather of Iceland, *The Zoology of Iceland*, **1(3)**, 1 - 62.

F

Furbish, D.J. and Andrew, J.T. (1984). The use of hypsometry to indicate long term stability and response of valley glaciers to changes in mass transfer, *Journal of Glaciology*, **30(105)**, 199 - 201.

G

Gellatly, A.F., Trevor, J.H., Chinn, T.J.H. and Röthlisberger, F. (1988). Holocene glacier variations in New Zealand: A review, *Quaternary Science Reviews*, **7**, 227-242.

Geirsdóttir Á. and Eiríksson, J. (1994). Growth of an Intermittent Ice Sheet in Iceland during the Late Pliocene and Early Pleistocene, *Quaternary Research*, **42**, 115 - 130.

Gordon, J. and Sharp M. (1983). Lichenometry in dating recent landforms and deposits, southeast Iceland, *Boreas*, **12**, 191 - 200.

Greene, D. (1995). The Loch Lomond Stadial Ice cap in western Lochaber, Scotland. Unpubl. PhD-thesis, University of Edinburgh, 173p.

Grove, J.M. (1988). *The Little Ice Age*, Methuen, London and New York.

Grove, J.M. and Switsur, R. (1994). Glacial Geological evidence for the Medieval Warm Period, *Climatic Change* **26**, 143 - 169.

Grönvold, K. (1972). Structural and petrochemical studies in the Kerlingarfjöll region, central Iceland, University of Oxford, Unpubl. Ph.D. thesis.

Grönvold, K. Óskarsson, N., Johnsen, S.J., Clausen, H.B, Hammer, C.U., Bond, G. and Bard, E. (1995). Ash layers from Iceland in the Greenland GRIP ice core correlated with oceanic and land sediments, *Earth and Planetary Science Letters*, **135**, 149-155.

Gudmundsson, H.J. (1992). *Eiríksjökull; Jöklabreytingar og gerð jarðlaga. Notkun fléttunnar Rhizocarpon geographicum við aldursgreiningar á jökulmenjum á Íslandi.* Unpubl. M.Sc.thesis, University of Iceland, 151p.

Gudmundsson, H.J. (1997). A Review of the Holocene Environmental History of Iceland, *Quaternary Science Reviews*, **16**, 81 - 92.

Gudmundsson, H.J. (in press,a): Holocene Glacier fluctuations of the Eiríksjökull ice cap, west central Iceland, *Jökull.*

Gudmundsson, H.J. and Norddahl, H. (in press, b). Holocene Glacier fluctuations in Iceland. *In:* Williams, R.S. Jr., & Sigurdsson, O. (eds.). *Glaciers of Iceland. In:*

Williams, J.R. & Ferrigno, J.G. (eds). *Satellite Image Atlas of the Glaciers of the World.* U.S. Geological Survey Professional Paper 1386-D, Submitted and accepted.

Gudmundsson, M.T., Sigmundsson, F. and Björnsson, H. (1997). Ice-volcanic interaction of the 1996 Gjálp subglacial eruption, Vatnajökull, Iceland, *Nature*, **389**, 954-957.

Goudie, A. (1981). *The Encyclopaedic Dictionary of Physical Geography*, Blackwell, Oxford, 528p.

H

Hafliðason, H., Larsen, G. and Ólafsson, G. (1992). The recent sedimentation history of Thingvallavatn, Iceland, *Okios*, **64**, 80 - 95.

Hallsdóttir, M. (1987). Pollen Analytical studies of human influence on vegetation in relation to the Landnám tephra layer in southwest Iceland. LINDQUA thesis, 18, Department of Quaternary Geology, University of Lund.

Hammer, C.U. (1984). Traces of Icelandic eruptions in the Greenland ice sheet, *Jökull*, **34**, 51 - 54.

Häberle, T. (1991). Holocene glacial history of the Hörgárdalur area, Tröllaskagi, Northern Iceland. In: Maizels and Caseldin (eds.). *Environmental Change in Iceland. Past and Present.* Kluwer, Dordrecht, 193 - 202.

Helgason, J. and Duncan, R.A. (1996). Jarðlagaskipan Svínafells í Öræfum: bergsegulstefna, aldursgreiningar og jöklunarsaga, *Abstract, Vorráðstefna Jarðfræðifélags Íslands 1996*, 46p.

Henderson, E. (1818). Iceland or the Journal of a Residence in that Island during the Years 1814 - 1815, 1, Edinburgh.

Henson, F.A. (1955). The Geology of Iceland. Survey. *Ed. Univ. of Nottingham*, **5(3)**, 34 - 46.

Hjartarson, Á. and Ingólfsson, Ó. (1988). Preboreal glaciation of southern Iceland, *Jökull*, **38**, 1 - 16.

Hjort, C., Ingólfsson, Ó., Möller, P. and Lirio, J.M. (1997). Holocene glacial history and sea-level changes on James Ross Island, Antarctic Peninsula, *Journal of Quaternary Science*, **12(4)**, 259-273.

Hospers, J. (1953). Reversals of the main Geomagnetic Field. I. *Koninkl. Nederl. Akad. Van Wetensch. Proceed. Ser. B*, **56(5)**.

Hubbard, A.L. (1996). High resolution modelling of glacier flow, Unpubl. Ph.D. thesis, University of Edinburgh, 83p.

Hulton, N.J., Sugden, D.E., Payne, A.J. and Clapperton, C.M. (1994). Glacier modelling and the climate of Patagonia during the Last Glacial Maximum, *Quaternary Research*, **42(1)**, 1 - 19.

I

Imsland, P. (1978). The petrology of Iceland; some general remarks, *Nordic Volcanological Institute Reports 7808*, 1 - 19.

Innes, J.L. (1985). Lichenometry, *Progress in Physical Geography*, **9**, 187 - 254.

Ingólfsson, Ó. and Norðdahl. H. (1994). A review of the environmental history of Iceland, 13000 - 9000 yr BP, *Journal of Quaternary Science*, **9(2)**, 147 - 150.

Isl. Ann. (1888). Islandske Annaler indtil 1578, Ed. G. Storm. Christiania.

Ives, J. (1956). Öræfi, Southeast Iceland: an essay in regional geomorphology, Unpubl. Ph.D-thesis, McGill University, Montreal, Canada, 231p.

Ives, J. (1991). Landscape change and human response during a thousand years of climatic fluctuations and volcanism: Skaftafell, Southeast Iceland, *Pirineos*, **137**, 5 - 50.

Ives, J. (1996). Glacier and Climate Reconstruction in Southeast Iceland During the Last Two Millennia: a Reconnaissance, Umwelt mensch gebirge beitrage zur dynamik von natur- und lebenstraum, Festschrift fur Bruno Messerli zum 65 - geburtstag, 17. September, 1996. *Geographica Bernensia, Geographischen Instituts der Universtiat Bern*, 123 - 132.

Ives, J. and King, C.A.M. (1954). Geological Observations on Morsárjökull. Part I: The Ogive Banding, *J. Glaciol.*, **2(16)**, 423 - 428.

Ives, J. and King, C.A.M. (1955). Glaciological observations on Morsárjökull, SW Vatnajokull. Part II. Regime of the Glacier, present and past, *J. Glaciol.*, **2(17)**, 477 - 482.

J

Jakobson, S.P. (1979). Petrology of recent basalts of the Eastern volcanic Zone, Iceland, *Acta Naturalia Islandica*, **26**, 1 - 103.

Jóhannesson, H. (1983). Gossaga Grímsvatna 1900-1983 í stuttu máli, *Jökull*, **33**, 146-147.

Jóhannesson, H. (1984). Grímsvatnagos 1933 og fleira frá því ári, *Jökull*, **34**, 151-158.

Jóhannesson, T., Raymond, C.F., and Waddington, E.D. (1989). A simple method for determining the response time of glaciers. *In*: Oerlemans, J. (ed.) *Glacier Fluctuations and Climatic Change*, Kluwer Academic Publishers, Dordrecht, 343 - 352.

Jóhannesson, T. (1997). The response of two Icelandic Glaciers to Climatic Warming Computed with a Degree-Day Mass Balance Model Coupled to a Dynamic Glacier Model, *Journal of Glaciology* **43(143)**, 321-327.

K

Karlén, W. (1988). Scandinavian glacial and climatic fluctuations during the Holocene, *Quaternary Science Reviews*, **7**, 199-200.

Karlén, W. and Matthews, J.A. (1992). Reconstructing Holocene glacier variations from glacial lake sediments: studies from Nordvestlanded and Jostedalsbreen - Jotunheim, southern Norway, *Geografiska Annaler*, **74(A)**, 327 - 348.

Kaldal, I. and Víkingsson, S. (1995). Höfuðborgarsvæði. Tillögur um staðal fyrir jarðgrunnskort, Orkustofnun, OS-1990-10-15.

Kerr, A. (1993). Topography, climate and ice masses: a review, Terra Nova, **5**, 332 - 342.

King, C.A.M. and Ives, J. (1955). Glaciological observations on some of the outlets of south-west Vatnajökull. Part I: Glacier regime, *J. Glaciol.*, **2(18)**, 563 - 569.

Kjartansson, G. (1964). Ísaldarlok og eldjöll á Kili, *Náttúrufræðingurinn*, **34**, 9-38.

Klitgaard-Krisensen, D., Serjup, H.P., Haflidason, H., Johnsen, S. and Spurk, M. (1998). A regional 8200 cal. yr. B.P. cooling event in Northwest Europe, induced by final stages of Laurentide ice-sheet, *Journal of Quaternary Science* **13(2)**, 165 - 169.

Knudsen, K. L., Henriksen, P., Rytter, F., Jiang, H. & Eiríksson, J. (1998). Palaeoclimatic shifts on the North Icelandic Shelf since 14,000 BP: Biostratigraphical results. In Wilson, J. R. and Plesner, S. (eds): 23rd Nordic Geological Winter Meeting Abstract Volume, p. 156. Århus, University of Aarhus.

Kristjánsson, L. (1979). The shelf area around Iceland, *Jökull*, **29**, 3 - 6.

Kroç, N., Jansen, E. and Hafliðason, H. (1993). Paleoceanographic reconstruction of surface ocean conditions in the Greenland, Iceland and Norwegian seas through the last 14 ka based on diatoms, *Quaternary Science Reviews*, **12**, 112-140.

L

Larsen, G. (1978). Gjóskulög í nágrenni Kötlu, Unpubl. B.S-Hons.-thesis, University of Iceland.

Larsen, G. (1979). Um aldur Eldgjárhrauna, *Náttúrufræðingurinn*, **49(1)**, 1-26.

Larsen, G. (1981). Tephrochronology by microprobe glass analysis. *In*: Self, S. and Sparks, R.S.J., (ed). *Tephra Studies*, Dordrecht, Reidel, 95 - 102.

Larsen, G. (1982). Gjóskutímatal Jökuldals og nágrennis. *In*: Thórarinsdóttir, J., Óskarsson, Ó.H., Steinthórsson, S. and Einarsson, Th., editors, *Eldur er í Norðri*, Reykjavík: Sögufélag Reykjavíkur, 51 - 66.

Larsen, G. (1984). Recent volcanic history of the Veidivötn fissure swarm, southern Iceland - an approach to volcanic risk assessment, *Journal of Volcanology and Geothermal Research*, **22**, 33 - 58.

Larsen, G. and Thórarinsson, (1977). H_4 and other Acid Hekla Tephra layers, *Jökull*, **27**, 28 - 46.

Le Maitre, R.W. (ed, 1989). *A classification of igneous rocks and glossary of terms*, Oxford, Basil Blackwell.

Lowe, D.J. (1986). Controls on the rates of weathering and clay mineral genesis in airfall tephras,: a review and New Zealand case study. *In*: Colman, S.M. and Dethier, D.P. (eds). *Rates of chemical weathering*. Academic Press, London, 265 - 330.

Luckman, B.H. and Osborn, G.D. (1979). Holocene glacial variations in the middle Canadian Rocky Mountains, *Quaternary Research*, **11**, 52 - 77.

M

Mackintosh, A.N., Dugmore, A.J. and Jacobsen, F.M. (in press). Ice-thickness measurements of Sólheimajökull, southern Iceland and their relevance to its recent behaviour, *J. Glaciol.*

MacDonald, R., McGarvie, D.W., Pinkerton, H., Smith, R.L. and Palacz, Z.A. (1990). Petrogenetic evolution of the Torfajökull volcanic complex, Iceland: 1: Relationship between the magma types, *Journal of Petrology*, **31**, 429 - 459.

Mangerud. J., Andersen, S.T., Beerglund, B.E. and Donner, J.J. (1974). Quaternary stratigraphy of the Norden, a proposal for terminology and classification, *Boreas*, **3**, 109 - 128.

Maizels, J. (1986). Lithofacies variations within sandur deposits. The role of runoff regime, flow dynamics and sediment supply characteristics, *Sedimentary Geology*, **85**, 299 - 325.

Maizels, J. and Dugmore, A.J. (1985). Lichenometrical dating and tephrochronology of sandur deposits, Sólheimajökull area, southern Iceland, *Jökull*, **35**, 69 - 77.

Mayewski, P.A., Meeker, L.D., Whitlow, S., Twickler, M.S., Morrison, M.C., Bloomfield, P., Bond, G.C., Alley, R.B., Gow, A.J., Grootes, P.M., Meese, D.A., Ram., M., Taylor, K.C., Wumkes, W. (1994). Changes in atmospheric circulation and ocean ice cores over the North Atlantic during the last 41.000 years, *Science*, **266**, 1680 - 1682.

McGarvie, D.W., McDonald, R., Pinkerton, H. and Smith, R.L. (1990). Petrogenetic evolution of the Torfajökull volcanic complex, Iceland: 2: The role of magma mixing. *Journal of Petrology*, **31**, 461 - 481.

Meese, D.A., Gow, A.J. Grootes, P., Mayewski, P.A., Ram, M., Stuiver, M., Taylor, K.C., Waddington, E.D. and Zelinski, G.A. (1994). The accumulation record from the GISP2 core as an indicator of climate change throughout the Holocene, *Science*, **266**, 1680 - 1682.

Meteorological Office (1963). *Weather in home fleet waters. Northern Seas*, H.M.S.O., 265, 265p.

N

Nielsen, N and Noe-Nygaard, A. (1936). Om den Islanske "Palagonitformations" Oprindelse, *Geogr. Tidskr.*, **39**, 3 - 36.

Noe-Nygaard, A. (1953). Notes on the nature of Some Indurated Moraines in South Iceland, *Geogr. Tidskr.*, **52**, 222 - 231.

O

Oerlemans, J. (1989). On the response of valley glaciers to climatic change. *In*: Oerlemans, J. (ed.). *Glacier Fluctuations and Climatic Change*. Kluwer Academic Publishers, 353-372.

Ogilvie, A.E. J. (1984). The past climate and sea-ice record from Iceland, part 1; data to A.D. 1780, *Climatic Change*, **6**, 131 - 152.

Ogilvie, A.E.J. (1991). Climatic Changes in Iceland A.D. c. 865 to 1598. *In*: Bigelow, G.F.(ed.). The Norse of the North Atlantic, *Acta Archaeologica*, **60**, 233 - 251.

Ogilvie, A.E.J. (1992). Documentary evidence for changes in the climate of Iceland, A.D. 1500 to 1800, Bradley R.S. and P.D. Jones (ed.), *Climate since A.D. 1500*, Routledge, London.

Osborn, G. and Luckman, B.H. (1988). Holocene glacier fluctuations in the Canadian Cordillera (Alberta and British Columbia), *Quaternary Science Reviews*, **7**, 115-128.

P

Palais, J.M., Taylor, K., Mayweski, P.A. and Grootes, P. (1991). Volcanic ash from the 1362 A.d. Öræfajökull eruption (Iceland) in the Greenland ice sheet, *Geophys. Res. Lett.*, **18**, 1241 - 1244.

Paterson, W.S.B. (1994). *The Physics of Glaciers*, Pergamon Press, 380p.

Payne, A and Sugden, D. (1990). Topography and ice-sheet growth, *Earth Surface Processes and Landforms*, **15(7)**, 625-639.

Pálsson, S. (1774). Ferðabók Sveins Pálssonar. Jöklarit. Frumdrög til lýsingar á staðháttum, sögu og eðlisfari íslenskra jökla. Skrifað 1773 - 1774, Reykjavík, Prenstsmiðjan Oddi.

Pilcher, J.R. and Hall, V.A. (1992). Towards a tephrochronology for the Holocene of the north of Ireland, *The Holocene*, **2**, 255 - 259.

Pilcher, J.R., Hall, V.A. and McComrac, F.G. (1995). Dates of Holocene eruptions from tephra layers in Irish peats, *The Holocene*, **5**, 105 - 110.

Piper, J.D.A (1971). Ground magnetic Studies of crustal growth in Iceland, *Earth and Planet. Sci. Letters*, **12**, 199 - 207.

Prestvik, T. (1979). Geology of the Öræfi district, Southeastern Iceland, *Nordic Volcanological Institute*, **79 01**, 28p.

R

Rose, J., Whiteman, C.A., Lee, J., Branch, N.P. Harkness, D.D. and Walden, J. (1997). Mid and Late Holocene vegetation, surface weathering and glaciation, Fjallsjökull, Southeast Iceland, *The Holocene*, **7(4)**, 457 - 471.

Rousseau, D.-D., Limondin, N., Magnin, F. and Puisségur, J.-J. (1994). Temperature oscillations over the last 10,000 years in western Europe estimated from terrestrial mollusc assemblages, *Boreas*, **23**, 66 - 73.

S

Sigfúsdóttir, A.B. (1975). Úrkoma á Vatnajökli, *Veðrið*, **2(19)**, 46 - 47.

Sigmundsson, F. (1990). Viscosity of the Earth beneath Iceland: A comparison of model calculations with geological data (in Icelandic with English summary), M.Sc. Thesis, University of Iceland, University Press, 121p.

Sigmundsson, F. and Einarsson, P. (1992). Glacio-isostatic crustal movements caused by historical volume change of the Vatnajökull ice cap, Iceland, *Geophys. Res. Letters*, **19**, 2123-2126.

Sigvaldason G. (1974). The petrology of Hekla and the origin of silicic rocks in Iceland, *The eruption of Hekla in 1947-1948 V*, 1-44.

Sigvaldason, G. (1982). Samspil vatns og kviku. Öskjugosið 1875. *In*: Thórarinsdóttir, J., Óskarsson, Ó.H., Steinthórsson, S. and Einarsson, Th., (eds). *Eldur er í Norðri*, Reykjavík, Sögufélag Reykjavíkur, 37 - 47.

Small, J. and Witherick, M. (1986). *A Modern Dictionary of Geography*. Edward Arnold, 233p.

Snorrason, S. (1984). Mýrarjöklar og Vatnsdalur. Unpubl. Cand. Real thesis, University of Oslo. 115p.

Sugden, D.E. and John, B.S. (1988). *Glaciers and Landscape*, Arnold, London, 376p.

Spedding, N. (1997). Meltwater controls on ice-marginal sedimentation, Unpubl. Ph.D thesis, University of Edinburgh, 325p.

Steinthórsson, S. (1977). Tephra layers in a drill core from the Vatnajökull ice cap. *Jökull*, **27**, 2 - 27.

Stötter, J. (1991). New Observations on the postglacial glacier history of Tröllaskagi, northern Iceland. *In*: Maizels and Caseldine (eds.). *Environmental Change in Iceland. Past and Present*. Kluwer, Dordrecht, 181 - 192.

Stötter, J. (1994). Changing the Holocene record - A call for International Interdisciplinary co-oporation, *Munchener Geogr. Abl.*, **B12**, 257 - 273.

Sweatman, T.R. and Long, J.V.P. (1969). Quantitative electron microprobe analysis of rock forming minerals, *Journal of Petrology*, 7, 332 - 379.

Sæmundsson, K. (1979). Outline of the Geology of Iceland, *Jökull*, **29**, 17 - 28.

Thompson, A. (1988). Historical Development of the Proglacial Landforms of Svínafellsjökull and Skaftafellsjökull, Southeast Iceland, *Jökull*, **38**, 17 - 31.

Thompson, A. and Jones, A. (1986). Rates and causes of proglacial river terrace formation in southeast Iceland: an application of lichenometric dating techniques, *Boreas*, **15**, 231 - 246.

Thórarinsson, S. (1943). Oscillations of the Iceland glaciers in the last 250 years, *Geogr. Ann.*, **25**, 1 - 54.

Thórarinsson, S. (1944). Tefrokronologiska studier på Island, *Geografiska Annaler*, **26A**, 1-217.

Thórarinsson, S. (1956). On the variations of Svínafellsjökull, Skaftafellsjökull and Kviárjökull in Öræfi, *Jökull*, **6**, 1-15.

Thórarinsson, S. (1957). Héraðið milli sanda og eyðing þess, *Andvari*, **82**, 35 - 47.

Thórarinsson, S. (1958). The Öræfajökull eruption of 1362, *Acta Nat. Isl. II(2)*, Reykjavík, Náttúrufræðistofnun Íslands.

Thórarinsson, S. (1961). Uppblástur í ljósi öskulagarannsókna. *Ársrit Skógræktarfélags Íslands*, 17-54.

Thórarinsson, S. (1963). The Svínafell layers. Plant-bearing interglacial sediments in Öræfi, southeast Iceland. *In*: Löve, A. and Löve, D. (eds.). *North Atlantic Biota and their History*, Pergamon Press, 377 - 389.

Thórarinsson, S. (1967). The eruptions of Hekla in historical times, *The eruption of Hekla 1947 - 1948 II/3*, 1 - 68.

Thórarinsson, S. (1974). Vötnin stríð. Saga Skeiðarárhlaupa og Grímsvatnagosa, Reykjavík, Bókaútgáfa Menningarsjóðs.

Thórarinsson, S. (1975). Katla og annáll Kötlgosa. *Árbók Ferðafélags Íslands*, Ferðafélag Íslands, 125-149.

Thórarinsson, S. (1981). The application of tephrochronology in Iceland. *In*: Self, S. and Sparks, R.S.J. (eds.), *Tephra Studies*, 1 - 12, Reidel, Dordrecht.

Thórarinsson, S., Sæmundsson, K. and William, R.S., Jr. (1973). ERTS-1 image of Vatnajökull: Analysis of Glaciological, Structural and Volcanic features, *Jökull*, **23**, 7 - 17.

Thórdarson, Th. (1990). *Skaftáreldar 1783 - 1785. Gjóskan og framvinda gossins.* B.Sc-Hons. thesis, University of Iceland and Science Institute, University Press.

Thoroddsen, Th. (1911). *Lýsing Íslands.* Hið Íslenska Bókmenntafélag, Kaupmannahöfn, 673p.

Tómasson, H. (1993). Jökulstífluð vötn á Kili og hamfarahlaup í Hvítá í Árnessýslu, *Náttúrufræðingurinn*, **62**, 77-98.

Tómasson, H (1996). The Jökulhlaup from Katla in 1918, *Annals of Glaciology*, **22**, 249-254.

W

Walker G.P.L. (1975). Excess spreading axis and spreading rate in Iceland, *Nature*, **255**, 468 - 471.

Wohlfarth, B. (1996). The chronology of the last Termination: a review of radiocarbon-dated, high-resolution terrestrial stratigraphy, *Quaternary Science Reviews*, **15**, 267 - 284.

Appendix I

Reprinted from *Quaternary Science Reviews*, **16**, Gudmundsson, H.J., "Review of the Holocene Environmental History of Iceland", pp 81 - 92, ©1997, with permission from Elsevier Science.

Pergamon

Quaternary Science Reviews, Vol. 16, pp. 81–92, 1997.

0277–3791/97 $32.00

PII: S0277-3791(96)00043-1

A REVIEW OF THE HOLOCENE ENVIRONMENTAL HISTORY OF ICELAND

HJALTI J. GUDMUNDSSON
The University of Edinburgh, Department of Geography, Drummond Street, Edinburgh EH8 9XP, U.K.
(E-mail: hjg@geovax.edu.ac.uk)

Abstract — The purpose of this paper is to review the present knowledge of the Holocene environmental history of Iceland, focusing on glacier fluctuations. The ideas of the Holocene being a relatively 'flat' epoch in terms of environmental changes have been superseded by new studies reflecting active fluctuations. The present paper promotes a revised model of the Holocene glacier fluctuation history of Iceland and recognises a long period of Neoglaciation. Present data suggests an onset of glacier expansion in Iceland around 5 ka BP which can be roughly correlated between different parts of the country and coincides with wider environmental changes. Specific glacier advances have been bracketed to 5–4.5 ka BP, ca. 4.2 ka BP, ca. 3 ka BP, 2 ka BP and 1.5–1.2 ka BP. During the Little Ice Age (LIA), glaciers in Iceland begun to advance in the late 18th century and were biggest in the late 19th century.

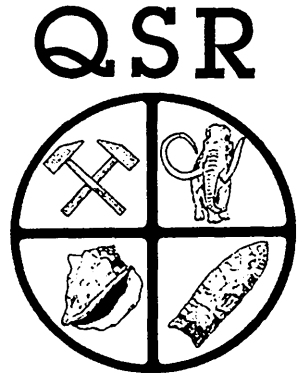

INTRODUCTION

Glacier fluctuations in temperate climates contain important palaeoclimatic data since they respond to changes in temperature and precipitation. The location of Iceland in the North Atlantic provides an ideal setting for studies of glacier fluctuations because small movements in the nearby oceanic and atmospheric Polar Fronts cause significant variation in glacier mass balance and consequently effect the frontal positions of the glaciers in Iceland. Case studies from all over the world have shown that precise indications of the scale and direction of climatic change may be recorded by glacier advances (Grove, 1988) although it is critically important to identify non-climatic influences that may inhibit or exaggerate a glacier response to temperature and precipitation change.

Local causes of changes in glacier extent are many: volcanism, sub-glacial geothermal activity, topographic thresholds and glacier dynamics are likely to effect the pattern of glacier oscillation (Hoppe, 1967; Björnsson, 1988; Dugmore and Sugden, 1991; Warren, 1991, 1993). Therefore, local effects on glacier fluctuations have to be filtered out before using individual glaciers as a source of palaeoclimatic reconstruction.

The aims of this paper are to review the present knowledge of the Holocene environmental history of Iceland, focusing on the role of glacier fluctuations. The Holocene is defined from 10 ka BP to present. The first part gives a short abstract of the decay of the last inland ice sheet based on four recent and detailed reviews by Ingólfsson (1991), Norddahl (1991), Kaldal and Víkingsson (1991), and Ingólfsson and Norddahl (1994). It is necessary to briefly summarise these to be able to make a link between the termination of the last inland ice sheet and the early Holocene. The rest of the paper is approached chronologically from the first signs of glaciers in the Holocene to the present, and involves Neoglaciation and the Little Ice Age (LIA).

THE DECAY OF THE LAST INLAND ICE SHEET IN ICELAND

The knowledge of the pattern and timing of the decay of the last major ice sheet has changed since the pioneering work of the late 19th and early to mid 20th century. The earliest work of Keilhack (1884), Thoroddsen (1891, 1906, 1911), Pjeturss (1910), Áskellson (1934), Kjartansson (1940, 1943) and Thórarinsson (1951) have been the foundation of geological thinking in Iceland. The first model of the deglaciation in Iceland was that of Einarsson (1961) which Norddahl (1991) has named the SAD model (Single Advance Deglaciation). In this model, the Hólkot moraine (Thórarinsson, 1951) in northern Iceland is correlated with the Búdi moraine (Kjartansson, 1964) in southern Iceland and called the Búdi stage (Fig. 1). This model was revised when it became apparent that end moraines in southwestern, western, southern, northern and northeastern Iceland, were formed before the Búdi stage. These later moraines have been described by Bárdarson (1923) and Tryggvason and Jónsson (1958). In the late 1960s, Einarsson (1967, 1968) revised his initial model and defined a second major still-stand, a readvance to a limit defined by the moraine sequences found in the Álftanes peninsula, southwestern Iceland, upper Borgar-

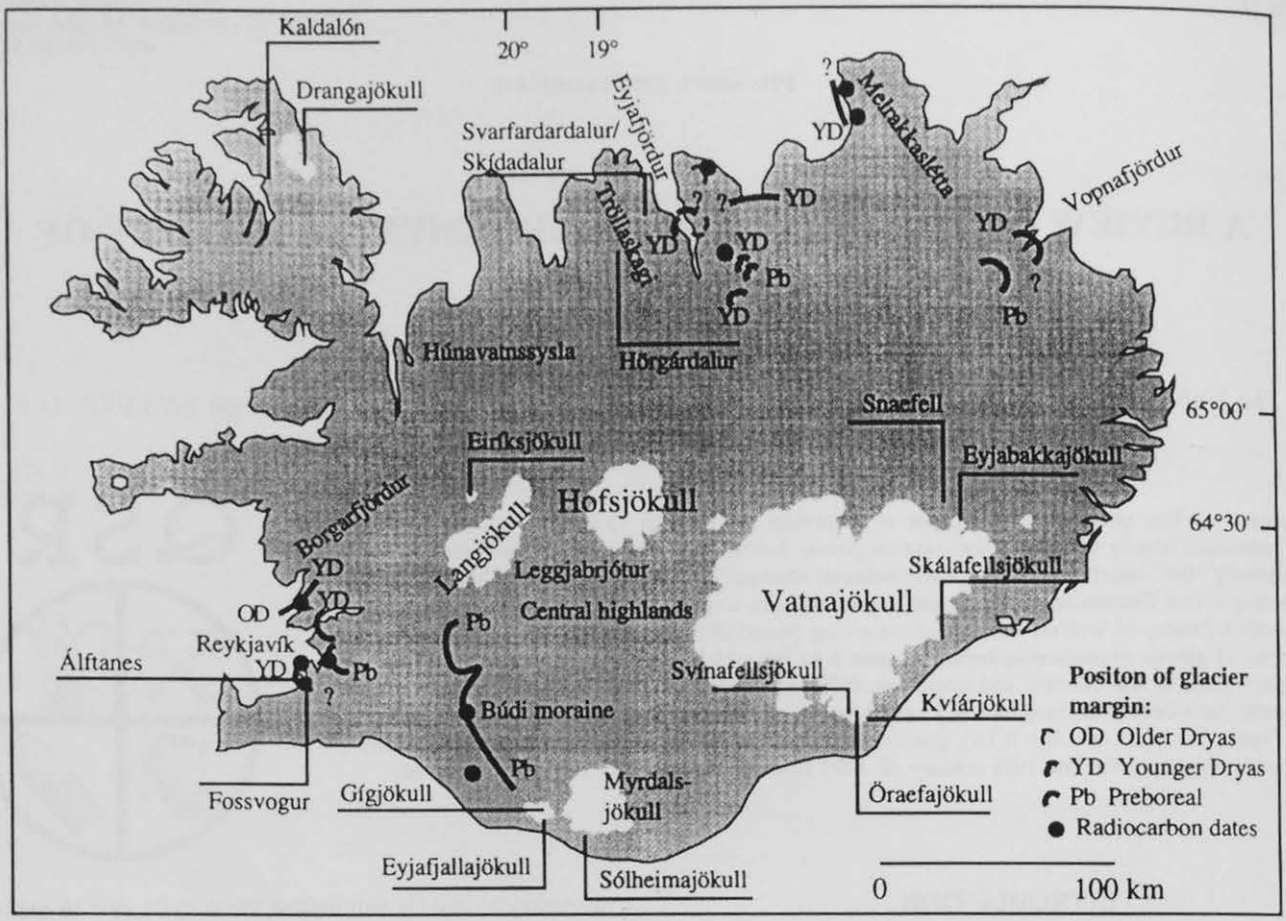

FIG. 1. Key map including the locations of important sites and place names in the Holocene glacier fluctuation history and the decay of the last inland ice sheet in Iceland. Data indicating different positons of ice margins during the termination of the last inland ice sheet is based on Norddahl (1991) and Ingólfsson and Norddahl (1994).

fjördur area, Húnavatnssysla and Eyjafjördur (Fig. 1). Norddahl (1991) has called this the DAD-model (Double Advance Deglaciation). When Einarsson (1967, 1968) introduced his DAD model he argued that the Búdi stage and the Álftanes Stage could be correlated with Older and Younger Dryas or Salpausselka-Ra stage, respectively, in Fennoscandia. Thórarinsson (1951) had also reached the same conclusion. At the same time, Einarsson (1967, 1968) had come to the conclusion that the Fossvogur layers, located near Reykjavik were formed during the last Pleistocene interglacial. The DAD model was generally accepted until Ingólfsson (1985, 1987a, b, 1988) suggested a revision based on his study of the Borgarfjördur area in western Iceland. This alternative model proposed more frequent glacier advances during the late glacial time in Iceland, probably at least nine in number, lasting from the Weichselian maximum, about 18 ka BP to early Preboreal around 9.6 ka BP. Subsequent support has come from studies from different parts of the country (Ingólfsson, 1991; Ingólfsson and Hjort, 1988; Hjartarson, 1989; Norddahl, 1991; Norddahl and Haflidason, 1990, 1992; Pétursson, 1986, 1991; Saemundsson, 1994, 1995). Norddahl (1991) called this new thinking the MAD model (Multi Advance Deglaciation; Fig. 1). This reassessment of the deglaciation pattern of Iceland has been developed mainly from dating of key sites of glaciogenic deposits, such as the Búdi moraines, south Iceland (Hjartarson and Ingólfsson, 1988), the Fossvogur layers, south-western Iceland (Hjartarson, 1989) and evidence of two separate glacier advances out of the Borgarfjördur main valley, western Iceland, considered to be of Younger and Older Dryas age (Ingólfsson, 1985, 1987a, b, 1988). Hjartarson and Ingólfsson (1988) studied the Búdi moraine in southern Iceland on the basis of its chronological position and came to the conclusion that it was of early Preboreal age instead of Younger Dryas age as Einarsson (1967, 1968) had proposed. The dating of the shell bearing section of the Fossvogur layers to the Alleröd Interstadial and early Younger Dryas (Hjartarson, 1989) necessitated a revision of Einarsson (1967) DAD model because of the location of the Fossvogur layers well within the Álftanes moraine complex. The revised age of the Fossvogur layers is based on 13 AMS ^{14}C dates, which are consistent and the precision of the measurements is good. The dates have not been calibrated according to Bard *et al.* (1993) and Stuiver and Reimer (1993) and cannot be correlated with the GISP2 ice core in terms of identifying lead and lag times of climatic change between Iceland and Greenland. Bartlein *et al.* (1995) have pointed out the need to calibrate conventional radiocarbon dates because it could have widespread implications for the interpretation of late-Quaternary palaeoecologcal and palaeoclimatic data.

Hammer *et al.* (1986) and more recently Dansgaard *et al.* (1989) argued that a warming of 7°C occurred over 50 years and that the climate of the Northern Atlantic turned

into a milder and less stormy regime in less than 20 years as a consequence of a rapid retreat of the sea-ice cover associated with the return of the northeast current to higher latitudes. Data from pollen studies in Iceland indicate a transition as well. By 10.4 ka BP plant colonisation of coastal north Iceland had begun (Björck *et al.*, 1992). The pollen stratigraphy shows a succession of pioneer plants from open tundra vegetation to birch and juniper heathlands in the north around 10.4 ka BP which probably reflects a transition from a cool climate to conditions more similar to today's oceanic sub-polar climate around 9.2 ka BP (Hallsdóttir, 1990; Björck *et al.*, 1992).

ENVIRONMENTAL HISTORY OF ICELAND FOLLOWING THE RETREAT FROM THE BÚDI MORAINE

The retreat of the glacier from the Búdi moraine was not continuous. Kaldal and Víkingsson (1991) have reported several still stands in the central highlands well within the Búdi moraine limit but did not manage to date them properly due to limited organic material. They interpreted the terminal moraines as being produced by surges of a constantly retreating glacier rather than climatically induced stillstand or readvance. The surging activity could have been instrumental in lowering the ice cap surface by making it sensitive to further retreat which eventually resulted in catastrophic collapse. The deglaciation produced very large volumes of meltwater which was probably drained immediately to the sea, but due to the regional bedrock topography some of it was trapped in glacier damned lagoons. Catastrophic floods have been described from these lagoons by Tómasson (1993). He reported geomorphologic evidence for these floods occurring near the end of the last glaciation in the basin of the Hvítá river in southern Iceland, hinting at the same pattern of deglaciation in the central highlands. This catastrophic change could also be enhanced by volcanism and sub-glacial geothermal activity that could have accompanied the unloading of the land caused by deglaciation. As a result, volcanism could have enlarged the ice-dammed lakes that caused the floods along the Hvítá river, in particular the Leggjabrjótur eruption (Fig. 1) at the end of the Búdi stage (Kjartansson, 1964).

Kaldal and Víkingsson (1991) conclude that the central highlands of Iceland were mostly ice free between 8 and 7 ka BP. This is supported by ^{14}C dating of lacustrine sediments in the area to the northwest of Myrdalsjökull, indicating an open lake about 9.4–7.8 ka BP and the vast Thjórsár lava dated to 7.8 ka BP (Kjartansson, 1964; Hjartarson, 1988, 1994), which erupted sub-aerially somewhere to the southeast of Thórisvatn (Vilmundardóttir, 1977) and is located well within the Búdi stage. They assume that all the end moraines in the southern highlands are younger than the Búdi stage and the same could also apply to the end moraines to the north of the present watershed, indicating deglaciation in the Preboreal. It is therefore inferred that all the moraines of the interior are probably younger than 9.4 ka BP and older than 7.8 ka BP.

Einarsson (1961, 1963, 1968, 1975) made generalised pollen diagrams for the Holocene, based on 20 different localities in Iceland, hinting at climatic change. A birch 'free' zone between 10 and 9 ka BP was followed by a birch woodland phase thought to indicate a warmer and dryer Boreal type of climate lasting to about 7 ka BP. Climate change towards more humid and cooler Atlantic type was inferred as a result of the apparent extension of the bogs over the woodlands, lasting until about 5 ka BP. Climatic improvement to warmer and drier conditions was indicated by the spread of the birch forests in the bogs. Around 2.7 ka BP re-expansion of the bogs is thought to indicate climate deterioration towards cooler and more humid conditions. Einarsson suggested that the temperature was at least 2–3°C higher during the warmer (birch) periods.

Studies of lake sediments from Vasari (1972, 1973) and other peats by Okko (1956), Straka (1956), Bartley (1973), Schwaar (1978), Pahlson (1981) and Hallsdóttir (1982, 1987, 1990) fit with some aspects of Einarsson's model but reveal some notable discrepancies. While Einarsson argued that the birch first expanded in Iceland ca. 9 ka BP, Vasari (1972, 1973) and Hallsdóttir (1987) argued for a date little before 8 ka BP. The different interpretations could be due to local variations, or as Ingólfsson (1991) has pointed out, the lack of radiocarbon dates from the lowest part of the Holocene biostratigraphical sequence.

Correlations between the various Greenland ice core results and the environmental record in Iceland are highly speculative at this stage, but not impossible. According to Meese *et al.* (1994) from the GISP2 project, cold periods are thought to have occurred between 8.8 to 8.0 ka cal. BP (very dramatic isotope low), 7.75 to 6.45 ka cal. BP, (this section includes some breaks in the pattern), and 4.35 to 3.95, 3.75 to 3.55, and 2.45 to 1.95 ka cal. BP. Meese *et al.* (1994) consider these periods to be similar to the LIA of recent centuries and they may indicate that such cool periods occurred throughout the Holocene. In Iceland evidence for cold periods, based on conventional dating, in the early Holocene have been reported by Thórarinsson (1966) and Dugmore (1987). Dating of tephras and soils, immediately on top of tills, around Sólheimajökull indicates a concentration of ages around 6.8 ka BP (Dugmore, 1987). This broadly correlates with similar dates of Thórarinsson (1966) in front of Hagafellsjökull eystri where he found tills only somewhat older than the H_5 tephra layer, dated to about 6 ka BP (Larsen and Thórarinsson, 1977; Vilmundardóttir and Kaldal, 1982; Häberle, 1991). Around Eyjafjallajökull, well beyond any later Holocene glacier activity, Dugmore (1987) reported basal date from around 8.8 to 8.0 ka BP indicating deglaciation sometime earlier.

According to Bartlein *et al.* (1995) a gap of approximately 1000 years occur between calibrated and

TABLE 1. Reported stages of Holocene glacier advances in Iceland

Southern Iceland	Local names	Northern Iceland	Local names
7–4.5 BP	Drangagil stage	Before 5 ka BP	Vatnsdalur I
Before 3.1 ka BP	Hólsárgil stage	Around 4.2 ka BP	Baegisárdalur I
1.2–1.4 ka BP	Ystagil stage	3.2–3 ka BP	Vatnsdalur II
		Around 2 ka BP	Barkárdalur I
		Around 1.5 ka BP	Barkárdalur II
		Around 1 ka BP	Baegisárdalur II

conventional dates between 10 ka to 5 ka BP. By applying this calibration to till dating from the early Holocene in Iceland and then comparing to known cold periods reported in the GISP2 ice core (Meese *et al.*, 1994) shows that the two sets of data do not match. This can be shown, for example, by linking till deposits from around 6.8 ka BP (Dugmore, 1987) or ca. 7.8 ka cal BP, with the cold period reported in the GISP2 ice core between 8.8 ka to 8 ka cal BP. If following calibrations, and this link is accepted, a lag of about 200 years is implied between the two areas.

THE NEOGLACIATION IN ICELAND

The earliest ideas of a Pre-historical glaciation in Iceland comes from Eythórsson (1935) based on his studies on Drangajökull, north-western Iceland. He concluded that, according to his observations on Icelandic glaciers and their terminal and lateral moraines, an advance must had taken place sometime between the last glaciation and historical time. The first scientific approach to this problem was taken by Thórarinsson (1949) when he argued that in front of some of the glacier outlets of Vatnajökull, terminal moraines existed "which might indicate that in early Subatlantic time these glaciers advanced a little further than during the last few centuries" (Thórarinsson, 1949: p. 250). In later papers Thórarinsson (1956, 1958) studied the Öraefajökull region and concluded, with the help of tephrochronology, that the Stóralda moraine and Kvíármyrar–Kambsmyr-arkambur moraine complex were older than the Öraefa-jökull eruption of 1362 (Ö1362). Application of tephrochronology to date the moraines of Hálsajökull, an outlet from Snaefell, a small ice cap north-east of Vatnajökull, indicated similar results (Thórarinsson, 1964; Fig. 1). Thorarinsson stated that the outermost moraine was older than the Ö1362 tephra layer and therefore probably pre-historical in age. A better minimum date could be produced by further tephrochronological studies using geochemical fingerprinting of constituent tephra grains, a method not available to Thórarinsson. In his observations, Thórarinsson suggested the age of these advances was Subatlantic, because of the then current model from Einarsson (1963) that suggested abrupt cooling around 2.7 ka BP. No other period of cooling was known at that time to cause the glacier expansions.

New data from Sólheimajökull (Dugmore, 1987, 1989), Tröllaskagi (Stötter, 1994), Skálafellsjökull (Sharp and Dugmore, 1985) and Skaftafellsjökull (Thompson, 1988; Fig. 1), hints at more extensive glaciation then previously thought. Dugmore (1987, 1989) study of Sólheimajökull, an outlet from the southern part of Myrdalsjökull, resulted in a more complicated glacier history than previously thought (Fig. 1). The oldest advance, called the Drangagil stage, is dated to older than 4.5 ka BP but younger than 7 ka BP (Table 1). Two other pre-historical stages were identified; Hólsárgil (>3.1 ka BP) and Ystagil (1.4–1.2 ka BP). The Ystagil stage correlates broadly with a cold spell detected in the Créte ice core in central Greenland (Sveinbjörnsdóttir, 1993) and the deterioration of climate observed by Pahlson (1981) in a pollen study in southern Iceland. The Drangagil and Hólsárgil stages broadly correlate with the GISP2 data (Meese *et al.*, 1994) but as in the early Holocene, environmental changes in Iceland seem to lag behind changes in Greenland recorded in the cores.

Dugmore and Sugden (1991) explained the relative extent of these different stages of Sólheimajökull by ice-divide migration during cycles of ice-cap growth and decay. They argued that a thin icefield with topographically controlled ice flow resulted in the glacier draining more of the ice cap and so becoming more advanced than neighbouring glaciers. During phases when the icefield thickened to form an ice cap, it is proposed that the ice divide migrated towards the principal precipitation supply from the Atlantic, resulting in reduced flow to Sólheimajökull and a reduction in glacier size. This explanation of glacier fluctuations is the first of its kind in Iceland highlighting the possibility of non-climatic factors determining the scale of glacier fluctuations. Although the timing of the fluctuations could still relate to climatic changes, the spatial pattern could be primarily determined by topography and precipitation gradients.

According to Sharp and Dugmore (1985) Eyjabakka-jökull and Skálafellsjökull, both outlets from Vatnajökull, advanced during the Holocene, although their mid-Holocene advance never exceeded the LIA moraines. Skálafellsjökull, a non-surging glacier from the south-eastern part of Vatnajökull (Fig. 1), shows an advance of a maximum date of about 5.7 ka BP but Eyjabakkajökull, a surging glacier from the north-eastern part of Vatnajökull (Fig. 1), shows a maximum extension about 6.9 ka BP.

Häberle (1991, 1994) and Stötter (1990, 1991, 1994) have reported advances of corrie glaciers in Buegisárdalur, Barkárdalur, Hörgárdalur, Skídadalur and Svarfadardalur all of which are located on the Tröllaskagi peninsula, northern Iceland (Fig. 1). As in southern Iceland, the glacier events are bracketed by ^{14}C dating and with the

TABLE 2. A tentative correlation of Holocene glacier advances in Iceland

Time of glacier advance (BP)	Southern Iceland	Bracketing dates	Northern Iceland	Bracketing dates
	Ystagil	900 A.D.[a]		
>1.2 ka <1.5 ka		1.5 ka BP	**Barkárdalur II**	1.555±90 BP
	Kvíarjökull	720-800±390 AD		(max.)
			Barkárdalur I	1.835 ka BP
Around 2 ka	**Kvíárjökull**	2.040±80 BP (min)		2.24 ka BP
Around 3 ka	**Hólsárgil**	2.660±60 BP	**Vatnsdalur II**	2.8 ka BP[c]
		3.480±60 BP		3.470 BP
>4 ka<7.000	**Drangagil**	7.210±60 BP	**Baegisárdalur I**	4.275 ka BP
		4.1 ka BP		4.700±205 BP
	Skálafellsjökull	5.710±90 BP	**Vatnsdalur I**	6 ka BP[d]
		1362 A.D.[b]		

Bold letters indicate tentatively correlated stages.
[a] Landnám tephra from around 900 AD.
[b] Ö1362 tephra.
[c] H_3 tephra.
[d] H_5 tephra.

application of tephrochronology (Table 1). The Barkárdalur II and Baegisárdalur II broadly correlate with a cold period presented from the Créte ice core in central Greenland (Sveinbjörnsdóttir, 1993) and the Baegisárdalur I, Vatnsdalur II and Barkárdalur I broadly correlate with the GISP2 data (Meese *et al.*, 1994) but showing leads and lags like in southern Iceland. Stötter (1994) argued that these results give only the first approximation of a more complex pre-LIA glacial history (Table 1).

The Late Holocene

Black (1990) studied the moraine sequences in front of Kvíárjökull, an outlet from southeastern part of Vatnajökull (Fig. 1) improving the work of Thórarinsson (1956). By applying tephrochronology, radiocarbon dating and lichenometry he argued that three stages of Holocene advances occurred, which he called the Little Ice Age stage, Pre-Settlement stage and Subatlantic stage. Of interest here is an advance which was constrained by tephrochronology to 720 A.D. ±395 and the Subatlantic stage, dated with ^{14}C and tephrochronology to minimum 2040±80 ^{14}C years BP. These data can be correlated to the Ystagil/Barkárdalur II stage and Barkárdalur I, respectively. A study relating a maximum glacier advance to the Subatlantic have been conducted by Gudmundsson (in press) at Klofajökull, an outlet of Eiríksjökull west central Iceland (Fig. 1). The results indicate a pre-settlement glaciation, deduced from the age of the Hallmundarhraun lava which flows around the outermost extension of the outermost moraine in front of the Klofajökull outlet glacier. The lava is dated to the settlement time, around 900 A.D. (Jóhannesson, 1989), and therefore gives a minimum relative date for this moraine. A moraine that pre-dates the historical time is located at Kaldalón, one of the outlets of Drangajökull, northwest Iceland (Fig. 1). The age of this moraine has never been established. Table 2 shows a compilation of known Holocene glacier advances in Iceland. On chronological grounds, Baegisárdalur I or Vatnsdalur I in northern Iceland can be correlated with the Drangagil stage and the minor advances of Skálafellsjökull, in southern Iceland. Likewise, Hólsárgil can be correlated with Vatnsdalur II; the Subatlantic moraines of Kvíárjökull with Barkárdalur I; and the Ystagil with the Barkárdalur II stages. The implication is that a regional pattern of glacier fluctuations in Iceland exists during the Holocene. Similar coincidence of environmental changes in the terrestrial environment occurs. As can be seen in Fig. 2, which summarises the knowledge of the Holocene environmental history of Iceland at present, changes in permafrost activity (Hirakawa, 1989; Friedman *et al.*, 1971), soil formation (Thórarinsson, 1961; Stötter, 1994; Dugmore and Buckland, 1991; Dugmore and Erskine, 1994), vegetation cover (Einarsson, 1963; Vasari, 1972, 1973; Hallsdóttir, 1987, 1990; Caseldine, 1991; Caseldine and Hatton, 1994) and landslide activity (Whalley *et al.*, 1983) broadly correlate. Stötter (1994) presented a ^{13}C isotope record extracted from cellulose in a peat core from a site in Vesturárdalur on Tröllaskagi, northern Iceland. The temperature interpretations (Fig. 2) indicate a short, but sharp, decline of temperature around 5 ka BP. These temperature changes match reasonably well with the record from Meese *et al.* (1994) from the GISP2 project. Stötter's record contrasts with Einarsson (1961, 1963) temperature curve which suggests relatively warm period about 5 ka BP but notes a low concentration of birch in pollen sections. A fairly good match appears to exist between glacier fluctuations, geomorphic processes and temperature change in general, although some lead and lag times are apparent as can be expected. The most dramatic change in the environment seems to be around 5 ka BP. The most likely explanation is a change in climate around this time. Koç *et al.* (1993) have studied diatoms in sediment cores to reconstruct the surface oceanic conditions in the Greenland, Iceland and Norwegian (GIN) seas. They recorded the first half of the Holocene as the warmest period during the last 13.4 ka BP but the second half was characterized by a cooling trend. This

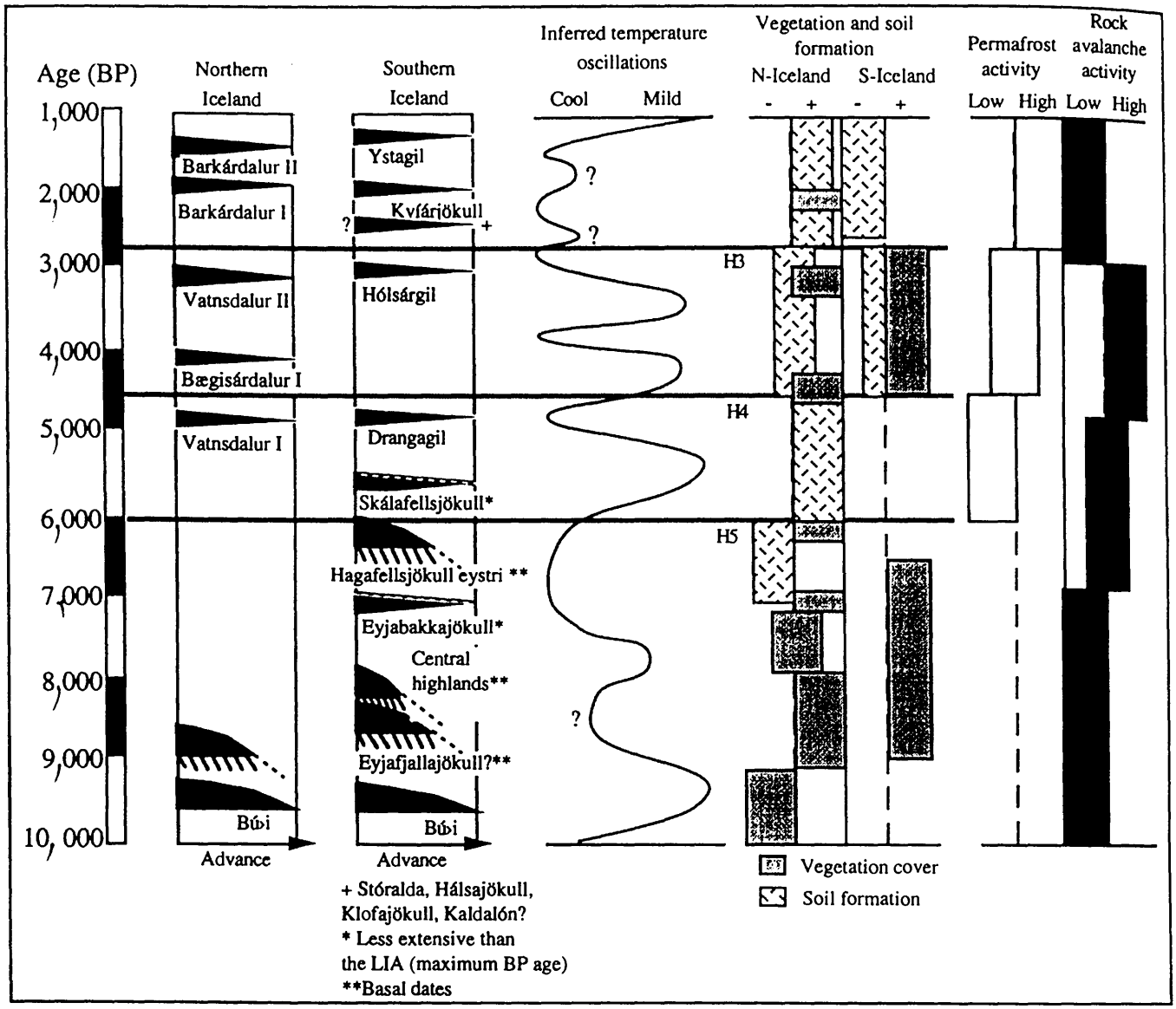

FIG. 2. Environmental changes during the Holocene in Iceland according to present knowledge. Frequent changes in the environment occur throughout the Holocene in Iceland. The temperature graph is indicative of tendancies only showing the general changes in the given period based on the observed environmental record and an isotope analysis from Stötter (1994) in northern Iceland. Major volcanic eruptions and other catastrophic events might influence the environmental record, especially vegetation and soil cover (e.g. Thórarinsson, 1944, 1961), regardless of climate. The tephra layers are used as time lines, not stratigraphic markes. Changes in vegetation are based on pollen studies from Einarsson (1963); Vasari (1972, 1973); Hallsdóttir (1987, 1990); Caseldine (1991); Caseldine and Hatton (1994). The changes in permafrost activity are based on Hirakawa (1989) and Friedman *et al.* (1971), soil formation on Thórarinsson (1961); Stötter (1994); Dugmore and Buckland (1991) and Dugmore and Erskine (1994) and the landslide activity was based on Whalley *et al.* (1983). Data showing glacier fluctuations comes from Sharp and Dugmore (1985); Dugmore (1987, 1989); Black (1990); Häberle (1991, 1994); Stötter (1990, 1994); Ingólfsson and Norddahl (1994) and Gudmundsson (*in press*).

matches with wider environmental data from Iceland. The most plausible cause of climate change in Iceland during the Holocene could therefore be connected to these observed changes in the oceanic currents.

The Little Ice Age (LIA)

The term 'Little Ice Age' (LIA) has been widely used to describe the cold period between the Medieval period and the warming that began at the beginning of the 20th century (Grove, 1988). During this time, many of the glaciers of the world expanded to more advanced positions than in previous centuries. In Iceland, glacier fluctuations during the LIA have been studied on the big outlets of Vatnajökull, Myrdalsjökull and Eyjafjallajökull in the southern part of the country and the small alpine glaciers on the Tröllaskagi peninsula, in northern Iceland (Fig. 1). The earliest scientific study of the maximum glaciation in the LIA comes from Thórarinsson (1936) where he argued that the outermost moraines in front of some of the outlets of Vatnajökull were probably from glacier maxima in historical time and that they probably represented the maxima of postglacial time. Further studies by Thórarinsson (1956, 1964, 1966) also indicated maximum Holocene glacier development during the later half of the 19th century. Thórarinsson's approach

included the use of archival data, maps, travelling books and other written sources that noted frontal positions of a glacier. He also integrated these sources with original fieldwork using tephrochronology that enabled him to date landforms in proglacial areas.

The dating techniques were expanded when Jaksch (1970, 1975) introduced lichenometry as a relative dating method of moraines in Iceland. The limitations of this technique have been assessed in general by Innes (1985) and in Iceland by Gordon and Sharp (1983); Maizels and Dugmore (1985) and Gudmundsson (1992). Different growth rates between regions and different altitudes above sea level (Gudmundsson, 1992) accompanied with severe environmental limits (Maizels and Dugmore, 1985; Caseldine, 1990) limit the application of the technique in Iceland. Lichenometry is often limited to the last 150 years or so because of environmental factors causing a re-population of most of the lichen thalli. For example, Maizels and Dugmore (1985) suggest a limit of 160 years in the southern part due to rock weathering. Limiting factors could also include aspect and exposure or even volcanic activty in the form of tephra acting as a pollutant inhibiting lichen growth. Gudmundsson (1992) has pointed out that in the north Iceland mean annual temperature is lower and the measurement sites are located at higher altitudes than the southern part and that this could result in regional variations in growth rate (Innes, 1985). Slow growth rates has been reported on Tröllaskagi by Kugelman (1990, 1991; Fig. 1) and Caseldine (1990) but this does not explain why older lichenometrical dates can be obtained in the northern part. The most probable cause is different substrate stability and rock weathering patterns between these two parts of Iceland, with northern sites being typified by more resistant basaltic rocks rather than the palagonite in the south, and having a more arid climate. In Scandinavia the use of lichenometry seems to be applicable for substrates up to 200 years old (e.g. Erikstad and Sollid, 1986) and even to 400 years old (Karlén, 1973) which does suggest local environmental constraints of the lichen growth in Iceland.

According to recent studies where lichenometry and tephrochronology were applied successfully together, the early maxima of the LIA glacial advances in southern Iceland was ca. 1850 and ended in the 1930s (Gordon and Sharp, 1983; Snorrason, 1984; Maizels and Dugmore, 1985; Thompson and Jones, 1986; Thompson, 1988). In the northern and western parts of Iceland the LIA glacier expansion in the middle of the 18th century and lasted until the 1940s (Caseldine, 1983, 1985, 1987, 1990; Hjort *et al.*, 1985; Häberle, 1991; Kugelman, 1990, 1991; Gudmundsson (*in press*). However Häberle (1991) questioned the oldest stage dated ca. 1744 A.D., because it was beyond the calibrated area of the lichen curve he used. At least four stages can be defined in the south vs. at least eight stages in the north and west of Iceland (Fig. 3). The overall pattern is therefore somewhat different. Although about 100 years difference exists between the first glacier advances of the LIA in the northern and the southern parts of the island, a certain synchroneity of glacier fluctuations existed during the late LIA.

Synchronous glacier fluctuations are also observable in modern historical records. Similar overall patterns occur, with nearly all glaciers measured retreating from the 1930s to 1990s. There is one major exemption, namely a group of outlets from Eyjafjalla and Myrdalsjökull (Fig. 1). They began to re-advance in the 1960s and are were still slowly advancing in 1992 (Sigurdson, 1993).

Complementary palaeoclimatic data

Incidence of sea-ice gives an effective proxy indication of temperature in Iceland (Bergthórsson, 1969; Ogilvie, 1984, 1991). The hypsothermal line, drawn from the sea-ice records, shows a long period of cooling lasting form the beginning of the 12th century until the start of the 20th. This was confirmed and refined by the rigorous work of Ogilvie (1984, 1991) and the northern hemisphere temperature index (Hammer *et al.*, 1980). A somewhat similar pattern, but with some notable mismatches, occurs in the GISP2 ice core where the cold periods are reported to around A.D. 1200, 1500 and 1800 but higher temperatures around A.D. 1400 and 1700 (Meese *et al.*, 1994). The mismatch is most apparent around A.D. 1500 and 1700 when the sea-ice data and the northern hemisphere temperature index indicate cold periods (Bergthórsson, 1969; Ogilvie, 1984; Hammer *et al.*, 1980). The cold spell around 1200 A.D. caused glacier advances in Iceland (Dugmore, 1987; Häberle, 1991, 1994) and therefore raises the question of when the LIA began. The present study suggests that it be defined according to the cold period between ca. 1600 A.D. and 1900 A.D. based on the temperature curve presented by Bergthórsson (1969), Ogilvie (1984, 1991), Hammer *et al.* (1980) and Meese *et al.* (1994) because this period is not interrupted by a major warming. The glacier advances that began in the mid 18th century in Iceland were a consequence of this prolonged cool period. According to Sveinbjörnsdóttir (1993) and Meese *et al.* (1994) a cold period began just before 1000 A.D. and lasted until ca. 1200 A.D. This correlates well with the Baegisárdalur II/ Sólheimajökull advances around the same time. The historical records, mainly from northwestern Europe, describe a Medieval Warm Period (MWP) between 800 and 1300 A.D. (Folland *et al.*, 1990) but this view is modified by recent results from Grove and Switzur (1994). Their results indicate a global glacial event between about 900 and 1250 A.D. which is in good agreement with the Icelandic data on a Medieval glacier advance. This indicates at least two periods of glacier advance can be defined in Iceland in the historical times, the Medieval Glacier Advance (MGA) and the Little Ice Age Glacier Advance (LIAGA). The reasons for other glaciers in Iceland not showing advances in Medieval time could be either that the evidence is hidden by soils or some factors such as topographic pinning points (Mercer, 1961) inhibited advance.

Alternative perspectives of the LIA can be gained by assessing rock avalanche and permafrost activity in historical time (Jónsson, 1957; Friedman *et al.*, 1971; Fig. 3). Incresed permafrost formation seems to have began when the climate got colder around 1000

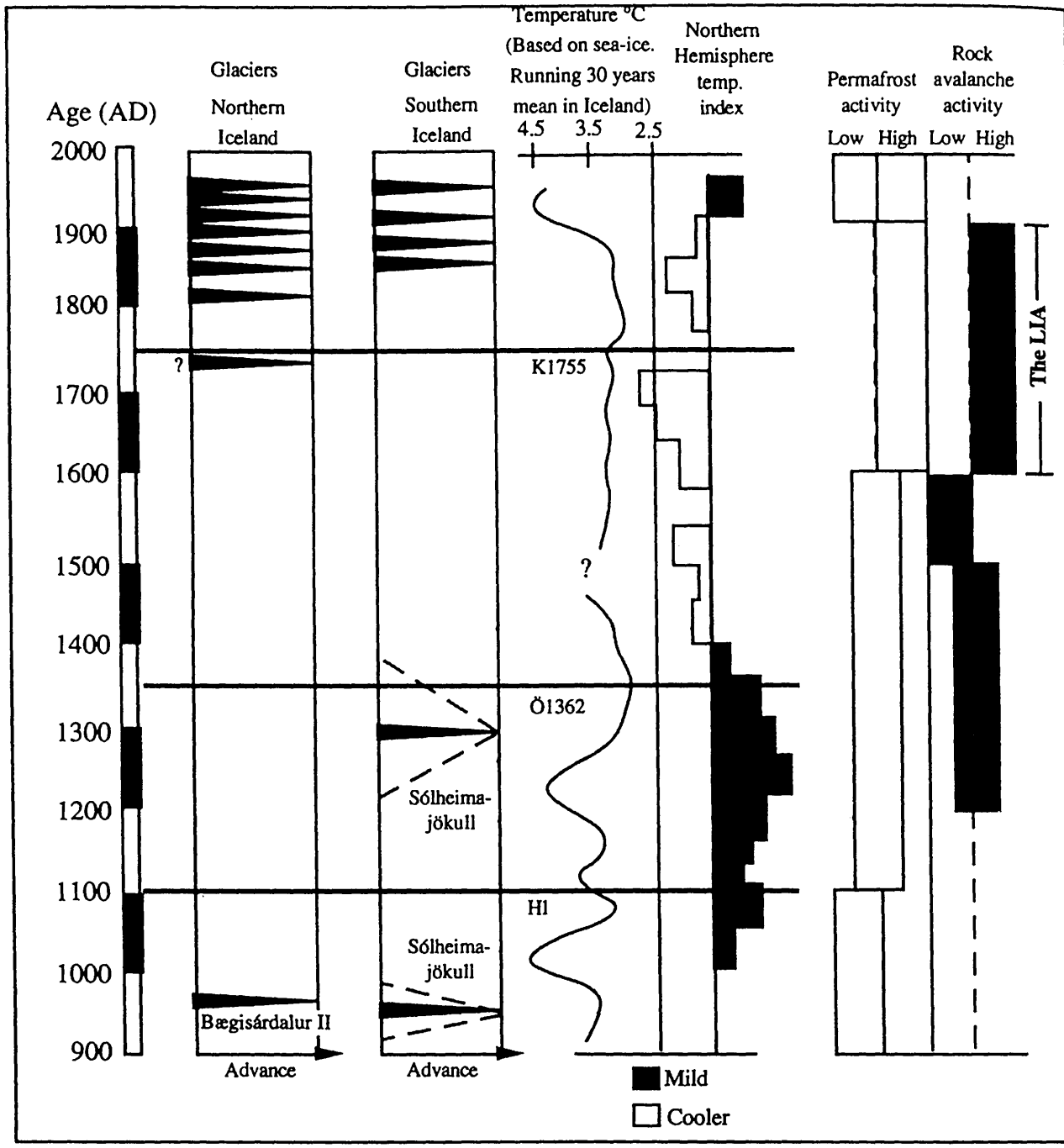

FIG. 3. Environmental changes during the historical time in Iceland according to present knowledge. Note that permafrost activity and rock avalanche activity broadly follows the temperature cooling of the LIA. As in Fig. 2., the tephra layers are used as time lines. The data on glacier fluctuations comes from Gordon and Sharp (1983); Snorrason (1984); Maizels and Dugmore (1985); Thompson and Jones (1986); Dugmore (1987); Thompson (1988); Caseldine (1983, 1985, 1987, 1990); Hjort *et al.* (1985); Häberle (1991); Kugelman (1990, 1991); Gudmundsson (*in press*). Temperature changes come from Bergthórsson (1969), based on incidence of sea-ice, and Hammer *et al.* (1980) and permafrost and rock avalanche activity from Jónsson (1957), and Friedman *et al.* (1971).

A.D. and escalated until the end of the LIAGA. This prolonged activity could be due to the long response time of permafrost to climate change or the warm periods during this time were not sufficient to inhibit the permafrost activity. Rock avalanche activity shows a similar pattern, increasing from 1200 A.D., and showing very high activity between ca. 1700 and 1900 A.D. In 30% of the cases, the rock avalanches coincide with years when heavy precipitation occurred during the summer, the autumn season, and in the winter. The occurence of rock avalanches was especially pronounced in the latter part of the period recorded, hinting at increasing precipitation, reaching a climax when the glaciers began to advance in the middle of the 1750s.

Human impact on vegetation and soils has been profound from the settlement of Iceland (Thórarinsson, 1961) and therefore the proxy climate signals tend to be heavily modified. Studies show that around the settlement of Iceland, at ca. 900 A.D., soil erosion in Iceland increased dramatically on a regional scale (e.g. Thórarinsson, 1944; Einarsson, 1961; Hallsdóttir, 1987; Dug-

more, 1987) and many distinct local patterns are apparent (Thórarinsson, 1961; Dugmore and Buckland, 1991; Dugmore and Erskine, 1994). Dugmore and Buckland (1991) argued that impact started early in most ecologically marginal upland areas with soil erosion developing at succeeding lower and less marginal locations through time. This pattern was reinforced by later work in the low lying area west of Eyjafjallajökull (Dugmore and Erskine, 1994). A general increase in the sediment accumulation began post ca. 900 but after 1341 A.D. local slopewash began, followed by widespread change beginning after 1510 A.D., linked to extensive breaching of vegetation cover. The low level pattern 'fits' general curves but Dugmore and Erskine (1994) show that this is probably only the most recent stage of a process beginning at higher altitude during the Settlement Period.

Discussion

In the light of present knowledge, the termination of the last inland ice sheet of Iceland began somtime prior to 13 ka BP (Ingólfsson and Norddahl, 1994). There was a cold spell, causing a glacier still-stand, around 9.7 ka BP (Ingólfsson and Norddahl, 1994). By 7.8 ka BP (Kaldal and Víkingsson, 1991) the inland ice sheet was probably almost gone, leaving the prototypes of current glaciers on highest mountains.

Coincidence of glacier fluctuations is considerable in Iceland during the Holocene (Table 2). The timing of the advances over wide areas in the late Holocene seems to match closely indicating that regional climatic factors were the primary cause. Therefore, a revised model of the Holocene glacier fluctuation is put forward here (Figs 2–4). One of the major implications of this model is firstly that it introduces the onset of a Neoglaciation around 5 ka BP and secondly it implies that frequent glacier fluctuations occurred throughout the Holocene in Iceland, suggesting that the present glaciers never disappeared during the Holocene.

The knowledge of the environmental history of Iceland earlier in the Holocene is relatively limited compared to the Alps and in northern Scandinavia, so some of the apparent correlation may be an artefact of the data sets. The paradigm of a 'Subatlantic glaciation' in Iceland has proved to be based on limited data and should be viewed with caution. Confirmation of glaciers that advanced during the Subatlantic is only known from Kvíárjökull (Black, 1990) and Barkárdalur (Häberle, 1994).

A comparison between Iceland, northern Scandinavia (Karlén, 1988) and the European Alps (Röthlisberger, 1986) is made in Fig. 4 and shows no clear links. No glacier advance has been found in Iceland, northern Scandinavia and in the European Alps between ca. 1300 A.D. and 1700 A.D. This might indicate that this period was not favourable for glacier expansion probably because it was milder compared to the cold spell in Medieval time and during the LIA. There is a reasonably good correlation between the Medieval glacier advance in all the three regions which substantiates a global glacial advance as suggested by Grove and Switzur (1994).

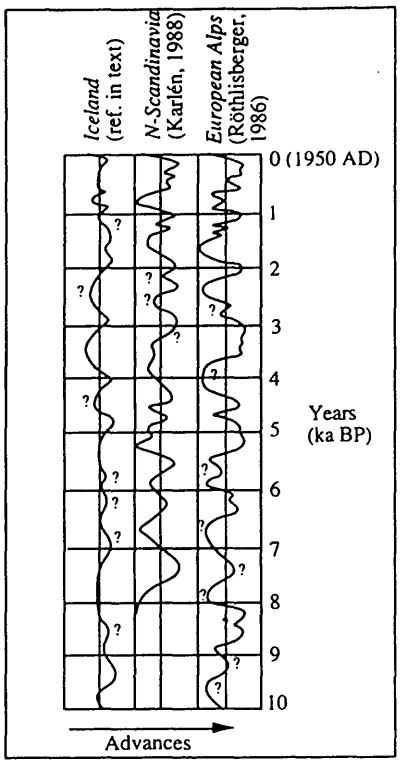

FIG. 4. A comparison of glacier fluctuations during the Holocene in Iceland, N. Scandinavia and the European Alps. In Iceland, the pattern indicates an onset of a Neoglaciation arround 5 ka BP. The model implies high glacier activity during the Holocene epoch in Iceland. The correlation between Iceland vs. N. Scandinavia and the European Alps is speculative at this stage.

Mismatches between the various Greenland ice core projects and the environmental record in Iceland are important to identify because of possible different responses to environmental change. Recently, an unambiguous correlation was made between the Greenland GRIP ice core and tephras originated from Iceland (Grönvold *et al.*, 1995). This is the first step in establishing an isochrone between Iceland and Greenland and will definately help to better understand the environmental history of Iceland. In order to compare the data sets at present, calibration of conventional dates is necessary. If conventional radiocarbon dates from Icelandic sites during the Holocene are calibrated using a simple relationship between equivalent calender (or calibrated) and radiocarbon years before present (Bartlein *et al.*, 1995), leads and lags become apparent. In most cases, environmental changes in Iceland tend to occur at least 200 years later than in Greenland. This might be explained in terms of environmental response time to climatic change. The most plausible explanation of climate change in Iceland are shifts in surface ocean conditions such as reported by Koç *et al.* (1993) throughout the Holocene.

Conclusions

The first glacier advance or still-stand of the Holocene time occurred in the early Preboreal ca. 9.8–9.6 ka BP and is called the Búdi stage (Hjartarson and Ingólfsson, 1988). It probably terminated in the central highlands around 7.8

ka BP when the current dirstribution of glaciers became established. Glacier advances occurred around 5 ka BP, identified in the Tröllaskagi peninsula, north Iceland, and south Iceland. The advances broadly correlate with temperature oscillations, but there are some notable mismatches. By comparing other proxy data of climatic change such as permafrost activity, rock avalanches activity, soil erosion and vegetation change, a distinct pattern of more frequent temperature oscillations can be observed in the latter part of Holocene compared to the earlier part. One climatic explanation could be the more frequent changes in oceanic currents around Iceland during the latter part of the Holocene.

The 'Subatlantic' glaciation in Iceland is poorly defined. At present only two glacier advances may be traced to this time, the Kvíárjökull advance in southern Iceland and the Barkárdalur I advance in northern Iceland, both occurring around 2 ka BP. Overall the data on glacier movement suggests that the onset of the Neoglaciation was around 5 ka BP. Evidence of a Medieval glacier advances have been found in Iceland suggesting a more complicated pattern of environmental change during this time than previously thought. This echoes with Ogilvie (1991) results which reported similar complexities in the climate during Medieval time. This Medieval glacier advance is in broad agreement with the Alps and in Scandinavia but the LIA optimum seem to be at least a decade ahead of Iceland in most cases (Grove, 1988). The first advances seem to have begun in the middle of the 18th and 19th century in northern and southern Iceland respectively, lasting well into the first decades of the 20th century.

ACKNOWLEDGEMENTS

I would like to thank Dr Andrew J. Dugmore and Professor David E. Sugden, Department of Geography, University of Edinburgh for comments and observations on the manuscript which also greatly benefited from the input of Dr Ólafur Ingólfsson and an anonymous reviewer.

REFERENCES

Áskellson, J. (1934). Quartergeologische Studien von Island I. *Geologiska Föreningen i Stockholm Förhandlinger,* **56,** 596–618.

Bard, E., Arnold, M., Fairbanks, R.G. and Hamlin, B. (1993). ^{230}Th, ^{234}U and ^{14}C ages obtained by mass-spectrometry on corals. *Radiocarbon,* **35,** 191–199.

Bartlein, G.J., Edwards, M.E., Shafer, S.L. and Baker, E.D., Jr (1995). Calibration of radiocarbon ages and the interpretation of paleoenvironmental records. *Quaternary Research,* **44,** 417–424.

Bartley, D.D. (1973). The stratigraphy and pollen analysis of peat deposits at Ytri Bægisá near Akureyri, Iceland. *Geologiska Föreningens i Stockholms Förhandlingar,* **95,** 410–414.

Bárdarson, G.G. (1923). Fornar sjávarminjar vid Borgarfjörd og Hvalfjörd. *Societas Scientiarum Islandica, Rit,* **I,** 116.

Bergthórsson, P. (1969). An estimate of drift ice temperature in Iceland in 1000 years. *Jökull,* **19,** 94–101.

Björck, G.S., Ingólfsson, Ó., Haflidason, H., Hallsdóttir, M. and Anderson, N.J. (1992). Lake Torfastadavatn. a high resolution record of the North Atlantic Ash zone I and the last glacial-interglacial environmental change in Iceland. *Boreas,* **21,** 15–21.

Björnsson, H. (1988). Hydrology of ice caps in volcanic regions. *Societas Scientarium Islandica, Rit,* XLV, Reykjavík.

Black, T.A. (1990). The Holocene fluctuation of the Kvíárjökull Glacier, southeastern Iceland. Unpubl. MA thesis, University of Colorado.

Caseldine, C.J. (1983). Resurvey of the margins of Gljúfurárjökull and the chronology of recent deglaciation. *Jökull,* **33,** 111–118.

Caseldine, C.J. (1985). Survey of Gljúfurárjökull and features associated with a glacier burst in Gljúfurárdalur. *Jökull,* **35,** 61–68.

Caseldine, C.J. (1987). Neoglacial Glacier Variation in Northern Iceland. Examples from the Eyjafjördur area. *Arctic and Alpine Research,* **19,** 296–304.

Caseldine, C.J. (1990). A review of dating methods and their applications in the development of chronology of Holocene glacier Varioation in Northern Iceland. *In*: Caseldine, C.J., Häberle, T., Kugelmann, O., Munzer, U., Stötter, J. and Wilhelm, F. (eds), *Geomoprhologische und landschaftsgeschichtliche Untersuchungen in Nordisland. Munchen Geogr. Abl.* B8, pp. 59–82.

Caseldine, C.J. (1991). Lichenometric dating, lichen population studies and Holocene glacial History of the Tröllaskagi, Northern Iceland. *In*: Maizels, J.K. and Caseldine, C.J. (eds), *Environmental Change in Iceland. Past and Present,* pp. 219–223. Dordrecht.

Caseldine, C.J. and Hatton, J. (1994). Interpretation of Holocene climatic change for the Eyjafjördur area of Northern Iceland form pollen data. Comments and preliminery results. *In*: Stötter, J. and Wilhelm, F. (eds), *Environmental Change in Iceland. Munchener Geog. Abl.* B12, pp. 41–63.

Dansgaard, W., White, W.C. and Johnsen, S.J. (1989). The abrupt termination of the Younger Dryas climate event. *Nature,* **3,** 532–534.

Dugmore, A.D. (1989). Tephrochronological studies of Holocene glacier fluctuations in south Iceland. *In*: Oerlemans (ed.), *Glacier Fluctuations and Climatic Change,* pp. 37–55. Kluwer. Dordrecht.

Dugmore, A.D. and Sugden, D.S. (1991). Do the anomalous fluctuation of Sólheimajökull reflect ice-devide migration?. *Boreas,* **20,** 105–113.

Dugmore, A.D. and Erskine, C.C. (1994). Local and regional pattern of soil erosion in Southern Iceland. *In*: Stötter, J. and Wilhelm, F. (eds), *Environmental Change in Iceland.* pp. 41–63. *Munchener Geog. Abl.* B12.

Dugmore, A.J. (1987). Holocene glacier fluctuation around Eyjafjallajökull, South Iceland. Unpubl. Ph.D thesis, University of Aberdeen, p. 114.

Dugmore, A.J. and Buckland, P. (1991). Tephrachronology and late Holocene soil erosion. *In:* Maizels, J.K. and Caseldine, C.J. (eds), *Environmental Change in Iceland. Past and Present,* pp. 147–161. Dordrecht.

Einarsson, Th. (1961). Pollenanalytische Untersuchungen fur spät- und postglazialen Klimatgeschichte Islands. *Sönderveroffentichungen des Geologischen Institutes der Universitat Köln,* 6.

Einarsson, Th. (1963). Pollen-analytical studies on vegetation and climate history of Iceland in late and post-glacial times. *In:* Löve, A. and Löve, D. (eds), *North Atlantic Biota and their History,* pp. 255–365. Pergamon.

Einarsson, Th. (1967). Zu der Ausdehung der weichselzeitlichen vereisung Nordislands. *Sönderöffentlichungen des Geologischen Institutes der Universitat Köln,* **1,** pp. 167–173.

Einarsson, Th. (1968). *Jardfraedi, saga bergs og lands.* Mál og Menning. Reykjavík.

Einarsson, Th. (1975). Um myndunarsögu íslensks myrlendis. *In:* Gardarson, A (ed.), *Votlendi,* pp. 15–21. Landvernd. Reykjavík.

Erikstad, L. and Sollid, J.L. (1986). Neoglaciation in South Norway using Lichenometric methods. *Norsk geografisk Tidskrift*, **40**, 85–105.

Eythórsson, J. (1935). On the variation of Glaciers in Iceland I. Drangajökull. *Geografiska Annaler*, **17**.

Folland, C.K., Karl, T. and Vannikov, Y (1990). *The IPCC (Intergovernmental Panel on Climatic Change) Scientific Assessment*. Hougthon, J.T., Jenkins, G.J. and Ephraunms, J.J. (eds). Cambridge, NY, pp. 195–238

Friedman, J.D., Johanson, L.E., Óskarsson, N., Svensson, H., Thórarinsson, S. and Williams, K.S., Jr (1971). Observation on Icelandic Polygon Surface and Palsas areas. Photo interpretations and Field studies. *Geografiska Annaler*, **53A**, 115–145.

Gordon, J. and Sharp, M. (1983). Lichenometry in dating recent landforms and deposits, southeast Iceland. *Boreas*, **12**, 191–200.

Grove, J.M. (1988). *The Little Ice Age*. Routledge, London and New York.

Grove, J.M. and Switzur, R. (1994). Glacial geological evidence for the Medieval warm period. *Climatic Change*, **26**, 143–169.

Grönvold, K., Óskarsson, N., Johnsen, S.J., Clausen, H.B., Hammer, C.U., Bond, G. and Bard, E. (1995). Ash layers from Iceland in the Greenland GRIP ice core correlated with oceanic and land sediments. *Earth and Planatery Science Letters*, **135**, 149–155.

Gudmundsson, H.J. (1992). Eiríkjsökull; Jöklabreytingar og gerd jardlaga. Notkun fléttunnar Rhizocarpon geographicum vid aldursgreiningar á jökulurdum á Íslandi. Unpubl. M.S.-thesis University of Iceland, 151.

Gudmundsson, H.J. (in press). Glacier fluctuation of the Eiríksjökull ice cap, west-central Iceland. *Jökull*.

Hallsdóttir, M. (1982). Frjógreining tveggja jardvegssnida úr Hrafnkellsdal. *In*: Thórarinsdóttir, H., Óskarsson, Ó., Steinthórsson, S. and Einarsson, Th. (eds), *Eldur er í Nordri*, pp. 253–266. Sögufélag. Reykjavík.

Hallsdóttir, M. (1987). Pollen analytical studies of human influence on vegetation in relation to the Landnám tephra layer in southwest Iceland. LINDQUA thesis, 18, Department of Quaternary Geology. University of Lund.

Hallsdóttir, M. (1990). Sudies in the vegetational history of North Iceland. A radiocarbon-dated pollen diagram from Flateyjardalur. *Jökull*, **40**, 67–81.

Hammer, C.U., Clausen, H.B. and Dansgaard, W. (1980). Greenland ice-sheet evidence of post-glacial volcanism and its climatic impact. *Nature*, **288**, 230–235.

Hammer, C.U., Clausen, B. and Tauber, H. (1986). Ice-core dating of the Pleistocene/Holocene applied to calibration of the ^{14}C. *Radiocarbon*, **28**, 284–291.

Hirakawa, K. (1989). Downslope movement of solifluction lobes in Iceland. A tephrochronological approach. *Tokyo Metropolitan University Geographical Reports No.*, **24**, 15–31.

Hjartarson, Á. (1988). Thjórsárhrauni› mikla - Staersta nútímahraun jardar. *Náttúrufreadingurinn*, **58**, 1–16.

Hjartarson, Á. (1989). The ages of the Fossvogur layers and the Álftanes end-moraines, SW-Iceland. *Jökull*, **3**, 21–31.

Hjartarson, Á. (1994). Environmental changes in Iceland following the Great Thjórsá lava eruption 7800 yrs B.P. *In*: Stötter, J. and Wilhelm, F. (eds), *Environmental Change in Iceland*, pp. 147–155. Munchener Geog. Abl. B12.

Hjartarson, Á. and Ingólfsson, Ó. (1988). Preboreal glaciation of southeastern Iceland. *Jökull*, **38**, 1–16.

Hjort, C., Ingólfsson, Ó. and Norddahl, H. (1985). Late Quaternary Geology and Glacial history of Hornstrandir. Northwest Iceland. A reconnaissance study. *Jökull*, **35**, 9–29.

Hoppe, G. (1967). Case studies of deglaciation patterns. *Geografiska Annaler*, **49A**, 204–212.

Häberle, T. (1991). Holocene glacial history of the Hörgardalur area, Tröllaskagi, northern Iceland. *In:* Maizels and Caseldine (eds), *Environmental Change in Iceland. Past and Present*, pp. 193–202. Kluwer, Dordrecht.

Häberle, T. (1994). Glacial, Late glacial and Holocene history of the Hörgárdalur area, Tröllaskagi, Northern Iceland. *In*: Stötter, J. and Wilhelm, F. (eds), *Environmental Change in Iceland. Munchener Geog. Abl.* **B12**, 41–63.

Ingólfsson, Ó. (1985). Late Weichselian glacial geology of the lower Borgarfjördur region, western Iceland. a prelimenary report. *Arctic*, **38**, 210–213.

Ingólfsson, Ó. (1987a). Investigation of the late Weichselian glacial history of the lower Borgarfjördur region, western Iceland. LUNDQUA thesis 19. Department of Quaternary Geology. University of Lund. 4. 4 appendix.

Ingólfsson, Ó. (1987b). The late Weichselian glacial Geology of the Melbakkar - Ásbakkar coastal cliffs, Borgarfjördur, W-Iceland. *Jökull*, **37**, 57–81.

Ingólfsson, Ó. (1988). Glacial history of the lower Borgarfjördur area, western Iceland. *Geologiska Föreningens i Stockholm Förhandlingar*, **110**, 293–309.

Ingólfsson, Ó. (1991). A review of the late Weichselian and early Holocene glacial and environmental history of Iceland. *In*: Caseldine, C.J. and Maizels, J. (eds), *Environmental Changes in Iceland, Past and Present*, pp. 13–29. Kluwer, Dordrecht.

Ingólfsson, Ó. and Hjort, C. (1988). Weichselian glaciation in Iceland. Present status and future research aims. *In*: Binazer, K., Marcussen. I. and Konradi, P. (eds), *Nordiske Geologiske Vintermöde. Abstracts*, 178–179.

Ingólfsson, Ó. and Norddahl, H. (1994). A review of the environmental history of Iceland, 13,000–9000 yr BP. *Journal of Quaternary Science*, **9**, 147–150.

Innes, J.L. (1985). Lichenometry. *Progress in Physical Geography*, **9**, 187–254.

Jaksch, K. (1970). Beobachtung in den Gletschervorfelden des Sólheima- und Sídujökull im Sommer 1970. *Jökull*, **20**, 45–49.

Jaksch, K. (1975). Das Gletschervorfeld des Sólheimajökull. *Jökull*, **25**, 34–38.

Jóhannesson, T. (1989). Aldur Hallmundarhrauns í Borgarfirdi. *Fjölrit Nátturufraedistofnunar*, **9**, 12.

Jónsson, Ó. (1957). *Snjóflód og skriduföll*. Akureyri. Nordri.

Kaldal, I. and Víkingsson, S. (1991). Early Holocene deglaciation in central Iceland. *Jökull*, **40**, 51–66.

Karlén, W. (1973). Holocene glacier and climatic variation. Kebnekaise Mountains, Swedish Lappland. *Geografiska Annaler*, **A55**, 29–63.

Karlén, W. (1988). Scandinavian glacial and climatic fluctuations during the Holocene. *Quaternary Science Reviews*, **7**, 199–209.

Keilhack, K. (1884). Uber postglaziale Meeresablagerungen in Island. *Zeitschrift Deutscher Geologische Gerselleschaft*, **35**, 145–160.

Kjartansson, G. (1940). Studier i isens tilbagerykning fra det sydvest-Islansk lavland. *Meddelser fra Dansk Geologiska Forening*, **9**, 426–458.

Kjartansson, G. (1943). *Árnesingasaga*. Árnesingafélagid í Reykjavík.

Kjartansson, G. (1964). Íslaldalok og eldfjöll a Kili. *Náttúrufraedingurinn*, **34**, 9–38.

Koç, N., Jansen, E. and Haflidason, H. (1993). Palaeoceanographic reconstructions of surface ocean conditions in the Greenland, Iceland and Norwegian seas through the last 14 ka based on diatoms. *Quaternary Science Reviews*, **12**, 115–140.

Kugelman, O. (1990). Datierung neuzeitlicher Gletschervorstöße im Svarfadardalur/Skídadalur (Nordisland) mit einer neu erstallten Flechtenwachstumskurve. *Münchener Geog. Abl.*, **B8**, 36–59.

Kugelman, O. (1991). Dating recent glacier advances in the Svarfadardalur/Skídadalur area of northern Iceland by means of a new lichen curve. *In*: Caseldine, C.J. and Maizels, J. (eds). *Environmental Changes in Iceland, Past and Present*, pp. 203–217. Kluwer, Dordrecht.

Larsen, G. and Thórarinsson, S. (1977). H_4 and other Acid Hekla Tephra layers. *Jökull,* **27,** 28–46.

Maizels, J.K. and Dugmore, A.J. (1985). Lichenometrical Dating and Tephrochronology of Sandur Deposits. Sólheimajökull Area, Southern Iceland. *Jökull,* **35,** 69–77.

Meese, D.A., Gow, A.J., Grootes, P., Mayewski, P.A., Ram, M., Stuiver, M., Taylor, K.C., Waddington, Waddington and Zielinski, G.A. (1994). The accumulation record from the GISP2 core as an indicator of climate change throughout the Holocene. *Science,* **266,** 1680–1682.

Mercer, J.H. (1961). The response of fjord glaciers to changes in the firn limit. *Journal of Glaciology,* **10,** 850–858.

Norddahl, H. (1991). Late Weichselian and early Holocene Deglaciation history of Iceland. *Jökull,* **40,** 27–50.

Norddahl, H. and Haflidason, H. (1990). Skogar tefran, en sen glacial kronostratigrafisk markera paa Nordisland. Abstract, 19 Nordic Geological Winter Meeting. Norsk Geologisk Förening. *Geonytt,* **17,** 84.

Norddahl, H. and Haflidason, H. (1992). The Skógar tephra, a Younger Dryas marker in North Iceland. *Boreas,* **21,** 23–41.

Okko, V. (1956). Glacial drift in Iceland, its origin and morphology. *Acta Geographica,* **15,** 1–133.

Ogilvie, A.E.J. (1984). The past climate and sea-ice record from Iceland, Part 1. Data to A.D. 1780. *Climatic Change,* **6,** 131–152.

Ogilvie, A.E.J. (1991). Climatic changes in Iceland A.D. c. 865 to 1598. *In:* The Norse of the North Atlantic. Presented by G.F. Bigelow. *Acta Archaeologica* (**60**), pp. 233–251.

Pahlson, I. (1981). A pollen analytical study on a peat deposit at Lágafell, southern Iceland. *Striae,* **15,** 60–64.

Pjeturss, H. (1910). Island. Handbuck der Regionalen. *Geologie,* **4,** 1–22.

Pétursson, H.G. (1986). Kvarteraergeologiske undersökelser på Vest-Melrakkaslétta, Nordöst Island. Cand. Real Thesis, University of Tromsö, p. 157.

Pétursson, H.G. (1991). The Wichselian glacieal history of West Melrakkaslétta, Norheastern Iceland. *In:* Caseldine, C.J. and Maizels, J. (eds). *Environmental Changes in Iceland, Past and Present,* pp. 49–65. Kluwer, Dordrecht.

Röthlisberger, F. (1986). *10000 jahre Gletschergeschicte der Erde.* Aarau

Schwaar, J. (1978). Moorkundliche Untersuchungen am Laugarvatn (Sudvest Island). *Berichte aus der Forschungstelle Ne›ri-Ás, Hveragerdi, Ísland,* **29,** 1-29.

Sharp, M. and Dugmore, A.J. (1985). Holocene glacier fluctuation in eastern Iceland. Zeitschrift fur Gletscherkunde und Glazialgeologi. *Band,* **21,** 341–349.

Sigurdson, O. (1993). Jöklabreytingar 1930-1960, 1960-1990 og 1991-1992. *Jökull,* **43,** 73–80.

Snorrason, S. (1984). Myrarjöklar og Vatnsdalur. Unpubl. Cand. Real. thesis. University of Oslo.

Straka, H. (1956). Pollenanalytische Untersuchungen eines Moorprofiles aus Nord-Island. *Neue Jahrbuch Geologische Palaontologische,* **6,** 262–272.

Stuiver, M. and Reimer, P.J. (1993). Extended ^{14}C database and revised calib 3.0 ^{14}C age calibration program. *Radiocarbon,* **35,** 215–230.

Stötter, J. (1990). Beobachtungen und Uberlegungen zur postglazialen Landschaftsgeschichte Islands am Beispiel des Svarfadar-Skídadals. *Munchener Geogr. Abh.,* **B8,** 83–104.

Stötter, J. (1991). New observations on the postglacial glacier history of Tröllaskagi, northern Iceland. *In:* Maizels and Caseldine (ed.). *Environmental Change in Iceland. Past and Present,* pp. 181–192. Kluwer, Dordrecht.

Stötter, J. (1994). Changing the Holocene record — A call for International Interdisciplinary co-oporation. *Munchener Geogr. Abl.,* **B12,** 257–273.

Sveinbjörnsdóttir, Á.E. (1993). Fornvedurfar lesid úr ískjörnum. *Náttúrufraeadingurinn,* **62,** 99–108.

Saemundsson, Th. (1994). The deglaciation history of the Hofsárdalur Valley, Northeast Iceland. *In:* Warren, W.P. and Croots, D. (eds). *Formation and Deformation of Glacial Deposits,* pp. 173–287. Balkema, Rotterdam.

Saemundsson, Th. (1995). Deglaciation and shorline displacement in Vopnafjördur, northeast Iceland. *LUNDQUA thesis* 33. Department of Quaternary Geology. University of Lund. p. 106.

Thompson, A. (1988). Historcal Development of the Proglacial area of Svínafellsjökull and Skaftafellsjökull, Southeast Iceland. *Jökull,* **38,** 17–31.

Thompson, A. and Jones, A. (1986). Rates and causes of proglacial river terrace formation in southeast Iceland. an application of lichenometric dating techniques. *Boreas,* **15,** 231–246.

Thórarinsson, S. (1936). Vatnajökull. Chapter III. *Geografiska Annaler,* **18,** 189–195.

Thórarinsson, S. (1944). Tefrokronologiska studier paa Island. *Geografiska Annaler,* **26A,** 1–217.

Thórarinsson, S. (1949). Some tephrochronological contributions to the volcanology and Glaciology of Iceland. *Geografiska Annaler,* **21,** 239–256.

Thórarinsson, S. (1951). Laxárgljúfur and Laxárhraun, a tephrochronological study. *Geografiska Annaler,* 33, 1–90.

Thórarinsson, S. (1956). On the variations of Svínafellsjökull. Skaftafellsjökull and Kviárjökull in Öraefi. *Jökull,* 6, 1–15.

Thórarinsson, S. (1958). The Öraefajökull eruption of 1362. *Acta Nat. Isl. II(2).* Reykjavík. Náttúrufraedistofnun Íslands.

Thórarinsson, S. (1961). Uppblástur í ljósi öskulagarannsókna. *Ársrit Skógraektarfélags Íslands,* pp. 17–54.

Thórarinsson, S. (1964). On the age of the terminal moraines of Brúárjökull and Hálsajökull. *Jökull,* **14,** 67–75.

Thórarinsson, S. (1966). The age of the maximum postglacial advance of Hagafellsjökull eystri. A tephrochronological study. *Jökull,* **16,** 207–210.

Thoroddsen, Th. (1891). Postglaciale marine aflejringer, kystrerrasser og strandlinjer i Island. *Geografisk Tidskrift,* XI, 209–225.

Thoroddsen, Th. (1906). Island. *Grundrisser der Geographie und Geologie.* Pettermans Mitteltungen. Erganzungsheft 152 und 153. Justus Perthes. Gotha, 358.

Thoroddsen, Th. (1911). *Lysing Íslands 2.* Hid Íslenska Bókmenntafélag. Köpenhamn.

Tómasson, H. (1993). Jökulstíflud vötn á Kili og hamfarahlaup í Hvítá í Árness‡slu. *Náttúrufraedingurinn,* **62,** 77–98.

Tryggvason, T. and Jónsson, J. (1958). *Jardfraedikort af nágrenni Reykjavíkur.* Department of Industry, University Research Institute, Reykjavík.

Vasari, Y. (1972). The history of the vegetation of Iceland during the Holocene. *In*: Vasari, Y., Hyvarinen, H. and Hicks, S. (eds). Climatic Changes in the Arctic during the last Ten Thousunds Years. *Acta Universitatis Ouluensis A3. Geologica,* **I,** 239–251.

Vasari, Y. (1973). Post-glacial plant succession in Iceland before the period of human interference. *Proceedings of the III International Palynological Conference,* Nauka, Moscow. pp. 7–14.

Vilmundardóttir, E.G. (1977). Tungnárhraun. Jardfraediskyrsla. *Orkustofnun OS-ROD,* **7702,** 156–.

Vilmundardóttir, E.G. and Kaldal, I. (1982). Holocene sedimentary sequence at Trjávidarlaekur basin. Thjórsárdalur, Southern Iceland. *Jökull,* **32,** 49–59.

Warren, C.R. (1991). Terminal environment, topographic control and fluctuation of West Greenland glaciers. *Boreas,* **20,** 1–15.

Warren, C.R. (1993). Rapid recent fluctuation of the calving San Rafael glacier, Chilien Patagonia. Climatic or non-climatic? *Geografiska Annaler,* **75A,** 111–125.

Whalley, B.W., Douglas, R.G. and Jónsson, A.E. (1983). The Magnitute and frequency of large rockslides in Iceland in the Postglacial. *Geografiska Annaler,* **65A,** 99–110.

Appendix II

Tables 4.1 - 4.40.

	SiO_2	Al_2O_3	FeO	MnO	MgO	CaO	Total
1	35,66	1,74	30,11	0,43	0,11	32,56	100,61
2	35,63	1,73	30,2	0,46	0,1	32,45	100,57
3	35,6	1,73	29,74	0,46	0,09	32,44	100,06
4	35,64	1,78	30,04	0,45	0,11	32,43	100,45
5	35,75	1,71	29,94	0,43	0,11	32,6	100,54
6	35,94	1,68	30,1	0,47	0,1	32,29	100,58
7	36,12	1,71	30,02	0,45	0,11	32,38	100,79
8	36,33	1,77	30,52	0,47	0,1	32,77	101,96
9	36,13	1,73	30,28	0,43	0,11	32,51	101,19
10	35,32	1,74	30,46	0,44	0,09	32,72	100,77
11	35,43	1,75	29,85	0,47	0,09	32,35	99,94
12	35,86	1,69	30,37	0,45	0,1	32,74	101,21
13	35,81	1,74	30,5	0,44	0,09	32,64	101,22
MEAN	35,79	1,73	30,16	0,45	0,1	32,53	100,76
S.D.	0,29	0,03	0,25	0,02	0,01	0,16	0,54
C.V.	0,81	1,64	0,83	3,39	8,56	0,48	0,53

Table 4.1. Selected andradite standard variation during all of the analysis in this study.

Sample no.	Material	Date (conv. BP)	1δ (cal. BP)	2δ (cal. BP)	$\delta^{13}C$ (0/00)
GU-4914	Peat	1540±50	1515-1358	1540-1320	-28,2
GU-4915	Wood	1830±70	1863-1700	1930-1577	-28,3
GU-4916	Peat	2080±60	2136-1984	2303-1898	-28,4
GU-4917	Wood	2240±50	2340-2156	2349-2129	-27,8

Table 4.2. Radiocarbon dating conducted in the study area.

Tables 4.3 - 4.37. Geochemical analyses of tephras in the Öræfi district. Each table is ordered in terms of descending silica

Table 4.3. Ö1727 tephra

SiO_2	TIO_2	Al_2O_3	FeO	MnO	MgO	CaO	Na_2O	K_2O	Total
58.92	1.72	13.74	13.08	0.39	1.36	5.41	3.44	1.61	99.67
58.33	1.57	13.48	12.85	0.43	1.43	5.36	4.61	1.65	99.71
58.10	1.52	13.27	12.71	0.33	1.24	5.33	4.24	1.62	98.36
58.05	1.61	13.53	12.33	0.38	1.47	5.35	3.84	1.65	98.21
57.99	1.71	13.55	12.76	0.37	1.46	5.44	4.68	1.60	99.56
57.83	1.47	13.25	12.34	0.37	1.33	5.37	4.22	1.62	97.80
57.74	1.70	13.37	12.68	0.33	1.48	5.59	4.68	1.58	99.15
57.74	1.68	13.46	12.71	0.35	1.45	5.54	4.21	1.64	98.78
57.63	1.58	13.41	12.49	0.35	1.48	5.35	4.42	1.68	98.39
57.62	1.81	11.64	14.32	0.40	1.56	4.97	3.96	1.92	98.20

Table 4.4. K1755 tephra

SiO_2	TIO_2	Al_2O_3	FeO	MnO	MgO	CaO	Na_2O	K_2O	Total
52.25	2.64	13.31	14.26	0.30	3.03	7.39	3.86	1.14	98.18
50.46	2.93	12.83	13.08	0.28	5.39	9.79	3.07	0.46	98.29
47.97	4.71	12.78	14.42	0.25	5.18	9.68	3.09	0.83	98.91
47.73	4.85	12.48	13.95	0.26	4.76	9.27	3.20	0.80	97.30
47.59	4.77	12.69	14.40	0.21	4.97	9.71	3.01	0.73	98.08
47.52	4.72	12.38	14.61	0.20	5.19	9.55	3.31	0.84	98.32
47.43	4.93	12.22	14.23	0.29	4.93	9.59	3.03	0.72	97.37
47.38	4.91	12.66	14.79	0.26	5.04	9.51	3.24	0.75	98.54
47.37	4.60	12.35	14.41	0.27	4.98	9.63	3.09	0.77	97.47
47.04	4.72	12.47	14.53	0.22	5.02	9.83	3.13	0.73	97.69
46.95	4.59	12.38	14.44	0.25	5.05	9.78	3.16	0.70	97.30
46.92	4.87	12.44	14.64	0.23	4.99	9.41	3.37	0.72	97.59
46.62	4.63	12.30	14.14	0.25	4.98	9.61	2.92	0.73	96.18
46.39	5.55	10.98	15.93	0.33	4.51	9.22	3.15	0.80	96.86
45.87	3.42	10.18	17.27	0.26	10.87	6.22	2.85	0.66	97.60

Table 4.5. G1784 tephra

SiO_2	TIO_2	Al_2O_3	FeO	MnO	MgO	CaO	Na_2O	K_2O	Total
50,53	2,82	14,89	11,95	0,27	4,52	10,06	3,21	0,37	98,62
50,17	2,95	12,76	13,52	0,22	5,31	9,93	2,9	0,48	98,24
50,03	2,96	13,07	13,65	0,21	5,57	9,83	3,07	0,46	98,85
49,67	3,02	12,88	13,78	0,16	5,32	9,47	2,99	0,42	97,71
49,65	2,92	12,83	13,84	0,24	5,54	9,71	2,84	0,5	98,07
49,57	3,22	12,9	13,8	0,2	5,36	9,66	2,92	0,43	98,06
49,3	2,98	12,73	13,83	0,24	5,4	10,05	2,81	0,48	97,82
46,69	4,33	12,38	14,05	0,22	4,93	9,69	3,03	0,77	96,09

Table 4.6. K1918 tephra

SiO_2	TIO_2	Al_2O_3	FeO	MnO	MgO	CaO	Na_2O	K_2O	Total
52,17	0,03	28,43	0,6	0	0,14	12,29	4,35	0,13	98,14
51,76	0,05	29,1	0,55	0	0,1	12,4	4,09	0,09	98,14
51,62	0,03	29,05	0,58	0	0,16	12,34	4,23	0,13	98,14
51,26	0,09	28,91	0,48	0	0,15	12,76	4,18	0,08	97,91
50,56	0,54	2,88	7,82	0,24	17,22	17,72	0,17	0	97,15
46,7	4,32	12,66	14,3	0,21	5,04	9,48	3,14	0,71	96,56
46,45	4,58	12,21	14,5	0,23	4,74	9,2	3	0,76	95,67

46,44	4,38	12,36	14,37	0,26	4,93	9,26	3,15	0,67	95,82
46,37	4,62	12,31	13,86	0,27	4,72	9,53	3,18	0,7	95,56
46.12	4,4	12,39	14,16	0,26	5,01	9,47	3,06	0,67	95,54
46,12	4,39	12,44	14,17	0,21	4,81	9,59	3,11	0,69	95,53
45,92	4,39	12,51	14,44	0,26	5	9,4	3,12	0,73	95,77
45,77	4,39	12,51	14,4	0,25	5,07	9,48	2,98	0,69	95,54
45,67	4,38	12,25	14,41	0,18	5,07	9,43	2,82	0,73	94,94

Table 4.7. Eystriheiði tephra

SiO_2	TIO_2	Al_2O_3	FeO	MnO	MgO	CaO	Na_2O	K_2O	Total
74,86	0,13	13,09	1,93	0,09	0,05	1,33	3,86	2,83	98,17
74,38	0,07	12,99	2,02	0,08	0,05	1,24	3,6	2,83	97,26
73,94	0,12	12,92	1,97	0,12	0,04	1,38	4,06	2,7	97,25
73,77	0,07	12,55	1,83	0,06	0,02	1,2	3,56	2,66	95,72
73,6	0,13	12,89	2,02	0,08	0,06	1,32	4,08	2,71	96,89
73,38	0,11	12,9	2,08	0,06	0,04	1,3	3,74	2,81	96,42
73,24	0,19	12,94	2,02	0,07	0,05	1,37	3,76	3,02	96,66
73,18	0,12	12,53	1,88	0,04	0,04	1,26	3,88	2,85	95,78
72,93	0,15	12,38	1,86	0,01	0,04	1,28	3,86	2,72	95,23
72,8	0,11	12,42	1,96	0,08	0,04	1,27	3,44	2,72	94,84
72,72	0,15	12,62	1,76	0,1	0,01	1,18	3,83	2,94	95,31
72,47	0,16	12,55	1,99	0,07	0,05	1,2	3,56	2,79	94,84
72,25	0,13	12,67	2,18	0,09	0,18	1,44	3,52	2,72	95,18

Table 4.8. Kviármýri 0 tephra

SiO_2	TIO_2	Al_2O_3	FeO	MnO	MgO	CaO	Na_2O	K_2O	Total
73,29	0,22	13,45	2,24	0,04	0,03	0,67	5,49	4,08	99,51
72,68	0,26	13,23	3,36	0,12	0,03	1,01	4,16	3,68	98,53
72,55	0,31	13,33	3,42	0,13	0,03	0,96	4,39	3,39	98,51
72,46	0,22	13,54	3,03	0,09	0,04	1,02	4,88	3,29	98,57
72,43	0,32	13,04	3,51	0,1	0,07	1,06	4,02	3,94	98,49
72,22	0,27	13,31	3,53	0,09	0,07	0,96	4,81	3,38	98,64
72,21	0,23	13,21	3,35	0,04	0,02	1,06	3,88	3,49	97,49
71,98	0,26	13,08	3,35	0,07	0,03	1,03	4,42	3,46	97,68
71,97	0,24	13,01	3,37	0,11	0,06	1,12	4,48	3,31	97,67
71,71	0,24	13,09	3,35	0,07	0,07	1,03	4,03	3,44	97,03
70,59	0,17	13,53	2,22	0,04	0,02	0,7	5,75	3,68	96,7
73,21	0,09	12,92	1,88	0,02	0,03	1,35	3,84	2,76	96,1
73,15	0,1	12,96	1,9	0,04	0,04	1,28	3,98	2,83	96,28
73,13	0,04	12,9	2,08	0,06	0,03	1,25	3,53	2,82	95,84
73,13	0,07	12,89	2,03	0,08	0,02	1,3	4,17	2,77	96,46
73,03	0,11	13,08	2,03	0,05	0,03	1,33	4,06	2,89	96,61
72,99	0,06	12,99	1,97	0,1	0,03	1,28	4,16	2,54	96,12
72,62	0,07	12,68	2,02	0,05	0,01	1,27	3,9	2,7	95,32
72,29	0,08	12,65	2,06	0,09	0,03	1,26	3,68	2,93	95,07
72,14	0,08	12,87	1,92	0,07	0,02	1,32	4,03	2,83	95,28
72,1	0,16	12,85	1,85	0,06	0,04	1,28	3,87	2,79	95

Table 4.9. Hekla-4 tephra

SiO_2	TIO_2	Al_2O_3	FeO	MnO	MgO	CaO	Na_2O	K_2O	Total
74.24	0.09	12.85	1.87	0.10	0.03	1.28	3.75	2.73	96.94
72.13	0.09	12.44	1.90	0.11	0.02	1.29	3.66	2.87	94.51
74,27	0,09	12,99	2,02	0	0,05	1,39	3,94	2,89	97,64
74,17	0,06	12,95	2,12	0,04	0,02	1,36	4,15	2,99	97,86
73,82	0,09	13	2,1	0,02	0,03	1,25	4,3	2,86	97,47

73,6	0,05	13,07	1,84	0,02	0,04	1,38	3,95	2,81	96,76
73,59	0,05	12,93	2,06	0,04	0,04	1,26	3,82	2,75	96,54
73,46	0,05	12,94	1,92	0,02	0,04	1,21	4,02	2,71	96,37
73,21	0,09	12,92	1,88	0,02	0,03	1,35	3,84	2,76	96,1
73,15	0,1	12,96	1,9	0,04	0,04	1,28	3,98	2,83	96,28
73,13	0,04	12,9	2,08	0,06	0,03	1,25	3,53	2,82	95,84
73,13	0,07	12,89	2,03	0,08	0,02	1,3	4,17	2,77	96,46
73,03	0,11	13,08	2,03	0,05	0,03	1,33	4,06	2,89	96,61
72,99	0,06	12,99	1,97	0,1	0,03	1,28	4,16	2,54	96,12
72,62	0,07	12,68	2,02	0,05	0,01	1,27	3,9	2,7	95,32
72,29	0,08	12,65	2,06	0,09	0,03	1,26	3,68	2,93	95,07
72,14	0,08	12,87	1,92	0,07	0,02	1,32	4,03	2,83	95,28
72,1	0,16	12,85	1,85	0,06	0,04	1,28	3,87	2,79	95

Table 4.10. Hekla-s tephra

SiO_2	TIO_2	Al_2O_3	FeO	MnO	MgO	CaO	Na_2O	K_2O	Total
72,8	0,2	13,88	2,77	0,13	0,15	1,9	3,68	2,42	97,93
71,68	0,19	13,83	2,8	0,08	0,15	1,82	3,77	2,39	96,71
68,87	0,44	14,99	4,59	0,14	0,33	2,97	4,68	2,83	99,84
67,52	0,53	15,02	6,13	0,17	0,54	3,43	4,11	2,16	99,61
67,15	0,43	14,93	5,74	0,23	0,61	3,22	3,92	2,01	98,24
67,06	0,47	14,77	5,95	0,14	0,544	3,25	3,62	2	97,8
66,89	0,53	14,82	5,79	0,16	0,52	3,31	4,43	1,91	98,36
66,89	0,54	15,33	5,51	0,19	0,54	3,39	3,97	2,07	98,43
66,78	0,44	15,14	6,41	0,16	0,66	3,48	3,63	2,08	98,78
66,31	0,51	14,7	5,91	0,13	0,54	3,28	4,3	2,01	97,69
66,3	0,48	14,93	6,13	0,17	0,55	3,48	4,23	1,98	98,25
66,22	0,53	14,68	6,1	0,2	0,6	3,34	4,4	1,7	97,77
66,15	0,49	14,65	5,86	0,13	0,59	3,48	4,63	2,03	98,01
66,01	0,61	15,47	5,74	0,13	0,51	4,07	5,24	1,58	99,36
65,75	0,56	14,88	5,94	0,13	0,61	3,48	4,19	1,95	97,49
65,12	0,38	14,78	6,23	0,11	0,59	3,4	4,12	1,96	96,69
64,99	0,49	14,73	5,86	0,14	0,63	3,21	4,06	1,9	96,01
64,71	0,82	13,83	8,13	0,23	0,8	3,86	4,46	2	98,84
64,03	0,7	14,63	7,26	0,2	0,89	4,16	3,89	1,84	97,6
63,77	0,44	14,21	6,07	0,21	0,57	3,28	3,54	1,92	94,01
62,85	0,93	13,71	8,98	0,24	0,93	4,29	3,94	1,85	97,72
62,43	0,93	14,67	8,43	0,19	1,1	4,5	4,37	1,66	98,28

Table 4.11. Miðheiði tephra

SiO_2	TIO_2	Al_2O_3	FeO	MnO	MgO	CaO	Na_2O	K_2O	Total
72,81	0,23	13,09	3,44	0,09	0,03	1,07	4,01	3,69	98,46
72,79	0,21	12,96	3,23	0,09	0,05	1,05	4,1	3,6	98,08
72,76	0,26	13,22	3,34	0,13	0,06	1,04	4,54	3,55	98,9
72,65	0,22	13,13	3,48	0,11	0,04	1,02	4,55	3,61	98,81
72,61	0,3	13,22	3,4	0,13	0,09	1,15	4,21	3,34	98,45
72,45	0,29	13,4	3,1	0,16	0,03	1,06	4,65	3,42	98,56
72,2	0,25	13,48	3,31	0,09	0,05	0,97	4,47	3,66	98,48
72,18	0,32	13,08	3,22	0,15	0,04	0,98	3,81	3,49	97,27
71,97	0,23	13,01	3,46	0,11	0,05	1,07	3,86	3,52	97,28
70,78	0,24	13,5	3,22	0,13	0,07	1,11	4,68	3,49	97,22
70,62	0,15	12,27	1,39	0,05	0,12	0,85	3,01	3,56	92,02

Table 4.12. Svínafellsheiði tephra

SiO_2	TIO_2	Al_2O_3	FeO	MnO	MgO	CaO	Na_2O	K_2O	Total

71.42	0.54	12.56	3.76	0.13	0.83	3.13	2.82	1.85	97.04
70.13	0.32	14.40	2.46	0.11	0.23	0.89	4.09	4.64	97.27
69.75	0.18	12.80	2.55	0.11	0.25	0.91	4.05	4.48	95.08
68.35	0.65	12.43	4.51	0.15	0.59	2.61	2.34	1.81	93.44
68.07	0.54	11.91	3.77	0.12	1.14	2.93	3.03	1.75	93.26
72,67	0,26	13,15	3,25	0,06	0,04	0,99	4,06	3,35	97,83
72,62	0,53	12,79	3,84	0,11	0,45	2,31	2,97	1,86	97,48
71,39	0,21	14,75	2,63	0,04	0,27	0,9	3,71	4,26	98,16
71,27	0,7	13,15	4,38	0,09	0,6	2,77	3,7	1,92	98,58
71,14	0,51	12,76	3,7	0,06	0,4	2,21	3,62	1,81	96,21
71,13	0,24	14,42	2,45	0,07	0,25	0,84	4,26	4,55	98,21
70,95	0,67	13,24	4,66	0,1	0,61	2,91	3,89	1,88	98,91
70,42	0,3	14,24	2,54	0,1	0,28	0,87	4,68	4,55	97,98
70,39	0,51	12,33	3,9	0,08	0,41	2,22	2,63	1,92	94,39
69,89	0,61	12,31	3,98	0,06	0,42	2,43	2,89	1,82	94,41
69,82	0,38	14,35	3,28	0,12	0,45	1,23	4,38	4,6	98,61
68,47	0,26	14,13	2,59	0,06	0,34	1,09	4,38	4,26	95,58
66,07	0,29	13,53	2,72	0,09	0,31	0,96	3,61	4,07	91,65
52,88	1,52	13,72	9,72	0,25	6,31	10,1	2,6	0,48	97,58

Table 4.13. Skerhóll tephra

SiO_2	TIO_2	Al_2O_3	FeO	MnO	MgO	CaO	Na_2O	K_2O	Total
73,33	0,18	13,17	3,37	0,15	0,05	1,14	4,16	3,4	98,95
72,94	0,49	11,97	2,61	0,1	0,23	1,25	3,69	3,7	96,98
72,2	0,27	12,87	3,24	0,1	0,06	1,14	4,63	3,5	98,01
68,04	0,39	15,66	2,01	0,05	0,18	3,09	5,22	2,37	97,01

Table 4.14. Skaftafellsheiði tephra

SiO_2	TIO_2	Al_2O_3	FeO	MnO	MgO	CaO	Na_2O	K_2O	Total
73,59	0,33	13,47	3,02	0,09	0,03	0,83	4,76	3,76	99,88
72,93	0,27	13,28	3,5	0,15	0,04	1,04	4,42	3,56	99,19
72,61	0,25	13,56	3,14	0,12	0,02	1,03	4,45	3,47	98,65
72,48	0,24	13,08	3,27	0,12	0,06	0,83	4,43	3,78	98,29
72,42	0,22	13,49	3,19	0,15	0,04	1,08	4,58	3,48	98,65
71,79	0,28	13,27	3,27	0,14	0,03	0,97	4,62	3,29	97,66
71,08	0,32	12,93	3,52	0,13	0,02	1,06	4,79	3,49	97,34
71,06	0,24	13,21	3,03	0,07	0,06	1,05	4,69	3,35	96,76
70,94	0,24	13,27	3,5	0,09	0,06	1,13	4,48	3,54	97,25
70,29	0,28	13,19	3,28	0,11	0,01	0,99	4,56	3,48	96,19

Table 4.15. Kvíárjökull/Skaftafellsheiði tephra

SiO_2	TIO_2	Al_2O_3	FeO	MnO	MgO	CaO	Na_2O	K_2O	Total
73,59	0,33	13,47	3,02	0,09	0,03	0,83	4,76	3,76	99,88
72,61	0,25	13,56	3,14	0,12	0,02	1,03	4,45	3,47	98,65
72,48	0,24	13,08	3,27	0,12	0,06	0,83	4,43	3,78	98,29
72,42	0,22	13,49	3,19	0,15	0,04	1,08	4,58	3,48	98,65
71,06	0,24	13,21	3,03	0,07	0,06	1,05	4,69	3,35	96,76

Table 4.16. Vö ca. 900 AD tephra

SiO_2	TIO_2	Al_2O_3	FeO	MnO	MgO	CaO	Na_2O	K_2O	Total
49,27	1,82	13,16	12,64	0,28	6,36	11,47	2,53	0,2	97,73
50,39	1,79	13,28	11,1	0,23	6,93	11,22	2,45	0,21	97,6
49,18	1,78	13,3	12,38	0,24	6,64	11,53	2,53	0,17	97,75
49,43	1,77	13,17	12,72	0,24	6,44	11,38	2,53	0,22	97,9
48,65	1,61	12,94	12,49	0,28	6,39	11,29	2,61	0,2	96,46

Table 4.17. Hekla-1 tephra (H1104)

SiO_2	TIO_2	Al_2O_3	FeO	MnO	MgO	CaO	Na_2O	K_2O	Total
74,35	0,1	11,66	3,19	0,14	0,13	1,29	3,95	3,22	98,03
72,12	0,23	13,45	2,96	0,1	0,1	1,91	4,74	2,74	98,35
71,79	0,18	13,97	2,26	0,08	0,06	1,9	5,28	2,43	97,95
71,59	0,16	13,45	2,99	0,06	0,1	1,8	4,45	2,64	97,24
71,34	0,21	13,7	3,22	0,04	0,1	2,02	4,07	2,47	97,17
71,34	0,16	13,58	3,14	0,02	0,1	1,7	3,9	2,92	96,86
71,27	0,15	14,09	2,13	0,02	0,05	2,02	5,29	2,55	97,57
70,95	0,17	13,67	3	0,05	0,08	1,98	4,62	2,75	97,27
70,92	0,19	13,72	3,27	0,05	0,1	1,86	4,25	2,74	97,1
70,15	0,16	15,08	2,47	0,06	0,07	2,31	5,45	2,32	98,07

Table 4.18. Kviármýri 7 tephra

SiO_2	TIO_2	Al_2O_3	FeO	MnO	MgO	CaO	Na_2O	K_2O	Total
72,85	0,5	12,78	3,98	0,08	0,35	2,23	3,21	2,04	98,02
72,73	12,36	0,11	0,45	2,31	0,58	3,8	3,35	1,96	97,65
72,21	0,63	12,43	3,87	0,05	0,38	2,28	2,43	2,09	96,37
72,13	12,45	0,09	0,42	2,53	0,48	3,72	3,47	1,88	97,17
72,03	0,6	12,38	4,09	0,07	0,38	2,49	3,37	2,2	97,61
72	12,42	0,11	0,39	2,12	0,56	3,75	2,94	2	96,29
72	12,38	0,05	0,37	2,15	0,59	3,74	3	2,04	96,32
71,72	12,36	0,05	0,4	2,23	0,54	3,81	3,16	1,89	96,16
70,7	14,63	0,07	0,22	0,78	0,24	2,51	4,44	4,59	98,18
69,86	14,19	0,09	0,25	0,81	0,21	2,54	4,49	4,56	97
69,78	0,75	12,88	4,6	0,09	0,61	2,97	3,42	1,72	96,82
69,32	14,36	0,06	0,26	0,94	0,27	2,72	4,22	4,45	96,6

Table 4.19. Kviármýri 6 tephra

SiO_2	TIO_2	Al_2O_3	FeO	MnO	MgO	CaO	Na_2O	K_2O	Total
73,21	0,27	13,19	3,02	0,09	0,06	0,96	4,06	3,7	98,56
73,21	0,26	12,61	3,07	0,07	0,02	0,75	4,52	3,51	98,02
72,67	0,26	13,15	3,25	0,06	0,04	0,99	4,06	3,35	97,83
72,67	0,26	13,15	3,25	0,06	0,03	0,99	4,05	3,34	97,8
72,39	0,28	13,23	3,4	0,06	0,01	1,08	3,84	3,48	97,77
72,25	0,29	13,13	3,23	0,13	0,05	1,1	3,65	3,51	97,34
72,19	0,29	13,05	3,29	0,1	0,04	0,87	4,08	3,73	97,64
72,12	0,25	13,35	3,19	0,15	0,04	0,95	4,06	3,38	97,49
71,92	0,29	12,96	3,2	0,11	0,02	0,99	4,34	3,58	97,41
71,87	0,25	13,47	2,78	0,04	0,01	0,92	5,43	3,24	98,01

Table 4.20. Kviármýri 3 tephra

SiO_2	TIO_2	Al_2O_3	FeO	MnO	MgO	CaO	Na_2O	K_2O	Total
77,35	0,19	10,92	1,29	0	0,02	0,57	3,87	3,14	97,35
72,28	0,11	15,16	0,44	0,02	0,08	0,58	5,11	5,35	99,13
70,87	0,24	12,94	2,21	0,08	0,22	0,79	3,63	4,61	95,59
70,44	0,29	13,16	2,08	0,04	0,22	0,84	4,1	4,46	95,63
70,03	0,28	13,3	2,17	0,05	0,24	0,94	4,11	4,17	95,29

Table 4.21. Kviármýri 2 tephra

SiO_2	TIO_2	Al_2O_3	FeO	MnO	MgO	CaO	Na_2O	K_2O	Total
78	0,11	12,69	0,35	0,05	0,02	0,52	4,89	4,3	100,9
74,08	0,27	13,72	2,54	0,08	0	0,83	4,86	3,72	100,1

72,44	0,05	14,69	0,39	0,05	0,04	0,27	5,28	5,52	98,73
71,24	0,33	13,24	2,15	0,05	0,26	0,88	3,93	4,31	96,39
71,22	0,3	13,04	3,14	0,1	0,04	0,98	5	3,2	97,02
69,96	0,16	13,05	1,86	0,04	0,15	0,81	4,14	4,26	94,43

Table 4.22. Kviármýri 1 tephra

SiO_2	TiO_2	Al_2O_3	FeO	MnO	MgO	CaO	Na_2O	K_2O	Total
73,63	0,26	11,69	3,6	0,09	0,03	0,66	4,25	3,99	98,2
73,03	0,29	12,38	3,17	0,1	0,04	0,71	5,19	3,61	98,52
72,47	0,3	13,08	2,6	0,07	0,03	0,65	5,45	3,6	98,25
72,39	0,24	13,35	3,48	0,17	0,04	1,07	4,66	3,46	98,86
72,35	0,27	13,78	2,89	0,11	0,04	0,93	5,29	3,26	98,92
70,61	0,14	15,9	1,54	0,02	0,02	1,01	7,61	2,66	99,51

Table 4.23. Botn 1 tephra

SiO_2	TiO_2	Al_2O_3	FeO	MnO	MgO	CaO	Na_2O	K_2O	Total
75,4	0,14	12,61	1,51	0,07	0,08	0,72	3,97	3,84	98,34
75,18	0,12	12,18	1,13	0,06	0,04	0,61	3,84	4,06	97,22
75,02	0,1	12,24	1,06	0,02	0,05	0,5	3,88	4,05	96,93
74,46	0,08	13,22	1,12	0,04	0,01	0,36	3,94	3,72	96,95
74,38	0,12	12,04	1,14	0,06	0,06	0,47	3,57	3,83	95,67
73,8	0,06	12,15	1,41	0,06	0,07	0,57	3,74	4,11	95,97
73,74	0,1	13,33	1,32	0,06	0,03	0,43	3,39	3,83	96,23
73,64	0,08	11,52	1,09	0	0,05	0,58	3,75	3,71	94,42
73,57	0,11	12,17	1,23	0,06	0,06	0,58	3,66	3,75	95,19
73,47	0,1	12,05	1,2	0,06	0,03	0,62	3,41	3,8	94,74
73,38	0,15	12,04	1,31	0,1	0,09	0,57	3,74	4,03	95,41
73,36	0,11	11,66	1,19	0,05	0,02	0,6	3,72	3,7	94,41
73,1	0,14	11,68	1,34	0	0,05	0,61	3,79	3,88	94,59
72,99	0,15	11,77	2,49	0,1	0,19	1,11	3,88	3,87	96,55
72,73	0,11	11,62	1,29	0,03	0,07	0,57	3,8	3,81	94,03
69,56	0,77	13,68	4,02	0,16	0,68	2,16	2,29	2,96	96,28

Table 4.24. Botn 2 tephra

SiO_2	TiO_2	Al_2O_3	FeO	MnO	MgO	CaO	Na_2O	K_2O	Total
73,4	0,23	11,84	2,49	0,08	0,23	1,48	3,89	2,61	96,25
71,81	0,29	11,65	2,78	0,11	0,25	1,53	3,83	2,31	94,56
68,04	0,9	13,53	4,08	0,22	0,64	1,88	4,3	2,99	96,58
67,99	0,93	13,92	3,88	0,18	0,66	1,89	4,41	3,13	96,99
67,71	0,85	13,43	4,32	0,15	0,76	2,19	4,63	3,1	97,14
67,25	0,75	13,56	4,05	0,17	0,76	2,02	4,43	2,93	95,92

Table 4.25. Botn 3 tephra

SiO_2	TiO_2	Al_2O_3	FeO	MnO	MgO	CaO	Na_2O	K_2O	Total
48,68	1,5	14,05	10,77	0,23	7,7	12,53	2,04	0,11	97,61
48,27	1,47	13,96	10,32	0,16	7,82	12,82	2,08	0,09	96,93
48,09	1,38	13,67	10,57	0,18	7,92	12,16	2,16	0,16	96,29
47,98	1,56	13,74	11,23	0,17	7,33	12,09	2,3	0,19	96,59
47,84	1,46	13,7	10,8	0,16	7,85	12,46	2,27	0,15	96,69

Table 4.26. Botn 4 tephra

SiO_2	TiO_2	Al_2O_3	FeO	MnO	MgO	CaO	Na_2O	K_2O	Total
72,41	0,13	12,69	1,28	0,07	0,02	0,44	3,72	4,48	95,24
72,14	0,15	13,01	1,15	0,03	0,02	0,4	4,25	3,94	95,09
70,5	0,17	14,27	2,7	0,08	0,07	0,98	5,88	3,51	98,16

70,12	0,12	13,47	2,46	0,1	0,03	0,56	3,68	5,07	95,61
67,4	1,29	12,62	5,38	0,15	0,68	2,14	4,47	3,32	97,45
66,76	1,22	13,62	5,34	0,19	0,91	2,65	4,44	2,87	98
66,16	1,3	13,35	5,64	0,19	0,96	2,74	4,23	2,98	97,55

Table 4.27. Botn 5 tephra

SiO_2	TIO_2	Al_2O_3	FeO	MnO	MgO	CaO	Na_2O	K_2O	Total
49,55	3,01	13,27	14,74	0,29	4,3	9,14	2,64	0,63	97,61
48,99	3,13	13,16	14,73	0,29	4,87	9,32	3,08	0,63	98,22

Table 4.28. Oddar tephra

SiO_2	TIO_2	Al_2O_3	FeO	MnO	MgO	CaO	Na_2O	K_2O	Total
74,66	0,11	12,84	1,89	0,06	0,02	1,17	3,67	2,94	97,36
74,16	0,11	13,16	1,94	0,05	0,01	1,35	3,91	2,87	97,56
73,63	0,11	12,64	2,16	0,1	0,02	1,35	3,4	2,92	96,33
73,54	0,09	12,69	1,95	0,04	0,03	1,29	4,01	2,89	96,53
73,36	0,09	12,89	2,06	0,08	0,01	1,34	3,8	2,56	96,19
72,52	0	12,88	2	0,06	0,04	1,36	3,78	2,8	95,44
72,42	0,09	12,66	1,94	0,07	0,02	1,33	3,85	2,81	95,19

Table 4.29. Sv14-12 tephra

SiO_2	TIO_2	Al_2O_3	FeO	MnO	MgO	CaO	Na_2O	K_2O	Total
74,99	0,26	12,91	1,94	0,02	0,12	0,97	3,49	3,78	98,48
74,95	0,16	12,88	1,78	0,03	0,07	0,78	3,7	3,71	98,06
74,68	0,14	12,7	1,82	0	0,1	0,9	3,56	3,78	97,68
74,65	0,13	12,78	1,64	0,02	0,11	0,78	4,07	3,83	98,01
74,19	0,11	12,84	1,54	0,08	0,09	0,77	3,95	3,49	97,06
73,83	0,12	12,58	1,86	0,04	0,09	0,86	3,77	3,67	96,82
73,15	0,16	12,57	1,74	0,05	0,12	0,86	3,63	3,67	95,95
73,13	0,14	12,48	1,67	0,02	0,07	0,84	3,47	3,78	95,6
72,77	0,18	12,46	1,76	0,05	0,11	0,7	3,33	3,58	94,94
72,72	0,16	12,28	1,73	0	0,08	0,85	3,43	3,59	94,84
72,53	0,16	12,57	1,73	0,1	0,08	0,79	4,01	3,8	95,77
72,27	0,17	12,29	1,7	0,03	0,09	0,74	3,45	3,68	94,42

Table 4.30. Sv14-11 tephra

SiO_2	TIO_2	Al_2O_3	FeO	MnO	MgO	CaO	Na_2O	K_2O	Total
71,04	0,37	14,19	4,04	0,12	0,31	1,8	3,79	3,35	99,01
65,75	1,18	13,94	5,41	0,2	1,1	3,15	4,11	2,82	97,66
65,69	1,18	13,99	5,34	0,15	1,1	3,04	4,29	2,87	97,65
65,66	1,05	13,98	5,47	0,2	1,14	3,02	4,16	2,87	97,55
65,65	1,18	13,6	5,35	0,14	1,13	3,17	4,07	2,73	97,02
57,83	2,33	14,55	8,13	0,18	3,37	6,79	3,48	1,69	98,35

Table 4.31. Sv14-9 tephra

SiO_2	TIO_2	Al_2O_3	FeO	MnO	MgO	CaO	Na_2O	K_2O	Total
69.36	0.08	16.78	2.65	0.07	0.39	2.22	5.24	2,82	99.61
69,04	0,13	16,64	2,36	0,02	0,35	2,15	5,52	2,93	99,14
67,22	0,24	16,33	2,19	0,05	0,31	2,03	4,88	2,68	95,93
54,11	2,24	13,87	11,4	0,26	2,78	6,57	3,53	1,33	96,09
52,66	2,34	13,6	12,15	0,15	2,96	6,8	3,33	1,08	95,07
52,52	2,52	13,96	12,58	0,18	3,08	7,31	3,74	1,17	97,06
52,15	2,45	13,71	12,59	0,25	2,98	7,35	3,52	1,2	96,2
52,13	2,33	13,71	12,59	0,22	3,08	7,04	3,78	1,18	96,06
50,95	2,41	13,99	11,3	0,19	2,74	6,82	3,44	1,02	92,86

Table 4.32. Sv14-7 tephra

SiO_2	TIO_2	Al_2O_3	FeO	MnO	MgO	CaO	Na_2O	K_2O	Total
73,39	0,11	12,9	1,92	0,11	0,03	1,35	4,25	2,72	96,78
70,41	0,46	13,61	4,84	0,17	0,23	1,59	4,65	3,64	99,6
70,38	0,26	12,92	3,41	0,12	0,01	0,91	4,18	3,53	95,78
69,99	0,28	12,72	3,44	0,11	0,03	0,87	4,64	3,48	95,56

Table 4.33. Sv61-1 tephra

SiO_2	TIO_2	Al_2O_3	FeO	MnO	MgO	CaO	Na_2O	K_2O	Total
74,07	0,26	13,25	2,34	0,01	0,36	1,44	4,02	3,65	99,4
73,43	0,12	12,54	1,61	0,04	0,1	0,82	3,61	3,83	96,1
73,43	0,18	12,47	1,76	0,01	0,15	0,8	3,74	3,86	96,4
72,97	0,22	12,74	1,89	0,04	0,14	1,04	3,57	3,78	96,39
72,65	0,09	12,41	1,56	0,02	0,1	0,73	4,03	4,63	96,22
71,43	0,33	12,89	2,27	0,01	0,28	1,37	3,01	4,11	95,7
71,42	0,24	12,95	2,25	0,01	0,27	1,34	3,77	3,93	96,18

Table 4.34. Virkisjökull tephra

SiO_2	TIO_2	Al_2O_3	FeO	MnO	MgO	CaO	Na_2O	K_2O	Total
73,81	0,17	13,52	2,07	0,04	0,08	0,61	4,56	4,22	99,08
72,64	0,27	12,46	3,24	0,1	0,05	0,99	3,8	3,67	97,22
71,35	0,43	12,94	3,24	0,14	0,19	1,1	3,99	3,88	97,26
70,94	0,33	13,78	4,15	0,14	0,1	1,43	4,17	3,42	98,46
70,69	0,35	13,46	4,12	0,15	0,07	1,44	4,41	3,21	97,9
70,57	0,44	13,43	3,48	0,09	0,26	1,28	4,61	3,47	97,63
69,94	0,28	13,44	3,94	0,13	0,09	1,44	4,21	3,45	96,92
65,99	0,27	13,2	3,85	0,13	0,09	1,06	3,36	3,61	91,56

Table 4.35. Kví64-1 tephra

SiO_2	TIO_2	Al_2O_3	FeO	MnO	MgO	CaO	Na_2O	K_2O	Total
76,16	0,05	12,63	1,9	0,1	0,06	1,38	4,08	2,95	99,31
74,88	0,05	13,04	1,98	0,07	0,01	1,27	4,3	2,91	98,51
74,37	0,08	13,05	2,09	0,09	0,01	1,33	4,16	2,87	98,05
74,11	0,166	13,27	2,01	0,11	0,01	1,34	4,08	2,77	97,87
73,84	0,1	12,91	1,85	0,1	0,03	1,2	4,01	2,88	96,92
72,59	0,09	12,75	1,87	0,13	0,02	1,31	4,1	2,88	95,74
72,45	0,11	12,9	2,01	0,11	0,01	1,1	3,76	2,77	95,22
72,26	0,1	12,78	1,82	0,1	0,04	1,27	3,99	2,87	95,23

Table 4.36. Kví64-2 tephra

SiO_2	TIO_2	Al_2O_3	FeO	MnO	MgO	CaO	Na_2O	K_2O	Total
73,97	0,28	12,15	1,87	0,06	0,07	0,64	3,05	4,84	96,93
73,97	0,21	13,21	1,7	0,09	0,07	0,63	4,52	4,42	98,82
73,05	0,24	13,02	1,87	0,08	0,08	0,7	3,84	4,33	97,21
71,58	0,2	13,94	3,19	0,1	0,16	1,83	4,01	2,39	97,4
71,26	0,29	13,03	2,2	0,08	0,2	0,88	4,05	4,34	96,33

Table 4.37. Kví64-4 tephra

SiO_2	TIO_2	Al_2O_3	FeO	MnO	MgO	CaO	Na_2O	K_2O	Total
74,89	0,34	11,55	2,02	0,06	0,09	0,56	3,12	5,08	97,71
74,47	0,16	12,04	1,51	0,09	0,02	0,26	3,94	5,11	97,6
72,74	0,17	12,8	1,53	0,06	0,05	0,51	4,06	4,41	96,33
72,09	0,27	13,28	1,81	0,09	0,18	0,9	3,25	4,46	96,33
71,84	0,24	13,61	2,1	0,07	0,1	0,79	3,33	4,32	96,4

Tephra layer	Eruption probability*	Date	Jökulhlaup	Relative size**
Ö1727	xxx	1727 AD	Yes	Intermediate
Ö1362	xxx	1362 AD	Yes	Big
The Skaftafellsheiði tephra	xxx	1540±50 BP	Yes	Intermediate
The Skerhóll tephra	x	1940±30 BP	?	Small?
The Miðheiði tephra	xxx	2860±160 BP	?	Intermediate
Sv14-9	x	5030±200	?	Small?
The Virkisjökull tephra	xx	4590±125 BP	?	Small?
Botn 6 tephra	xx	4430±100 BP	?	Small?
SV14-11 and	x	6430±140	?	Small?
Botn 4 tephras	x	Mid-Holocene	?	Small?
Sv14-12	x	9790±980 BP	?	Small?
Sv61-1	x	8590±780 BP	?	Small?
Botn 1	x	Early Holocene	?	Small?

*x Likely; xx Very likely; xxx Took place

** In terms of the Ö1362 AD eruption

Table 4.38. Probable eruptions of the Öræfajökull stratovolcano in the Holocene. Assuming that the silicic tephras reflect the true number of eruptions over the the Holocene, an eruption occurred every ca. 600 BP years on avarage. Jökulhlaup is likely to have followed each eruption.

Table 4.39. Pre-1362 AD MSAR in the Öræfi district

Profile	*Soil thickness (mm)*	*Year interval (BP)*	*SAR (mm/a)*
14	685	H4 - Ö1362	0.211
18	680	H4 - Vö ca. 900	0.247
7	755	H4 - Vö ca. 900	0.274
31	620	H4 - Vö ca. 900	0.225
67	940	H4 - Ö1362	0.289
68	941	H4 - Ö1362	0.29
Mean	736	2949	0.249±0.04

Table 4.40. Post-1362 AD MSAR in the Öræfi district

Profile	*Soil thickness (mm)*	*Year interval (yrs)*	*SAR (mm/a)*
1	110	1727 - 1362	0.301
6	150	1727 - 1362	0.41
11	340	1727 - 1362	0.931
14	120	1727 - 1362	0.328
18	350	1727 - 1362	0.958
27	165	1727 - 1362	0.452
33	350	1727 - 1362	0.958
35	130	1727 - 1362	0.365
Mean	214	365	0.587±0.02

The tables indicate the difference in sediment accumulation rates before and after the big eruption of Öræfajökull in 1362 AD.

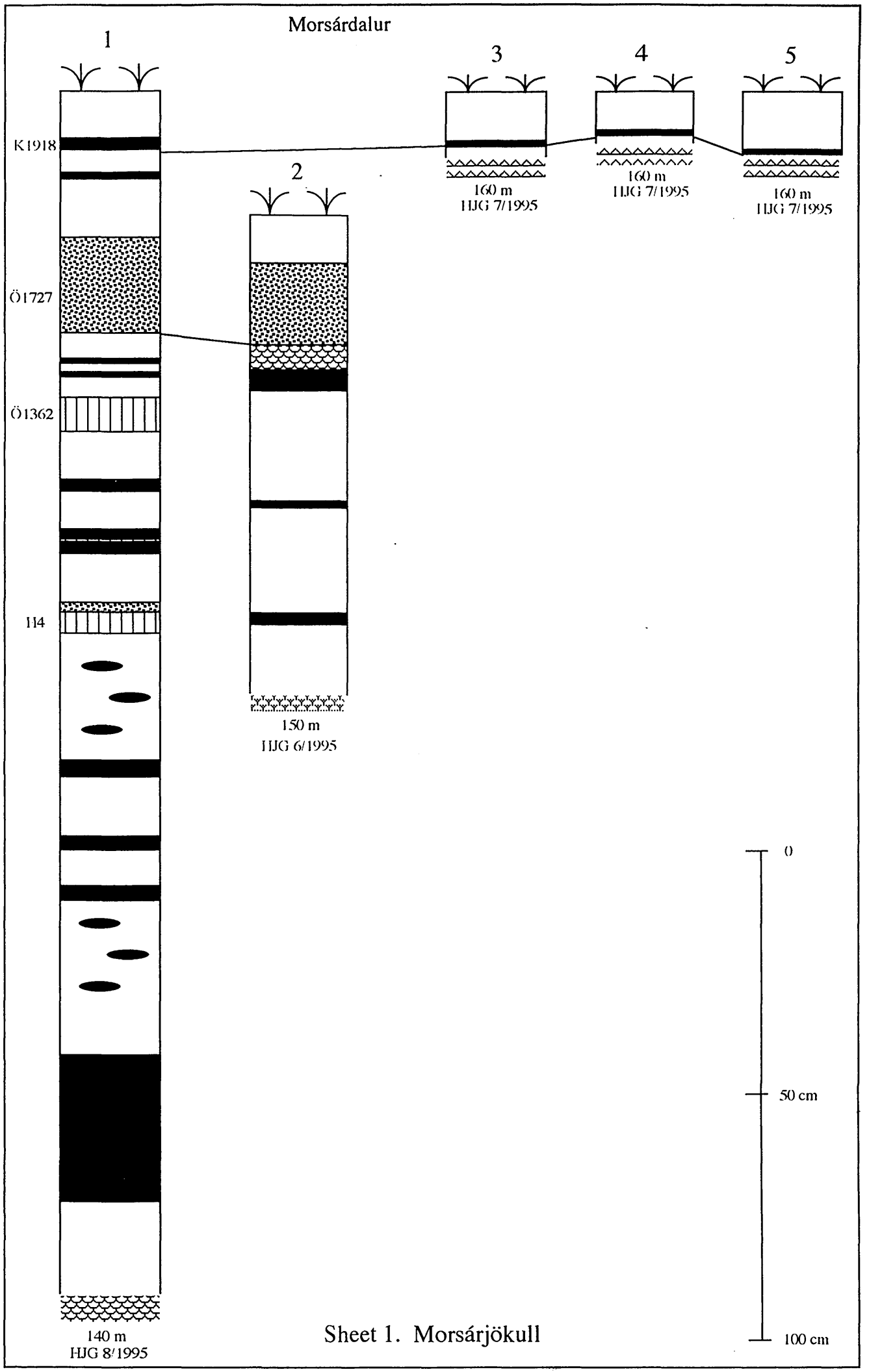

Sheet 1. Morsárjökull

Skaftafellsheidi/jökull

Sheet II. Skaftafellsheidi

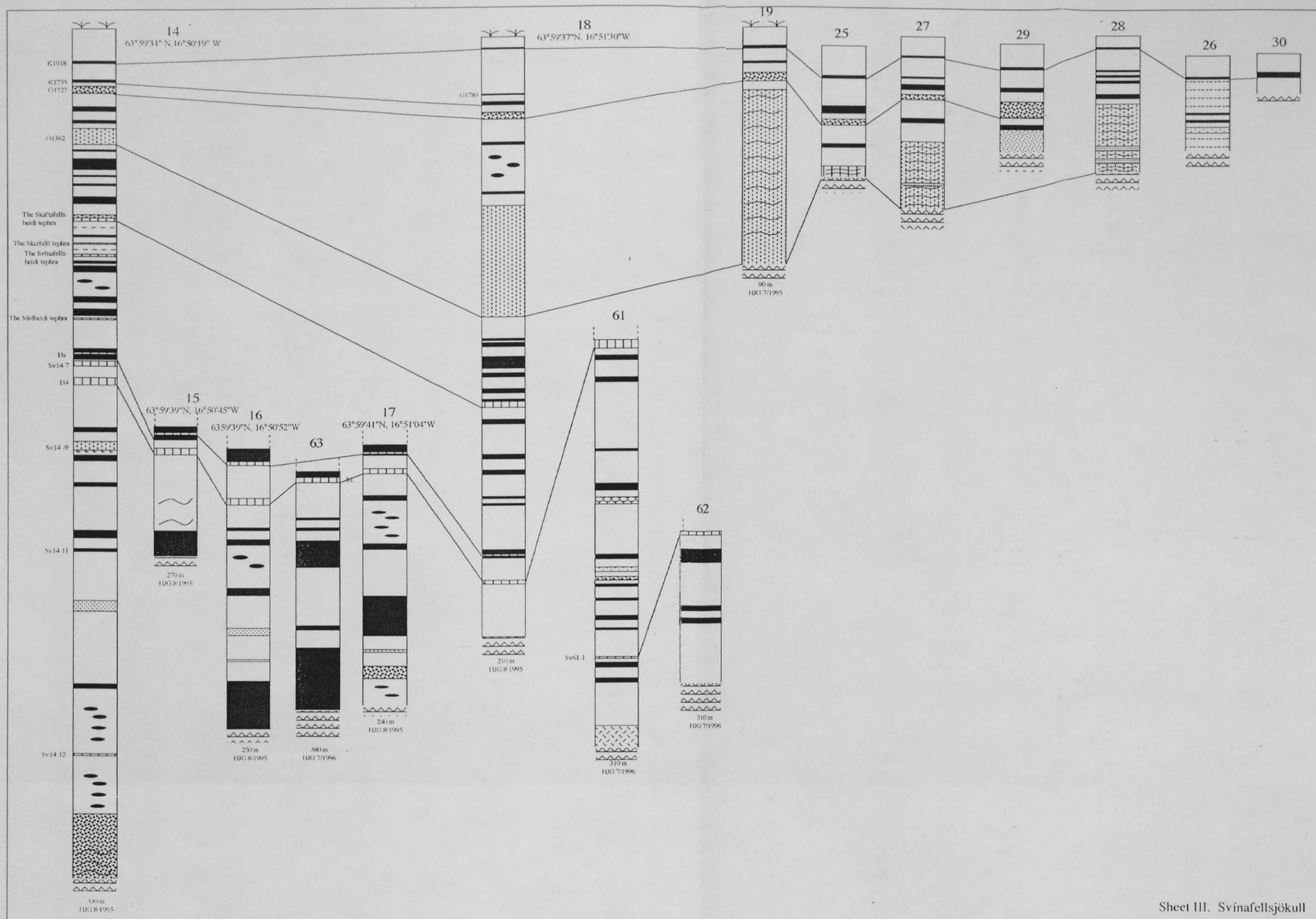

Sheet III. Svínafellsjökull

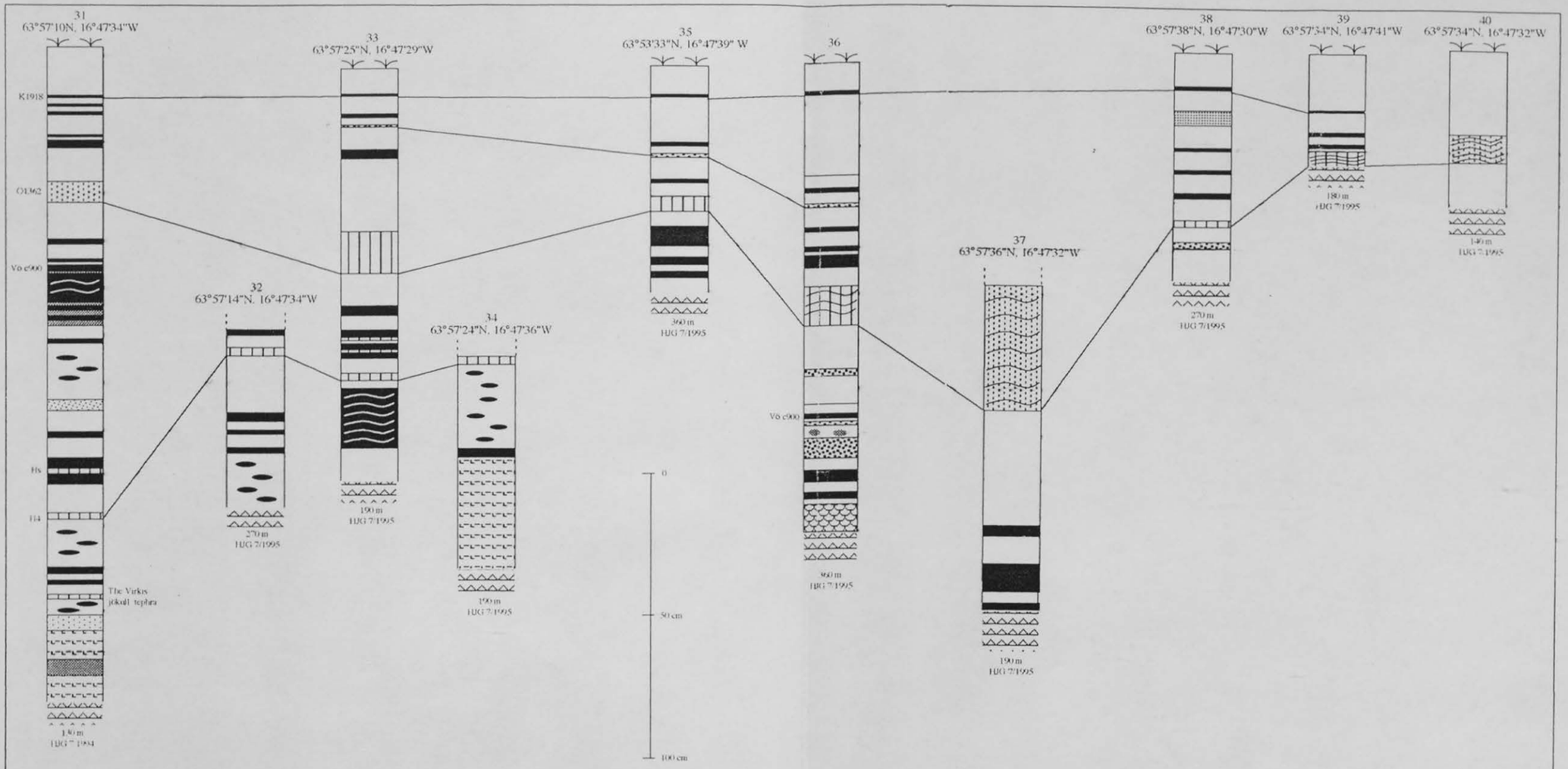

Sheet IV. Virkisjökull

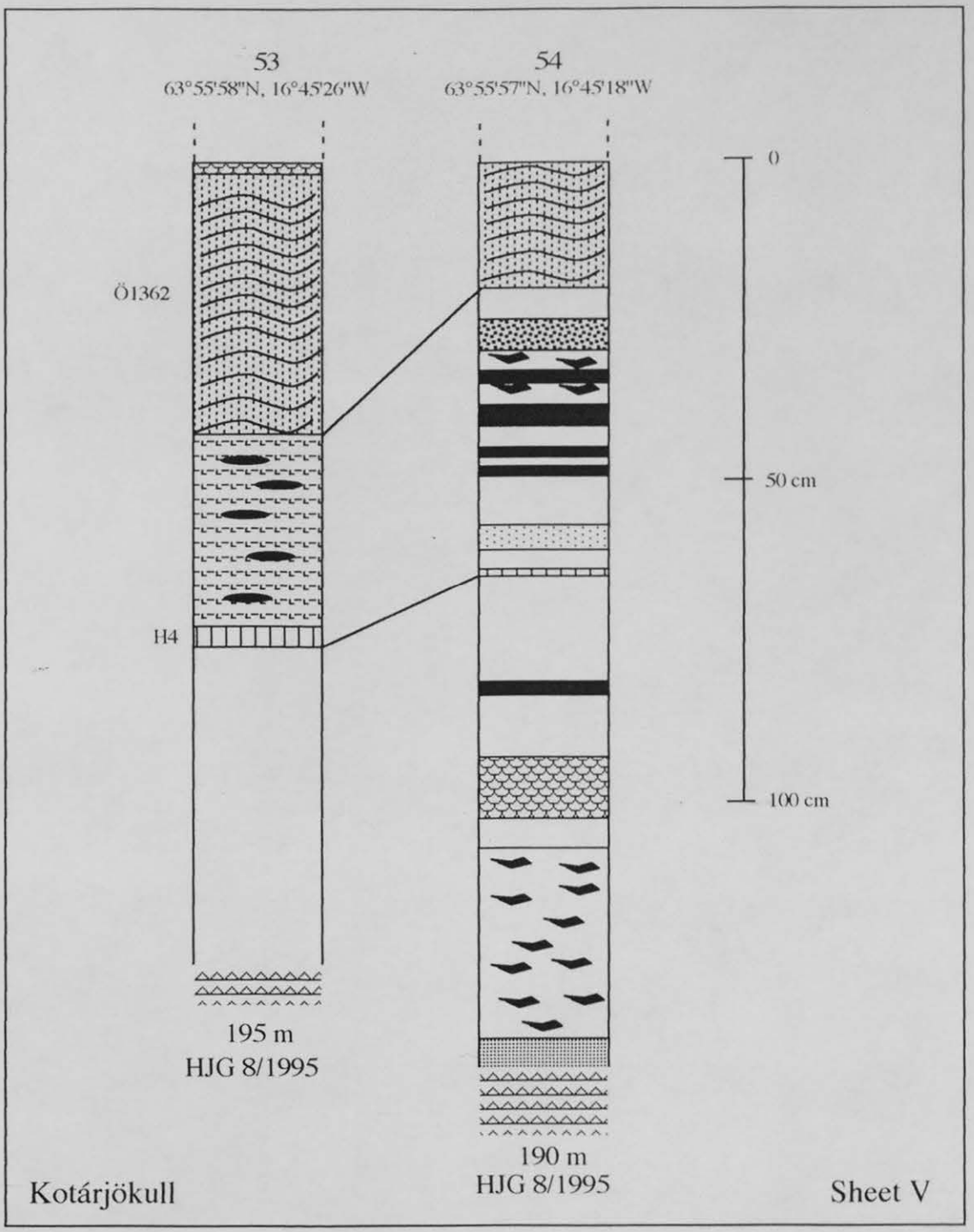
53
63°55'58"N, 16°45'26"W
54
63°55'57"N, 16°45'18"W
Ö1362
H4
0
50 cm
100 cm
195 m
HJG 8/1995
190 m
HJG 8/1995
Kotárjökull
Sheet V

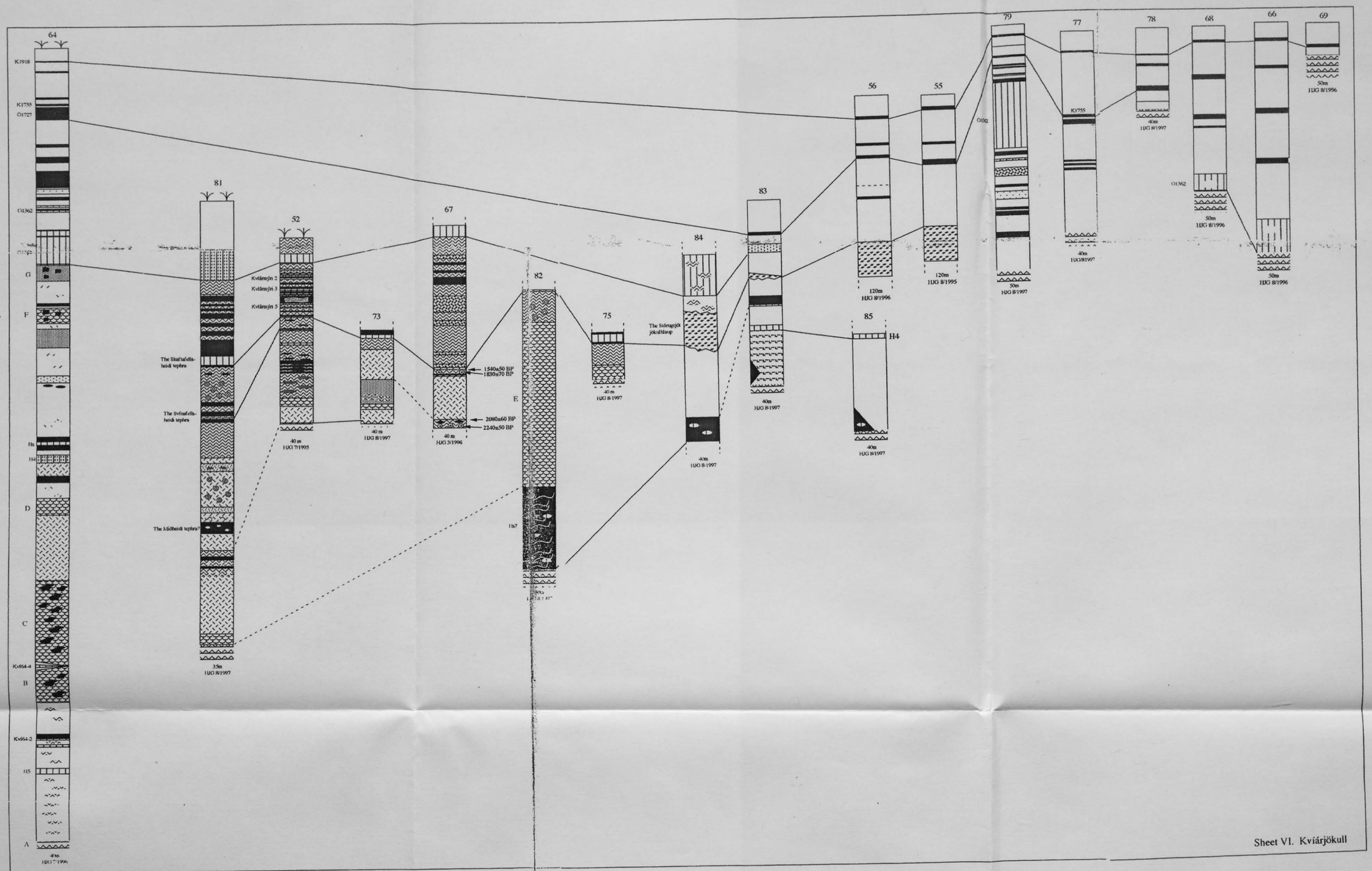

Sheet VI. Kvíárjökull